U.S. Department
of Commerce

Volume 104
Number 1
January 2006

Fishery Bulletin

U.S. Department of Commerce
Carlos M. Gutierrez
Secretary

National Oceanic and Atmospheric Administration
Vice Admiral
Conrad C. Lautenbacher Jr., USN (ret.)
Under Secretary for Oceans and Atmosphere

National Marine Fisheries Service
William T. Hogarth
Assistant Administrator for Fisheries

The *Fishery Bulletin* (ISSN 0090-0656) is published quarterly by the Scientific Publications Office, National Marine Fisheries Service, NOAA, 7600 Sand Point Way NE, BIN C15700, Seattle, WA 98115-0070. Periodicals postage is paid at Seattle, WA, and at additional mailing offices. POSTMASTER: Send address changes for subscriptions to Fishery Bulletin, Superintendent of Documents, Attn.: Chief, Mail List Branch, Mail Stop SSOM, Washington, DC 20402-9373.

Although the contents of this publication have not been copyrighted and may be reprinted entirely, reference to source is appreciated.

The Secretary of Commerce has determined that the publication of this periodical is necessary according to law for the transaction of public business of this Department. Use of funds for printing of this periodical has been approved by the Director of the Office of Management and Budget.

For sale by the Superintendent of Documents, U.S. Government Printing Office, Washington, DC 20402. Subscription price per year: $55.00 domestic and $68.75 foreign. Cost per single issue: $28.00 domestic and $35.00 foreign. **See back for order form.**

Fishery Bulletin

Scientific Editor
Adam Moles, Ph.D.

Technical Editor
Elizabeth Calvert

11305 Glacier Highway
Juneau, Alaska 99801-8626

Managing Editor
Sharyn Matriotti

National Marine Fisheries Service
Scientific Publications Office
7600 Sand Point Way NE, BIN C15700
Seattle, Washington 98115-0070

Editorial Committee

Harlyn O. Halvorson, Ph.D.	University of Massachusetts, Boston
Ronald W. Hardy, Ph.D.	University of Idaho, Hagerman
Richard D. Methot, Ph.D.	National Marine Fisheries Service
Theodore W. Pietsch, Ph.D.	University of Washington, Seattle
Joseph E. Powers, Ph.D.	National Marine Fisheries Service
Harald Rosenthal, Ph.D.	Universität Kiel, Germany
Fredric M. Serchuk, Ph.D.	National Marine Fisheries Service
George Watters, Ph.D.	National Marine Fisheries Service

***Fishery Bulletin* web site: www.fishbull.noaa.gov**

The *Fishery Bulletin* carries original research reports and technical notes on investigations in fishery science, engineering, and economics. It began as the Bulletin of the United States Fish Commission in 1881; it became the Bulletin of the Bureau of Fisheries in 1904 and the *Fishery Bulletin* of the Fish and Wildlife Service in 1941. Separates were issued as documents through volume 46; the last document was No. 1103. Beginning with volume 47 in 1931 and continuing through volume 62 in 1963, each separate appeared as a numbered bulletin. A new system began in 1963 with volume 63 in which papers are bound together in a single issue of the bulletin. Beginning with volume 70, number 1, January 1972, the *Fishery Bulletin* became a periodical, issued quarterly. In this form, it is available by subscription from the Superintendent of Documents, U.S. Government Printing Office, Washington, DC 20402. It is also available free in limited numbers to libraries, research institutions, State and Federal agencies, and in exchange for other scientific publications.

U.S. Department of Commerce
Seattle, Washington

Volume 104
Number 1
January 2006

Fishery Bulletin

Contents

Articles

1 **Rochet, Marie-Joëlle, Jean-François Cadiou, and Verena M. Trenkel**
Precision and accuracy of fish length measurements obtained with two visual underwater methods

10 **Witteveen, Briana H., Robert J. Foy, and Kate M. Wynne**
The effect of predation (current and historical) by humpback whales (*Megaptera novaeangliae*) on fish abundance near Kodiak Island, Alaska

Companion papers

21 **Weinberg, Kenneth L., and David A Somerton**
Variation in trawl geometry due to unequal warp length

35 **Kotwicki, Stan, Kenneth L. Weinberg, and David A. Somerton**
The effect of autotrawl systems on the performance of a survey trawl

46 **Zeidberg, Louis D., William M. Hamner, Nikolay P. Nezlin, and Annette Henry**
The fishery for California market squid (*Loligo opalescens*) (Cephalopoda: Myopsida), from 1981 through 2003

60 **Criales, Maria M. John D. Wang, Joan A. Browder, Michael B. Robblee, Thomas L. Jackson, and Clinton Hittle**
Variability in supply and cross-shelf transport of pink shrimp (Farfantepenaeus duorarum) postlarvae into western Florida Bay

75 **Grandcourt, Edwin M., Thabit Z. Al Abdessalaam, Ahmed T. Al Shamsi, and Franklin Francis**
Biology and assessment of the painted sweetlips (Diagramma pictum (Thunberg, 1792)) and the spangled emperor (Lethrinus nebulosus (Forsskål, 1775)) in the southern Arabian Gulf

The conclusions and opinions expressed in *Fishery Bulletin* are solely those of the authors and do not represent the official position of the National Marine Fisher-ies Service (NOAA) or any other agency or institution.

The National Marine Fisheries Service (NMFS) does not approve, recommend, or endorse any proprietary product or proprietary material mentioned in this publication. No reference shall be made to NMFS, or to this publication furnished by NMFS, in any advertising or sales promotion which would indicate or imply that NMFS approves, recommends, or endorses any proprietary product or proprietary material mentioned herein, or which has as its purpose an intent to cause directly or indirectly the advertised product to be used or purchased because of this NMFS publication.

89 **Porch, Clay E., Anne-Marie Eklund, and Gerald P. Scott**
A catch-free stoack assessment model with application to goliath grouper (*Epinephelus itajara*) off southern Florida

102 **Tuckey, Troy D., and Mark Dehaven**
Fish assemblages found in tidal-creek and seagrass habitats in the Suwannee River estuary

118 **Clarke, Lora M., Alistair D. M. Dove, and David O. Conover**
Prevalence, intensity, and effect of a nematode (*Philometra saltatrix*) in the ovaries of bluefish (*Pomatomus saltatrix*)

125 **Edwards, Elizabeth F.**
Duration of unassisted swimming activity for spotted dolphin (*Stenella attenuata*) calves: implications for mother-calf separation during tuna purse-seine sets

136 **Saillant, Eric, and John R. Gold**
Population structure and variance effective size of red snapper (*Lutjanus campechanus*) in the northern Gulf of Mexico

Note

149 **Friedland, Kevin D., Lora M. Clarke, Jean-Denis Dutil, and Matti Salminen**
The relationship between smolt and postsmolt growth for Atlantic salmon (*Salmo salar*) in the Gulf of St. Lawrence

156 **Erratum**

157 **Guidelines for authors**

Precision and accuracy of fish length measurements obtained with two visual underwater methods

Marie-Joëlle Rochet
Laboratoire MAERHA, IFREMER
Rue de l'Ile d'Yeu, B.P. 21105
44311 Nantes, Cedex 03, France
E-mail address: mjrochet@ifremer.fr

Jean-François Cadiou
IFREMER (DNIS/SM/IM)—Centre Méditerranée
B.P. 330
83507 La Seyne, France

Verena M. Trenkel
Laboratoire MAERHA, IFREMER
Rue de l'Ile d'Yeu, B.P. 21105
44311 Nantes, Cedex 03, France

Abstract—During the *VITAL* cruise in the Bay of Biscay in summer 2002, two devices for measuring the length of swimming fish were tested: 1) a mechanical crown that emitted a pair of parallel laser beams and that was mounted on the main camera and 2) an underwater auto-focus video camera. The precision and accuracy of these devices were compared and the various sources of measurement errors were estimated by repeatedly measuring fixed and mobile objects and live fish. It was found that fish mobility is the main source of error for these devices because they require that the objects to be measured are perpendicular to the field of vision. The best performance was obtained with the laser method where a video-replay of laser spots (projected on fish bodies) carrying real-time size information was used. The auto-focus system performed poorly because of a delay in obtaining focus and because of some technical problems.

Manuscript submitted 22 July 2003
to the Scientific Editor's Office.

Manuscript approved for publication
20 April 2005 by the Scientific Editor.

Fish. Bull. 104:1–9 (2006).

Visual sampling of marine systems by SCUBA divers and underwater vehicles is increasingly used to estimate animal abundances, to observe natural behavior and response behavior to fishing gear *in situ*, and to assess community interactions (e.g., Bublitz, 1996; Auster et al., 1997; Davis et al., 1997; Uiblein et al., 2002; Trenkel et al., 2004). Visual methods also allow estimates of population-size structures without the bias caused by the size selectivity of fishing gear. Visual techniques have been used in the wild for measuring the length of animals by SCUBA divers (e.g., Yoshihara, 1997; Pfister and Goulet, 1999; Harvey et al., 2002a) or by submersibles (Love et al., 2000; Yoklavich et al., 2000). They have also been employed for estimating the length frequency of the catch of live tuna to be fattened after capture (Harvey et al., 2003), and in aquaculture to estimate the size range of fish (Petrell et al., 1997). Until now these techniques were mainly used in shallow waters or tanks. Because of the optical characteristics of sea water—its turbidity, the variations in light intensity with depth and water movements and fish movements, these methods are subject to measurement errors. Estimating the order of magnitude of this measurement error has been the focus of many studies (van Rooij and Videler, 1996; Yoshihara, 1997; Harvey et al., 2001, 2002a, 2002b, 2003).

Efficient methods for measuring fish length *in situ* can also be used in deeper waters not accessible to divers. Parallel laser projected from a video camera onto the seafloor or fish bodies permit accurate measurements (Love et al., 2000; Yoklavich et al., 2000). Albert et al. (2003) measured fish lengths on a video screen and then transformed these measurements into real length knowing the distance of the camera from the ground, its tilt angle, and the horizontal opening angle of the camera. If fish are not on or close to the bottom, it is necessary to know their distance off the bottom to apply this method. Auster et al. (1997) and Norcross and Mueter (1999) measured fish size on a video screen when the fish appeared between the skids of their ROV. The screen measurement is then related to the known distance of the skids. This method relies on the fish and skids being in the same horizontal plane and on the fish being perpendicular to the axis of the camera. Krieger (1992) used a submersible to estimate the size of rockfish.

Two methods were tested during the *VITAL* cruise in the Bay of Biscay, in late August and early Septem-

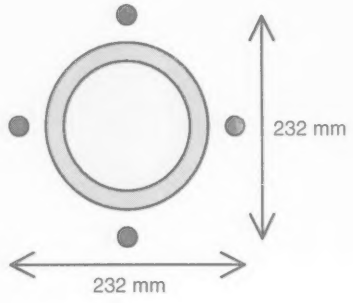

Figure 1

The four laser pointers mounted on a crown around the main camera in front of the ROV *Victor 6000*. The inner circle is the camera lens.

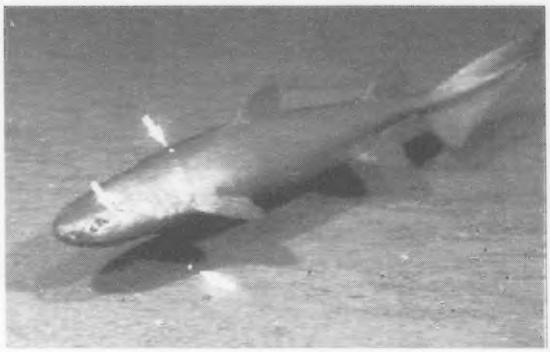

Figure 2

Laser spots (indicated by arrows) visible on and under a fish. These laser spots documented on videotape provided size information both in real time and during video replay.

ber 2002.[1] *Victor 6000*, a remotely operated vehicle (ROV) equipped with several video cameras and recorders, was operated at depths ranging from 1100 to 1500 m. Fish size was measured both by using a pair of parallel laser beams, and an auto-focus video camera linked to software for estimating object size based on the focal distance of the object in focus. In this study three sources of measurement variability were investigated: 1) systematic errors inherent to each method; 2) variability due to observer differences; 3) variability due to continuous fish movements and horizontal body orientation. To estimate these error components separately, rigid and articulated artificial objects ("artificial fish") of known size were measured repeatedly by several independent observers. Individuals belonging to several deep-sea fish species were also repeatedly measured. Mixed-effects models and heteroscedastic error models were fitted to the resulting measurements to compare the magnitude of errors due to different sources.

Materials and methods

Measurement devices

Both measurement devices were installed close to each other on the ROV *Victor*. The laser-beam crown was mounted on the main camera, which was itself attached to the pan and tilt unit. The METRAU© (SONY, model FCB-1X 47P) autofocus camera was mounted on the same pan and tilt unit.

Laser-beam pointers Four red laser pointers (10 mW, 635 nanometers [nm]) were mounted around the main camera housing (Fig. 1). The distance between each two opposite lasers was 232 mm. Red light is strongly attenuated by water but because of the relatively high power of the laser light-emitting diode (LED), a range of up to 7 m is reachable in clear waters.

To measure the fish and objects, the laser beams were projected on the target (Fig. 2). The laser spots, visible on the video, give size information both in real time and during video replay. The principle is simple, but several limitations exist. First, the measurement is correct only for an object located in a plane perpendicular to the laser axis. Second, the target should be large enough to be reached by at least two laser beams; the more laser impacts that are seen on the object to be measured, the easier the measurement.

For the measurement to be accurate, there must be a strict parallelism between the laser beams. This is complicated by the fact that the laser component itself (the diode with its optic lens) does not necessarily have a beam parallel to the axis of the component package. Further, designing an accurate alignment mechanism that is compatible with offshore and deep underwater operating conditions is difficult. The residual error after alignment is about 0.15°, which entails an error of 10 mm for the distance between two opposite spots at a distance of 4 meters (i.e., 4% of size).

METRAU camera The METRAU system is based on the autofocus video camera. The imaging device is an original equipment manufacturer (OEM) camera module similar to those used in off-the-shelf camcorders. The

[1] Trenkel, V. M., N. Bailly, O. Berthelé, O. Brosseau, R. Causse, F. de Corbière, O. Dugornay, A. Ferrant, J. D. M. ordon, D. Latrouite, D. Le Piver, B. Kergoat, P. Lorance, S. Mahévas, B. Mesnil, J.-C. Poulard, M.-J. Rochet, D. Tracey, J.-P. Vacherot, G. Veron, and H. Zibrowius. 2002. First results of a quantitative study of deep-sea fish on the continental slope of the Bay of Biscay: visual observations and trawling. ICES CM 2002/L:18, 2002, 15 p.

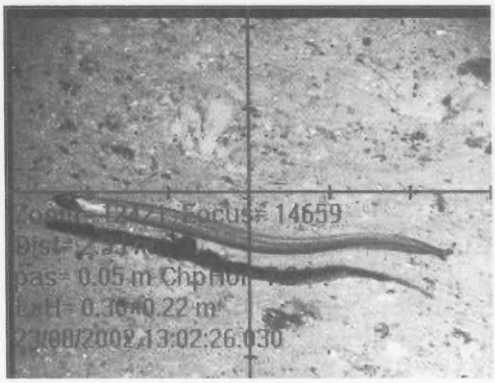

Figure 3
A METRAU video camera image with overlaid grid.

camera has a built-in automatic focus unit which adjusts lens settings to provide a sharp image. The camera is remotely controlled by a RS323 digital link and sends data back over this link, including zoom position and focal value (see details in Cadiou et al., 2004). A previous calibration in air and in a test tank provided correlation rules between raw data and field angle or focal distance.

When the system is operated, the data received by the computer are processed in real time. The object distance and the field angle are computed and a scale is overlaid on the video image (Fig. 3).

According to optical laws, the depth of focus decreases as the focal length increases. This means that in order to obtain an accurate measure of focal distance, a narrow field angle is required. In addition, the depth of focus increases when the focal distance moves towards infinity. Consequently, a domain of validity of the measurement can be defined. With the METRAU camera, there must be a target distance under three meters and a field angle of less than 6°. These constraints have to be combined with the following conditions: a steady image that would allow the automatic focal servo to stabilize; and avoidance of scenes with several image planes. In turbid waters, particles can create disturbing focal planes and affect the measurement process.

Measurement experiments

Artificial objects and live fish Objects of known size were used to estimate the potential bias in the length measurements obtained with the two devices. Three rigid objects—a can, a bottle, and a plastic tube measuring respectively 13, 30, and 66 cm—were repeatedly measured to evaluate device performance and observer-induced variability in the absence of errors induced by fish movement and variations in horizontal observation angles.

Fish movement makes the horizontal observation angle vary continuously. As a result, it is difficult to judge if and when an individual fish is perpendicular to the measurement axis. Further, fish seldom lie in a straight plane. Some species continuously flex their tail, others bend their whole body. To mimic the mobility of a real fish, a mobile object was built consisting of several pieces of Ertalyte (Quadrant Engineering Plastic Products, Bridgeport, CT) plates linked together with rope rings. This artificial fish was designed to be neutrally buoyant so that it could be moved by water currents and undulate like a real swimming fish. The "artificial fish" had three distinctively colored parts. Thus depending on how many parts were measured, a small (13 cm), medium (17 cm), or large (41 cm) "artificial fish" was the result. The real size of rigid objects and of the artificial fish was unknown to the observers throughout the measurement experiment.

In addition to measuring each of the rigid objects and the artificial fish, 351 individuals belonging to 21 deep-sea fish species were measured with both methods. The body sizes of these species ranged from 5 to 110 cm. Each individual fish was measured up to nine times. Altogether 2373 measurements were carried out.

Real time and postoperation measurements While the ROV was in operation, four to five observers were able to watch the video images. Real time measurements were performed by estimating sizes directly from the screen, without using any measuring instrument. Each observer was asked to write down his or her length estimate without announcing it, so that independent measurements were obtained. All artificial objects were measured by both trained and novice observers; real fish were measured only by trained observers, namely scientists and ROV pilots. All objects and fish were measured at distances of 2 to 5 meters.

Postoperation measurements were also performed on registered videos and digital images. For the laser method, the video tape was replayed. The tape was stopped when the image with an object or fish seemed to be in the best possible position. The fish or object was then measured with a ruler on the still video image. Postoperation measurements made with a ruler were also performed on digital snapshots taken from the videos in real time for both the laser and the METRAU method. A ruler was used rather than computer image analysis because it was easy and cost-efficient and it was felt appropriate for this trial appraisal of measurement methods. The bias introduced by this method was assumed to be negligible compared to observer-induced and fish-movement-induced errors.

Operational constraints prevented a full factorial design where all observers could use all methods and measure all objects.

Data analysis

Variance components for observers and fish movements The measurement variability due to observer differences

and fish movements was estimated from the measurements of the artificial objects, for which the true size was known. Because the measurement variance was expected to be larger for the mobile artificial fish than for the rigid objects, an extended linear mixed-effects model (Pinheiro and Bates, 2000) was used to account for this expected heteroscedasticity. The model included true length as a fixed effect and observer as a random effect. Fixed objects and mobile objects (artificial fish) were allowed separate variances. The resulting model was

$$L_{i,f} = \mu + \beta L^* + o_i + f_j + \varepsilon_{ij}, \quad (1)$$

where $L_{i,j}$ = length measured by observer i of an object of class j={fixed, mobile} and of true size L^*;
$o_i \sim N(0,\sigma(o))$; and
$\varepsilon_{ij} \sim N(0,\sigma)$, whereas $f_j \sim N(0, \sigma_j(f_t))$.

The model was fitted to the data from the eight observers who had measured all objects with the laser method.

Accuracy and precision for artificial objects An extended linear model including heteroscedastic variance terms was used to compare the precision and accuracy of the two methods. The model included fixed effects for true length and the measurement method. The estimated fixed effects allow assessment of the potential measurement bias of each method. The measurement errors for fixed and mobile artificial objects were modeled separately for each method. This allowed us to compare the precision of the methods. Thus, the fitted model was

$$L_{j,k} = \mu_k + \beta L^* + f_{jk} + \varepsilon_{jk}, \quad (2)$$

where k = the measurement method and j the object class as before. As in model 1, $\varepsilon_{jk} \sim N(0, \sigma)$. In contrast, $f_{jk} \sim N(0, \sigma_{jk}(f_{jk}))$ allowed for separate variances for each object-type and method pair. Only two trained observers used both measurement methods for all objects. Because there was no significant difference between their measurements, and in order to reduce the number of parameters to be estimated, no observer effect was included in this model.

Precision of fish measurements The precision of fish-length estimates was compared for two species, *Bathypterois dubius* and *Lepidion eques*. These species were selected for this analysis because they are abundant and relatively easy to measure, compared to other species that move faster or flex their body more often. Twenty-four individuals belonging to these two species were measured repeatedly by up to five observers using the real-time laser measurement method.

Because true fish size was unknown, measurement accuracy could not be estimated. For estimating the precision of fish measurements, an extended linear model with heteroscedastic errors was fitted to the fish length measurements. The model included a fixed individual fish effect (each fish had a different, unknown size) and a random observer effect; and fish species were allowed heteroscedastic variances to account for species behavior differences (*Lepidion* versus *Bathypterois*). The stationary species, *B. dubius*, is easier to measure compared to the more lively *L. eques*. The model was

$$L_{n,i,l} = \mu_n + o_i + s_l + \varepsilon_{nil}, \quad (3)$$

where $L_{n,i,l}$ = the length measurement obtained by observer i for individual fish n belonging to species l;
$o_i \sim N(0, \sigma(o))$; and
$\varepsilon_{nil} \sim N(0, \sigma)$, whereas $s_l \sim N(0, \sigma_l(s_l))$.

Unfortunately, it was not possible to carry out a direct comparison between the precision of size estimates of fish and artificial objects because the latter were measured seven to 11 times, whereas the former were measured only two to seven times. Random subsamples could be carried out to obtain comparable sample size; unfortunately, subsamples from large samples would still have a larger variance than small samples.

All models were fitted by using Splus 6.0 for Unix (MathSoft, Seattle, WA). For heteroscedastic models, because of identifiability constraints, the fitting algorithm provided estimates of the ratio between the standard deviations of each class in relation to the standard deviation of a specified class instead of the full set of standard deviations.

Results

Precision and accuracy of measurements varied among objects and methods (Table 1). The best precision was obtained with the video-replays of laser measurements, whereas METRAU generally did not perform very well, especially on snapshots. The precision was generally much lower for mobile objects than for rigid objects. Measurement bias was generally low for the laser method, whereas the METRAU method systematically underestimated the size of objects. A variety of fish species with various sizes were measured. CVs for individual fish measurements varied from 3% to 23% (Table 2). Species were grouped according to their motion behavior (1=sitting on bottom motionless, 2=station holding or drifting, 3=slow swimming, 4=fast swimming [Lorance and Trenkel[2]]). CVs were found to differ between groups, increasing with mobility (mean CV in group 1: 8.9%; group 2: 9.7%; group 3: 12.9%; group 4 was excluded because there was only one individual, $P<10^{-5}$).

[2] Lorance, P., and V. Trenkel. In preparation. Natural behaviour and reaction to an approaching ROV of large mid-slope species. IFREMER, Centre do Brest, B.P. 70, 29280 Plouzané, France.

Table 1

Summary of length measurements for artificial objects by five visual methods. Lengths (in cm) are given along with their coefficient of variation (%) and number of observations in parentheses. a.f. = artificial fish. The laser method entailed viewing laser points (that permit accurate length data) projected on fish. The METRAU method is based on an autofocus video camera.

Object	True size	Laser	Laser + video	Laser + snapshot	METRAU	METRAU + snapshot
Can	13	14.31 (13%, 26)	13.76 (3%, 5)	13.55 (4%, 5)	11.25 (7%, 10)	10.96 (7%, 5)
Bottle	30	30.87 (7%, 26)	31.90 (2%, 5)	31.47 (2%, 5)	26.90 (18%, 10)	32.05 (41%, 5)
Tube	66	65.62 (9%, 26)	66.40 (2%, 5)	66.66 (1%, 5)	44.25 (14%, 8)	40.75 (25%, 4)
Short a.f.	13	13.30 (13%, 21)	13.32 (6%, 3)	22.10 (23%, 2)	11.50 (6%, 2)	7.55 (33%, 6)
Medium a.f.	17	16.49 (14%, 21)	17.11 (5%, 3)	24.86 (25%, 2)	11.50 (18%, 2)	9.25 (32%, 6)
Large a.f.	41	40.80 (17%, 21)	44.87 (14%, 3)	63.23 (25%, 2)	30.00 (14%, 4)	23.21 (31%, 6)

Table 2

Summary of fish length measurements. n = number of individual fish measured for each species. m = total number of measurements. m/n = mean number of observations per individual. Mean length = average individual fish length (cm) per species. Mean CV = average individual coefficient of variation per species. Group = behavioral group of the species (1=sitting on bottom motionless, 2=station holding or drifting, 3=slow swimming, 4=fast swimming).

Species	n	m	m/n	Mean length	Mean CV	Group
Alepocephalus bairdi	2	4	2.0	48.4	8.2%	2
Bathypterois	87	586	6.7	19.2	8.9%	1
Breviraja caerulea	3	13	4.3	29.6	4.8%	2
Caelorinchus labiatus	15	73	4.9	28.7	10.2%	2
Cataetyx latyceps	1	5	5.0	24.1	12.4%	2
Chimaera monstrosa	6	23	3.8	91.4	9.2%	3
Coelorhyncus labiatus	2	8	4.0	25.4	14.9%	2
Coryphaenoides rupestris	21	77	3.7	45.4	12.1%	2
Cottunculus thomsoni	2	17	8.5	29.1	16.1%	1
Galeus melastomus	1	4	4.0	30.7	2.8%	4
Hoplostethus atlanticus	6	27	4.5	32.6	9.4%	2
Hydrolagus affinis	1	6	6.0	74.9	23.3%	3
Hydrolagus mirabilis	3	6	2.0	78.4	11.9%	3
Lepidion eques	161	814	5.1	26.6	9.6%	2
Mora moro	3	8	2.7	60.0	7.9%	2
Nezumia aequalis	10	22	2.2	32.8	8.9%	2
Notacanthus	2	5	2.5	44.6	10.6%	2
Phycis blenoides	1	4	4.0	44.8	15.3%	2
Syphobranchus kaupii	7	23	3.3	27.2	16.2%	3
Trachyrincus murrayi	4	7	1.8	38.9	3.5%	2
Trachyscorpia cristulata echinata	14	67	4.8	40.7	8.1%	1

Measurement variance for observers and fish movements

The standard deviation of the observer random effect, $\sigma(o)$, amounted to approximately 20% of the residual standard deviation. The standard deviation of the random effect for mobile objects, $\sigma_{mobile}(f_{mobile})$, was 40% higher than that for rigid objects, indicating that the measurement variability was lower for fixed than for mobile objects, as expected. The slope and intercept of the fixed effects did not significantly differ from 1 and 0, respectively. Thus the laser method is unbiased and performs equally well for all sizes in the range tested (Table 3).

Accuracy and precision of measurements for artificial objects

Size measurements carried out using the laser beams in real time or on registered videos were found to be

Table 3

Estimated fixed-effect coefficients and standard deviations for model 1 for the measurements of rigid and mobile objects by eight independent observers using the laser method. SE = standard error; CL =confidence limit.

Coefficient	Estimate	SE	*P*-value
μ	1.53	0.97	0.12
β	0.976	0.023	<0.0001
Standard deviation	Lower CL	Estimated	Upper CL
$\sigma(o)$	0.296	1.126	4.435
σ	4.369	5.535	7.014
$\sigma_{rigid}(f_{rigid})/\sigma_{mobile}(f_{mobile})$[1]	0.523	0.710	0.964

[1] Standard deviations were estimated in relation to the standard deviation for mobile objects.

Table 4

Estimated coefficients for model 2 for measurements of rigid and mobile objects by five variants of the two methods.

Coefficient	Estimate	SE	*P*-value
μ_{laser}	0.106	0.934	0.91
μ_{METRAU}	−7.198	1.621	<0.0001
$\mu_{laser+video}$	1.466	0.937	0.15
$\mu_{laser+snapshot}$	1.348	0.932	0.19
$\mu_{METRAU+snapshot}$	−9.516	1.806	<0.0001
β	0.976	0.023	<0.0001
σ	4.592		

Table 5

Estimates of the standard deviations of length measurements for rigid and mobile objects obtained by five variants of the two methods, from model 2. Number of measurements are given in parentheses. Estimates significantly different from 1 are in bold font.

Method	Rigid objects	Mobile objects
Laser	1.12 (21)	1.00[1] (9)
Laser + video	**0.21** (15)	1.03 (9)
Laser + snapshot	**0.19** (15)	3.43 (6)
METRAU	2.11 (20)	1.06 (8)
METRAU + snapshot	3.16 (14)	1.58 (18)

[1] All standard deviations are relative to the standard deviation for laser measurements of mobile objects.

unbiased, whereas the METRAU-based measurements underestimated the true length of objects by as much as 7 cm for real-time measurements and 10 cm for time-delayed measurements (Table 4, Fig. 4). In addition, the variance of METRAU measurements was systematically larger than the corresponding laser measurements (Table 5: ratios larger than 1). For rigid objects, laser-based video-replays had a lower variance than real time measurements. This lower variance for postoperational measurements was due to the allowance of videos to be replayed as many times as necessary in order to select the best image where an object was perpendicular to the optical axis. Use of a ruler also improves the measurement. The high estimation variance obtained for mobile objects measured with the laser method on digital snapshots was partially due to one outlier (Fig. 4B). The object was measured at a relatively great distance in somewhat turbid water. The outlier was not removed because these kinds of errors are to be expected under common measurement conditions in the field. Generally the most precise results were obtained for video-replays with the laser beam method.

Precision of fish measurements

The variance of the random effect for *B. dubius* was about 66% of the variance estimated for *L. eques*. For live fish, the standard deviation of the observer random effect was approximately 16% of the residual standard deviation (Table 6). This standard deviation is lower than that obtained for objects of known size because the residual variance was larger owing to the small number of repeated measurements obtained for each fish. It was not easy to repeatedly measure fish because of escapement behavior. In addition, only trained observers took part in this experiment, which reduced observer variability.

Discussion

The potential sources of errors and variability in visual fish length measurements are 1) the design and calibra-

Table 6

Estimates and 95% confidence limits for the standard deviations of the components of model 3 for fish size measurements obtained for two species by five independent observers using the laser method.

Standard deviation	Lower	Estimate	Upper
$\sigma(o)$	0.068	0.278	1.130
σ	1.096	1.702	2.642
$\sigma_{B.dubius}(S_{B.dubius})/\sigma_{L.eques}(S_{L.eques})$[1]	0.41	0.66	1.06

[1] Standard deviations provided in relation to the standard deviation for *Lepidion* measurements.

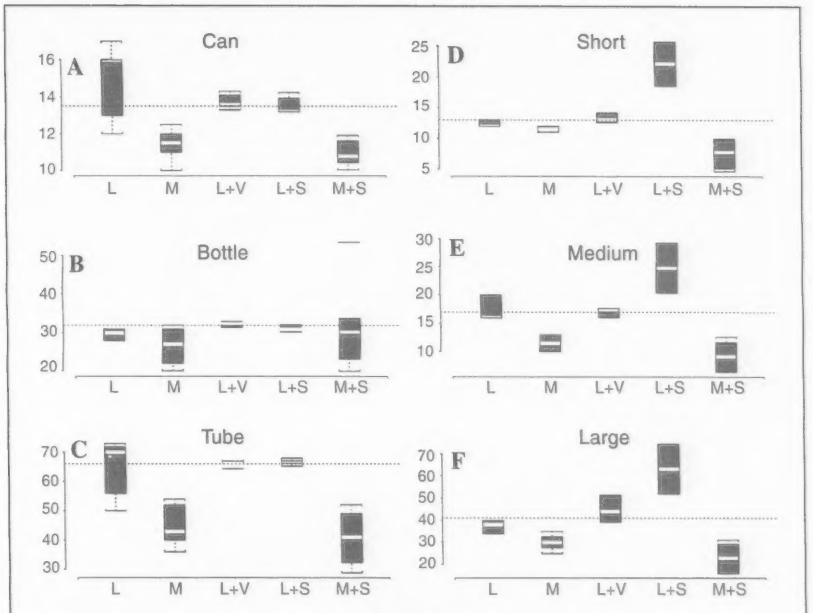

Figure 4

Boxplots for the distributions of length measurements (cm) obtained by five measurement methods for each of three fixed (left) and three mobile (right) objects. Boxes = interquartile range, white line = median, whiskers = extremes (excluding outliers). Dotted line is the true size of the object. L = laser method; M = METRAU method; L+V = laser video-replay; L+S = laser snapshot measurement; M+S = METRAU snapshot measurement.

tion of the measurement devices, 2) differences among observers, 3) orientation and position of fish in relation to the camera, and 4) swimming motion. We investigated each of these featuress.

Among the two methods tested during this study, the METRAU method performed poorly. It has several disadvantages. First, METRAU system needs the fish brought into focus when it is perpendicular to the field of vision. This may take time during which the fish can escape. Second, the registered video images do not include the superimposed calculated scales. Thus, unlike the laser method, it is not possible to replay the video to identify the best image. Postoperational measurements can be performed only by using the digital snapshots registered in real time. Third, this method had a higher variance than the laser method, probably because of the technical constraints just mentioned. Fourth, during the *VITAL* cruise the estimates were systematically biased downwards. Measurements carried out after the cruise in a laboratory pool confirmed this systematic underestimation to be ~20% of the real sizes. This result may be due to errors in the software which processes the output of the camera. Although the errors could probably be fixed, and the hardware improved to generate a video signal with the overlaid scale for recording, the other disadvantages are more difficult to eliminate, because of the intrinsic limitations of the system. Hence the method is not promising for estimating the size of fish in the wild.

By contrast, the laser beam method performed rather well, at least for rigid objects. We obtained CVs of 7–13% for rigid objects in real time and 1–4% with image postprocessing (Table 1), both of which compare well with CVs for silhouette measurements obtained with a single camera placed in a laboratory pool (with scale bars placed on the bottom of the pool) and with computer image processing (1%, Harvey et al., 2002b), or even with stereo-video measurements of silhouettes (0.6–7.5%, Harvey and Shortis, 1996). Length measurements were always unbiased and postoperational measurements on video images reached a high precision for rigid objects and for small- to medium-size mobile objects. Thus the method seems suited for measuring the size of animals of low mobility, like invertebrates, along visual observation transects.

The variance due to differences between observers was about 20% of the residual variance. This variance was reduced to 16% when measurements were performed by trained observers. This is true for real-time measurements. For video-replays of the laser-beam data, the variance due to observers was very small because of the use of a ruler instead of subjective extrapolation of

the known laser distance. The use of automated analysis of video images may further reduce the observer error source.

The major difficulty in measuring fish length *in situ* is caused by fish mobility, which causes them to be in variable orientations and positions in relation to the camera, and also to be flexed. We addressed both variance components together by comparing measurements of mobile objects ("artificial fish") and rigid objects. With the laser beam method, the measurement standard deviation of rigid objects was estimated to be 20% of the standard deviation of mobile objects (95% confidence limits: 6–75%). These components may be of the same order of magnitude as those for fish measurements, although fish measurements could not be estimated in our study because the true size of the fish was unknown. An attempt to disentangle both components is provided by estimating the difference between the precision obtained for species with contrasting behaviors. *Bathypterois dubius* individuals lie motionless on the bottom and seldom move, but because they stand on their fins they are never exactly perpendicular to the camera. By contrast, *L. eques* swims close to the bottom and tends to escape when the ROV is approaching too closely. This species continuously moves its tail; therefore it is very difficult to obtain an image with the whole body properly orientated and straight. The standard deviation of *B. dubius* length measurements was estimated to be 66% of that of *L. eques*. This difference is smaller than the difference between rigid and mobile objects above; therefore we conclude that the major part of variance is due to the orientation of the fish in relation to the camera. Similarly, the estimated CVs of 21 species grouped by motion behavior differed only slightly. This is consistent with previous studies which have shown that relative errors of single-camera or stereo-video measurements of silhouettes or frozen fish could reach 10% to 30%, depending on the distance to the camera, when the angle to the camera was increased from 0° to 60°, whereas the measurement CVs increased fourfold (Harvey and Shortis, 1996; Petrell et al., 1997; Harvey et al., 2002b). By contrast, error due to tail flexion and muscle contractions during swimming motions was estimated at ~5% in a comparison of "linear" to "sinusoidal" length of dorsally photographed sharks (Klimley and Brown, 1983) and at 0.5% for repeated stereo-video measurements of swimming tunas (Harvey et al., 2003).

In conclusion, the major source of measurement error for live fish may be their orientation and position in relation to the camera. For animals that are sessile or lying immobile on the ocean floor, this would be much reduced if the camera and laser beams were mounted vertically instead of obliquely. Thus the laser-beam method may be potentially useful for measuring benthic animals. For mobile animals, however, stereo-video methods (Harvey et al., 2001; Harvey et al., 2002a; van Rooij and Videler, 1996) may be more promising, and are continuously improving (Harvey et al., 2003).

Acknowledgments

We thank all observers for taking part in the experiment, and the ROV pilots for their willingness and skill at pursuing fish and in obtaining positions suitable for being measured. An anonymous referee gave very helpful comments on a previous version of this manuscript.

Literature cited

Albert, O. T., A. Harbitz, and Å. S. Høines.
2003. Greenland halibut observed by video in front of survey trawl: behaviour, escapement, and spatial patterns. J. Sea Res. 50:117–127.

Auster, P., R. Malatest, and C. Donaldson.
1997. Distributional responses to small-scale habitat variability by early juvenile silver hake, *Merluccius bilinearis*. Environ. Biol. Fish. 56:195–200.

Bublitz, C.
1996. Quantitative evaluation of flatfish behaviour during capture by trawl gear. Fish. Res. 25:293–304.

Cadiou, J.-F., V. Trenkel, and M.-J. Rochet
2004 Comparison of several methods for *in situ* size measurements of moving animals. *In* Proceedings of the fourteenth (2004) international offshore and polar engineering conference; Toulon, France, May 23–28, 2004, p. 438–444. Int. Soc. Offshore Polar Engineers, Danvers, MA.

Davis, C. L., L. Carl, and D. Evans.
1997. Use of a remotely operated vehicle to study habitat and population density of juvenile lake trout. Trans. Am. Fish. Soc. 126:871–875.

Harvey, E., M. Cappo, M. Shortis, S. Robson, J. Buchanan, and P. Speare.
2003. The accuracy and precision of underwater measurements of lentgh and maximum body depth of southern bluefin tuna (*Thunnus maccoyii*) with a stereo-video camera system. Fish. Res. 63:315–326.

Harvey, E., D. Fletcher, and M. Shortis.
2001. A comparison of the precision and accuracy of estimates of reef-fish lengths determined visually by divers with estimates produced by a stereo-video system. Fish. Bull. 99:63–71.
2002a. Estimation of reef fish length by divers and by stereo-video. A first comparison of the accuracy and precision in the field on living fish under operational conditions. Fish. Res. 57:255–265.

Harvey, E., and M. Shortis.
1996. A system for stereo-video measurement of sub-tidal organisms. Mar. Technol. Soc. J. 29:10–22.

Harvey, E., M. Shortis, M. Stadler, and M. Cappo.
2002b. A comparison of the accuracy and precision of measurements from single and stereo-video systems. Mar. Technol. Soc. J. 36:38–49.

Klimley, A. P., and S. T. Brown.
1983. Stereophotography for the field biologist: measurement of lengths and three-dimensional positions of free-swimming sharks. Mar. Biol. 74:175–185.

Krieger, K. J.
1992. Distribution and abundance of rockfish determined from a submersible and by bottom trawling. Fish. Bull. 91:87–96.

Love, M. S., J. E. Caselle, and L. Snook.
2000. Fish assemblages around seven oil platforms in the Santa Barbara Channel area. Fish. Bull. 98:96–117.

Norcross, B., and F.-J. Mueter.
1999. The use of an ROV in the study of juvenile flatfish. Fish. Res. 39:241–251.
Petrell, R. J., X. Shi, R. K. Ward, A. Naiberg, and C. R. Savage.
1997. Determining fish size and swimming speed in cages and tanks using simple video techniques. Aquacult. Engineer. 16:63–84.
Pfister, R. D., and D. Goulet.
1999. Nonintrusive video technique for in situ sizing of coral reef fishes. Copeia 1999:789–793.
Pinheiro, J. C., and D. M. Bates.
2000. Mixed-effects models in S and S-PLUS, 528 p. Springer, New York, NY.
Trenkel, V. M., P. Lorance, and S. Mahévas.
2004. Do visual transects provide true population density estimates for deep-water fish? ICES J. Mar. Sci. 61:1050–1056.
Uiblein, F., P. Lorance, and D. Latrouite.
2002. Variation in locomotion behaviour in northern cutthroat eel (*Synaphobranchus kaupi*) on the Bay of Biscay continental slope. Deep-Sea Res. 49(1):1689–1703.
van Rooij, J. M., and J. J. Videler.
1996. A simple field method for stereo-photographic length measurement of free-swimming fish: merits and constraints. J. Exp. Mar. Biol. Ecol. 195:237–249.
Yoklavich, M. M., H. G. Greene, G. M. Cailliet, D. E. Sullivan, R. N. Lea, and M. S. Love.
2000. Habitat associations of deep-water rockfishes in a submarine canyon: an example of a natural refuge. Fish. Bull. 98:625–641.
Yoshihara, K.
1997. A fish body length measuring method using an underwater video camera in combination with laser discharge equipment. Fish. Sci. 63:676–680.

The effect of predation (current and historical) by humpback whales (*Megaptera novaeangliae*) on fish abundance near Kodiak Island, Alaska

Briana H. Witteveen
Robert J. Foy
Kate M. Wynne
School of Fisheries and Ocean Sciences
University of Alaska Fairbanks
118 Trident Way
Kodiak, Alaska 99615
E-mail address (for B. H. Witteveen): bwitteveen@sfos.uaf.edu

Abstract—Humpback whales (*Megaptera novaeangliae*) are significant marine consumers. To examine the potential effect of predation by humpback whales, consumption (kg of prey daily) and prey removal (kg of prey annually) were modeled for a current and historic feeding aggregation of humpback whales off northeastern Kodiak Island, Alaska. A current prey biomass removal rate was modeled by using an estimate of the 2002 humpback whale abundance. A historic rate of removal was modeled from a prewhaling abundance estimate (population size prior to 1926). Two provisional humpback whale diets were simulated in order to model consumption rate. One diet was based on the stomach contents of whales that were commercially harvested from Port Hobron whaling station in Kodiak, Alaska, between 1926 and 1937, and the second diet, based on local prey availability as determined by fish surveys conducted within the study area, was used to model consumption rate by the historic population. The latter diet was also used to model consumption by the current population and to project a consumption rate if the current population were to grow to reach the historic population size. Models of these simulated diets showed that the current population likely removes nearly 8.83×10^6 kg of prey during a 5-month humpback whale feeding season, which could include around 3.26×10^6 kg of juvenile pollock (*Theragra chalcogramma*), 2.55×10^6 kg of capelin (*Mallotus villosus*), if these species are consumed in proportion to their availability. The historic humpback whale population may have removed over 1.76×10^7 kg of prey annually.

Manuscript submitted 22 April 2004 to the Scientific Editor's Office.
Manscript approved for publication 25 April 2005 by the Scientific Editor.
Fish. Bull. 104:10–20 (2006).

Numerous studies have revealed that an increased awareness of trophic-level interactions is essential in assessing the status of complex marine ecosystems (Overholtz et al., 1991; Hairston and Hairston, 1993; Pascual et al., 1993; Estes, 1994; Kenney et al., 1997; Trites et al., 1997). Such studies have shown that predator-prey relationships in marine systems can have direct and indirect effects on all ecosystem members, but predictions of their effects cannot be made without multispecies models.

Cetaceans are top predators in marine ecosystems and consume significant amounts of prey. Knowledge of the distribution, abundance, and foraging habits of cetaceans is, therefore, an essential element of any pelagic ecosystem study (van Franeker, 1992). Many species preyed upon by cetacean populations are targeted by other marine predators and commercial fisheries or are linked to fisheries through complex food webs. Previous studies have reported that prey removal due to cetacean consumption approaches or exceeds removals due to commercial fishing (Laws, 1977; Laevastu and Larkins, 1981; Bax, 1991, Markussen et al., 1992; Nordøy et al., 1995; Kenney et al., 1997). Such high levels of consumption can have significant effects on the distribution and abundance of prey species and the structure of marine communities (Perez and McAlister, 1993; Kenney et al., 1997; Croll et al., 1998). Therefore, examining consumption by cetaceans contributes information about complex ecosystem relationships and the long-term sustainability of marine resources (Perez and McAlister, 1993; Kenney et al., 1997; Tamura and Ohsumi[1]).

Humpback whales (*Megaptera novaeangliae)* feed in the waters off Kodiak Island and, because they are considered apex predators, may influence the structure of the Kodiak Island marine ecosystem (Fig. 1) (Trites et. al., 1997; Croll et. al., 1998). Modeling the amount of prey consumed (kg of prey annually) by feeding humpback whales is, therefore, a useful tool for evaluating their role as marine predators.

Cetaceans, in general, are described as opportunistic in their food selection, although species tend to select broad categories of prey such as cephalopods, fish, or zooplankton (Tomilin, 1954; Nemoto, 1959; Klumov, 1966; Sigurjónsson and Víkingsson, 1998). Humpback whales are classified as generalists and target a wide variety of prey species (Nemoto, 1970; Perry et al., 1999). They have been shown to be seasonal feeders on euphausiids (*Thysanoessa* spp.) and schooling fish species up to 30 cm in length, including capelin (*Mallotus villosus*), Pacific herring (*Clupea pal-*

[1] Tamura, T., and S. Ohsumi. 2000. Regional assessments of prey consumption by marine cetaceans in the world. International Whaling Commission document SC/52/E6, 45 p. Website: www.icrwhale.org/eng/SC52E6.pdf [Accessed on 30 November 2002].

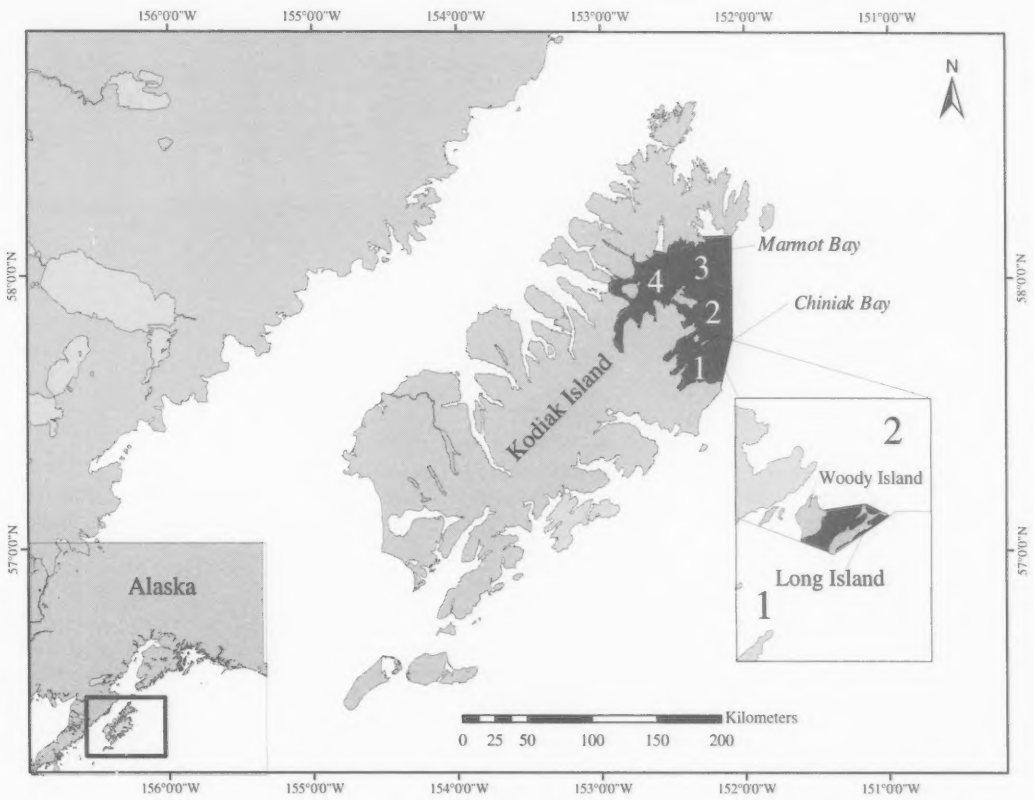

Figure 1

Map of Kodiak Island study area. Study area is shown as shaded area and subareas (1–4) are outlined and numbered. In detail is the nearshore subarea between Woody Island and Long Island.

lasi), walleye pollock (*Theragra chalcogramma*), Atka mackerel (*Pleurogrammus monopterygius),* cod (*Gadus* spp.), sardines (*Sardinops* spp.), and sandlance (*Ammodytes* spp.) (Nemoto, 1957, 1959; Mitchell, 1973; Payne et al., 1990). The variety, as well as the amount, of prey removed from Kodiak waters may therefore be significant. Resource removal from Kodiak waters is of particular importance when considering the high value of Kodiak Island commercial fisheries, which totaled 63.3 million dollars in exvessel (wholesale) value in 2002 (NMFS[2]).

Modeling consumption by humpback whales as they recover from severe population declines could shed light on patterns of change seen in prey and sympatric consumer populations, such as marine birds and pinnipeds (Merrick, 1997; Anderson and Piatt, 1999). Commercial whaling in the 1900s significantly reduced the number of humpback whales, both within coastal Kodiak waters and throughout the North Pacific (Rice, 1978). Following the protection of humpback whales in 1965, however, their numbers in the central North Pacific increased, possibly by as much as 10%, between the early 1980s and early 1990s for some North Pacific stocks (Baker and Herman, 1987; Calambokidis et al.[3]). Removal and subsequent recovery of a marine predator of this magnitude may cause large variations in the biomass removal of prey in the ecosystem, as has been hypothesized in other studies (Laws, 1985; Springer et al., 2003). However, no empirical evidence exists to demonstrate such trophic interactions in the Gulf of Alaska. In this article,

[2] NMFS (National Marine Fisheries Service). 2002. Unpubl. data. Website: http://www.st.nmfs.gov/pls/webpls/MF_LPORT_YEARD.RESULTS [Accessed on 31 May 2003.]

[3] Calambokidis, J., G. H. Steiger, J. M. Straley, T. Quinn, L. M. Herman, S. Cerchio, D. R. Salden, M. Yamaguchi, F. Sato, J. R. Urbán, J. Jacobson, O. von Ziegesar, K. C. Balcomb, C. M. Gabriele, M. E. Dalheim, N. Higashi, S. Uchida, J. K. B. Ford, Y. Miyamura, P. Ladron de Guevara, S. A. Mizroch, L. Schlender, and K. Rasmussen. 1997. Abundance and population structure of humpback whales in the North Pacific basin. Cascadia Research Cooperative Final Contract Report 50ABNF500113 to Southwest Fisheries Science Center, La Jolla, CA 92038, 72 p. Website: http://www.cascadiaresearch.org/reports/rep-NPAC.pdf. [Accessed on 19 April 1999.]

we model the historic and current consumption rate by humpback whales within waters of northeastern Kodiak Island in order to assess the impact these whales have as predators on local prey populations.

Materials and methods

Study area

The study area encompassed waters of northeastern Kodiak Island, including Chiniak and Marmot Bays (Fig. 1). The study area was divided into four subareas of approximately equal size in order to equalize sampling effort and maximize coverage of the study area. Subareas were also used to separate sightings of humpback whales for the purpose of weighting diet composition in relation to prey availability. An additional subarea, including the waters near Woody and Long Islands, was not considered a survey subarea but was designated in the poststudy period for calculating diet composition ("nearshore," Fig. 1).

Sightings and abundance of humpback whales

Data on humpback whale sightings were collected during vessel surveys conducted between June and September in 2001 and 2002. Individual whales were identified from photographs of the black and white pigment patterns (and other natural markings) on the ventral surface of their tail flukes (Katona et al., 1979). A humpback whale sighting was defined as a sighting of an individual whale on a single day. Therefore, no whale was counted twice on one day, but may have been counted multiple times during the study period. Humpback whale sightings were summed by month and then by subarea for calculation of whale diet (see "Materials and methods" section: "Composition of simulated diets").

These sightings and fluke photographs were used in an associated study to estimate current humpback whale abundance within the study area (Witteveen, 2003). The estimate determined from this associated study was used in conjunction with historic catch data from the Port Hobron whaling station to estimate historic humpback whale abundance. The whaling grounds of Port Hobron encompassed most of eastern Kodiak waters—an area approximately four times that of the study area. To account for the size difference between whaling grounds and the study area, catch values were divided by four under the assumption of a random harvest throughout the grounds. The prewhaling and current estimates of humpback whale population size in the study area are 343 individuals (95% CI: 331, 376) and 157 individuals (95% CI: 114, 241), respectively (Witteveen, 2003).

Composition of simulated diets

Two diets were simulated: one that reflected the historic diet and the other that reflected the current diet for humpback whales. The diets were simulated because direct observation of humpback whale feeding behavior is rare and, even when observed, cannot produce a precise account of the prey species being eaten.

Diet A simulated historic target species and was based on the stomach contents of 39 humpback whales harvested at the Port Hobron whaling station from southeast Kodiak waters between 30 May and 9 August 1937 as analyzed by Thompson (1940).

Diet B simulated current target species and assumed no prey selectivity. It was based on the assumption that humpback whales will eat prey of a suitable size (<30 cm) in proportion to the relative occurrence of the prey in areas used by humpback whales. Euphausiid proportions in the diet were based on historic stomach contents and assumed to be constant over time (no current euphausiid abundance estimate is available).

Information on seasonal prey availability was collected from mid-water trawl surveys that were conducted within eastern Kodiak waters in July 2001 and from June through September 2002. Multiple passes with a commercial mid-water trawl net with a 22-mm mesh codend liner were made through acoustic scattering layers, ensuring an accurate representation of mid-water fish composition and occurrence. Species composition, species counts, and fish size were determined for each tow and grouped within the study subareas. Only data from tows conducted during the study period in 2001 and 2002 in areas utilized by humpback whales were included in our analysis. Therefore, prey surveys overlapped humpback whale sightings both temporally and spatially. A separate series of acoustic and purse-seine (center panel with a 3.2-mm mesh net) surveys was used to determine prey availability within the nearshore subarea from June through September 2002 (Foy[4]). Prey composition determined by these surveys was assumed to be homogeneous throughout the nearshore habitat within the study area.

To calculate diet B, the occurrence of fish smaller than 30 cm was determined from the mid-water trawl surveys within each subarea and month for both 2001 and 2002. Tow data were first separated by subarea and month. Percent composition of prey species in each tow was calculated by dividing the total number of fish of each species caught by the total number of all fish caught in each tow, excluding species larger than 30 cm (Nemoto, 1959) and species that were not previously documented as prey, such as flatfish and other nonschooling fishes (Nemoto, 1957, 1959; Klumov, 1963; Krieger and Wing, 1984, 1986; Perry et al., 1999).

To calculate diet B for the entire study area, prey proportions were weighted by the number of whales in each subarea. The weighted proportions were then summed across all months and subareas and multiplied by one minus the percentage of assumed euphausiid

[4] Foy, R. 2002. Unpubl. data. Fishery Industrial Technology Center, University of Alaska Fairbanks, Kodiak, AK 99615.

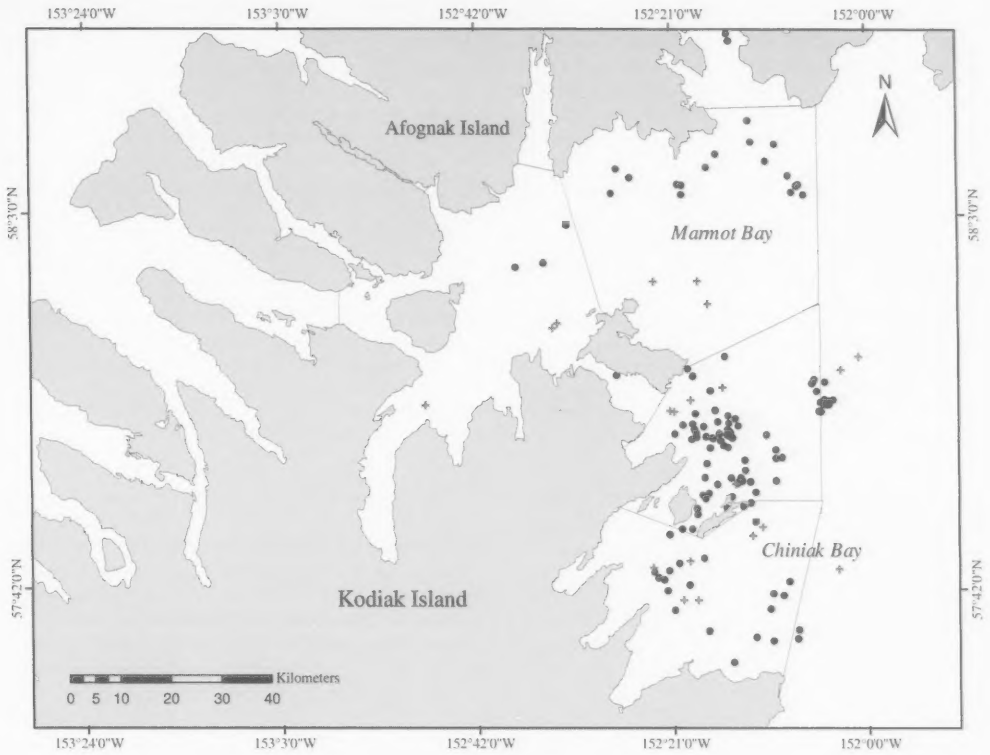

Figure 2

A close-up of the study area showing locations of humpback whale (*Megaptera novaeangliae*) sightings and prey tows (+) for 2001 and 2002. Only mid-water trawl locations are shown.

occurrence within the diet. Thus, diet B simulated a weighted availability of prey species based on temporal and spatial overlap between prey surveys and humpback whale sightings within the study period (Fig. 2).

Consumption rate

A seasonal consumption rate was estimated for both the current humpback whale population and the prewhaling humpback whale population. The prewhaling consumption rate was estimated by using diet A only. Diet B was used to estimate the consumption rate by the current humpback whale population and to project the consumption rate by a humpback whale population at the prewhaling abundance level.

The active metabolic rate (kcal/day) of feeding humpback whales was estimated in this study as $E=192M^{0.75}$, where Kleiber's (1961) model for basal metabolic rate (BMR; $E=70M^{0.75}$) was modified by using average oxygen consumption estimates for feeding baleen whales, where M is average body weight (kg) (Wahrenbrock et al., 1974: Sumich, 1983; Perez and McAlister, 1993).

Daily prey consumption was then estimated as

$$I = \frac{E}{K}\frac{1}{1{,}000},$$

where I = total prey consumption (kg/day);
E = estimated daily energy requirements (kcal/day); and
K = the estimated energy density (kcal/gram wet weight) of presumed prey.

The average body mass for humpback whales (M) was set equal to 30,408 kg (Trites and Pauly, 1998). The total energy density (K) of each diet was calculated by multiplying the average seasonal energy density of each prey species sampled in the study area by the percentage of that species within each diet and summing across all species. Values of K for individual prey species came from proximate compositions that were determined from prey collected during 2002 trawl surveys for all months within the study period (Foy[4]). For each month, energy density was calculated by multiplying percent lipid by 9.4 kcal/g and percent protein by 4.3 kcal/g, which are conversion factors based on heat produced during metabolism of food (Schmidt-Nielson, 1997). Carbohydrates were considered to be bound and not available for nutrition (Gaskin,

1982). The average seasonal energy density of each prey species was calculated by summing all values of energy density and dividing by the number of months in the study period. Previously published proximate composition values for surf smelt (*Hypomesus pretious)* and energy density data for euphausiids (*Thysanoessa* spp.*)* were used (Davis et al., 1997; Payne et al., 1999).

Seasonal prey consumption for the population was estimated by multiplying I by estimates of abundance (N) and the total number of days in the humpback whale feeding season. Consumption estimates were calculated for both the upper and lower 95% confidence limits on the abundance estimates to show a possible range of consumption. The length of the feeding season was presumed to be 152 days (Perez and McAllister, 1993).

Table 1

Number of sightings of humpback whales (*Megaptera novaeangliae*) for 2001 and 2002 by subarea and month in the Kodiak Island study area.

	2001 and 2002				
Area	June	July	August	September	Total
1	10	7	10	3	30
2	29	89	22	3	143
3	20	8	0	12	40
4	0	3	0	7	10
Nearshore	5	14	0	0	19
Total	64	121	32	25	242

Results

Analysis of sightings showed that humpback whales were not uniformly distributed within the study area (Table 1). Occurrence of humpback whales within subareas was variable, indicating within-season shifts of habitat use. Peak humpback whale sightings occurred in subarea 2 in July of both years. No humpback whales were sighted in the nearshore area after the month of July in either year.

Only two prey items were identified in the 27 stomachs that contained appreciable quantities of prey of 39 stomachs analyzed by Thompson (1940). Surf smelt were found in 21 of 27 (78%) stomachs and euphausiids were found in 6 of 27 (22%) stomachs (Table 2). These percentages represent diet A. Energy densities of these two species combined to give a total energy density of 1.31 kcal/gram (Table 3).

The fish species in areas used by humpback whales in 2001 and 2002, as shown by mid-water trawl surveys, were pollock (36.96%), capelin (28.89%), eulachon (7.60%), Pacific sandlance (4.44%), Pacific sandfish (0.08%), and Pacific herring (0.03%) (Table 2). These percentages represent diet B. Calculated energy densities of prey species ranged from a high (eulachon) of 2.52 kcal/gram to a low of 1.12 kcal/gram (juvenile pollock). The total energy density for diet B was 1.19 kcal/gram (Table 3).

Based on energetic content of the above diets, the model indicated that each humpback whale in the study area would consume 338 kg/day on diet A and 370 kg/day on diet B. Using a prewhaling estimate of 343 (95% CI=331–376) animals in the study area, we determined that humpback whales feeding on diet A prior to 1927 would have removed an estimated 1.76×10^7 kg of prey annually (95% CI= 1.70×10^7 to 1.93×10^7), including nearly 3.87×10^6 (3.74×10^6 to 4.24×10^6) kg of euphausiids and approximately 1.37×10^7 (1.32×10^7 to 1.50×10^7) kg of surf smelt (Table 4). If diet B accurately reflects prey selection by the estimated 157 (95% CI=114–241)

Table 2

Composition and relative occurrence of prey species represented in simulated humpback whale (*Megaptera novaeangliae*) diet A (historic) and diet B (current).

Diet	Prey species	Common name	Percent of total diet
A	*Hypomesus pretious*	surf smelt	78.00%
	Thysanoessa spp.	euphausiid spp.	22.00%
		Total	100%
B	*Theragra chalcogramma*	walleye pollock	36.96%
	Mallotus villosus	capelin	28.88%
	Thysanoessa spp.	euphausiid spp.	22.00%
	Thaleichthys pacificus	eulachon	7.60%
	Ammodytes hexapterus	Pacific sandlance	4.44%
	Trichodon trichodon	Pacific sandfish	0.08%
	Clupea harengus pallasi	Pacific herring	0.03%
		Total	100%

Table 3

Monthly and average energy densities (kcal/gram) of prey species represented in simulated humpback whale (*Megaptera novaeangliae*) diets A and B based on lipid and protein composition. Energy densities were used to estimate consumption by humpback whales. Average values in parentheses have been adjusted to reflect standard deviations of lipid and protein composition. N/A = not available.

	Energy densities (kcal/gram)				
Species	June	July	August	September	Average
Capelin	1.1285	1.2632	1.1956	1.4298	1.2542 (1.1665, 1.3755)
Pacific sandlance	1.4179	1.4179	1.4179	1.4179	1.4179 (1.3211, 1.5590)
Pacific sandfish	0.8661	1.2126	1.1165	1.1165	1.0779 (1.0449, 1.1300)
Eulachon	2.1582	2.5218	2.6758	2.7424	2.5245 (2.3761, 2.6860)
Herring	2.0999	2.0999	1.9454	2.1205	2.0664 (1.9432, 2.2942)
Juvenile pollock	1.0144	1.0657	1.1380	1.2461	1.1160 (0.9730, 1.2994)
Euphausiids	N/A	N/A	N/A	N/A	0.7430
Surf smelt	N/A	N/A	N/A	N/A	1.4698

Table 4

Daily and annual (over a 152-day feeding season) consumption of prey from two different diets off northeastern Kodiak Island by humpback whales (*Megaptera novaeangliae*) at two levels of population abundance: the current population of 157 and the historic population of 343 (also presumed to be the carrying capacity to which the current population will recover). Diet A is the simulated diet of the historic population through analysis of stomach contents of 39 whales in 1937; Diet B is the simulated diet of the historic and current population based on currently available prey of suitable size for consumption.

		Annual prey removal (kg)		
Prey species	Daily prey removal (kg)	Mean	Lower limit	Upper limit
Historic population				
Diet A				
Surf smelt	90,301	13,725,715	13,245,515	15,046,264
Euphausiids	25,469	3,871,355	3,735,914	4,243,818
Total	115,770	17,597,070	16,981,429	19,290,083
Diet B				
Euphausiids	27,934	4,246,006	4,097,458	4,654,514
Walleye pollock	46,924	7,132,406	6,882,876	7,818,614
Capelin	36,671	5,573,943	5,378,936	6,110,211
Eulachon	9,652	1,467,057	1,415,731	1,608,202
Pacific sandlance	5,635	856,475	826,511	938,876
Pacific sandfish	98	14,907	14,386	16,342
Pacific herring	33	5,038	4,862	5,523
Total	126,974	19,300,028	18,624,808	21,156,882
Current population				
Diet B				
Euphausiids	12,786	1,943,507	1,411,209	2,983,345
Walleye pollock	21,478	3,264,687	2,370,537	5,011,399
Capelin	16,785	2,551,338	1,852,564	3,916,385
Eulachon	4,418	671,510	487,593	1,030,789
Pacific sandlance	2,579	392,031	284,659	601,780
Pacific sandfish	45	6,824	4,955	10,474
Pacific herring	15	2,306	1,675	3,540
Total	58,119	8,834,124	6,414,587	13,560,661

humpback whales currently feeding in the study area, these whales would be removing nearly 8.83×10^6 (6.41×10^6 to 1.36×10^7) kg annually, including 3.26×10^6 (2.37×10^6 to 5.01×10^6) kg of pollock, nearly 2.55×10^6 (1.85×10^6 to 3.92×10^6) kg of capelin, and 6.71×10^5 (4.88×10^5 to 1.03×10^6) kg of eulachon. If the same diet were consumed by a population of humpback whales allowed to return to prewhaling abundance, the projected population would remove 1.9×10^7 (1.86×10^7 to 2.12×10^7) kg of prey annually, including approximately 7.13×10^6 (6.88×10^6 to 7.82×10^6) kg of pollock, 5.57×10^6 (5.38×10^6 to 6.11×10^6) kg of capelin, and 4.25×10^6 (4.10×10^6 to 4.65×10^6) kg of euphausiids (Table 4).

Discussion

Consumption rate

Estimating the energy requirements of large cetaceans is inherently difficult and values presented in the present study may be subject to substantial uncertainty. Previous studies in which consumption rates for cetaceans were estimated have used a range of values to adjust BMR ($E=70M^{0.75}$) for active metabolism. These values generally range from approximately 1.5 to 3 times BMR (Hinga, 1979; Lockyer, 1981; Sigurjónsson and Víkingsson, 1998). Our value of 192 is 2.7 times larger than 70 and is, therefore, a reasonable estimate because it fits within this range and is based on the observed oxygen consumption rates of baleen whales. However, the consumption estimates are highly sensitive to perturbations of model input; a 5% error in this value would cause deviation of the same percentage (5%) in final consumption values. Further, all values in our consumption model are assumed to be constant when body mass, physiological status, and assimilation efficiency are likely subject to large seasonal fluctuations (Innes et al., 1987; Perez and McAlister, 1993, Kenney et al., 1997; Trites et al., 1997; Sigurjónsson and Víkingsson, 1998). Our model, however, did account for seasonal changes in the energy density of local prey sources; previous models, on the other hand, did not account for these changes (Perez and McAlister, 1993). Further research is necessary to obtain reliable field estimates of metabolic rates if model uncertainty is to be reduced.

The historic prevalence of surf smelt in diet A could imply a dramatic change in surf smelt availability, misidentification, or an overestimation of smelt found in stomachs. Thompson's (1940) analysis resulted from "samples of stomach contents" obtained from catcher vessels; therefore, these samples may have completely missed less prevalent species. Further, stomach samples may have only reflected the most recent meal of the whale and therefore be biased toward a single species. This potential bias, however, could have been minimized by sampling stomachs throughout the season (May 30–August 09) (Thompson, 1940). Diet B was dominated by walleye pollock, a species not present in historic diet A. The increased importance of juvenile pollock in contemporary humpback whale diet B could reflect changes in prey species availability and use, foraging selectivity, or reflect our diet reconstruction method.

Diet B is considered provisional for two reasons. First, it is assumed that humpback whales eat prey species in proportion to their availability within foraging areas. Humpback whales select preferred prey species and consumption, therefore, may be disproportional to availability. That is, they may be selectively foraging from all available prey sources. Previous foraging studies have described humpback whale distribution as being correlated with areas of capelin (Whitehead and Carscadden 1985; Piatt et al. 1989) and sandlance abundance (Payne et al. 1986; Kenney et al. 1996) and this correlation may indicate a possible preference for small forage fish species. Given that in the decades since whaling, the Gulf of Alaska has shifted from a system dominated by forage fish to one dominated by pollock and other groundfish (Merrick 1997; Anderson and Piatt 1999; Benson and Trites 2002), a shift in prevalence from surf smelt in the historic diet to pollock in the current diet is not unexpected. Pollock have been shown to be a dominant prey source of humpback whales harvested in Russia (Klumov, 1963). Additionally, humpback whales in southeastern Alaska have been observed near schools of juvenile pollock and are believed to eat pollock to an unknown, but potentially large, extent in some years (Gabriele[5]).

The second source of uncertainty in diet B stems from the assumption that our mid-water trawl surveys provide unbiased samples of all available prey. Because these surveys were not designed to sample zooplankton, they may have produced a biased estimate of euphausiid availability. This bias may not be significant, however, because the 22% value we used in diet B was based on historic usage and falls within the range of euphausiid consumption (5–30% of the total diet) estimated in other humpback whale studies (Perez and McAlister, 1993; Kenney et al., 1997).

Further, diet B was constructed from the results of mid-water trawl surveys that may underestimate the availability of some forage fishes, particularly Pacific sandlance. Pacific sandlance are often small enough to swim through the meshes in the net or are found in benthic habitats and cannot be captured by mid-water trawl methods. To minimize this potential sampling bias, we supplemented our trawl surveys with purse seine sampling in the nearshore subarea. Despite this effort we may have underestimated the prevalence of Pacific sandlance in the area because it was found to dominate the diets of other coastal piscivores; stomach contents of 34 coho salmon (*Oncorhynchus kisutch*) and Pacific halibut (*Hippoglossus stenolepis*) in 2002 (Witteveen[6]) and regurgitants from blacklegged kittiwakes

[5] Gabriele, C. 2001–2002. Personal commun. Glacier Bay National Park, P.O. Box 140. Gustavus, AK 99826-0140.

[6] Witteveen, B. H. 2002. Unpubl. data. Fishery Industrial Technology Center, University of Alaska Fairbanks, Kodiak, AK 99615.

in 2001 (n=96) and 2002 (n=147) were dominated by Pacific sandlance (Murra et al., 2003).

Ecological effects from humpback whale prey consumption

Although estimates of consumption are highly dependent on estimates of population abundance and metabolic rates, these values indicate that humpback whales were, and still are, significant predators within the Kodiak Island ecosystem.

Historic commercial whaling reduced the population in our study area to an estimated low of 27 animals by 1938 (Witteveen, 2003). The removal of so many large consumers likely had significant impacts on the surrounding ecosystem. As modeled, reducing historic consumption to that of current levels would release nearly 10,000 tons of prey within the study area in a single feeding season. Such a release could have caused a trophic cascade effect.

Cetacean removals in the Southern Ocean have demonstrated how trophic cascades can affect marine ecosystems through removal of large marine predators, including whales (Laws, 1985). It has been hypothesized that a similar reorganization of the marine community may have occurred in the Bering Sea and Gulf of Alaska, although the mechanisms of such a cascade are not well understood (Merrick, 1997; Trites, 1997; Springer et al. 2003). Removal of whales during commercial harvest reduced predation on certain fish, cephalopod, and zooplankton species, which were then available to other consumers. This large number of unconsumed prey, when combined with environmental factors such as the 1977 regime shift, may have contributed to the growth of sympatric marine predator populations from the late 1940s to late 1970s. It is hypothesized that whale stock resurgence, coupled with the 1977 regime shift that favored the proliferation of groundfish species, may have reduced prey availability to other piscivores in the system and may have led to declines seen in harbor seal (*Phoca vitulina)*, Steller sea lion, northern fur seal (*Callorhinus ursinus),* common murre (*Uria aalge*), thick-billed murre (*U. lomvia*), and red-legged kittiwake (*Rissa brevirostris*) populations (Merrick, 1995, 1997; NRC, 1996; Trites, 1997). The Gulf of Alaska and Bering Sea ecosystems may still be affected by changes caused by baleen whale removals and their recovery (NRC, 1996).

Assuming that the Kodiak Island study area was similarly affected by this trophic reorganization, an estimate of the current consumption by humpback whales would help elucidate the role that a humpback whale recovery is playing in ecosystem dynamics. If our diet composition and subsequent consumption estimates are accurate, our results indicate that the diet of humpback whales in Kodiak waters directly overlaps those of sympatric piscivores and the biomass that is removed may be substantial. The top species modeled in the humpback whale diet represent important sources of energy for multiple higher-trophic-level species and are known to be significant dietary species for Steller sea lions (Wynne[7]), harbor seals (Jemison[8]), tufted puffins (*Fratercula cirrhata)* (Piatt et al., 1997), blacklegged kittiwakes (Murra et al., 2003), adult pollock, Pacific halibut, and arrowtooth flounder (Livingston, 1993; Yang, 1995; Merrick, 1997; Best and St. Pierre[9]).

Our model indicates that humpback whales within the study area may currently be consuming a significant amount of fish, including over 3.26×10^6 kg of juvenile pollock and nearly 3.62×10^6 kg of small forage fish, such as capelin, eulachon and Pacific sandlance, during a 152-day feeding season. In comparison, tufted puffins consume less juvenile pollock (6.40×10^4 kg) between mid-July and mid-September, but this amount still accounts for one-tenth of the age-0 pollock stock in the Gulf of Alaska during early July (Hatch and Sanger, 1992). In addition, gadid removal by Steller sea lions in 1998 was estimated to be 1.79×10^8 kg, or 12% of the total gadid biomass that is removed by commercial fisheries for that year (Winship and Trites, 2003). This amount, although nearly 55 times the amount of pollock removal due to consumption by humpback whales, includes all gadid (not only pollock) species removals in all Alaskan waters. More importantly, these fish are likely larger (≥60 cm vs. ≤30 cm) than fish targeted by humpback whales.

Although humpback whales generally feed on smaller age classes than are targeted by commercial fisheries or Steller sea lions (Perez and McAlister[1]; Kenney et al., 1997), consumption of younger age classes may affect future recruitment into the fishery. Barrett et al. (1990) stated that consumption of young cod (*Gadus morhua)* and saithe (*Pollachius virens)* by shags (*Phalacrocorax aristotelis)* and cormorants *(P. carbo)* in the Northeast Atlantic could be a limiting factor in recruitment in years of low stock size, even if consumption of these species was overestimated by an order of magnitude. Thus, it is noteworthy that the removal by humpback whales of an estimated 3.26×10^6 kg of pollock (age 0–2) equals 30% of the 2002 commercial pollock harvest of 1.09×10^7 kg (ages 3 to 8) for the entire Kodiak Island management area and 2.1% of the 2002 spawning biomass of pollock for the entire Gulf of Alaska, which was estimated at 1.58×10^8 kg (NMFS[10]; NPFMC[11,12]).

These comparisons are based on mean estimates of prey removal and do not take into account model uncer-

[7] Wynne, K. M. 2002. Unpubl. data. Fishery Industrial Technology Center, Univ. Alaska Fairbanks, Kodiak, AK 99615.

[8] Jemison, L. A. 2001. Summary of harbor seal diet data collected in Alaska from 1990–1999. *In* Harbor seal investigations in Alaska (R. J. Small, ed.), p. 314–22. Ann. Rep. NOAA Grant NA 87Fx0300. Alaska Departmart of Fish and Game, P.O. Box 240020, Douglas, AK 99824.

[9] Best, E. A., and G. St. Pierre. 1986. Pacific halibut as predator and prey. International Pacific Halibut Commission Technical Report 21, 27 p. Website: http://www.iphc.washington.edu/halcom/pubs/techrep/tech0021.pdf. [Accessed on 31 May 2003.]

[10, 11, 12] *See next page for footnote text.*

tainty. When uncertainty is considered, comparison to even the lower end of estimates of prey removal are still of note. For example, assuming that removal of juvenile pollock is equal to the lower estimate, or 2.37×10^6 kg, the removal of pollock by humpback whales could still equal 21.7% of the 2002 commercial pollock catch and 1.5% of 2002 spawning biomass. Thus, it follows that if true consumption is actually closer to the upper estimates, the impact of prey removal by humpback whales would likely increase.

The humpback whale represents only one of a myriad of marine consumers within the Kodiak Island ecosystem whose ecological role cannot be determined without sophisticated multispecies models and an analysis of ecosystem interactions. This study was designed to provide essential baseline data and a model for estimating prey removal by foraging humpback whales. Our results show that the potential for biomass removal due to consumption by humpback whales is significant and that the foraging strategies of these whales warrant further investigation. Continued research efforts can improve estimates of biomass removal by identifying target prey, determining the degree of prey selectivity, and assessing variable foraging efficiency.

Acknowledgments

The authors are grateful for the insight and guidance provided by Janice M. Straley, Terry J. Quinn II, Brendan P. Kelly, and Chris Gabriele. Field and laboratory assistance was provided by Lisa Baraff and Katie Brenner. Financial support for this project was provided by the Rasmuson Fisheries Research Center and NOAA Grant no. NA16FX1270 to the University of Alaska Gulf Apex Predator-Prey Project. All research was conducted until provisions of NMFS Scientific Research Permit 473-1433.

Literature cited

Anderson, P. J., and J. F. Piatt.
1999. Community reorganization in the Gulf of Alaska following ocean climate regime shift. Mar. Ecol. Prog. Ser. 189:117–123.

[10] NMFS 2002. 2002. Gulf of Alaska groundfish quotas and preliminary catch in round metric tons. NMFS/AKR Fish Management, Juneau, AK 99802.

[11] North Pacific Fisheries Management Council (NPFMC). 2003. Stock assessment and fishery evaluation (SAFE) report for the groundfish resources of the Gulf of Alaska, 846 p. Website: http://www.afsc.noaa.gov/refm/stocks/Historic_Assess.htm [Accessed on 24 February 2004.]

[12] NPFMC. 2002. SAFE report for the groundfish resources of the Gulf of Alaska, Assessment of Walleye Pollock Stock in the Gulf of Alaska, 90 p. Website: http://www.afsc.noaa.gov/refm/stocks/Historic_Assess.htm [Accessed on 24 February 2004.]

Baker, C. S., and L. M. Herman.
1987. Alternative population estimates of humpback whales (*Megaptera novaeangliae)* in Hawaiian waters. Can. J. Zool. 65:2818–2821.

Barrett. R. T., N. Rov, J. Loen, and W.A. Montevecchi.
1990. Diets of shags *Phalacrocorax aristotelis* and cormorants *P. carbo* in Norway and possible implications in gadoid stock recruitment. Mar. Ecol. Prog. Ser. 66:205–218.

Bax, N. J.
1991. A comparison of the fish biomass flow to fish, fisheries, and mammals in six marine ecosystems. ICES Mar. Sci. Symp. 193:217–224.

Benson, A. J., and A. W. Trites.
2002. Ecological effects of regime shifts in the Bering Sea and eastern North Pacific Ocean. Fish Fish. 3:95–113.

Croll, D. A., B. R. Tershy, R. P. Hewitt, D. A. Demer, P. C. Fiedler, S. E. Smith, W. Armstrong, J. M. Popp, T. Keikhefer, V. R. Lopez, J. Urban, and D. Gendron.
1998. An integrated approach to the foraging ecology of marine birds and mammals. Deep-Sea Res. 45: 1353–1371.

Davis, N. D., K. W. Meyers, and Y. Ishida.
1997. Caloric value of high-seas salmon prey organisms and simulated salmon ocean growth and prey consumption. North Pacific Anadromous Fish Commission (NPAFC) 1:146–162.

Estes, J. A.
1994. Top-level carnivores and ecosystem effects: questions and approaches. *In* Linking species and ecosystems (C. G. Jones and J. H. Lawton, eds.) p. 151–158. Chapman Hall, New York, NY.

Gaskin, D. E.
1982. The ecology of whales and dolphins, 459 p. Heinemann, London.

Hairston, N. G., and N. G. Hairston.
1993. Cause-effect relationships in energy flow, trophic structure, and interspecific interactions. Am. Nat. 142:379–411.

Hatch, S. A., and G. A. Sanger.
1992. Puffins as samplers of juvenile pollock and other forage fish in the Gulf of Alaska. Mar. Ecol. Prog. Ser. 80:1–14.

Hinga, K. R.
1979. The food requirements of whales in the Southern Hemisphere. Deep-Sea Res. 26:569–577.

Innes, S., D. M. Lavigne, W. M. Eagle, and K. M. Kovacs.
1987. Feeding rates of seals and whales. J. Anim. Ecol. 56:115–130.

Katona, S., P. Baxter, O. Brazier, S. Kraus, J. Perkins, and H. Whitehead.
1979. Identification of humpback whales by fluke photographs. *In* Vol. 3: behavior of marine animals (H. E. Winn and B. L. Olla, eds.), p. 33–44. Pages Plenum Press, New York, NY.

Kenney, R. D., P. M. Payne, D. W. Heinmann, and H. E. Winn.
1996. Shifts in northeast shelf cetacean distributions relative to trends in the Gulf of Maine/Georges Bank finfish abundance. *In* The northeast shelf ecosystem: assessment, sustainability, and management (K. Sherman, N. A. Jaworski, and T. J. Smayda, eds.). p.169–197. Blackwell Science, Cambridge, MA.

Kenney, R. D., G. P. Scott, T. J. Thompson, and H. E. Winn.
1997. Estimates of prey consumption and trophic impacts

of cetaceans in the USA Northeast continental shelf ecosystem. J. Northwest Atl. Fish. Sci. 22: 55–171.

Kleiber, M.
1961. The fire of life: an introduction to animal energetics, 454 p. John Wiley and Sons, New York, NY.

Klumov, S. K.
1963. Food and helminth fauna of whalebone whales in the main whaling regions of the world ocean. Trudy Instituta Okeanologii 71:94–194.
1966. Plankton and the feeding of the whalebone whales (Mystacoceti). Trans. Inst. Oceanol. 51:142–156.

Krieger, K. J., and B. L. Wing.
1984. Hydroacoustic surveys and identification of humpback whale forage in Glacier Bay, Stephens Passage, and Frederick Sound, Southeastern Alaska, Summer 1983. NOAA Tech. Memo. NMFS F/NWC-66, 60 p. Auke Bay Laboratory National Marine Fisheries Service P.O. Box 210155 Auke Bay, Alaska 99821.
1986. Hydroacoustic monitoring of prey to determine humpback whale movements. NOAA Tech. Memo. NMFS F/NWC-98, 62 p. Auke Bay Laboratory National Marine Fisheries Service P.O. Box 210155 Auke Bay, Alaska 99821.

Laevastu, T., and H. A. Larkins.
1981. Marine fisheries ecosystems, its quantitative evaluation in management, 167 p. Fishing News Books, Farnham, Surrey, UK.

Laws, R. M.
1977. Seals and whales in the Southern Ocean. Phil. Trans. R. Soc. of London Series B Biol. Sci. 279:81–96.
1985. The ecology of the Southern Ocean. Am. Sci. 73:26–40.

Livingston, P. A., A. Ward, G. M. Lang, and M-S. Yang.
1993. Groundfish food habits and predation on commercially important prey species in the eastern Bering Sea from 1987 to 1989. NOAA Tech. Memo. NMFS F/NWC-54, 192 p.

Lockyer, C.
1981. Estimation of the energy costs of growth, maintenance and reproduction in the female minke whale (*Balaenoptera acutorostrata*), from the Southern Hemisphere. Rep. Int. Whal. Comm. 31:337–343.

Markussen, N. H., M. Ryg, and C. Lydersen.
1992. Food consumption of the NE Atlantic minke whale (*Balaenoptera acutorostrata)* population estimated with a simulation model. ICES J. Mar. Sci. 49:317–323.

Merrick, R. L.
1995. The relationship of the foraging ecology of Steller sea lions (*Eumetopias jubatus)* to their population decline in Alaska. Ph.D. diss., 172 p. Univ. Washington, Seattle, WA.
1997. Current and historical roles of apex predators in the Bering Sea ecosystem. J. Northwest Atl. Fish. Sci. 22:343–355.

Mitchell, E.
1973. Draft report on humpback whales taken under special scientific permit by eastern Canadian land stations, 1969-1971. Rep. Int. Whal. Comm. 23:138–154.

Murra, K. A., C. L. Buck, S. D. Kildaw, J. B. Gamble, C. T. Williams.
2003. Forage location, diet, and productivity of black-legged kittiwakes in 2001 and 2002 in Chiniak Bay, Kodiak Alaska (Abstract). *In* Marine science in the Northeast Pacific: science for resource dependent communities joint science symposium (book of abstracts); January 13–17, 2003, Anchorage, Alaska.

NRC (National Research Council).
1996. The Bering Sea ecosystem, 307 p. National Academy Press, Washington D.C.

Nemoto, T.
1957. Foods of baleen whales in the northern Pacific. Sci. Rep. Whales Res. Inst. Tokyo 12:33–89.
1959. Foods of baleen whales with reference to whale movements. Sci. Rep. Whales Res. Inst. Tokyo 14:244–290.
1970. Feeding patterns of baleen whales in the ocean. *In* Marine food chains (J. H. Steele, ed.) p. 241–252. Oliver and Boyd, Edinburgh, Scotland.

Nordøy, E. S., L. P. Falkov, P.-E. Måtensson, and A. S. Blix.
1995. Food requirements of northeast Atlantic minke whales. *In* Whales, seals, fish, and man (A. S. Blix, L. Walløe, and Ø. Ulltang, eds.), p. 307–317. Elsevier Science, Amsterdam, The Netherlands.

Overholtz, W. J., S.A. Murawski and K.L. Foster.
1991. Impacts of predatory fish, marine mammals, and seabirds on pelagic fish ecosystems of the northeastern USA. *In* Multispecies models relevant to management of living resources (N. Daan and M.P. Sissenwine, eds.) p. 198–208. ICES Mar. Sci. Symp. 193. International Council for the Exploration of the Sea (ICES), Copenhagen V, Denmark.

Pascual, M., R. Hilborn, L. Fritz, H. Xi, and J. Moss.
1993. Modeling the trophic relationships between fish and marine mammal populations in Alaskan waters. *In* Is it food? Addressing marine mammal and seabird declines, p. 30–44. Alaska Sea Grant Rep. 93-01. Alaska Sea Grant Program, Univ. Alaska, Fairbanks, AK.

Payne, S. A., B. A. Johnson, and R. S. Otto.
1999. Proximate composition of some northeastern Pacific forage fish species. Fish. Oceanogr. 8:159–177.

Payne, P. M., J. R. Nicolas, L. O'Brien, and K. D. Powers.
1986. The distibution of the humpback whales *Megaptera novaeangliae* on Georges Bank and in the Gulf of Maine in relation to densities of the sand eel *Ammodytes americanus*. Fish. Bull. 84:271–277.

Payne, P. M., D. N. Wiley, S. B. Young, S. Pittman, P. J. Clapham, and J. W. Jossi.
1990. Recent fluctuations in the abundance of baleen whales in the southern Gulf of Maine in relation to changes in selected prey. Fish. Bull. 88:687–696.

Perez, M. A., and W .B. McAlister.
1993. Estimates of food consumption by marine mammals in the eastern Bering Sea. NOAA Tech. Memo. NMFS-AFSC-14, 36 p. National Marine Fisheries Service Alaska Fisheries Science Center 7600 Sand Point Way N.E., Building 4, Seattle, WA 98115.

Perry, S. L., D. P. DeMaster, and G. K. Silber.
1999. The great whales: History and status of six species listed as endangered under the Endangered Species Act of 1973. Mar. Fish. Rev. 61(1):1–74.

Piatt, J. F., D. A. Methven, A. E. Burger, R. L. McLagan, V. Mercer, and E. Creelman.
1989. Baleen whales and their prey in a coastal environment. Can. J. Zool. 67:1523–1530.

Piatt, J. F., D. D. Roby, L. Henkel, and K. Neuman.
1997. Habitat use, diet, and breeding biology of tufted puffins in Prince William Sound, Alaska. Northwest. Nat. 78:102–109.

Rice, D. W.
1978. The humpback whale in the North Pacific: distribution, exploitation and numbers. Appendix 4 *in* Report on a workshop on problems related to humpback whales

(*Megaptera novaeangliae*) in Hawaii (K. S. Norris and R. R. Reeves, eds.), p. 29–44. U.S. Dep. Commer., Nat. Tech. Info. Serv. PB-280 794, Springfield, VA.

Schmidt-Nielson, K.
1997. Animal physiology: adaptation and environment, 5th ed., 607 p. Cambridge Press, Cambridge, UK.

Sigurjónsson, J., and G. A. Víkingsson.
1998. Seasonal abundance of and estimated food consumption by cetaceans in Icelandic and adjacent waters. J. Northwest Atl. Fish. Sci.. 22:271–287

Springer, A. M., J. A. Estes, G. B. van Vilet, T. M. Williams, D. F. Doak, E. M. Danner, K. A. Forney, and B. Pfister.
2003. Sequential megafaunal collapse in the North Pacific Ocean: An ongoing legacy of industrial whaling? Proc. Acad. Nat. Sci. 100:12223–12228.

Sumich, J. L.
1983. Swimming velocities, breathing patterns, and estimated costs of locomotion in migrating gray whales, *Eschrichtius robustus*. Can. J. Zool. 61:647–652.

Thompson, R.J.
1940. Analysis of stomach contents taken during the years 1937 and 1938 from the North Pacific. M.Sc. thesis, 82 p. Univ. Washington, Seattle. WA.

Tomilin, A. G.
1954. Adaptive types in the order Cetacea (the problem of ecological classification of Cetacea). Zool. Zh. 33:677–692.

Trites, A. W.
1997. The role of pinnipeds in the ecosystem. *In* Pinniped populations, eastern north Pacific: status, trends, and issues. A symposium of the 127th annual meeting of the American Fisheries Society (G. Stong, J. Goebel, and S. Webster, eds.), p. 31–38. New England Aquarium, Conservation Department, Boston, MA.

Trites, A. W, and D. Pauly.
1998. Estimating mean body masses of marine mammals from maximum body lengths. Can. J. Zool. 78:886–896.

Trites, A. W., V. Christensen, and D. Pauly.
1997. Competition between fisheries and marine mammals for prey and primary production in the Pacific Ocean. J. Northwest Atl. Fish. Sci. 22:173–187.

van Franeker, J. A.
1992. Top predators as indicators for ecosystem events in the confluence zone and marginal ice zone of the Weddell and Scotia seas, Antarctica, November 1988 to January 1989 (EPOS Leg 2). Polar Biol. 12:93–102.

Wahrenbrock, E. A., G. F. Maruschak, R. Elsner, and D. W. Kenney.
1974. Respiration and metabolism in two baleen whale calves. Mar. Fish. Rev. 36:1–9.

Whitehead, H., and J. E. Carscadden.
1985. Predicting inshore whale abundance—whales and capelin off the Newfoundland coast. Can. J. Fish. Aquat. Sci. 42:976–981.

Winship, A. J., and A. W. Trites.
2003. Prey consumption of Steller sea lions (*Eumetopias jubatus*) off Alaska: how much prey do they require? Fish. Bull. 101:147–163.

Witteveen, B. H.
2003. Abundance and feeding ecology of humpback whales (*Megaptera novaeangliae)* in Kodiak, Alaska. M.Sc. thesis, 109 p. Univ. Alaska Fairbanks. Fairbanks, AK.

Yang, M. S.
1995. Food habits and diet overlap of arrowtooth flounder (*Atheresthes stomias)* and Pacific halibut (*Hippoglossus stenolepis)* in the Gulf of Alaska. *In* Proceedings of the international symposium on North Pacific flatfish, p. 205–223. Alaska Sea Grant Program Report 95-04, Univ. of Alaska, Fairbanks, AK.

Variation in trawl geometry due to unequal warp length

Kenneth L. Weinberg
David A. Somerton
National Marine Fisheries Service
Alaska Fisheries Science Center
7600 Sand Point Way N.E.
Seattle, Washington 98115-0070
E-mail address (for K. L. Weinberg): ken.weinberg@noaa.gov

Abstract—Survey standardization procedures can reduce the variability in trawl catch efficiency thus producing more precise estimates of biomass. One such procedure, towing with equal amounts of trawl warp on both sides of the net, was experimentally investigated for its importance in determining optimal trawl geometry and for evaluating the effectiveness of the recent National Oceanic and Atmospheric Administration (NOAA) national protocol on accurate measurement of trawl warps. This recent standard for measuring warp length requires that the difference between warp lengths can be no more than 4% of the distance between the otter doors measured along the bridles and footrope. Trawl performance data from repetitive towing with warp differentials of 0, 3, 5, 7, 9, 11, and 20 m were analyzed for their effect on three determinants of flatfish catch efficiency: footrope distance off-bottom, bridle length in contact with the bottom, and area swept by the net. Our results indicated that the distortion of the trawl caused by asymmetry in trawl warp length could have a negative influence on flatfish catch efficiency. At a difference of 7 m in warp length, the NOAA 4% threshold value for the 83-112 Eastern survey trawl used in our study, we found no effect on the acoustic-based measures of door spread, wing spread, and headrope height off-bottom. However, the sensitivity of the trawl to 7 m of warp offset could be seen as footrope distances off-bottom increased slightly (particularly in the center region of the net where flatfish escapement is highest), and as the width of the bridle path responsible for flatfish herding, together with the effective net width, was reduced. For this survey trawl, a NOAA threshold value of 4% should be considered a maximum. A more conservative value (less than 4%) would likely reduce potential bias in estimates of relative abundance caused by large differences in warp length approaching 7 m.

Manuscript submitted 20 October 2004 to the Scientific Editor's Office.
Manuscript approved for publication 6 June 2005 by the Scientific Editor.
Fish. Bull. 104:21–34 (2006).

Standardization of trawl survey procedures can reduce the variability in abundance indices between samples, survey vessels, and over time by reducing the variability in trawl catch efficiency. Such standardization was the focus of the recently developed U.S. National Oceanic and Atmospheric Administration (NOAA) protocols for the operation of its groundfish bottom trawl surveys (Stauffer, 2004). The first of these protocols concerns the measurement of towing cables or warps. For vessels towing with two warps, the NOAA protocols specify that the difference in length between port and starboard warps may not exceed 4% of the wire length between otter doors measured along the bridles and footrope. The need for adopting such a critical value was considered essential because of the belief that unequal warp lengths—from inaccurate measurement or subsequent stretching—would lead to distortion of trawl geometry and a change in catch efficiency, particularly for operations that use trawl winches with the brakes set or locked. The adopted value, however, was chosen somewhat arbitrarily because experimental data showing the dependency of trawl geometry or fishing performance on warp symmetry was lacking for any of the bottom trawl surveys subject to the protocols.

In this study, we examine the effect of unequal warp lengths on the geometry of the 83-112 Eastern trawl which is used by the Alaska Fisheries Science Center (AFSC) to conduct the annual eastern Bering Sea shelf survey. Although we monitor a full suite of trawl dimensions, such as door spread, wing spread, and headrope height that are typically measured on trawl surveys, our attention was primarily focused on the distance between the footrope and lower bridles with the sea floor. Prior studies with this trawl have demonstrated that escapement under the footrope (Somerton and Otto, 1999; Munro and Somerton, 2002; Weinberg et al., 2004) and herding by the bridles (Somerton and Munro, 2001) are the most important determinants of catch efficiency for flatfishes and other benthic species. Although we understand that catch efficiency depends on animal behavior as well as trawl geometry, a goal of our study was to assess whether the 4% critical value is appropriate to prevent an appreciable degradation of catch efficiency due to warp asymmetry, the result of unequal trawl warp lengths.

Materials and methods

Experimental design

The experiment was conducted during 14–17 September 2003 along the Alaska Peninsula in Bristol Bay approximately 85 km NE of Amak Island (55°58′N, 162°55′W) on smooth, relatively level bottom at a depth of 82 m. Trawling was performed with the chartered 38-m stern trawler FV *Vesteraalen*. The *Vesteraalen* is powered by a single 1725-hp engine and is equipped with split Rapp Hydema (Rapp Hydema AS, Bodø, Norway) trawl winches carrying 2.5 cm (1″) diameter, compacted, solid-core trawl warp.

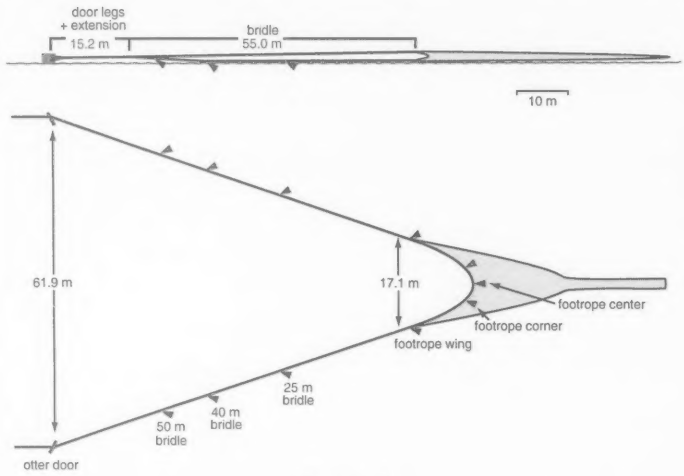

Figure 1

Schematic diagram of the 83-112 Eastern survey trawl and rigging shown from the side (upper panel) and from above (lower panel). The experimentally determined mean door spread and wing spread dimensions shown apply when towing at a depth of 82 m with 274 m of trawl warp on each side. Bottom contact sensor units, shown as oversized triangles along the bridles and footrope, are labeled by position as discussed in the text.

The 83-112 Eastern is a low-rise, 2-seam, flatfish trawl designed for use on smooth, soft bottom. The nylon net is constructed of 10.1-cm stretch mesh in the wing and body, 8.9 cm in the intermediate, and double 8.9-cm mesh lined with a 3.1-cm mesh in the codend. It is towed behind a pair of 1.8×2.7 m steel "V" doors, weighing approximately 816 kg apiece, which are attached to the net by two 3-m-long door legs (consisting of 1.6-cm long-link chain); a 12.2-m-long door leg extension (consisting of 1.9-cm diameter stranded wire); and a pair of 55-m-long, bridles (consisting of 1.6-cm diameter bare stranded wire) on each side of the net (Fig. 1). The 25.5-m-long (83 ft) headrope has 41 evenly spaced, 20.3-cm diameter floats that provide 116.4 kg of total lift. The 34.1-m-long (112 ft), 5.2-cm diameter footrope is constructed of 1.6-cm diameter stranded-wire rope protected by a single wrap of both 1.3-cm diameter polypropylene line and split rubber hose. The footrope is weighted with 51.8 m of chain (0.8-cm proof-coil) attached at every tenth link, forming 168 loops to which the netting is hung. An additional 0.6-m-long, 1.3-cm long-link chain extension connects each lower bridle to the trawl wing tips to help keep the footrope close to the bottom. Because the wire length between otter doors measured along the bridles and footrope is 175.6 m, the critical value for differential warp length for this trawl established by the NOAA 4% rule is 7 m.

Prior to the experiment, the warp length to be used was measured to the nearest 0.1 m with a calibrated, in-line wire counter (Olympic 750-N, Vashon, WA). A zero reference point was painted on each trawl warp, as determined by first setting the wire counter to zero with the trawl door just beneath the water surface and then measuring out 274 m (150 fm), the survey standard warp length for a fishing depth of 82 m. To verify this benchmark measurement, the process was repeated and all replicate measurements were found to be within 0.3 m, which is less than the 1 m specified by the NOAA trawl survey protocols for replicate measurements. Subsequent reference marks, measured by tape, were then placed along each warp at 3, 5, 7, 9, 11, and 20 m from the zero mark.

The experiment consisted of examining the effect of seven differences in warp length, henceforth referred to as "offsets," where one warp was positioned at values of 0, 3, 5, 7, 9, 11, or 20 m longer. An experimental set consisted of all seven offsets, chosen in random order. A treatment consisted of towing the trawl, with the winch brakes locked, at the specified offset for 5 minutes at 3 knots while maintaining a constant vessel heading. Treatments were preceded by a 2-min equalization period at the specified offset. A haul consisted of two treatment sets: one with a port offset and the other with a starboard offset—the order having been chosen randomly for each haul. To minimize the effect of bottom currents on trawl symmetry, hauls were made in pairs along the axis of the dominant current direction, either with or against the current—again, the order having been chosen randomly. This direction was determined by deploying a current meter (Nobska MAVS-3, Woods Hole, MA) 3 m above the bottom for one day

prior to the start of the experiment. Hauls were made with the trawl codend open to eliminate any catch effects on trawl geometry.

Several measures of trawl geometry and performance were taken during each treatment. The distance between the doors (door spread), the wing tips (wing spread), and the center of the headrope to the sea floor were measured acoustically with Scanmar sensors (Scanmar, Asgardstrand, Norway) to 0.1 m at 4-s intervals. Water flow, both perpendicular and tangential to the headrope, was measured to 0.1 knot at 24-s intervals with a Scanmar trawl speed sensor placed at the center of the headrope. Vessel position was measured with satellite navigation at 2-s intervals. Bridle tension was measured in kilograms at 2-s intervals using in-line tension recorders (Billings Ind. TR-999, N. Falmouth, MA) attached behind the door legs. Bottom current velocity in cm/s and direction data were recorded at 10-s intervals.

Footrope off-bottom distance was measured at five positions simultaneously by placing bottom contact sensors (BCS) at the center of the footrope, at the corners located 3 m to either side of the center, and on each wing 1 m behind the wing tip (Fig. 1). These sensors are self-contained units consisting of a tilt meter, which measured angle to the nearest half degree at 0.5 s elapsed time intervals, and a data logger housed in a watertight stainless steel container that fits inside a steel sled (Somerton and Weinberg, 2001). One side of this sled clips into a clamp on the footrope, which allows that end of the sled to pivot freely about the footrope while the other end drags along the bottom (Fig. 2). In this way, changes in the distance of the footrope from the bottom produced changes in the recorded tilt angle. Conversion from tilt angle to distance off-bottom was accomplished by applying a calibration function derived for each BCS unit by fitting a quadratic function to data from an experiment in which angles associated with known distances from a hard surface were measured. The BCS unit extended 44 cm behind the footrope and weighed (BCS, sled, and footrope clamp) 8.9 kg in seawater. The clamp extended beneath the footrope by 2 cm and, depending on the extent of penetration into the sediment, could raise the footrope off the bottom (Fig. 2). Because the degree of penetration is unknown, no adjustments to our calibration functions were made.

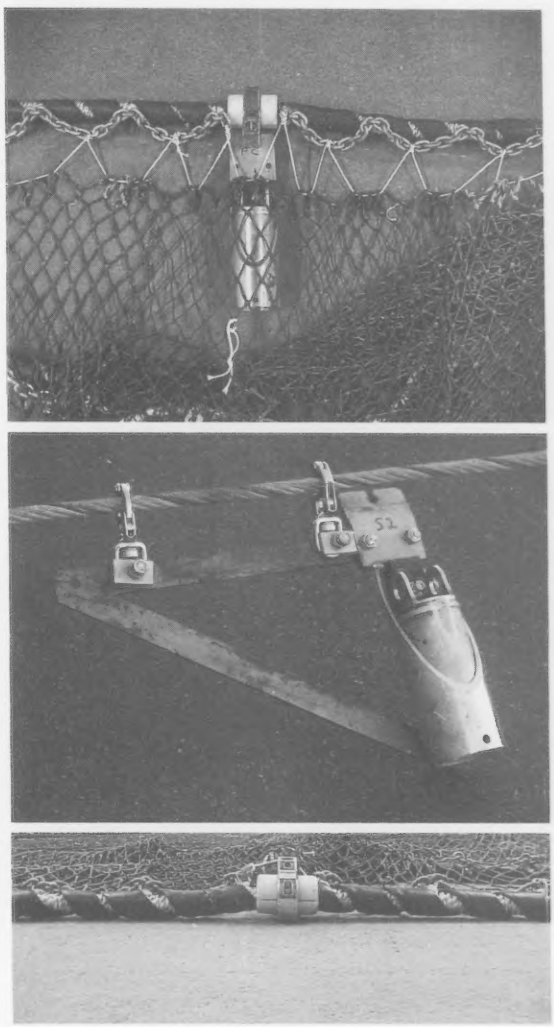

Figure 2

Bottom contact sensors shown mounted to the footrope (upper) and bridle (middle). The footrope shown in the "on-bottom" position without lateral tension and on a hard surface is elevated 2 cm by the footrope clamp (lower).

Bridle off-bottom distance was measured at six positions simultaneously by placing BCS units on the lower bridle at distances of 25, 40, and 50 m forward of the wing tip on both sides of the trawl (Fig. 1). However, the BCS units used on the bridles differed from those used on the footrope. These units were mounted on a triangular frame designed to hold the BCS perpendicular to the bridle (Fig. 2; Somerton, 2003). The triangular frame measured 49 cm in its longest dimension and was held in place by a cable stop that also extended beneath the bridle by about 2 cm. The weight of a bridle BCS unit and frame was 8.7 kg in seawater.

Data analyses

Three tilt angle measurements from each BCS unit were averaged for each 1.5-s interval, converted to distance off-bottom by applying the calibration function determined for that unit, and then the off-bottom distances

were averaged for each experimental treatment on each haul. Mean off-bottom distances for each bridle and footrope position, except the footrope center, were grouped by offset distance (i.e., long side vs. short side of an experimental treatment) where, for example, the distance measurements from the 25-m position on the starboard bridle collected on a starboard treatment (long side) was grouped with the measurements from the 25-m position on the port bridle during a port treatment. Under these groupings, we assumed equality and subsequently refer to the offsets by whether they were on the long or short side (e.g., long 5 m) rather than whether they were on the port or starboard side (e.g., port 5 m).

To allow interpolation between the experimental offsets, cubic spline models (Venables and Ripley, 1994) were fitted to door spread, wing spread, headrope height, and the off-bottom distances for each bridle and footrope position as a function of offset. Bootstrapped empirical 95% confidence intervals (CI; Efron and Tibshirani, 1993) were estimated for all measured categories as described in the following example for off-bottom distance as follows: 1) assuming that mean off-bottom distances within a set were correlated because of local environmental conditions, we chose 1000 bootstrap replicates by sampling entire sets of measurements with replacement; 2) we fitted a cubic spline, weighted by the inverse of the variance, to each bootstrap sample, and then predicted the mean off-bottom distance for each 1 m of offset; and 3) we ranked the predicted values, then chose the 25th highest and lowest values as the CI bounds. Similarly, we estimated the empirical 95% CIs about the mean off-bottom distance at zero offset in the same manner except that only zero offset treatments were considered.

Modeling trawl shape

To help visualize the distortion of the trawl that occurs in response to offset, we created three views of the trawl: 1) the shape of the lower bridle when viewed laterally, 2) the shape of the headrope when viewed from above, and 3) the shape of the footrope when viewed from in front of the trawl. In addition, we calculated the area swept by the bridles (herding area) and the effective net width (i.e., the greatest lateral dimension of the net).

Bridle shape and herding area

The shape of the lower bridle, when viewed laterally (i.e., off-bottom distance as a function of position along the bridles), was approximated by linear interpolation between the mean off-bottom distances measured at the wing, and the 25-, 40-, and 50-m bridle positions. Such shape functions were calculated for both the long side and the short side of the trawl at each offset increment.

The herding area can be considered as a function of the bridle contact length, that is, the length of the bridle that is sufficiently close to the bottom to elicit a herding response (Somerton and Munro, 2001) and the angle-of-attack between the bridle and the direction of travel (α). For flatfish, the vertical distance of the bridle from the sea floor at which a herding response is initiated (reaction height) will vary with species, size, viewing conditions, arousal state, and other variables, but for illustrative purposes, we considered a reaction height of 1 cm where video observations indicated that this value is appropriate for a small flatfish, initially at rest and unaware of the approaching bridle (Somerton, unpubl. data). Thus the value of the bridle contact length was determined as the distance between the wing tip and the point along the bridle at which the interpolated value of off-bottom distance reached the reaction height. The angle-of-attack, α, was not measured during the experiment; however, when the trawl is symmetric, α can be modeled as

$$\alpha = \mathrm{Sin}^{-1}\left(0.5(D-W)/B\right),$$

where D = the distance between doors;
W = the distance between wing tips; and
B = the distance between the wing tip and the door.

It is not clear, however, how α will differ between the long and short side of the trawl when warp offsets occur. For illustrative purposes, we assumed that α is symmetrical and remains constant during all experimental values of warp offset. Thus, for each side of the trawl and for each offset, a value of bridle contact length and α were first calculated as above, then the width of the herding area on each side of the trawl was computed as the bridle contact length times sin (α) and the two areas were summed together.

Headrope shape and effective net width

The curved shape of the headrope when viewed from above can be approximated as a quadratic (parabolic) function when the warps are equal in length and there are no external forces to distort the symmetry of the net (Fridman, 1969). If the shape remains parabolic as the warp offset is increased, then the headrope shape can be uniquely determined with three geometric measurements: 1) the length of the headrope; 2) the distance between wing tips; and 3) the tangent to the headrope at its center. The first quantity was measured at the start of the experiment. The second quantity was measured acoustically on all hauls, and then averaged by treatment. The third quantity was calculated as the quotient of the tangential water velocity (U) divided by the perpendicular velocity (V) measured by the headrope speed sensor (i.e., U/V). With these quantities, the headrope shape was determined as described in Appendix A.

Although the shape of the headrope determined by this method is assumed to be parabolic, the headrope becomes increasingly asymmetric about the direction of travel as the degree of warp offset increases because the wing tip on the short side of the net precedes that on the long side. When this distortion occurs, the mea-

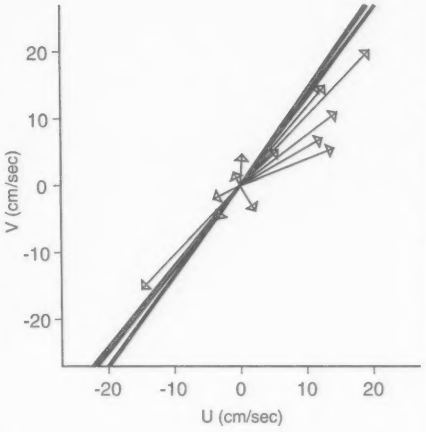

Figure 3

Current velocity vectors during each of the 13 experimental tows are shown with arrows. Vessel direction during these tows is shown with the dark lines. The axes, labeled U and V, indicate the latitudinal and meriodonial components of the velocity vectors in cm/s.

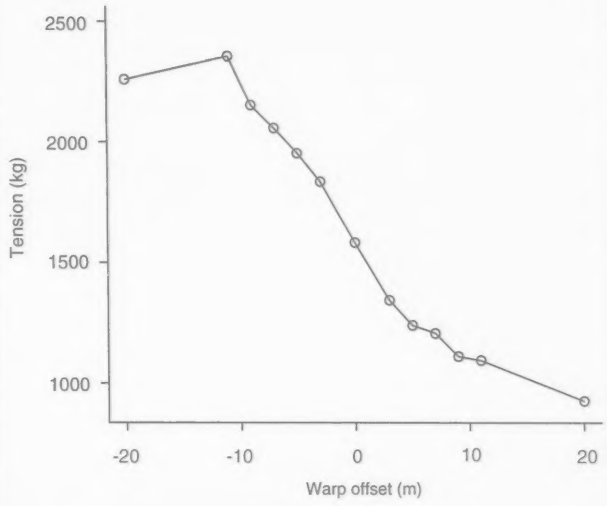

Figure 4

Mean tension (in kilograms) measured on both port and starboard door legs is shown plotted as a function of warp offset in meters. Note that on the side with the shorter warp (negative offset), tension is higher than when the warps are equal and that on the side with the longer warp, the tension is lower.

sured distance between wing tips becomes increasingly greater than the effective net width (i.e., the distance from wing tip to wing tip projected on a plane perpendicular to the direction of travel). The method used to estimate effective net width was based on headrope geometry and is described in Appendix A.

Footrope shape viewed from the net mouth

Because of footrope geometry, the importance of footrope bottom contact to overall net efficiency varies along the length of the footrope. This feature is true not only because escapement probability likely changes with the angle of the footrope in relation to the direction of travel but also because the proportion of the net width spanned by a unit length of footrope varies. To help visualize the latter effect better, we projected the off-bottom distances from their positions along the footrope onto a plane that was perpendicular to the direction of travel and spanned by the effective net width, using the footrope shape model determined for each offset increment described in Appendix A.

Results

Twelve successful tows consisting of 24 sets of treatments were completed during the experiment. Bottom current velocities ranged from about 5 cm/s to about 30 cm/s and current direction was approximately parallel to the trawl towing direction (Fig. 3); consequently the mean current velocity perpendicular to the towing direction was quite small (1.8 cm/s).

Bridle tension and geometry

For the single haul in which both tension meters worked successfully, the bridle tension, combined over both sides, did not change significantly when regressed on the warp offset (df=11, P=0.69). This result indicates that any distortion of the trawl due to the offset treatments was not sufficient to appreciably affect the combined tension and, therefore, the hydrodynamic and frictional drag of the net and the bridles. However, changing the relative length of the warps resulted in a progressive transfer of the tension to the shorter warp (Fig. 4). For example, based on the average combined bridle tension (3248 kg), when the difference in warp lengths was 11 m, the shorter warp carried 72% of the total net and bridle drag.

Headrope speed through the water

The velocity component perpendicular to the headrope (U) decreased with increasing warp offset, whereas the absolute value of the velocity tangential (velocities from the port side of the sensor are opposite in sign to velocities from the starboard side) to the headrope (V) at its

center increased (Fig. 5). We interpret this as indication that the speed sensor at the headrope was rotated in relation to the direction of travel as the warp offset was increased. Calculating the angle between the perpendicular at the center of the headrope and the direction of travel as $\tan^{-1}(U/V)$, the angle increased from 11° at 3 m offset to 61° at 20 m offset. Although the absolute value of the tangential velocity was measured at values >0 at zero offset, the tangential velocity was not significantly different than zero (t-test, P=0.71). This result indicates that the alignment of the experimental tows in relation to the prevailing current was sufficient to reduce the cross current to negligible levels.

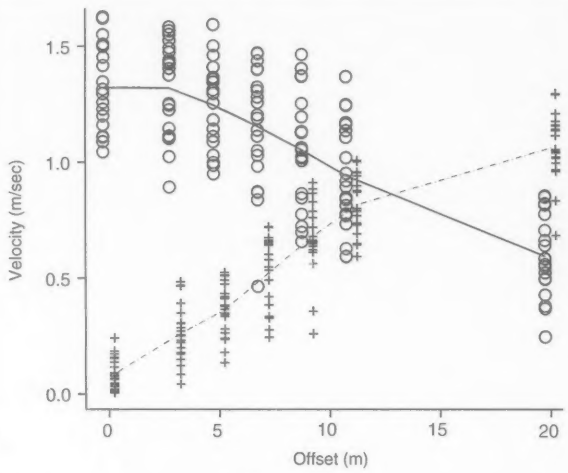

Figure 5

Current velocity (in m/sec) measured at the center of the headrope for each tow is shown separated into the component perpendicular to the headrope (O) and the component tangential to the headrope (+). The solid and dashed lines connect the means at each offset increment. Note, for clarity, that the offsets are incremented by plus or minus 0.1 m for the tangential and perpendicular components.

Net and door measurements

At zero offset, the mean door spread obtained was 61.9 m. The mean wing spread was 17.1 m, and the mean headrope height was 2.0 m. Differences in the means of all three quantities were not apparent at lower offsets, however headrope height and wing spread were more sensitive to changes in large offsets because both were significantly (P<0.05) greater than the zero offset means when offset was increased to 11 m, whereas door spread did not differ significantly until the offset was approximately 14 m (Fig. 6).

Bridle and footrope distance off-bottom by position

Bridle and footrope off-bottom distance varied considerably with position, not only with respect to the mean value but also with respect to the sensitivity of the mean to changes in offset. At zero offset, the mean off-bottom distance of the bridle declined from 12.3 cm at 50 m from the wing tips, to 3.2 cm at 40 m and 2.0 cm at 25 m (Fig. 7). Mean off-bottom distance remained small along the footrope, varying from 1.7 cm at 1 m behind the wing tip to 2.5 cm at the corner and 1.9 cm at the center.

The mean response to changes in offset varied greatly by position. Along the bridles, the most sensitive location was at 50 m, where off-bottom distance increased on the short side and decreased on the long side with increasing offset (Fig. 7). At 40 m, a similar pattern was repeated, but for most offsets on the long side, the off-bottom distance was near the minimum recorded, indicating that the bridle was resting on the bottom. At 25 m, the bridle was nearly always in contact with the bottom and off-bottom distance was insensitive to variations in warp offset. Along the footrope, the most sensitive position was the corner where off-bottom distance increased greatly with offset, particularly with positive offsets due to the relaxation in warp tension. At the center of the footrope, off-bottom distance was also sensitive to warp offset, responding almost identically on the long and short sides. At 1 m behind the wing tip, sensitivity to warp offset was quite low and the off-bottom distance indicated that the footrope was in contact with the bottom except for large offsets on the long side.

An alternate method of assessing the sensitivity of geometry of the 83-112 Eastern trawl to changes in offset is to determine if the mean off-bottom distance at 7 m, the maximum offset allowed under the NOAA protocols for the 83-112 Eastern trawl, differs statistically from the mean off-bottom distance at zero offset. Based on the bootstrapped confidence intervals (Fig. 7), off-bottom distance is significantly different from what it is at zero offset at the 50-m and 40-m bridle positions and at the center and corner footrope positions but is not significantly different at the wing and the 25-m bridle position.

Bridle shape and herding area

To understand better how the change in tension that accompanies offsets in warp leads to changes in bridle shape, we show the mean off-bottom distances plotted against the BCS positions on the wing and bridles for both the short side and long side of the trawl. From this perspective it is clear that as the tension is increased, off-bottom distance increases on the forward part of the bridle. Likewise, as the tension is reduced, the off-bottom distance decreases (Fig. 8). For flatfish, the effect of these changes in off-bottom distance is a change in the area subjected to herding stimuli. For the case where the reaction height is 1 cm, the bridle contact length is determined by the intersection of the line depicting

the reaction height with the lines depicting the bridle shape at each offset (Fig. 8). The change in these lengths on the short and long sides of the trawl is asymmetric with changes in warp offset (Fig 9). For the long side, bridle contact length increases linearly with positive offset. However, for the short side, bridle contact length decreases nonlinearly with warp offset—the greatest changes occurring with small offsets. This difference likely leads to a change in the total width of the herding area with changes in warp offset. If, for example, it is assumed that the angle-of-attack (α) is the same for the long and short sides of the trawl, then the width of the herded area declines to a minimum at about 8 m offset, at which the herded area is reduced by 10.3% compared to that at zero offset.

Headrope shape and effective net width

With increasing difference in warp length, the model we used to describe headrope shape predicts three distinct changes in shape. First, the headrope is distorted so that the wing tip on the short side of the trawl precedes that on the long side in the direction of travel (Fig. 10). The difference in the forward position of the wing tips, however, is much less than the warp offset. For example, an 11-m difference in warp length resulted in an offset in the position of the wing tips of only 2–3 m. This difference occurs because the increased tension on the short warp changes the catenary in both the bridles and the warps (i.e., both become effectively longer as the sag is reduced). Second, the headrope is distorted so that its center is increasingly displaced away from the midpoint between wings and toward the short side of the trawl. When this displacement occurs, the perpendicular at the center of the headrope is no longer aligned with the direction of travel. Third, the headrope is distorted so that the effective width of the net (i.e., the wing spread projected to the line perpendicular to the towing direction) becomes increasingly shorter than the distance measured by the acoustic net sensors. The difference between the effective and the measured net width is negligible for offsets up to 7 m but rapidly increases at greater offsets (Fig. 11).

Footrope shape viewed from in front of the net

The distance of the footrope off-bottom, when viewed from a position in front of the net, increases with increasing offset; however, the location of the maximum off-bottom distance in relation to the midpoint between wings, shifts slightly with increasing offset (Fig. 12). With offsets of 9 m or less, the position of maximum off-bottom distance is at the corner of the footrope on the long side of the trawl. However, with increasing offset, the shift in the position of the footrope corner changes because of the rotation of the trawl in relation to the direction of travel; and at a 20-m offset the footrope corner on the long side of the trawl is positioned, when viewed on a plane perpendicular to the direction of travel, almost exactly midway between the wing tips.

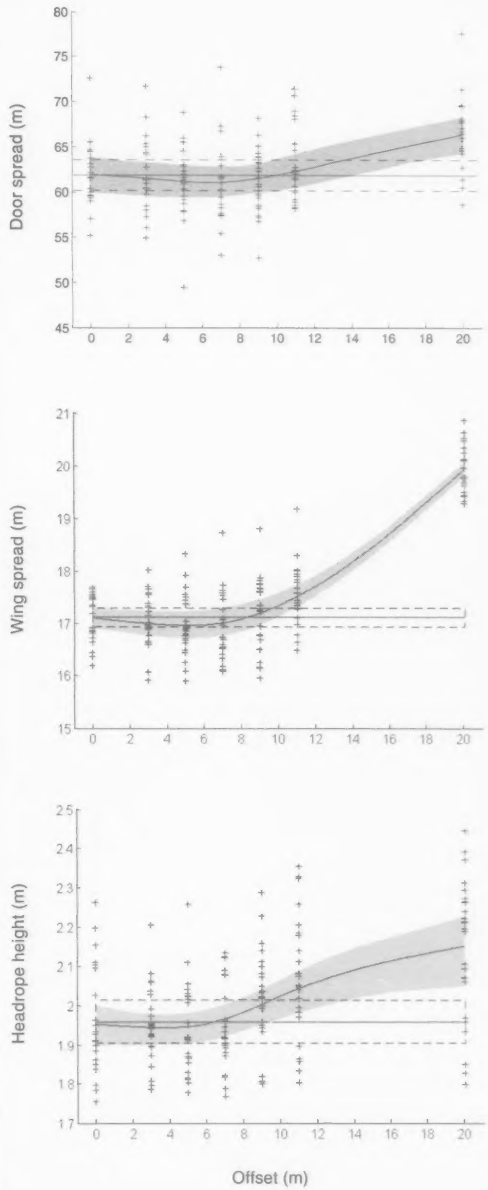

Figure 6

Mean door spread, wing spread, and headrope height are shown (+) plotted against offset increment. The means for all values of offset increment were fitted with a cubic spline function (solid curve). Bootstrapped 95% confidence bounds are shown with shading. Also shown are the mean door spread, wing spread, and headrope height for treatments with zero offset (solid horizontal line) and the corresponding bootstrapped 95% confidence bounds (dashed horizontal lines).

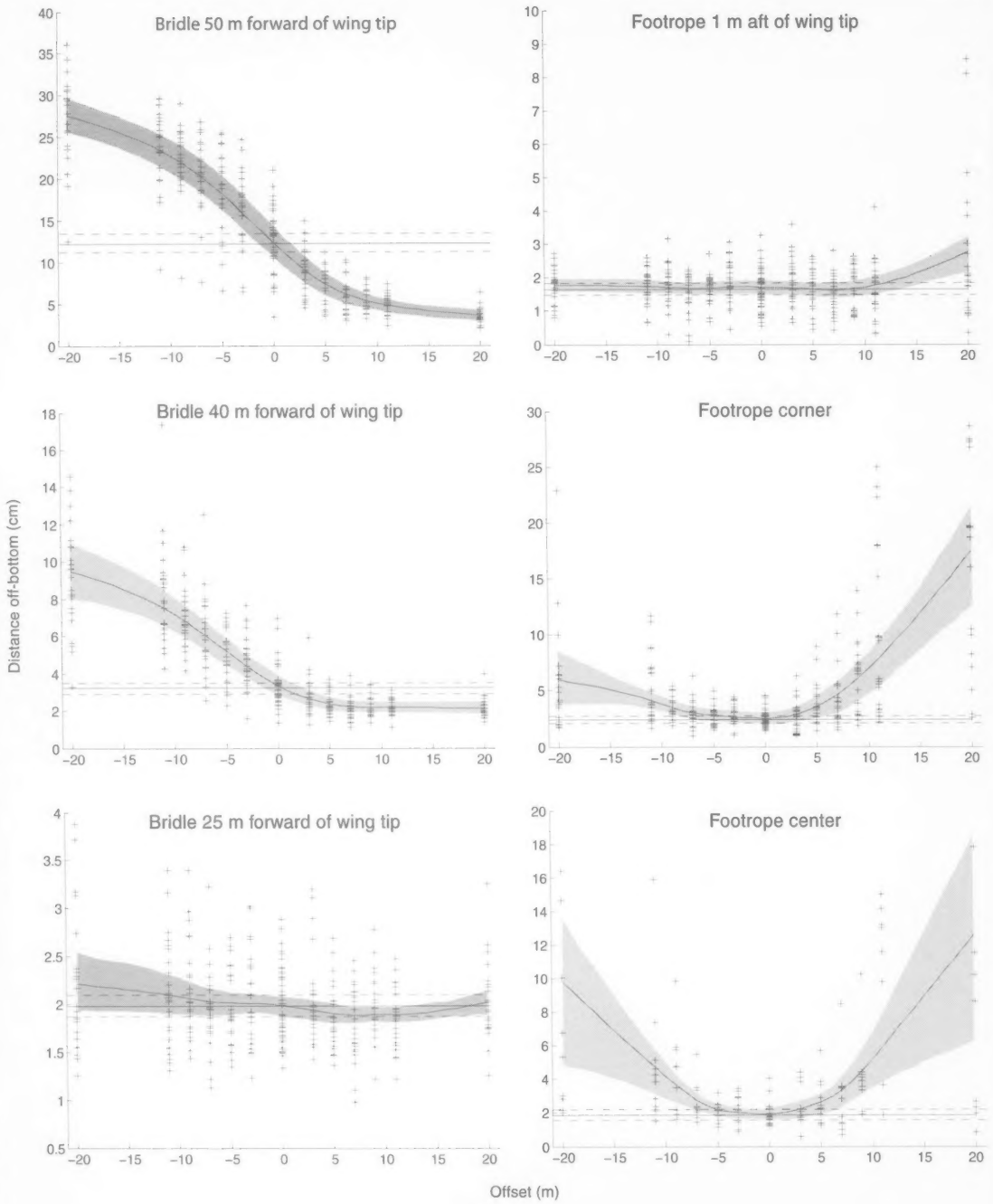
Bridle 50 m forward of wing tip
Footrope 1 m aft of wing tip
Bridle 40 m forward of wing tip
Footrope corner
Bridle 25 m forward of wing tip
Footrope center
Distance off-bottom (cm)
Offset (m)

Figure 7

Mean bridle and footrope distance at each bottom contact sensor position is shown (+) plotted against offset increment. The means for all values of offset increment were fitted with a cubic spline function (solid curve). Bootstrapped 95% confidence bounds are shown with shading. Also shown is the mean distance off-bottom for only treatments with zero offset (solid horizontal line) and the bootstrapped 95% confidence bounds (dashed horizontal lines).

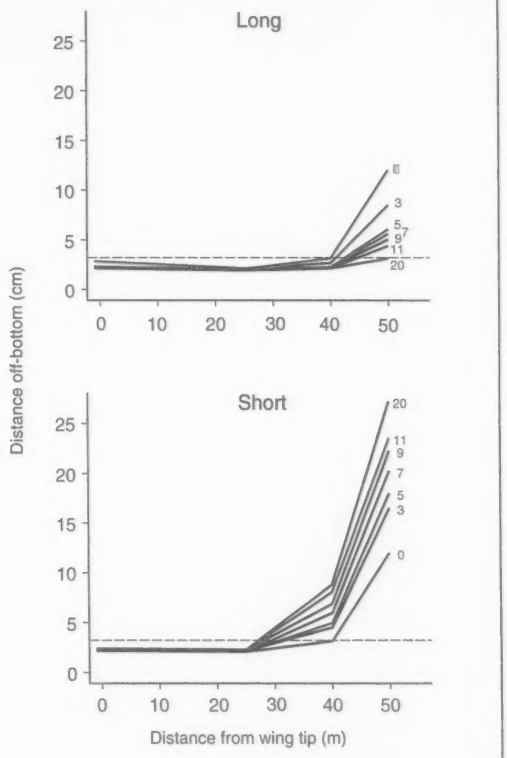

Figure 8

Mean off-bottom distance is shown plotted against the distance measured from the wing tip to the positions of the wing and the three bridle bottom contact sensors. This approximation to the shape of the bridle when viewed laterally is shown for each of the offset increments for both the side with the longer warp and the side with the shorter warp. The dashed line represents the hypothetical reaction height of a fish. The intersection of the dashed line with the solid line for each configuration defines the bridle length that is sufficiently close to the bottom to elicit a herding response.

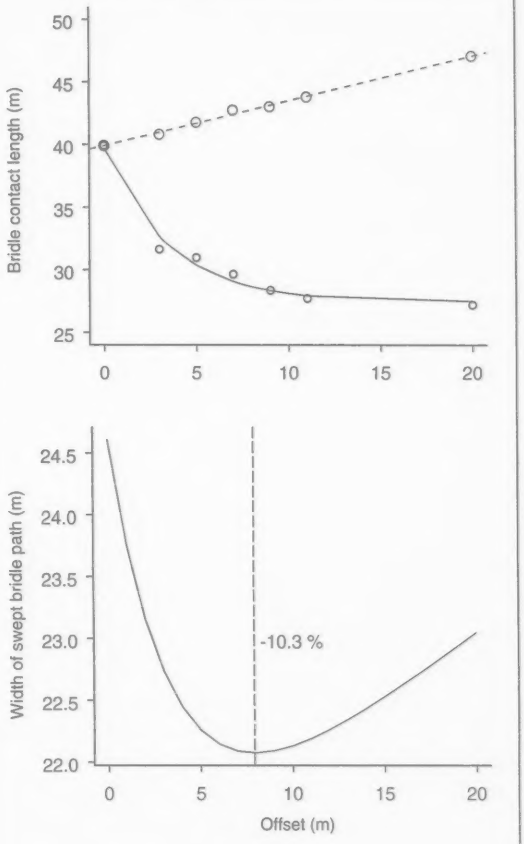

Figure 9

The length of the bridle with the off-bottom distance <1 cm is shown plotted against the offset increment in meters for both the short warp (solid line) and long warp (dashed line) sides of the trawl (upper panel). In both cases the lines are represented using cubic spline smoothing functions. The width of the swept bridle path as a function of warp offset is represented in the lower panel.

Discussion

There are two distinct approaches for judging whether a difference in warp length between the sides of a survey trawl will lead to a significant bias in estimates of relative abundance. In both approaches we focused on the adequacy of the maximum 7-m offset allowed for the 83-112 Eastern trawl under NOAA trawl survey protocols. In the first approach, we simply asked whether, given the sampling effort used in the experiment, any of the measured dimensions at 7-m offset were statistically different from zero offset. In our experiment, none of the three standard measures of trawl geometry (i.e., door spread, wing spread, and headrope height) differed from mean values at zero offset. This finding indicates that either these dimensions are fairly robust to changes in warp offset or that the acoustic measurement of these dimensions was insufficiently precise to detect a difference. Off-bottom distance, however, was significantly different at the two forward positions on the bridles and along the footrope at the center and corner positions.

From the perspective of trawl survey standardization, however, the detectability of changes in geometry is not of primary importance; these changes, however, may produce a significant effect on estimates of relative abundance. Bias in these estimates could result either because the change in trawl geometry leads to an inac-

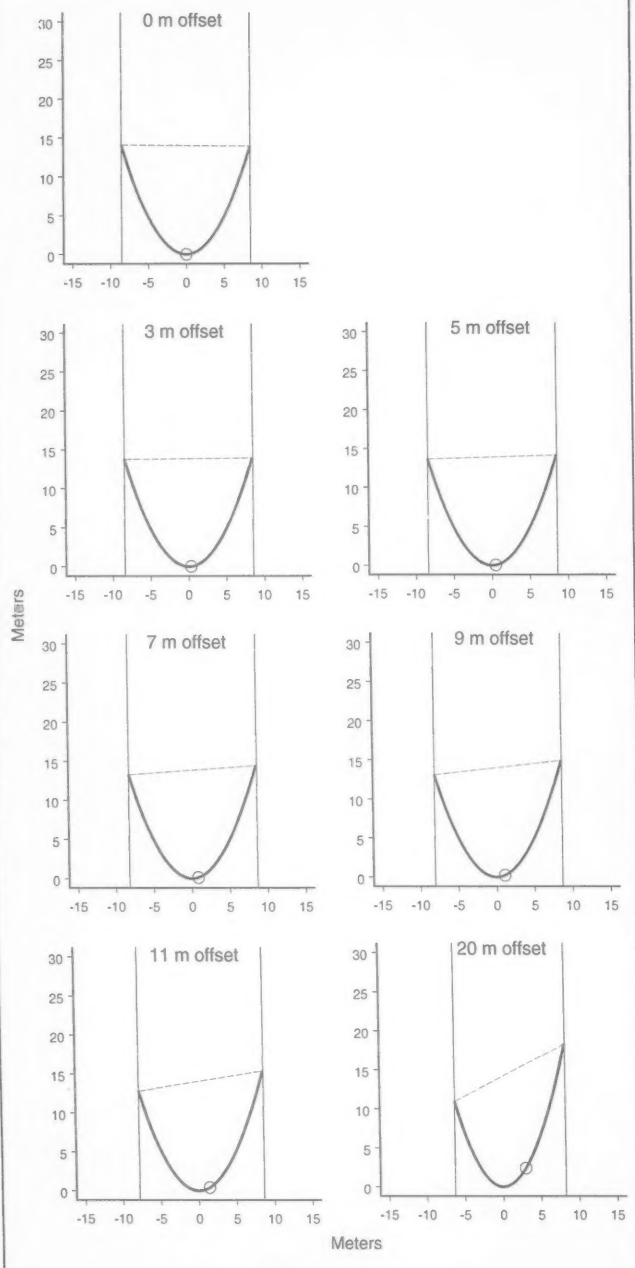

Figure 10

Estimated net shape (curve) and position of headrope center (O) at varying levels of warp offset. The mean distance between wing tips that was acoustically measured during the experimental tows is indicated with a dashed line. The maximum lateral dimensions of the net are indicated with solid vertical lines. The distance between these lines is the effective net width needed for estimating the area swept by the net.

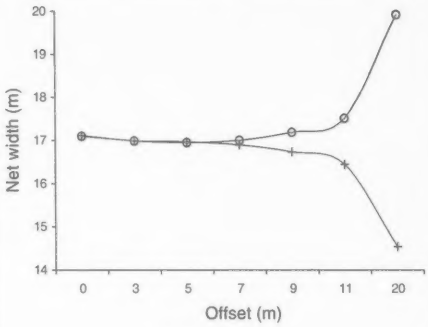

Figure 11

The mean distance between wing tips measured acoustically (O) during the experimental tows (net width) and the calculated effective net width (+) are shown plotted against the offset increment in meters. Note that there is little difference between the two measures of net width until the offset increment is increased to 9 m.

curate measurement of swept area or because it leads to a change in catch efficiency.

Relative abundance indices produced for the eastern Bering Sea shelf survey are based on catch per area swept between the trawl wings. As the net distorts on account of differential warp length, the effective net width will become increasing less than the width that is acoustically measured during the survey. Thus, net width will become increasingly overestimated and relative abundance of fish species therefore will be underestimated. At 7-m offset, however, the measured net width differed from the effective net width by only 0.5%, and therefore this source of error is unlikely to contribute to bias in the swept area estimates. However, the difference between measured and effective net width increases rapidly at greater offsets and could present a problem if a less restrictive threshold value of offset were used.

Catch efficiency of the 83-112 Eastern trawl depends primarily on 1) herding by the bridles, doors, and the mud clouds they create; 2) the escapement under the footrope; and 3) the escapement through the mesh in the body of the net. The relative importance of these three processes, however, will vary for the major species groups that are targeted in the surveys. Gadoids (primarily walleye pollock [*Theragra chalcogramma*] and Pacific cod [*Gadus macrocephalus*] appear to have little or no herding response to the 83-112 Eastern trawl (Somerton, 2004) and rarely pass under the footrope (Somerton, unpubl. data). However, both Pa-

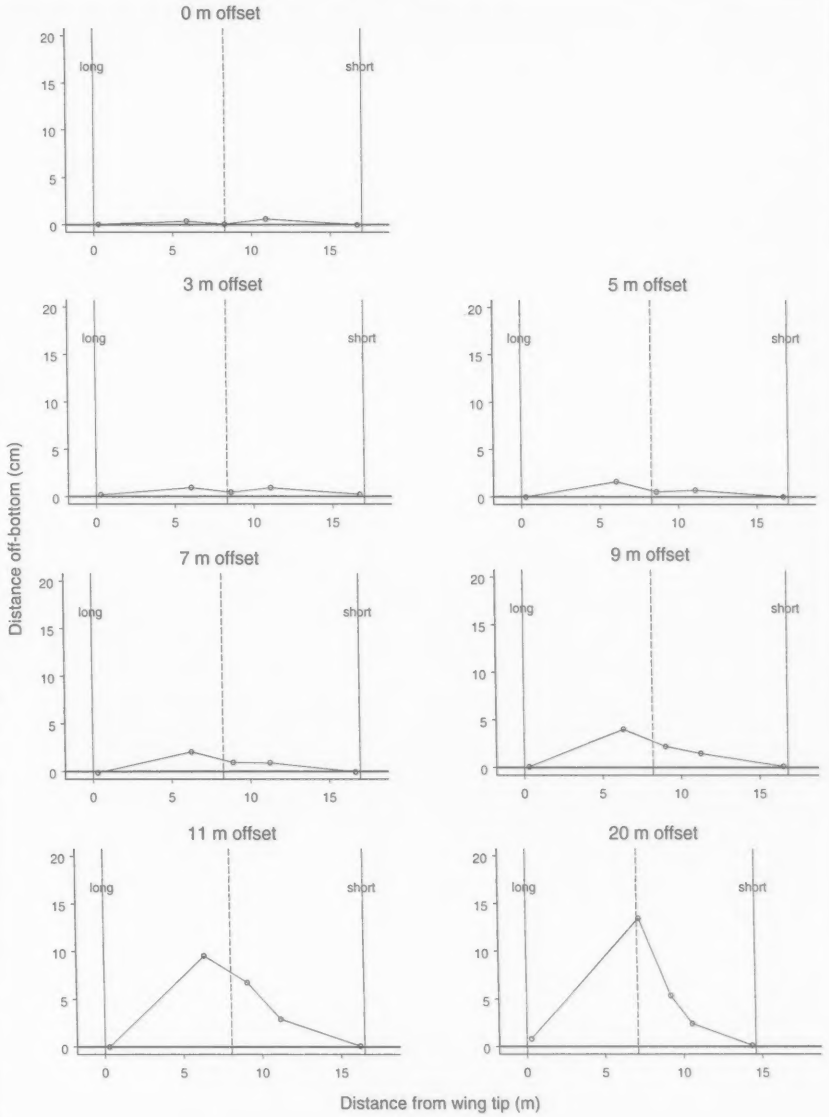

Figure 12

Mean off-bottom distances (in cm) at the five bottom contact sensor positions along the footrope (circles) are shown for each warp offset. The positions are projected onto the wing tip to wing tip plane to depict the footrope as it would appear if one were looking into the net from the direction of travel. The vertical solid lines indicate the positions of the wing tips on the long warp and short warp sides of the trawl. The dashed line indicates the midpoint between wing tips. Note that the projection considers the reduction in effective net width with increasing offset.

cific cod and walleye pollock are found gilled in the body of the net; therefore some mesh escapement may occur, especially if any distortion of the net results in altered water flow through the meshes. Video observations of crabs (snow and Tanner crabs [*Chionoecetes* sp.] and king crabs [*Paralithodes* sp.] show that they also exhibit little or no herding response to the 83-112 Eastern trawl (Weinberg, unpubl. data). However, both

Chionoecetes species (Somerton and Otto, 1999) and red king crab (Weinberg et al., 2004) do escape under the footrope. Flatfishes (including yellowfin sole [*Limanda aspera*], flathead sole [*Hippoglossoides elassodon*], and rock sole [*Lepidopsetta bilineata*] display a strong herding response to the 83-112 Eastern trawl (Somerton and Munro, 2001); as much as 49% of the catch consisted of fish that were herded by the bridles into the net path. Likewise, flatfishes are readily capable of escaping under the footrope and, for species such as yellowfin sole, at least 25% of the largest individuals escape in this manner (Munro and Somerton, 2002). Thus, the capture efficiency of the trawl is species-specific. The change in catch efficiency due to warp offset is likely minimal for species not captured as a function of herding and footrope escapement behaviors; however, because flatfish are susceptible to herding and are adept at footrope escapement, their catch rate could potentially be affected most by warp offsets.

Bridle efficiency (i.e., the fraction of fish in the area between the wing tips and doors that are herded into the path of the net) for flatfish catch is strongly influenced by the size of the herding area or area swept by the bridles because flatfish are stimulated to herd by the close approach or direct contact of the lower bridle. Although we were able to measure the off-bottom distance along the bridle and thereby predict the shape of the bridle, there is still considerable uncertainty as to the exact size of the herding area because the reaction height of a fish will vary with species, size, physiological state, state of arousal to the approaching bridle, viewing conditions for the fish, and, perhaps, other variables. Additionally, there is uncertainty in the estimate of the size of the herding area because it is based on the assumption of symmetry in the bridle angle-of-attack—a symmetry that is increasingly untenable with increasing offset. Despite this uncertainty, it is likely that the loss of herding area on one side of the trawl is not countered by an increase on the other side; thus some overall loss of herding efficiency is to be expected. In the hypothetical case chosen in our study, the reduction in herded area was 10.3%, which when applied to a strong herding flatfish such as rock sole (the herded component of the catch has been estimated to be about 49%, Somerton and Munro, 2001), the expected reduction in catch with an 8-m offset would be roughly 5%.

Flatfish escapement under the footrope will be influenced not only by the increase in off-bottom distance but also by the location along the footrope where the increase occurs. At a 7-m offset, the footrope off-bottom distance is about 2 cm higher in the footrope corner on the long side of the trawl and approximately 1 cm higher at the center and opposing corner than at zero offset (Fig. 12). Footrope off-bottom distances increased appreciably with greater offsets. Weinberg et al. (2002) demonstrated that flatfish escapement can increase with similar increases in footrope off-bottom distance; however their study focused on a different trawl and considered escapement for the entire footrope rather than by position along the footrope. Although we are unaware of any studies that quantify escapement rate by position along the footrope, our video observations indicate that flatfish are less likely to escape under the footrope near the wings than in the center (Somerton, unpubl. data). Because it is the center portion of the footrope where most of the increases in off-bottom distance occur in the 83-112 trawl, flatfish escapement is likely increased and potentially could represent a significant, but presently unquantifiable, loss in catch and a source of bias in estimates of relative abundance.

In conclusion, most aspects of the 83-112 Eastern trawl geometry were significantly degraded by warp offset differences equal to or greater than 7 m compared to zero offset. More importantly, the locations where the detectable differences occurred could affect catch efficiency; therefore a NOAA threshold value of 4% should be considered a maximum value for the 83-112 Eastern trawl and perhaps a more conservative value (less than 4%) would be prudent. However, given today's standardized survey procedures for measuring warp and for real-time monitoring of warp offset, the probability of warp offsets even approaching 7 m is highly unlikely on our surveys when locked-winches are used. Likewise, we argue that any appreciable differences in warp lengths between sides due to stretching are unrealistic because AFSC charter vessels use large diameter, compressed, solid-core wire. In fact, a review of the 413 hauls made during the 2004 EBS survey revealed that only three tows had a recorded maximum 1-m length difference between sides (Weinberg, unpubl. data).

Acknowledgments

We would like to thank Captain Brad Lougheed and the FV *Vesteraalen* crew, Niles Griffen, Waldemar Janezak, Van Ngo, and Todd Becker for their outstanding professionalism, positive attitudes, and constant attention to detail; AFSC scientists Stan Kotwicki and Dennis Benjamin for their assistance at sea; reviewers Guy Fleischer and Henry Milliken for their helpful comments; and the AFSC editorial staff, including Gary Duker, Jim Lee, and Karna McKinney for their help during the in-house review and manuscript preparation process.

Literature cited

Efron, B., and R. Tibshirani.
1993. An introduction to the bootstrap, 436 p. Chapman and Hall, New York, NY.

Fridman, A. L.
1969. Theory and design of commercial fishing gear. (Transl. from Russian by Israel Program Sci. Transl., Jerusalem) 1973, 489 p. [Available as TT 71-50129 from Natl. Tech. Inf. Serv., Springfield, VA.]

Munro, P. T., and D. A. Somerton.
2002. Estimating net efficiency of a survey trawl for flatfishes. Fish. Res. 55:267–279.

Somerton, D. A.
2004. Do Pacific cod (*Gadus macrocephalus*) and wall-

eye pollock (*Theragra chalcogramma*) lack a herding response to the doors, bridles and mudclouds of survey trawls? ICES J. Mar. Sci. 61:1186–1189.

2003. Bridle efficiency of a survey trawl for flatfish: measuring the length of the bridles in contact with the bottom. Fish. Res. 60:273–279.

Somerton, D. A., and P. T. Munro.

2001. Bridle efficiency of a survey trawl for flatfish. Fish. Bull. 99:641–652.

Somerton, D. A., and R. S. Otto.

1999. Net efficiency of a survey trawl for snow crab, *Chionoecetes opilio*, and Tanner crab, *C. bairdi*. Fish. Bull. 97:617–625.

Somerton, D. A., and K. L. Weinberg.

2001. The affect of speed through the water on footrope contact of a survey trawl. Fish. Res. 53:17–24.

Stauffer, G.

2004. NOAA protocols for groundfish bottom trawl surveys of the nation's fishery resources. NOAA. Tech. Memo. NMFS-F/SPO-65, 205 p. Alaska Fisheries Science Center, 7600 Sand Point Way N.E., Seattle, WA, 98115.

Venables, W. N., and B. D. Ripley.

1994. Modern applied statistics with S-plus, 462 p. Springer-Verlag, New York, NY.

Weinberg, K. L., D. A. Somerton, and P. T. Munro.

2002. The effect of trawl speed on the footrope capture efficiency of a survey trawl. Fish. Res. 58:303–313.

Weinberg, K. L., R. S. Otto, and D. A. Somerton.

2004. Capture probability of a survey trawl for red king crab (*Paralithodes camtschaticus*). Fish. Bull. 102:740–749.

Appendix 1: Estimating headrope and footrope shape when the warps differ in length

If a trawl headrope has the same shape as a flexible twine under a uniformly distributed load, then the shape of the headrope can be approximated as a quadratic (parabolic) function (Fridman, 1969; p. 84) as

$$y = cx^2, \tag{1}$$

where c is a constant controlling the shape (Fig. A1). As the headrope is distorted by a differential in warp length, not only does the value of c change, but the headrope is displaced along the path of the parabola, so that its center is no longer aligned with the vertex of the parabola. A unique solution to the shape of the headrope when it is distorted in this manner can be determined from three types of data: the total headrope length (L), the measured distance between the wing tips (W), and the measured slope (tangent) of the parabola at the center of the headrope (tan). The third quantity can be obtained from the V (perpendicular to the footrope) and U (tangential to the footrope) velocities measured by the headrope speed sensor as the quotient U/V. With these quantities, the solution can be obtained as follows.

A small length interval measured along the headrope can be expressed as

$$ds = (dy^2 + dx^2)^{\frac{1}{2}}. \tag{2}$$

Which, after substitution of the derivative of Equation 1, is

$$ds = \left(1 + (2cx)^2\right)^{\frac{1}{2}} dx. \tag{3}$$

The length of any segment of the headrope, measured from the port end (x_{lower}), is then

$$S = \int_{x_{lower}}^{x} \left(1 + (2cx)^2\right)^{\frac{1}{2}} ds. \tag{4}$$

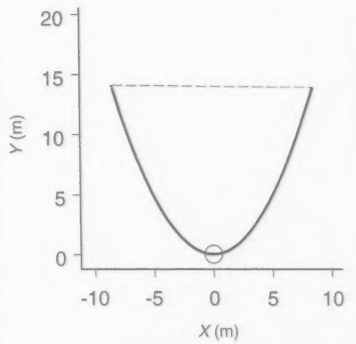

Figure A1

Shape of a trawl headrope as described by a parabola. The total length of the headrope (shown with a solid line) is equal to L. The measured width of the trawl (shown with a dashed line) is equal to W. The circle indicates the center of the headrope where a speed sensor is located. The speed sensor measures water speed both perpendicular and parallel to the headrope.

A segment equal to the total length of the headrope is obtained by integrating up to the starboard end (x_{upper}).

The solution is approximated numerically in two stages. First, for a trial value of c, Equation 4 is integrated from trial values of x_{lower} up to the value of x at which S=L/2 (i.e., x_{middle}). The tangent at this position is then evaluated as $2cx_{middle}$ (based on the derivative of Eq. 1). This process is then repeated iteratively to find the value of x_{lower} for the specified value of c at which the calculated tangent equals the tangent value determined from the headrope speed sensor. The value of x_{upper} is

then determined by integrating Equation 4 from x_{lower} to the value of x at which $S=L$. The wing tip to wing tip distance $D_{wingtip}$ is then calculated as

$$D_{wingtip} = \left((y_{upper} - y_{lower})^2 + (x_{upper} - x_{lower})^2\right)^{\frac{1}{2}}, \quad (5)$$

where y_{upper} and y_{lower} are obtained from Equation 1. In the second stage, c is varied and the above process is repeated iteratively until the value of $D_{wingtip}$ is found that is closest to the measured net spread. At this point the calculated values of $D_{wingtip}$ and the tangent at the headrope center will equal the measured values.

The headrope-shape model for each offset was used to project the off-bottom distances measured at the five positions along the footrope onto a plane orientated perpendicular to the direction of travel to depict the shape of the footrope as it would appear from a position in front of the trawl. To do this, a shape function was developed for the footrope. Assuming that the coordinates of the endpoints of the footrope (x_{lower}, x_{upper}, y_{lower}, y_{upper}) were the same as the headrope, Equation 5 was iteratively integrated with varying values of c until the estimated value of the footrope length (S) equaled the true length (34.1 m):

$$S = \int_{x_{lower}}^{x_{upper}} \left(1+(2cx)^2\right)^{\frac{1}{2}} dx. \quad (6)$$

Once c is determined, Equation 4 is integrated to find the value of x associated with the value of S at each BCS (bottom current sensor) position on the footrope.

The effect of autotrawl systems on the performance of a survey trawl

Stan Kotwicki*
Kenneth L. Weinberg*
David A. Somerton

National Marine Fisheries Service
Alaska Fisheries Science Center,
7600 Sand Point Way N.E.
Seattle, WA 98115

E-mail address (for K. L. Weinberg, contact author): ken.weinberg@noaa.gov

*Equal authorship.

Abstract—Three aspects of a survey bottom trawl performance—1) trawl geometry (i.e., net spread, door spread, and headrope height); 2) footrope distance off-bottom; and 3) bridle distance off-bottom—were compared among hauls by using either of two autotrawl systems (equal tension and net symmetry) and hauls conducted with towing cables of equal length and locked winches. The effects of environmental conditions, vessel heave, crabbing (i.e., the difference between vessel heading and actual vessel course over ground), and bottom current on trawl performance with three trawling modes were investigated. Means and standard deviations of trawl geometry measures were not significantly different between autotrawl and locked-winch systems. Bottom trawls performed better with either autotrawl system as compared to trawling with locked winches by reducing the variance and increasing the symmetry of the footrope contact with the bottom. The equal tension autotrawl system was most effective in counteracting effects of environmental conditions on footrope bottom contact. Footrope bottom contact was most influenced by environmental conditions during tows with locked winches. Both of the autotrawl systems also reduced the variance and increased the symmetry of bridle bottom contact.

Autotrawl systems proved to be effective in decreasing the effects of environmental factors on some aspects of trawl performance and, as a result, have the potential to reduce among-haul variance in catchability of survey trawls. Therefore, by incorporating an autotrawl system into standard survey procedures, precision of survey estimates of relative abundance may be improved.

Manuscript submitted 27 October 2004 to the Scientific Editor's Office.

Manuscript approved for publication 6 June 2005 by the Scientific Editor.

Fish. Bull. 104:35–45 (2006).

Bottom trawl survey operating procedures are standardized in order to reduce the variability of catch per unit of effort (CPUE) estimates. Many of the current standardization procedures address the efficiency of the trawl gear and the maintenance of constant catchability among samples and over time. Despite these efforts, variability in trawl catchability can be exacerbated by uncontrollable environmental conditions. Variables such as surface and bottom currents, sea state, wind direction, varying substrate types and inclinations, and depth of tow may all contribute to differences in gear efficiency by influencing the area swept by the net (Rose and Nunnallee, 1998), the herding efficiency of the bridles (Somerton and Munro, 2001; Somerton, 2003), and escapement beneath the footrope (Weinberg et al., 2002).

Many bottom trawl surveys conducted by the National Marine Fisheries Service, such as the Alaska Fisheries Science Center's (AFSC) eastern Bering Sea (EBS) shelf survey, operate with trawl winch brakes, set or locked, and tows are made with equal amounts of towing cable (warp) on both sides of the vessel. Other than by controlling towing speed and direction, these surveys are unable to compensate for changing environmental conditions. In contrast, autotrawl systems are widely used by the commercial fleet and are purported to improve fishing performance by stabilizing trawl geometry over varying environmental conditions, such as rough weather when vessel heave produces an upward lift on the trawl door resulting in loss of ground shear and wing spread, or over rough bottom when doors and nets have a greater probability of snagging. If autotrawl systems are able to reduce some of the variability in gear efficiency that is due to environmental variability, such as sea state and currents, then including the use of autotrawl systems as a standard survey bottom trawl procedure may improve the precision of survey results.

In simple terms, autotrawls are dynamic systems that operate on the principle of ensuring that the trawl is being towed in a direction perpendicular to the center of the footrope and headrope in order to optimize its performance. We are aware of two styles of autotrawl systems currently marketed. The first is a tension-controlled system that reacts to the difference in warp tension between winches by equalizing hydraulic pressure (equal tension). When the tension on either side exceeds that of the other side (a user-defined threshold) due to factors such as increased drag, currents, sediments, or steep slopes, the system lengthens that warp to equalize the pressure between the two winches. Conversely, when the tension decreases on one warp, the system compensates by shortening that warp to equalize pressure between the two winches. The second autotrawl style is a symmetry-controlled system that actively adjusts warp length in response to cross flow

signals from a sensor mounted on the trawl headrope. This system operates on the principle that net skewing can be caused by a crosscurrent. If the net is pulled square to the direction of flow then, its geometry will be symmetrical and trawl performance will be optimized.

In the late summer of 2003, the AFSC conducted an experiment to examine the effect of these two types of autotrawl systems on the geometry of a survey trawl, comparing them to towing with equal amounts of warp on each side with the winches locked. The study considers three aspects of trawl performance: 1) the factors of trawl geometry influencing the area and volume swept by the trawl (door spread, wing spread, and headrope height); 2) the bottom-tending performance of the footrope; and 3) the bottom-tending performance of the lower bridles.

Materials and methods

Operations and instrumentation

The experiment was conducted during 19–25 September 2003 aboard the chartered 38-m-long commercial stern trawler FV *Vesteraalen* on smooth, relatively level bottom in 115 m of water at a site approximately 70 km north of Unimak Pass in the Bering Sea (55°10′N, 166°15′W). The *Vesteraalen* is powered by a single 1725-hp engine and is equipped with split Rapp Hydema (Rapp Hydema AS, Bodø, Norway) trawl winches carrying 2.5 cm (1″) diameter, compacted, solid-core trawl warp. The winches are controlled by a Scantrol 2000 (Scantrol, Bergen, Norway) winch control system capable of quickly switching to different towing modes as requested by the vessel operator. For this experiment towing was performed with the codend open and with three different winch control modes: locked winches with equal amounts of warp on the port and starboard side (locked); a tension-controlled autotrawl, which maintains equal tension on both warps by adjusting warp length based on the drag forces on each side (tension); and a symmetry-controlled autotrawl, which adjusts warp length according to side current forces in order to "optimize" water flow through the net (symmetry). The symmetry-controlled system requires a real-time speed sensor capable of detecting the direction of water flow across the headrope. We used an acoustically linked Scanmar (Scanmar, Asgardstrand, Norway) trawlspeed sensor that transmits flow data at 24-sec intervals both perpendicular and tangential to the headrope at its center. For this experiment and when in symmetry mode, the Scantrol system adjusted warp length at 30-sec intervals in response to changes in tangential velocity.

The experiment was conducted with the AFSC standardized trawl for the EBS shelf survey, the 83-112 Eastern bottom trawl. The 83-112 Eastern is a low-rise, 2-seam flatfish trawl designed to fish on smooth, soft bottom. The nylon net is constructed of 10.1-cm stretch mesh in the wing and body, 8.9-cm mesh in the intermediate, and double 8.9-cm mesh lined with 3.1-cm mesh in the codend. It is towed behind a pair of 1.8×2.7 m steel "V" doors, weighing approximately 816 kg apiece, which are attached to the net by two 3-m-long, 1.6-cm long-link chain door legs, a 12.2-m-long, 1.9-cm diameter stranded-wire door leg extension, and a pair of 55-m-long, 1.6-cm diameter bare stranded-wire bridles on each side (Fig. 1). The 25.5-m-long (83 feet) headrope has forty-one evenly spaced, 20.3-cm diameter floats providing 116.4 kg of total lift. The 34.1-m-long (112 feet), 5.2-cm diameter footrope is constructed of 1.6-cm diameter stranded-wire rope that is protected with a single wrap of both 1.3-cm diameter polypropylene line and split rubber hose. The footrope is weighted with 51.8 m of chain (0.8-cm proof-coil) attached at every tenth link, forming 168 loops to which the netting is hung. An additional 0.6-m-long, 1.3-cm long-link chain extension connects each lower bridle to the trawl wing tips to help keep the footrope close to the bottom.

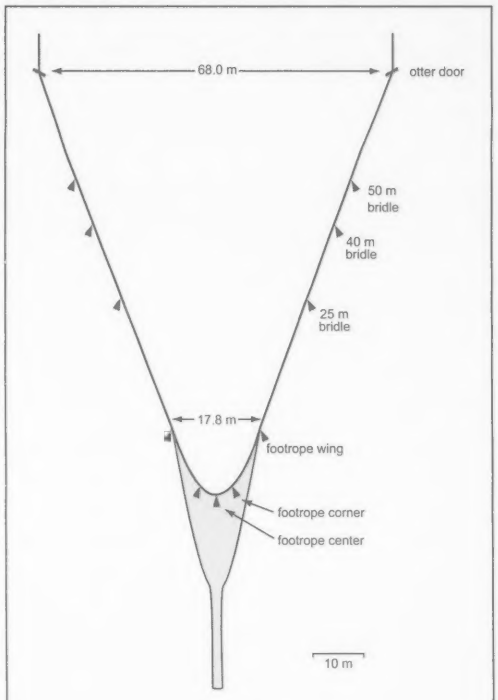

Figure 1

Schematic diagram of the 83-112 Eastern bottom trawl and rigging shown from above. Mean door spread (68.0 m) and mean wing spread (17.8 m) were calculated from experimental tows made at a depth of 115 m with the winches locked and 366 m of trawl warp out on each side. Bottom contact sensor units, shown as oversized triangles along the bridle and footrope, are labeled by position, as discussed in the text.

Prior to experimental towing, trawl warps were measured and marked at 366 m, the amount of warp used on the EBS survey when stations are fished at a depth of 115 m, the depth of our study site. Warps were measured and marked in accordance with AFSC protocol (Stauffer, 2004) by using in-line wire counters (Olympic 750-N, Vashon, WA) while at the same time, calibration of the geometric winch counters associated with the autotrawl system was performed.

A haul consisted of towing at a vessel speed of 3 knots while steering a steady course over ground. Tow direction was selected by attempting to expose the trawl to the maximum amount of side current. Vessel speed and position were measured at 2-sec intervals with satellite navigation. Each haul consisted of two treatment sets in which three 15-min towing treatments (locked winches [locked], tension-controlled autotrawl [tension], symmetry-controlled autotrawl [symmetry]) were conducted, allowing at least two minutes between treatments for the net to equilibrate. Randomizing the order of treatments within each treatment set reduced the influence of treatment order on trawl performance introduced by sea state, wind, and tidal currents. Likewise, towing at the same site for the duration of the experiment eliminated bias that could be attributed to varying substrate.

Wing spread, door spread, and headrope height were measured acoustically with Scanmar sensors at 4-sec intervals to the nearest 0.1 m. Footrope distance from the sea floor (cm) was measured at 0.5-sec intervals and averaged over 1.5-sec periods at five positions along the footrope simultaneously by placing bottom contact sensors (BCS) at the center, at both trawl corners (located 3 m to either side of the center), and on each wing 1 m aft of the wing tips (Fig. 1). These sensors are self-contained units consisting of a tilt meter capable of measuring angle to the nearest 0.5° and a data logger housed in a watertight stainless steel container that fits inside a steel sled (Somerton and Weinberg, 2001). One side of the sled clips into a clamp that pivots freely on the trawl footrope and the other end drags along the bottom (Fig. 2). Changes in the distance of the footrope from the bottom produce changes in the recorded tilt angle. Conversion from tilt angle to distance off-bottom was accomplished with a calibration function determined for each BCS unit by fitting a quadratic function to data derived from a separate calibration experiment in which tilt angles were recorded when the footrope clamp was elevated set distances from a hard surface. The BCS unit extended out from the footrope 44 cm and its combined weight (consisting of BCS, sled, and footrope clamp) was 8.9 kg in seawater. The thickness of the clamp beneath the footrope was 2 cm. Because underwater video equipment was unavailable for this experiment, the extent to which this clamp penetrates into variable substrates was not estimated.

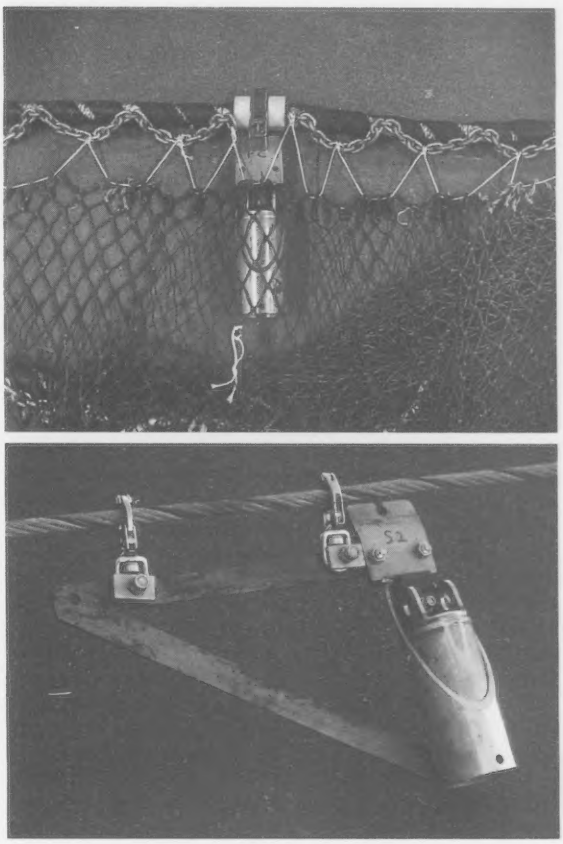

Figure 2

Bottom contact sensors mounted to the footrope (top) and the bridle (bottom).

Bridle distance from the bottom was measured at three positions simultaneously on both port and starboard sides by placing BCS units 25, 40, and 50 m forward of each wing tip. The BCS units and sled were mounted on triangular frames designed to hold them perpendicular to the bridle (Fig. 2, Somerton, 2003). The triangular frame measured 49 cm in its longest dimension. The combined weight of a BCS unit and frame was 8.7 kg in seawater.

In addition to trawl mensuration, data were also collected on certain environmental variables during the different towing modes. Three variables were studied: 1) vessel heave measured at the trawl block; 2) the relative degree of offset of the warps from the heading of the vessel (crabbing); and 3) bottom current velocity both parallel and perpendicular to the direction of the vessel.

The effect of sea state on the vertical displacement and attitude of the vessel is transmitted to the footrope from the trawl blocks through the trawl warps and

likely causes variable bridle and footrope contact with the bottom. Vessel heave at the starboard trawl block was used as a proxy for sea state. Heave, pitch, and roll data were collected at 1-sec intervals with a heave sensor (VT TSS, DMS-25, Watford, UK) mounted in the bridge along the centerline of the vessel. Heave data at the starboard block were then predicted, given the x, y, z coordinates of the block from the heave sensor, as distance (cm) from its equilibrium position. In the analyses, the standard deviation of the heave was used as the index of sea state.

Net crabbing was subjectively assessed on a four-point scale by a single observer, then numerically coded as follows; 1) none—the net trailed straight behind the vessel; 2) slight—the warp could be seen entering the water between the side rail and the aft gantry; 3) moderate—the point of entry of the warp into the water was blocked from view by the aft gantry; and 4) severe—the warp was observed entering the water behind the stern ramp. Conditions usually remained constant and one observation was made per towing-mode treatment. However, in some instances conditions changed rapidly and warranted more than one code. In such cases the average of the observation codes was used in the analyses.

Bottom current direction and velocity (cm/sec) were measured at 10-sec intervals with an oceanographic current meter (Nobska, MAVS-3, Woods Hole, MA) moored in the vicinity of our trawling activity three meters from the bottom. The current data were partitioned into two directional components, one parallel to the course of the vessel and the other perpendicular, and averaged for each sample treatment.

Data analyses

Comparison of the means and standard deviations among treatments Our null hypothesis, that the three treatments had the same effect, was tested with a Kruskal-Wallis one-way ANOVA for all measures of trawl performance. We selected this test because of the skewed nature of the data. To describe the effect of the three treatments on trawl geometry features the mean and standard deviation (SD) were calculated for the wing spread, door spread, and headrope height off-bottom from each treatment in each haul.

To describe the bottom-tending performance of the footrope we calculated the following statistics for each treatment:

1 mean footrope distance off-bottom—the sum of mean distances off-bottom along the footrope, from five footrope BCS units;
2 standard deviation of the footrope distance off-bottom—the sum of standard deviations along the footrope, from five footrope BCS units; and
3 symmetry of the footrope distance off-bottom—the sum of the absolute difference between the means of the two wing positions and the absolute difference between the means of the two corner positions on the footrope.

To describe the bottom-tending performance of the lower bridle, we considered only the BCS unit positioned 40 m from the wing tip. The variability in bottom-tending performance of the bridles 40 m from the wing tip may have the highest impact on the catchability of the trawl because the BCS at the 25 m position was always on the bottom and the BCS at the 50 m position was always off the bottom. Performance of the bridles at the 40 m position was characterized by

1 mean bridle distance off-bottom—the sum of the mean distances off-bottom from the BCS units located 40 m forward of the wing tip on both lower bridles;
2 standard deviation of the bridle distance off-bottom—the sum of the standard deviations from the BCS units located 40 m forward of the wing tip on both lower bridles; and
3 symmetry of the bridle distance off-bottom—the absolute difference between means from the BCS units located 40 m forward of the wing tip on both lower bridles.

Assessment of the effect of environmental factors If differences among towing mode treatments were found by the ANOVA ($P<0.05$), then the effects of heave, crabbing, and bottom current on gear performance within each treatment were explored. Multiple regression analyses were performed for each of the treatment statistics with environmental variables as dependents. At the start of the analyses, the models included all four dependent variables (heave, crabbing, current parallel, and current perpendicular to the tow direction). Variance inflation factors (VIFs) were calculated for all variables to test for multicollinearity (Neter et al., 1996). Dependent variables in all models had VIFs ranging from 1 to 1.4, indicating that no serious multicollinearity existed among dependent variables. Models were simplified (backward deletion) until all P-values of the individual slopes were lower than 0.05. This procedure enabled us to establish which variables had a statistically significant impact on performance of the trawl within each treatment.

Results

A total of 21 successful hauls were performed during the experiment, yielding 42 possible treatment sets for analyses. The number of successful treatment sets included in the analyses varied for each of our performance statistics as a result of either malfunctions or poor survey trawl performance caused by conflicts with abandoned fishing gear.

Comparison of the means and standard deviations among treatments

Trawl geometry A total of 41 treatment sets were used to analyze the six trawl geometry statistics (means and

Table 1

Means of the trawl geometry statistics (m) and *P*-values of the Kruskal-Wallis test for differences between three towing-mode treatments. Locked=locked winches; symmetry=symmetry-controlled autotrawl; and tension=tension-controlled autotrawl.

Statistic		Locked	Symmetry	Tension	*P*-value
Wing	mean	17.76	17.77	17.85	0.6952
	SD	0.69	0.70	0.73	0.9157
Door	mean	68.03	67.67	67.71	0.8380
	SD	1.87	1.73	2.14	0.0977
Height	mean	1.82	1.81	1.81	0.7618
	SD	0.21	0.20	0.20	0.8618

Table 2

Means of the footrope and bridle statistics (cm) and *P*-values of the Kruskal-Wallis test for differences between three towing-mode treatments. Locked=locked winches; symmetry=symmetry-controlled autotrawl; and tension=tension-controlled autotrawl.

Statistic		Locked	Symmetry	Tension	*P*-value
Footrope	mean	13.98	13.09	12.08	0.0441
	SD	6.39	5.67	5.24	0.0391
	symmetry	1.95	1.44	1.45	0.0554
Bridle	mean	7.50	6.69	6.28	0.0286
	SD	4.91	4.03	3.37	0.0046
	symmetry	1.59	0.93	0.88	0.0030

standard deviations of the wing spread, door spread, and net height). No significant differences were detected among the three towing modes (Table 1); consequently, no environmental variables were tested for their influence on trawl geometry.

Footrope distance off-bottom Analyses based on 33 successful treatment sets produced varying results among the three measures describing the bottom tending performance of the footrope. Mean footrope distance off-bottom differed significantly among the three towing modes (Table 2, Fig. 3). Footrope distance was lowest for the tension treatment followed by the symmetry treatment and locked winches. The greatest observed difference occurred between the locked (13.98 cm) and the tension treatment (12.08 cm). Standard deviation in footrope distance off-bottom also differed significantly among treatments. Differences were similar to those observed for the mean, in that the lowest SD was observed for the tension treatment (5.24 cm) and the highest SD was observed for the locked treatment (6.39 cm). Because the variance equals the square of the standard deviation, this seemingly small reduction in standard deviation corresponds to a fairly large reduction in the variance (~30%). Symmetry in the footrope off-bottom distance did not differ significantly (P=0.0554) among the three towing modes.

Bridle distance off-bottom A total of 34 successful treatment sets were used to analyze the bridle distance off-bottom data. Mean bridle distance off-bottom differed significantly among treatments (Table 2, Fig. 4); it was lowest for the tension treatment (6.28 cm) and highest with the winches locked (7.50 cm). Standard deviation of bridle distance off-bottom also differed significantly among the three towing modes. SD values were significantly lower in the autotrawl towing modes, being lowest in the tension treatment (3.37 cm) and highest in the locked treatment (4.91 cm). Bridle distance off-bottom was most symmetrical in the symmetry and tension towing modes. Symmetry and tension means were similar (0.93 cm and 0.88 cm, respectively) and significantly lower than that observed for the locked-winches treatment (1.59 cm).

Assessment of the effect of environmental factors

Footrope distance off-bottom The effect of environmental factors on our three measures describing the bottom tending performance of the footrope produced varying results. Mean distance off-bottom was significantly affected by heave only, during all treatments (Table 3, Fig. 5). The standard deviation of the footrope distance off-bottom was also significantly affected by heave, crabbing, and bottom current parallel to the direction of the

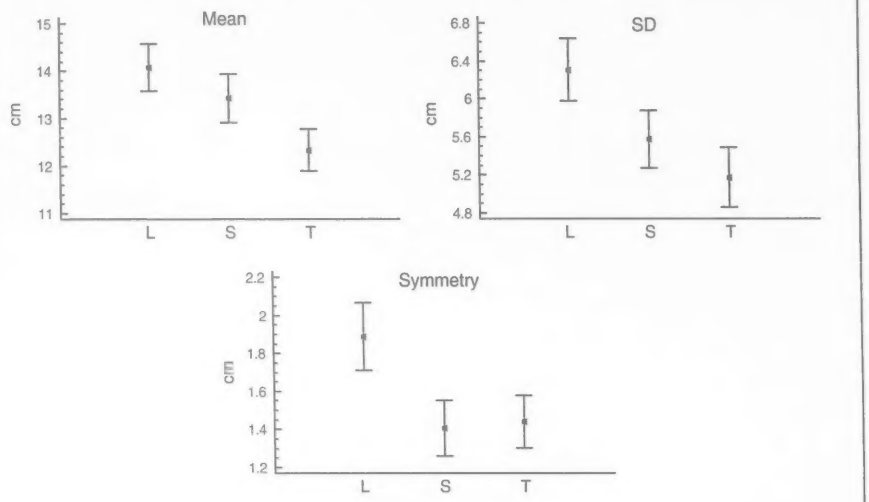

Figure 3

Means and standard errors of the footrope distance off-bottom, standard deviation of the footrope distance off-bottom, and footrope symmetry for the locked winches (L), symmetry (S), and tension (T) treatments.

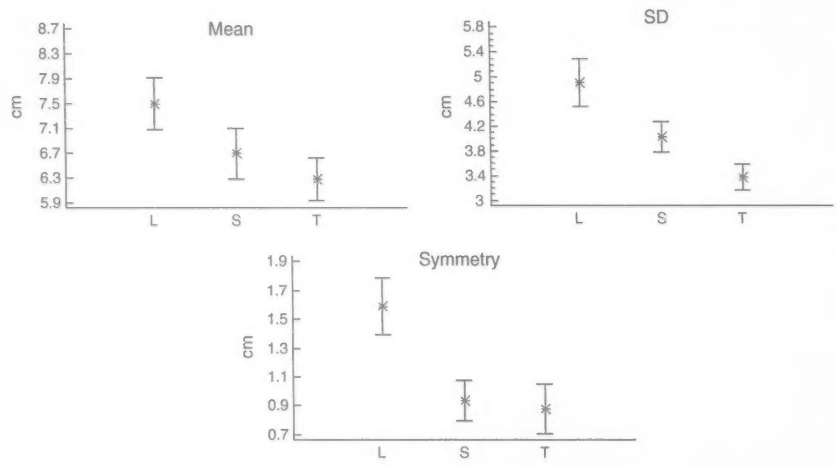

Figure 4

Means and standard errors of the bridle distance off-bottom, standard deviation of the bridle distance off-bottom, and bridle symmetry for the locked winches (L), symmetry (S), and tension (T) treatments.

tow during some treatments (Table 3, Fig. 6). Heave had a greater effect on footrope SD during the locked-winches treatment (slope=0.0610) than during the symmetry treatment (slope=0.0381). Similar effects were also detected for crabbing (slopes=1.2355 and 0.8493, respectively). Current speed in the direction of the tow affected footrope SD only during the symmetry mode. Heave, crabbing, and current velocity had no effect on

Table 3

Multiple regression model slope coefficients with P-value <0.05, for locked winches, symmetry-controlled, and tension-controlled towing modes (Y=bottom current parallel to the direction of the tow, Abs$X$=absolute value of the crosscurrent).

Statistic		Treatment	Heave	Crabbing	Y	Abs$X$	R^2	P-value
Footrope	mean	locked	0.0572	—	—	—	9.04	0.0495
		symmetry	0.0713	—	—	—	15.64	0.0227
		tension	0.0544	—	—	—	16.14	0.0205
	SD	locked	0.0610	1.2355	—	—	58.93	<0.0001
		symmetry	0.0381	0.8493	−0.0446	—	33.96	0.0066
		tension	—	—	—	—	—	>0.05
	symmetry	locked	—	—	0.0255	—	15.42	.0238
		symmetry	—	—	—	—	—	>0.05
		tension	—	—	—	—	—	>0.05
Bridle	mean	locked	0.0680	—	—	—	19.66	0.0086
		symmetry	—	—	—	—	—	>0.05
		tension	0.0491	—	—	—	14.88	0.0242
	SD	locked	0.0796	0.9536	—	—	60.30	<0.0001
		symmetry	—	—	—	—	—	>0.05
		tension	0.0411	0.3023	—	—	33.83	0.0017
	symmetry	locked	—	—	—	0.0556	26.58	0.0018
		symmetry	—	—	—	—	—	>0.05
		tension	—	—	—	0.0361	13.25	0.0343

footrope SD during the tension mode. The symmetry in footrope distance off-bottom was significantly affected by the current parallel to the direction of the tow during the locked-winches treatment only (Table 3, Fig. 7).

Bridle distance off-bottom Mean bridle distance off-bottom was affected by heave only during some of the treatments (Table 3, Fig. 8). Heave had a greater impact on the mean bridle distance off-bottom during the locked-winches treatment (slope=0.0680) than during the tension treatment (slope=0.0491). The standard deviation of the bridle distance off-bottom was affected by heave and crabbing during two of the treatments (Table 3, Fig. 9). Heave had an effect on the SD of the bridle distance off-bottom during both locked (slope=0.0796) and tension (slope=0.0411) treatments. A significant effect due to crabbing was also detected during these same two treatments (slopes 0.9536 and 0.3023, respectively). During the symmetry mode no effect due to any of the environmental conditions was detected, even though SD was almost always higher than that observed in the tension mode, with the exception of extreme heave conditions. Symmetry in the bridle distance off-bottom was affected only by crosscurrent (Table 3, Fig. 10). Crosscurrent had an effect on the symmetry during the locked (slope=0.0556) and tension (slope=0.0361) treatments.

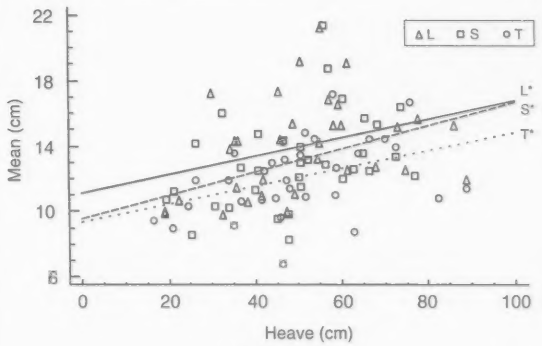

Figure 5

Comparison of regression lines illustrating the relationship between the mean footrope distance off-bottom and heave for locked winches (L), symmetry (S), and tension (T) treatments. Treatments in which heave had a statistically significant effect on the mean are identified with an asterisk (*).

Discussion

The objective of this study was to identify towing modes that could potentially reduce variance in the catchability of the 83-112 Eastern bottom trawl among hauls. Three separate aspects of trawl performance affecting catchability were investigated: trawl geometry, bottom tend-

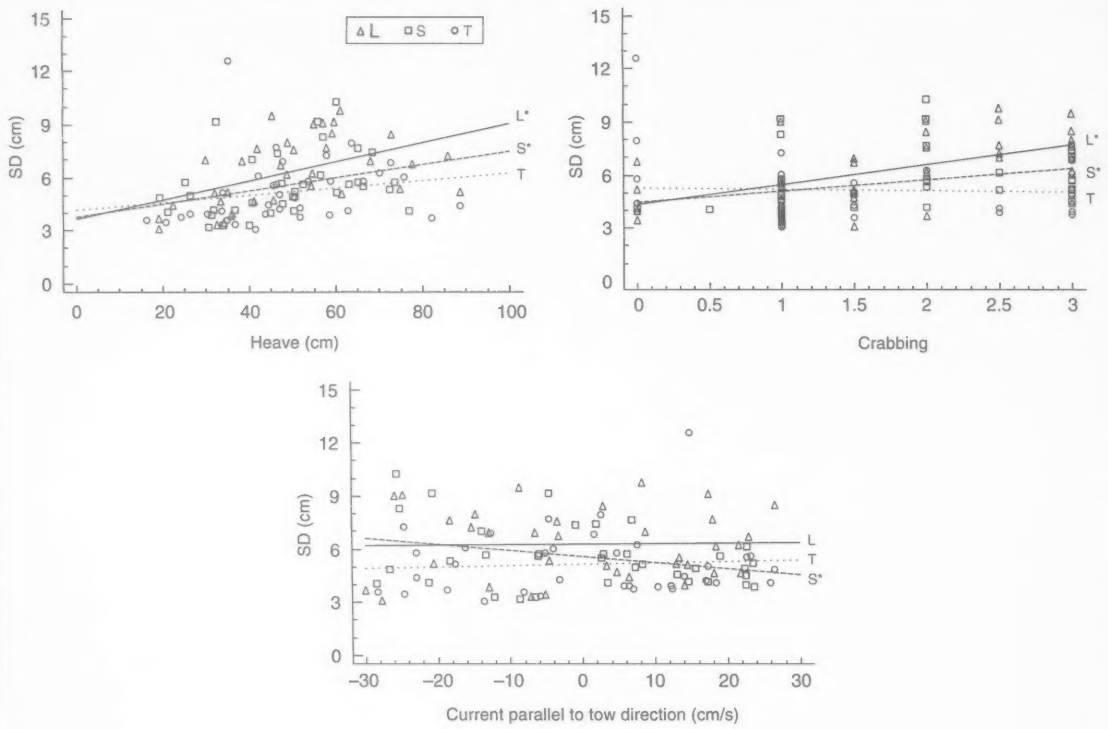

Figure 6

Comparison of regression lines illustrating the relationship between the standard deviation (SD) of the footrope distance off-bottom and environmental variables for locked winches (L), symmetry (S), and tension (T) treatments. Treatments in which the environmental variable had a statistically significant effect on the SD are identified with an asterisk (*).

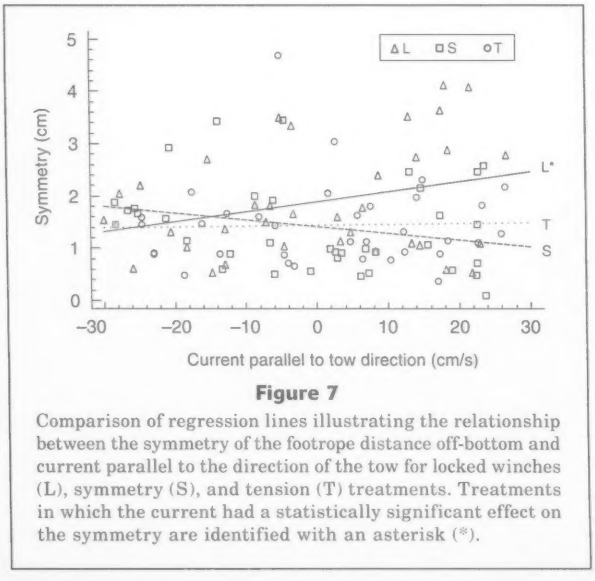

Figure 7

Comparison of regression lines illustrating the relationship between the symmetry of the footrope distance off-bottom and current parallel to the direction of the tow for locked winches (L), symmetry (S), and tension (T) treatments. Treatments in which the current had a statistically significant effect on the symmetry are identified with an asterisk (*).

ing performance of the footrope, and bottom-tending performance of the lower bridles.

Trawl geometry

Because wing and door spread and net height variability all influence catchability of a trawl (Rose and Nunnallee, 1998), surveys would stand to benefit from autotrawl systems if variances in the trawl geometry features were reduced. Our study showed that neither autotrawl system improved trawl geometry over the conventional locked-winches towing mode.

Footrope

Previous studies have demonstrated that escapement under the footrope is an important factor determining the catchability of the 83-112 Eastern survey trawl (Somerton and Otto 1999; Munro and Somerton, 2002; Weinberg et al., 2004). Periodic separation between the footrope and the bottom contribute to variability in catchability and have

been shown to be influenced by a variety of factors, such as net speed through the water (Somerton and Weinberg, 2001) that can increase footrope distances off-bottom. Weinberg et al. (2002), using a different survey bottom trawl, found capture probability of some benthic species to decrease as a result of footrope separations with the bottom. These findings likely apply to the 83-112 Eastern trawl as well. Because capture probability is generally size dependent (Munro and Somerton, 2002), an unstable footrope may not only increase the variance of overall biomass estimates, but may bias the size distribution data generated by a survey as well. If autotrawl systems can help maintain footrope contact with the bottom, then the use of an autotrawl during surveys may be warranted.

In our experiment, the tension-controlled autotrawl system provided the best footrope contact overall and the lowest standard deviation (Fig 3). High heave and moderate to strong crabbing were largely responsible for the differences observed in the bottom-tending performance of the footrope among treatments (Figs. 5–7). The tension treatment was most effective in counteracting the effects of environmental conditions, whereas the locked-winches treatment was the least stable of the three treatments given the changing environmental conditions.

We found both autotrawl systems have a potential to improve bottom trawl survey biomass estimates by increasing the dynamic stability of the trawl, thereby reducing the variance in its catchability. The equal-tension system proved better than the symmetry system in improving the overall stability of the footrope bottom-tending performance given the low bottom current velocities observed. Symmetry autotrawl systems, designed to react to crosscurrent conditions at towing depth, could prove to be more effective under stronger current conditions, but during our experiment, current velocities may have been too low (≤35 cm/s) for us to be able to detect a difference between the symmetry and tension towing modes.

Bridles

Flatfish are stimulated to herd by close proximity to or actual contact with the lower bridle (Main and Sangster, 1981a), whereas semipelagic species such as Atlantic cod (*Gadus morhua*) are probably stimulated to herd by the sight of the otter doors and mud clouds created by the doors and lower bridles (Main and Sangster, 1981b). For this reason, the length of the lower bridle in contact with the bottom and the frequency of this contact affect the herding efficiency of the trawl (Somerton, 2003). If the among- and within-tow variability of the bridle bottom-tending distance could be reduced by using an autotrawl system, then standardizing survey

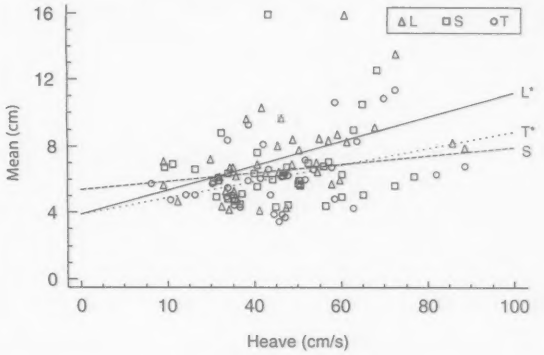

Figure 8

Comparison of regression lines illustrating the relationship between mean bridle distance off-bottom and heave for locked winches (L), symmetry (S), and tension (T) treatments. Treatments in which the heave had a statistically significant effect on the mean are identified with an asterisk (*).

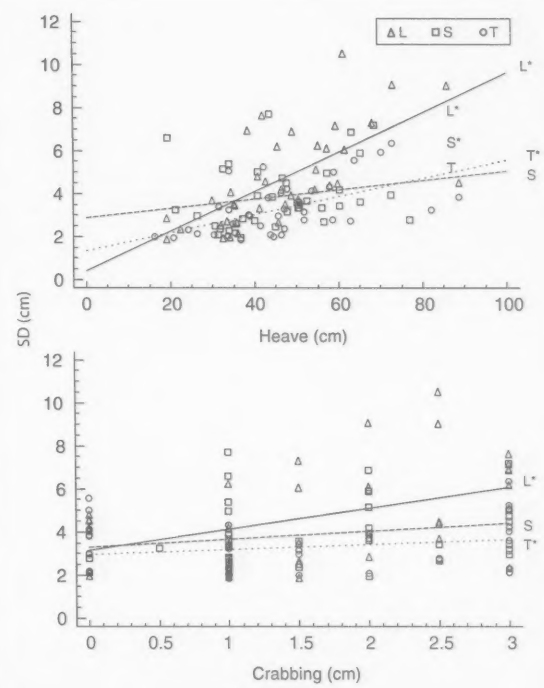

Figure 9

Comparison of regression lines illustrating the relationship between standard deviation (SD) in bridle distance off-bottom and environmental variables for locked winches (L), symmetry (S), and tension (T) treatments. Treatments in which the environmental variable had a statistically significant effect on the SD are identified with an asterisk (*).

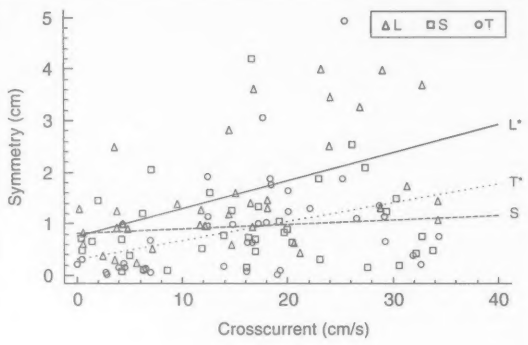

Figure 10

Comparison of regression lines illustrating the relationship between bridle symmetry and crosscurrent for locked winches (L), symmetry (S), and tension (T) treatments. Treatments in which crosscurrent had a statistically significant effect on bridle symmetry are identified with an asterisk (*).

procedures to include towing with an autotrawl system would likely be beneficial.

Our results showed that both autotrawl systems reduced the mean distance of the bridles off-bottom and the standard deviation of this distance and increased the symmetry between bridles (Fig. 4) over the locked-winches treatment. Our experiment also demonstrated that both autotrawl systems increased the stability of lower bridle bottom contact in changing environmental conditions, but we were unable to discern which of the systems was better. The data indicate that bridle bottom-tending performance was the least affected by environmental conditions during the symmetry treatment; however the standard deviation in the bridle distance off-bottom was almost always lower during the tension treatment, the exception being under extreme heave conditions (Fig. 9). The locked-winches treatment had the highest standard deviation and was affected the most by heave, crabbing, and crosscurrent velocity.

Autotrawl systems counteract the effects of warp length differential created by trawl crabbing. During our locked-winches treatment crabbing likely caused unequal tension in the warps similar to that seen while towing straight behind the boat with unequal warp lengths. Weinberg and Somerton (2006) reported that warp tension changes significantly with offset in warp lengths. To compensate for the crabbing angle and to assure that the trawl is pulled square to the direction of the tow during crabbing, one warp should be shorter than the other. Tension-controlled autotrawl systems adjust the length of the warps to equalize the tension on them. Symmetry-controlled autotrawl systems change the length of the warps to minimize crosscurrent and also increase the symmetry of the trawl in relation to the tow direction.

In summary, autotrawl systems proved to be effective in decreasing some of the adverse effects of environmental factors on some aspects of the 83-112 bottom trawl performance and, as a result, have the potential to reduce variance in among-haul catchability of the survey trawl. For this trawl, footrope and bridle distances off-bottom were significantly different among the three towing modes, albeit the differences in actual distances off-bottom were small. Trawls deploying heavier groundgear, thus enabling more constant contact with the bottom, may not be as affected. Further investigations are needed to assess the effects of the two types of autotrawl systems on other types of survey trawl gear, such as high-opening bottom trawls, trawls using different footropes, shrimp trawls, and midwater trawls. The effect of using autotrawls in areas with stronger current and different depths also needs to be investigated for the different types of trawl gear.

For bottom trawl surveys, we are concerned with two potential shortcomings in the symmetry-controlled autotrawl system tested. First, videos of trawling in rough terrain have revealed footrope distortion occurring when the footrope or doors snag on the bottom (Weinberg, unpublished data). Typically, the side opposite the snag is pulled forward while the snagged side remains stationary or is pulled ahead at a slower pace. This uneven pull on the net causes asymmetry in the headrope shape, by skewing it from the general tow direction (Weinberg and Somerton, 2006). Distortion of the headrope introduces error in the current direction and velocity values obtained by the current sensor mounted on the headrope from which warp length is determined, and thus impacts trawl performance. Our second concern involves the overall warp adjustment period required for the trawl to equilibrate to current

direction and velocity based on the current sensor input. Because many surveys standardize to a 15-min tow duration, a proportionally large percentage of tow time may be involved with adjusting warp lengths in pursuit of optimal symmetry and therefore vary trawl catchability during the tow. Under commercial trawling conditions, the manufacturer of the symmetry winch control system recommends using a 2-min minimum signal collection and analysis period between warp adjustments. After each adjustment, new sensor signals would be received and evaluated, followed by another warp adjustment, if necessary. We are uncertain as to how many warp adjustments may be necessary to orient the trawl in relation to crosscurrent flow, but based on our experiences and the frequency with which warp lengths changed during our experiment, it is conceivable that several adjustment periods spanning the majority of the survey tow may be necessary, leaving minimal time for the net to actually fish symmetrically. Furthermore, each 2-min warp adjustment would be based on a maximum of only five current flow readings because the current sensor refreshes data at 24-s intervals. Should signal loss occur, then fewer data points would be available.

We recommend taking a cautious approach before switching a trawl survey from locked winches to autotrawl. A change in survey method may require an extensive calibration experiment between the two trawling methods in order to maintain the continuity of a survey time series. Furthermore, autotrawl systems, like other mechanical devices, require service, appropriate inspections and periodic testing to ensure that they are functioning correctly within manufacturer specifications. Autotrawl calibration parameters are dependent upon accurate measurements of the diameter and length of each winch drum, warp diameter, and construction (e.g., compacted vs. traditional or wire core vs. fiber core), layers of warp, and the number of windings per layer on each drum. Hydraulic pumps and lines, electric motors, valves, solenoids, computerized control panels, and geometric counters must all be inspected to assure proper operation. Of course, should surveys operate with a symmetry-style autotrawl system, then all of the above procedures would hold true in addition to the need for accurate calibration of the current sensor and the proper mounting of the sensor to the headrope.

Acknowledgments

The success of this project is due to the efforts of many. We extend our gratitude to Tim Cosgrove, Brad Lougheed, and the crew of the FV *Vesteraalen*. Our knowledge of winch control systems was greatly enhanced by the guidance of Doug Dixon and Ed Ramberg, as was our ability to communicate at-sea with a wide range of instruments thanks to Scott Furnish, David Roetcisoender, Jon French, and Dennis Benjamin. We are also grateful to our reviewers including Captain John Gruver, Mark Wilkins, Gary Walters, and Peter Munro.

Literature cited

Main, J., and G. I. Sangster.
1981a. A study of the sand clouds produced by trawl boards and their possible effect on fish capture. Scott. Fish. Res. Rep. 20:1–20.
1981b. A study of fish capture process in a bottom trawl by the direct observations from a towed underwater vehicle. Scott. Fish. Res. Rep. 23:1–23.

Munro, P. T., and D. A. Somerton.
2002. Estimating net efficiency of a survey trawl for flatfishes. Fish. Res. 55:267–279.

Neter, J., M. H. Kutner, C. J. Nachtsheim, and W. Wasserman.
1996. Applied linear regression models, third ed., 720 p. Irwin, Chicago, IL.

Rose, C. S., and E. P. Nunnallee.
1998. A study of changes in groundfish trawl catching efficiency due to differences in operating width, and measures to reduce width variation. Fish. Res. 36:139–147.

Somerton, D. A.
2003. Bridle efficiency of a survey trawl for flatfish: measuring the length of the bridles in contact with the bottom. Fish. Res. 60:273-279.

Somerton D. A., and P. T. Munro.
2001. Bridle efficiency of a survey trawl for flatfish. Fish. Bull. 99:641–652.

Somerton, D.A., and R. S. Otto.
1999. Net efficiency of a survey trawl for snow crab, *Chionoecetes opilio*, and Tanner crab, *C. bairdi*. Fish. Bull. 97:617–625.

Somerton, D.A., and K. L. Weinberg.
2001. The affect of speed through the water on footrope contact of a survey trawl. Fish. Res. 53:1724.

Stauffer, G.
2004. NOAA protocols for groundfish bottom trawl surveys of the nation's fishery resources. NOAA Tech. Memo. NMFS-F/SPO-65, 205 p. Alaska Fish. Sci. Center, 7600 Sand Point Way NE, Seattle, WA 98115.

Weinberg, K. L., R. S. Otto, and D. A. Somerton.
2004. Capture probability of a survey trawl for red king crab (*Paralithodes camtschaticus*). Fish. Bull. 102:740–749.

Weinberg, K. L., and D. A. Somerton.
2006. Variation in trawl geometry due to unequal warp length. Fish. Bull. 104:21–34.

Weinberg, K. L., D. A. Somerton, and P. T. Munro.
2002. The effect of trawl speed on the footrope capture efficiency of a survey trawl. Fish. Res. 58:303–313.

The fishery for California market squid (*Loligo opalescens*) (Cephalopoda: Myopsida), from 1981 through 2003

Louis D. Zeidberg
Monterey Bay Aquarium Research Institute
7700 Sandholdt Rd.
Moss Landing, California 95039-9644
E-mail address: zelo@mbari.org

William M. Hamner
Dept. of Ecology and Evolutionary Biology
Univ. California, Los Angeles
621 Charles E. Young Drive South
Box 951606
Los Angeles, California 90095-1606

Nikolay P. Nezlin
Southern California Coastal Water Research Project
7171 Fenwick Lane
Westminster, California 92683-5218

Annette Henry
California Department of Fish and Game
Southwest Fisheries Science Center
Marine Region, La Jolla Field Office
8604 La Jolla Shores Drive
La Jolla, California 92037

Abstract—The California market squid (*Loligo opalescens*) has been harvested since the 1860s and it has become the largest fishery in California in terms of tonnage and dollars since 1993. The fishery began in Monterey Bay and then shifted to southern California, where effort has increased steadily since 1983. The California Department of Fish and Game (CDFG) collects information on landings of squid, including tonnage, location, and date of capture. We compared landings data gathered by CDFG with sea surface temperature (SST), upwelling index (UI), the southern oscillation index (SOI), and their respective anomalies. We found that the squid fishery in Monterey Bay expends twice the effort of that in southern California. Squid landings decreased substantially following large El Niño events in 1982–83 and 1997–98, but not following the smaller El Niño events of 1987 and 1992. Spectral analysis revealed autocorrelation at annual and 4.5-year intervals (similar to the time period between El Niño cycles). But this analysis did not reveal any fortnightly or monthly spawning peaks, thus squid spawning did not correlate with tides. A paralarvae density index (PDI) for February correlated well with catch per unit of effort (CPUE) for the following November recruitment of adults to the spawning grounds. This stock–recruitment analysis was significant for 2000–03 ($CPUE=8.42+0.41PDI$, adjusted coefficient of determination, $r^2=0.978$, $P=0.0074$). Surveys of squid paralarvae explained 97.8% of the variance for catches of adult squid nine months later. The regression of CPUE on PDI could be used to manage the fishery. Catch limits for the fishery could be set on the basis of paralarvae abundance surveyed nine months earlier.

Manuscript submitted 7 May 2004
to the Scientific Editor's Office.
Manuscript approved for publication
20 June 2005 by the Scientific Editor.
Fish. Bull. 104:46–59 (2006).

The recent discovery of falsification in Chinese fisheries reporting has led to the realization that the majority of the world's fisheries surpassed sustainability in 1988 (Watson and Pauly, 2001). The food chain has been fished down by removal of apex predators like swordfish and snapper beyond sustainability, and fisheries have subsequently shifted to prey items like sardine and mackerel (Pauly et al., 1998). We have reached the point where cephalopods are regularly the largest biomass of all commercial species harvested. Since 1970, groundfish landings of flounders, cods, and haddocks have either decreased or maintained their levels while landings in cephalopod fisheries have increased (Caddy and Rodhouse, 1998). Some of the larger cephalopod landings may be due to increased demand, but lower levels of predation and competition from finfish, and the shorter lifespan of squid may have allowed cephalopods to increase in abundance worldwide.

Loligo opalescens is a small squid (130 mm mantle length) that occupies the middle trophic level in California waters, and it may be the state's most important forage species. Market squid are principal forage items for a minimum of 19 species of fishes, 13 species of birds, and six species of mammals (Morejohn et al., 1978). The effective management of this fishery is of paramount importance not only to the fishermen involved but also to the millions of fishes, birds, and mammals that compete for this resource. Because cephalopods eat mostly zooplankton (Loukashkin, 1976), if we also deplete the squid population, it is not clear how oceanic food chains will respond. If the subannual population of *L. opalescens* fails to recruit a large biomass in a given year, the long-lived predators of this species in

the California Current may encounter severe metabolic stress.

Since the decline of the anchovy fishery, market squid probably constitutes the largest biomass of any single marketable species in the coastal environment of California (Rogers-Bennett, 2000). In the 1999–2000 season, fishermen landed 105,005 metric tons of California market squid (*Loligo opalescens*) with an exvessel (wholesale) revenue of $36 million (California Department of Fish and Game [CDFG] landing receipts). These squid deposit egg capsules on sandy substrates at depths of 15–50 m in Monterey Bay (Zeidberg et al., 2004) and 20–90 m in the Southern California Bight. The majority of squid landings occur around the California Channel Islands, from Pt. Dume to Santa Monica Bay, and in southern Monterey Bay. The fishery comprises chiefly light-boats with high wattage illumination to attract and aggregate spawning squid to the surface, and seine vessels that net the squid (Vojkovich, 1998).

Management to date has followed methods that are not dependent upon an estimate of population abundance because no estimate of squid biomass exists. In addition to limiting the catch and the number of vessels, management of the fishery has included weekend closures north of Point Conception since 1983, and these closures have recently extended to all of California coastal waters. This regulation is designed to allow a 48-hour period each week for undisturbed spawning. For Monterey Bay, the weekend closure resulted in highest landings on Mondays and decreasing daily landings through Friday (Leos, 1998). Since 2000, light boat and seine vessel operators have been required to complete logbooks for CDFG, such that CPUE can be estimated from data on the cumulative effort required to land squid.

Because of their short lifespan, many squid populations have been more effectively correlated with local oceanographic conditions than have pelagic fish species with life spans of 4–8 years. Squid landings from all regions of the world fluctuate in conjunction with the temperatures of the previous season. McInnis and Broenkow (1978) found positive temperature anomalies preceded good *Loligo opalescens* landings by 18 months, and poor squid catches followed periods of anomalous low temperatures in Monterey Bay. Robin and Denis (1999) found similar results. Warmer waters (mild winters) were followed by increased cohort success for *Loligo forbesi* in the English Channel, but this effect was not constant throughout the year. Conversely, Roberts and Sauer (1994) found *Loligo vulgaris reynaudii* landings in South Africa to increase with upwelling that coincided with La Niña (cold water) conditions in the equatorial Pacific. Rocha et al. (1999) also found an increase in squid paralarvae of many species during upwelling conditions on the Galacian-coast.

Modern instruments for monitoring coastal ocean conditions, including weather buoys and satellites, provide a vast amount of information on the physical environment of fish and squid populations. The correlation between cold, upwelled nutrient-rich water at the sea surface resulting from Eckman transport and phytoplankton blooms a few days later is well established (Nezlin and Li, 2003). Mesoscale eddies generated by coastal processes and islands also serve to concentrate phytoplankton (Falkowski et al., 1991; Aristegui et al., 1997; DiGiacomo and Holt, 2001). The subsequent effect upon zooplankton grazers rapidly follows the cycles of upwelling and relaxation (Wing et al., 1995; Graham and Largier, 1997; Hernandez-Trujillo, 1999).

Waluda et al. (1999) found that the CPUE for the *Illex argentinus* fishery was not related to monthly local sea surface temperature (SST), but CPUE was inversely related to SST on the hatching grounds for the previous July, when hatchlings were in their exponential growth phase (Yang et al., 1986; Grist and des Clers, 1998). The largest catches followed cold water. Waluda et al. (2001) found a large CPUE when the Brazilian Current dominated and frontal waters diminished in the location where squid hatching occurs. Agnew et al. (2000, 2002) found that CPUE for *Loligo gahi* was inversely correlated with SST for hatching areas six months earlier. Sakurai et al. (2000) found that *Todarodes pacificus* CPUE was highest following periods when there were large regions of hatchling-favorable habitat (17–23°C waters). They found a positive correlation between the density of paralarvae and the catch per unit of effort (CPUE) of adults in the same year (r^2=0.91) and also in the CPUE of the following year (r^2=0.77).

The CDFG has an extensive database of landings data from 1981 to the present for market squid. Because there is no record of effort prior to 2000 and because the market is driven by demand, it is difficult to use landings and vessel-day data to calculate a CPUE and therefore estimate biomass. Fishermen report that even if squid are available, they may not be harvested when processors are not accepting squid (Brockman[1]). However, there is no other database as large and widespread temporally and spatially as fishery data. Even though there are no data recorded when boats attempt to catch squid and fail, we can still use landings and vessel-days to create a CPUE. This CPUE therefore is not a methodically collected estimate of biomass, but is still a robust enough estimate of abundance to draw preliminary conclusions as we wait for logbook data to accumulate.

It is important to determine the effects of the environment on the California market squid fishery so that we can predict future landings from present conditions. Our investigation uses California market squid landings for 1981–2003 to examine correlations of landings and CPUE with physical oceanography. We compare landings data (time, location, vessel-days, and landings [in pounds]) to sea surface temperature (SST), upwelling index (UI), the Southern Oscillation index (SOI), the index of sea surface temperature in the eastern equatorial tropcial Pacific NINO3, and their respective anomalies. We also compare CPUE to a paralarvae density index

[1] Brockman, D. 2002. Personal commun. Davies Locker Sportfishing, 400 Main St. Newport Beach, CA 92611.

(PDI) based upon distributions determined in the Southern California Bight (Zeidberg and Hamner, 2002).

Materials and methods

The CDFG database for commercial California market squid landings from 1981 to present includes weight, date, location (based on CDFG 10×10 nm blocks), and gear type. Accounting for general physical oceanographic properties (Harms and Winant, 1998; Bray et al., 1999; Brink et al., 2000; Hickey et al., 2003) and following our previous studies (Nezlin et al., 2005), we organized the landings data into six areas to look at subtle differences between them: MB=northern coastal (because the majority of the landings in this area occur in southern Monterey Bay), CC=central coastal, SB=Santa Barbara Channel, SCB=Southern California Bight, SM=Santa Monica, and SD=San Diego. Also we grouped the fishery into two larger regions April (APR, equal to MB above) and October (OCT, a combination of the other five areas) based upon the month of greatest recruitment (Fig. 1). For the purpose of our study, recruitment is the aggregation of reproductive adults on the spawning grounds. When CDFG reports squid data, they make a distinction at Point Conception, thus our MB and CC areas are grouped as the "north" and our SB, SCB, SM, and SD are named "south." For this fishery we defined CPUE as the recorded tons landed in a day, divided by the number of seine vessels that landed these squid. Those days in which there were no landings were assigned a value of zero. This CPUE is important because, although not truly a quantifying effort, it does provide a means for estimating the abundance of squid by providing some basis for the amount of time taken to make a landing. Lampara, brail, and light boat data were not included because of increased variability in landings and effort and the fact that these vessels have dwindled from ten to zero percent since 1981.

The landings and boat data for each area were summed for each block by day. For example, assume that on a particular day fishermen caught 10,000 metric tons with four boats in the area of SM, 18,000 tons from three boats in SCB, and 12,000 tons from three boats in SB. We would calculate a CPUE of 2500 tons/vessel-day in SM, 6000 tons/VD in SCB, and 4000 tons/VD in SB, respectively. Thus for every date for which there was a landing we were able to calculate CPUE value for each area. Until 2002, there had never been a landing in Monterey in January, when one vessel captured 75 tons. Data such as this produce misleadingly high CPUEs; therefore all months with less than seven vessel-days for the entire 22-year period were removed from the analysis.

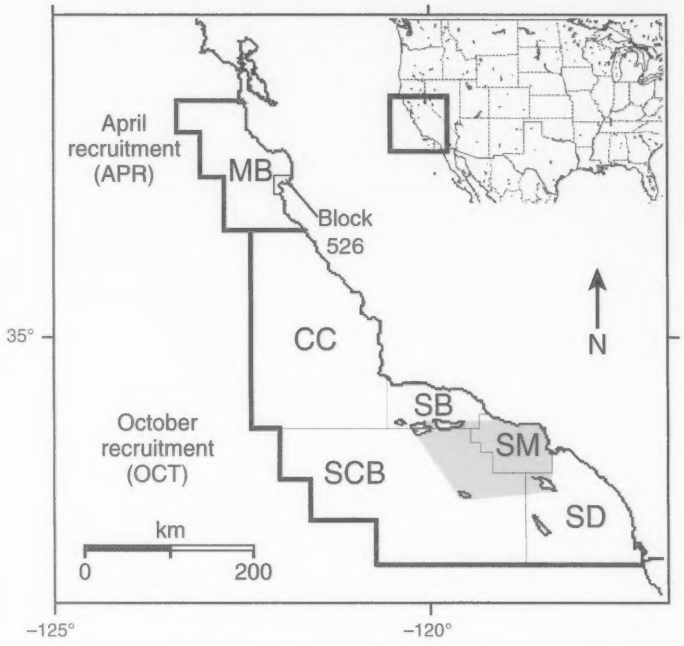

Figure 1

The California coast with the fishery areas for the California market squid (*Loligo opalescens*) identified. Areas were classified according to physical oceanographic features: Northern Coast (MB), Central Coast (CC), Santa Barbara Channel (SB), Southern California Bight (SCB), Santa Monica Bay (SM), and San Diego (SD). Regions were also classified by fishery recruitment month: April recruiting (APR: same as MB area) and October recruiting (OCT: CC, SB, SCB, SM, and SD areas combined). Block 526 (indicated with a slender arrow) is where the majority of the MB-APR landings occur. Shaded area indicates the location of the paired-net surveys used to generate the paralarvae density index (PDI).

Physical oceanography data were gathered from the Internet for sea surface temperature (SST),[2] upwelling index (UI),[3] southern oscillation index (SOI),[4] and NINO3.[5] Upwelling index (UI) is an Ekman offshore water transport (m^3/s per 100 m of the coastline) estimated from fields of atmospheric pressure (Bakun, 1973). Southern Oscillation index (SOI) is the difference between the standardized measurements of the sea level atmospheric

[2] NOAA (National Oceanic and Atmospheric Administration). National Data Buoy Center. 2000. Website: http://facs.scripps.edu/surf/buoys.html [Accessed on 24 April 2003.]

[3] NOAA Pacific Fisheries Environmental Laboratory. 2003. Website: http://www.pfeg.noaa.gov/products/las.html [Accessed on 20 March 2003.]

[4] Australian Government Bureau of Meteorology. 2005. Website: http://www.bom.gov.au/climate/current/soihtm1.shtml [Accessed on 29 March 2003.]

[5] IRI (International Research Institute for Climate Prediction). 2005. Website: http://ingrid.ldgo.columbia.edu/SOURCES/.Indices/.nino/.EXTENDED/.NINO3/ [Accessed on 20 April 2004.]

Table 1

Totals of vessel-days, landings (metric tons), and CPUE (tons/vessel-day) for two time periods of the California market squid (*Loligo opalescens*) fishery (1981–2003). The majority of the fishery occurred in Monterey Bay, 1981–89, and in southern California, 1990–2003. The six small areas represent physical oceanographic features and the larger regions (APR and OCT) are grouped by the month of greatest recruitment of spawning adults to the fishery (see bolder border in Fig. 1). MB and APR are synonymous terms. MB=northern coastal area, predominantly southern Monterey Bay; CC=central coast; SB=Santa Barbara; SCB=Southern California Bight; SM=Santa Monica; and SD=San Diego. VD=vessel days.

Years	Region and area	Vessel-days (VD)	Percent VD	Landing (tons)	Percent landings (tons)	CPUE (tons/VD)
1981–89	APR					
	MB	4918	87.4	27242	66.5	5.5
	OCT					
	CC	38	0.7	1040	2.5	27.4
	SB	186	3.3	3811	9.3	20.5
	SCB	169	3.0	3475	8.5	20.6
	SM	122	2.2	1811	4.4	14.8
	SD	194	3.4	3597	8.8	18.5
Subtotal		709	12.6	13735	33.5	19.4
Total		5627		40977		7.3
1990–2003	APR					
	MB	6508	22.5	92323	13.6	14.2
	OCT					
	CC	1283	4.4	33964	5.0	26.5
	SB	3822	13.2	104172	15.3	27.3
	SCB	8037	27.7	212986	31.3	26.5
	SM	4408	15.2	113569	16.7	25.8
	SD	4918	17.0	124147	18.2	25.2
Subtotal		22468	77.5	588838	86.4	26.2
Total		28976		681161		23.5

pressure in Tahiti and Darwin. NINO3 is determined by averaging the SST anomalies over the eastern tropical Pacific (5°S–5°N; 150°W–90°W). The buoys used were the Monterey buoy (46042, 36°N 122°W) for the MB region, the east Santa Barbara buoy (46053, 34.24°N 119.85°W) for the SB region, and the Santa Monica buoy (46025, 33°N 119°W) for the remaining regions.

We performed a spectral analysis of the entire time series to look for significant periodicities in the daily data for the entire 22-year data set. CPUE values were natural log-transformed and smoothed with a Parzen window (Ravier and Fromentin, 2001). We used a time series analysis method of cross correlation to determine the lag period in months between CPUE and the physical features of SST, SOI, NINO3, and UI and their anomalies from averaged seasonal cycles. Using this lag period we calculated linear regression of the CPUE from SST.

Sea surface temperature (SST) time series was obtained from infrared satellite measurements with advanced very high resolution radiometers (AVHRRs) on National Oceanic and Atmospheric Administration (NOAA) meteorological satellites. The data were processed at the University of Miami's Rosenstiel School of Marine and Atmospheric Science (RSMAS) and the NOAA National Oceanographic Data Center (NODC) within the scope of Pathfinder Project (version 4.1, available from the Jet Propulsion Laboratory Physical Oceanography Distributed Active Archive Center [JPL PO DAAC]).[6]

We performed a stock-recruitment analysis from a paralarvae density index (PDI). Paralarvae were collected with paired nets (505-μm mesh) without bridles, deployed like bongo-nets, and towed in a double oblique mode to 100 m depth. Samples were taken in February from 1999 to 2003, every 7.5 km on transects in regions SCB and SM (Zeidberg and Hamner, 2002). Flow meters were used to standardize the number of paralarvae per 1000 m^3 of water. The PDI is the average number of paralarvae/1000 m^3 from all tows. We used linear regression to compare the February PDI with the CPUE for the large November adult recruitment event in the SCB and SM regions of the same year.

Statistics were performed with Statview 3.0 (Abacus Concepts, Berkeley, CA) or Statistica 6.0 (Statsoft, Tulsa, OK). Interpretations of *t*-test, regression, ANOVA,

[6] http://podaac.jpl.nasa.gov/ [Accessed on 15 March 2003.]

spectral analysis, and cross correlation time series were made in accordance with Zar (1984).

Results

Decadal-regional analysis

The 22-year fishery data for *Loligo opalescens* were divided into two periods: 1981–89 and 1990–2003 (Table 1) due to a southward shift in the fishery after 1989. For the first period (1981–89), 87% of the effort and 66% of the landings were predominantly focused in the MB or APR region, specifically in the southern portion of Monterey Bay. The amount of squid captured in 1981 and 1982 was not matched again in Monterey Bay until 2002. The MB region was the most focused region; 62% of the total catch and 83% of the CPUE came from a very small area (block 526, Fig. 1)—just off Monterey harbor. CPUE in this region and time period was low, 5.54 tons/vessel-day (Table 1). SM had 4.43% of the landings and 2.2% of the vessels, yielding a CPUE of 14.85 tons/vessel-day. The SB, SCB, and SD areas were similar in the 1980s with landings around 9%, vessels at 3%, and CPUEs varying from 18.5 to 20.5 tons/vessel-days. The CC area had the smallest percentage of landings (2.5%) and vessels (0.7%), but the highest CPUE (27.4%)—most likely due to squid being hauled as a secondary target species in this region. Few fishermen choose to harvest squid in the central California area because of rough seas and rocky, gear-fouling ocean bottoms.

The focus of the market squid fishery shifted to southern California in the 1980s and landings surpassed those of Monterey Bay in 1990 (Fig. 2, Table 1). Whereas vessel-days per year decreased by 17.6% in the MB area, vessel-days increased 20-fold in the other areas. For the period 1990–2003, SM and SB ranked third and fourth for landings and vessel-days because of hauls made on the northern coasts of the Channel Islands and off the Malibu and Redondo Canyons, respectively. CC is the area least targeted, with only 5% of landings and vessels. CPUE for this period was 26 tons/vessel for all areas except MB, where it was little more than half that at 14 tons/vessel. CPUE in APR/MB has nearly tripled since 1981–82. CPUE in the OCT region has increased more modestly, except in SM.

Since 1999, annual landings have decreased in OCT (91,229 tons to 22,180 tons) and increased in APR (289 to 14,521 tons—with 22,770 tons in 2002, Fig. 2A). Effort has increased as well in the last 23 years (Fig. 2B). With the exception of MB 1981–82, all areas saw the number of vessel-days/month increase until the 1997–98 season. The number of vessel-days has decreased since 1999—in OCT (4011 to 1573)— and has increased in APR (20 to 978). The average number of days between landings for individual boats in APR (2.3) and OCT (2.1) was not significantly different (t-test$_{0.05(2)}$, df=977, t-value 0.87, P=0.39).

There have been increases in CPUE concomitant with gains in experience, and advances in technology have enhanced the ability of fishermen to locate squid. There has been a "ratcheting up," both in terms of size of vessel and in the amount of sonar (from single to dual frequency [50 to 200 kHz]) used in the competition among fishermen. However, CPUE decreased substantially in all regions in 1984 and 1998, the second years of the two biggest El Niño events recorded. Milder El Niño events in 1987 and 1992 preceded dips in CPUE values in 1988 and 1993 (Fig. 2C). Average CPUE was calculated for the APR and OCT regions by splitting the data

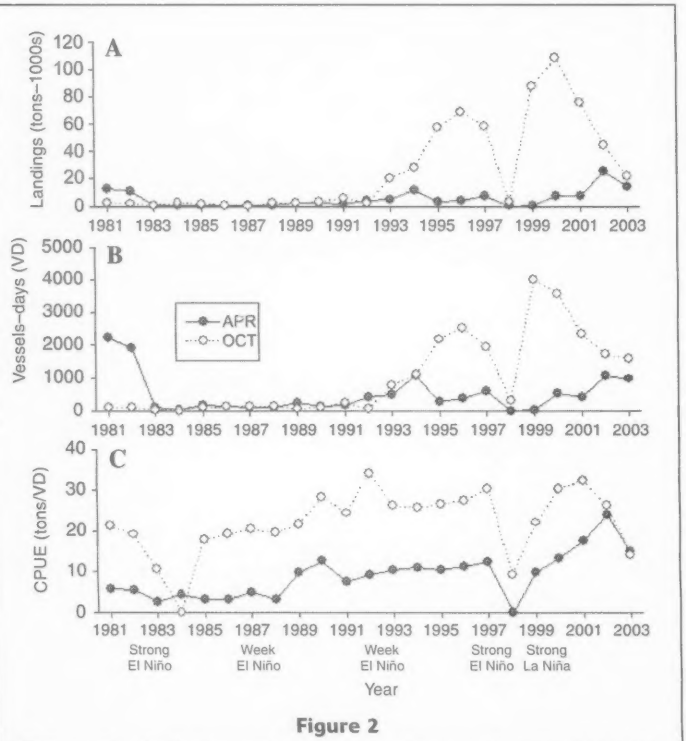

Figure 2

Fishery data for *Loligo opalescens*, summed by year for 1981–2003. (**A**) landings, (**B**) vessel days, and (**C**) catch per unit of effort (CPUE) by year for Monterey Bay (April [APR]—black circles) and southern California (October [OCT]—unfilled circles) regions. Scale of y-axis changes between A, B, and C. Note the lack of landings in OCT in 1984 and APR in 1998, following strong El Niño events.

by the frequencies determined from the spectral analysis. These splits resulted in three separate means for CPUE in APR (7.5-year frequency) and five means for the OCT region (4.5-year frequencies). Anomalies of CPUE from these means were compared to the climatic indices, and had significant linear regressions to NINO3, SOI, and UI anomalies, but explained less than 5% of the variance (data not shown).

1981–2003 squid fishery data

In comparisons of landings (Fig. 3A) by month, the six areas fell into two categories: APR and OCT. Effort in vessel-days and CPUE showed similar trends. The *Loligo opalescens* squid fishery generally occurs from April through November in APR. Although landings peak in May, by then there are so many vessels in operation that CPUE has dwindled to half that of April (Fig. 3, B and C). There is a second landings pulse in August.

In the five areas of the OCT grouping, landings typically begin in October, build to a peak in January, and diminish to lows in August (Fig. 3A). A large unimodal pulse of squid landings occurred in November for all areas except SCB. The SCB had a bimodal recruitment pulse, the two largest recruitment events in all of California: one in November and a larger one in January. In SD, like SCB, landings peaked in January, but there was no strong November signal in this region.

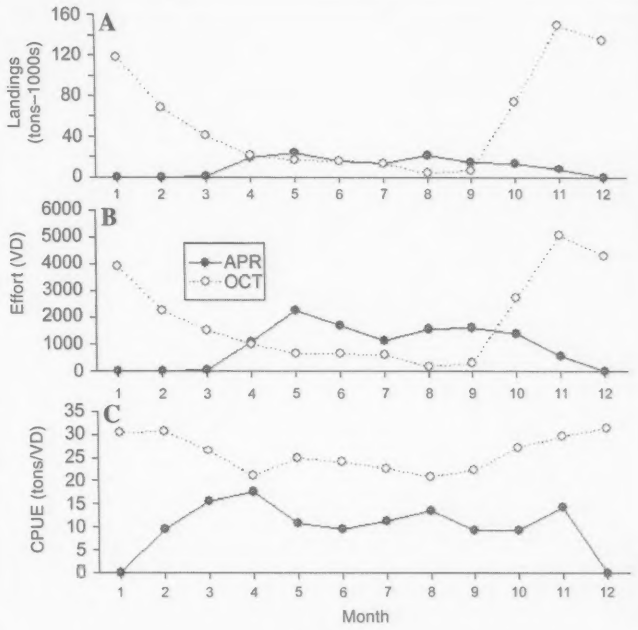

Figure 3

Fishery data for *Loligo opalescens*, summed by month for 1981–2003. (**A**) Landings (metric tons). (**B**) Effort in vessel-days (VD). (**C**) Catch per unit of effort (tons/VD). Monterey Bay (April [APR]—black circles) and southern California (October [OCT]—unfilled circles). Scale of *y*-axis changes between A, B, and C. Largest landings occurred one month later in May in the APR region and in November in the OCT region when SST was 11.7°C and 16.1°C, respectively.

CPUE by month for APR was typically half that of OCT. The APR CPUE varied between 8 and 20 tons/vessel-day, for months with more than seven vessel-days, whereas CPUE for the southern California (OCT) areas ranged from 17–36 tons/vessel-day (Fig. 3C).

Time-series analysis

The periods of the ten highest peaks of the variance spectrum were determined for all six areas (Table 2). The largest peaks from the spectral analysis occurred at periods of 372 and 356 days, or roughly 1 year for all areas. There was a 7.5-year peak in the MB and CC areas. There was a 4.5-year peak (for all areas except MB) that was similar to the period of the four El Niño events that occurred in this area during the 22-year period. There was a 3.7-year peak for all areas except CC and SM. The seven-day cycle is most likely a stochastic factor of fishermen working within weekend closures because data before 1998 did not have this periodicity. There was no 28- or 14-day cycle in any of the areas; this finding likely indicates that spawning squid do not respond to tidal currents or lunar light.

The most significant cross correlations of time lag analysis for CPUE to SST are listed in Table 3. In all cases of biological significance, CPUE lagged SST by 4, 5, or 10 months. MB CPUEs were highest (in May) when SST was low four months earlier (Jan), and hence gave a negative correlation. In all other regions, the four or five month correlation was positive, with CPUE high (Nov) when SSTs were high four months earlier (Jul). For the southern California areas there was a negative correlation with SSTs 10 months earlier (Jan). Therefore, cold winters and warm summers correlate with larger landings. Recruitment of spawning adults to the fishery occurs during the productive seasons in both APR, MB, and OCT. Productivity in APR and MB co-occurs with the spring–summer upwelling season, and in OCT productivity correlates with winter storms that lead to a deeper mixed layer. There were significant cross correlations with SOI, NINO3, and UI, but not with the anomalies of SOI and UI. Interestingly correlations for NINO3 were greater than those for SOI (Fig. 4), indicating that the CPUE of *Loligo opalescens* is more closely related to the "oceanic teleconnection" than to "atmospheric teleconnection."

Table 2

Periods of greatest spectral variance in the daily CPUE data of the market squid (*Loligo opalescens*) fishery for 1981–2003. Significance: $P<0.01$. Numbers in bold are repeated in more than one area. Harmonics of factors of 2: 2, 4, ... 4096 (blank spaces) are omitted because they are inherent in spectral analysis and not relevant to this species. MB=northern coastal area, predominantly southern Monterey Bay; CC=central coast; SB=Santa Barbara; SCB=Southern California Bight; SM=Santa Monica; and SD=San Diego.

	Top ten periods of spectral variance					
	MB			CC		
Rank	Days	Years	Month	Days	Years	Month
1	**372.4**	1	12.2			
2	**356.2**	1	11.7	**372.4**	1	12.2
3				**1638.4**	4.5	53.7
4	**7**	0	0.2	**2730.7**	7.5	89.5
5	**315.1**	0.9	10.3	**455.1**	1.2	14.9
6	**2730.7**	7.5	89.5	481.9	1.3	15.8
7	**341.3**	0.9	11.2	**356.2**	1	11.7
8	**455.1**	1.2	14.9	**390.1**	1.1	12.8
9	3.5	0	0.1			
10	**1365.3**	3.7	44.8			
	SB			SCB		
Rank	Days	Years	Month	Days	Years	Month
1	**372.4**	1	12.2	**372.4**	1	12.2
2	**356.2**	1	11.7	**1638.4**	4.5	53.7
3	**390.1**	1.1	12.8	**356.2**	1	11.7
4	**1365.3**	3.7	44.8	**1365.3**	3.7	44.8
5	**1638.4**	4.5	53.7	**390.1**	1.1	12.8
6	910.2	2.5	29.8			
7						
8	264.3	0.7	8.7			
9				819.2	2.2	26.9
10	**182**	0.5	6	**682.7**	1.9	22.4
	SM			SD		
Rank	Days	Years	Month	Days	Years	Month
1	**372.4**	1	12.2	**356.2**	1	11.7
2	**1638.4**	4.5	53.7			
3	**182**	0.5	6	**372.4**	1	12.2
4				**182**	0.5	6
5				**1638.4**	4.5	53.7
6	**356.2**	1	11.7	**682.7**	1.9	22.4
7	**390.1**	1.1	12.8	**341.3**	0.9	11.2
8	**315.1**	0.9	10.3	**1365.3**	3.7	44.8
9	204.8	0.6	6.7	**390.1**	1.1	12.8
10	**7**	0	0.2	178.1	0.5	5.8

Table 3

Results of the time series analysis. Significant correlation coefficients occurred when CPUE lagged behind sea surface temperature (SST) from buoys and advanced very high resolution radiometers (AVHRRs) by 4–10 months for all areas, except CC. Negative correlation coefficients demonstrate that high CPUE corresponds with low water temperatures in the lagged month from column two; positive values may indicate a direct relationship. MB=northern coastal area, predominantly southern Monterey Bay; CC=central coast; SB=Santa Barbara; SCB=Southern California Bight; SM=Santa Monica; and SD=San Diego.

CPUE region	Lagged (months)	SST source	Correlation coefficient
MB	4	MB buoy	−0.481
	5	AVHRR	−0.358
SCB	4	SM buoy	0.206
	10	SM buoy	−0.344
	9	AVHRR	−0.340
SD	4	SM buoy	0.220
	10	SM buoy	−0.398
	10	AVHRR	-0.387
SM	5	SM buoy	0.176
	10	SM buoy	−0.340
	10	AVHRR	−0.334
SB	4	ESB buoy	0.387
	4	SM buoy	0.415
	9	AVHRR	−0.372

Assuming a 6–9 month lifespan for *L. opalescens*, we used linear regression to compare SST from buoy data for the previous 6–10 months. We performed comparisons up to 10 months because squid eggs take 30 days to hatch at 12°C, which is a typical time period for eggs to hatch in winter in Southern California and spring–summer in Monterey Bay. The only significant regression occurred in the SM region with SSTs 10-months earlier ($r^2=0.46$, $P=0.0033$, Fig. 5). We compared satellite-derived (AVHRR) estimates of SST for 1985–2002 from areas with high densities of paralarvae and juveniles (within 8 km of shore) with CPUE by using cross correlation time series analysis. Although there were significant correlations, linear regression yielded no significant predictions for landings or CPUE from SST.

Stock recruitment analysis

We compared a paralarvae density index (PDI) with CPUE for the SCB and SM regions (Fig. 6, shaded area of Fig. 1). Collections of paralarvae were made in February (Fig. 6). After the initial surveys of 1999, methods developed in Zeidberg and Hamner (2002) resulted in 34–50 stations for oblique bongo tows to collect paralarvae in SCB and SM regions. Paralarvae/1000 m^3 from

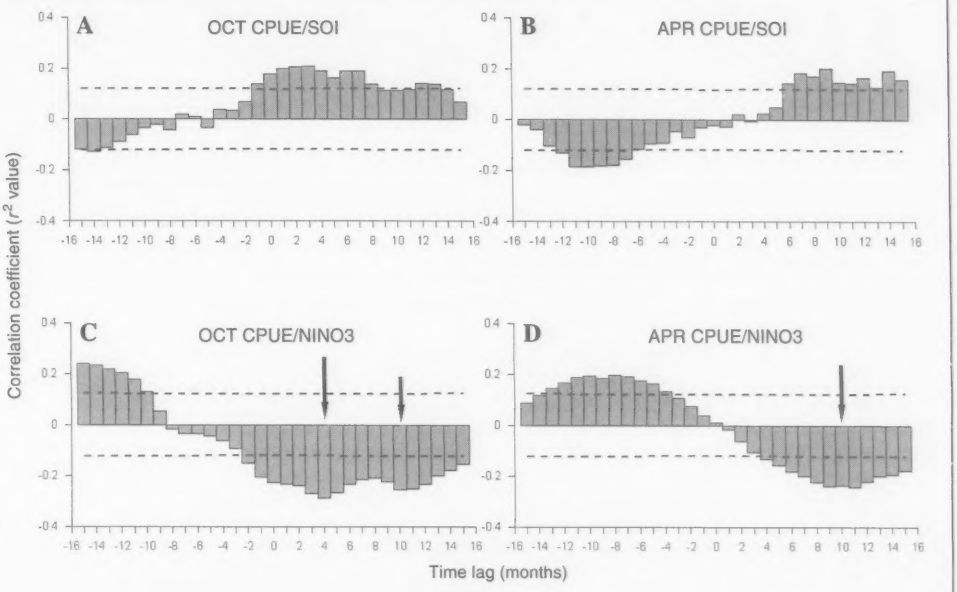

Figure 4

Time-series analysis: cross-correlation between CPUE and the global climatic indices: Southern Oscillation index (SOI for atmospheric pressure differences between Tahiti and Darwin, **A** and **B**) and NINO3 (SST anomaly in eastern equatorial Pacific, **C** and **D**) for regions OCT (A, C) and APR/MB (B, D). The correlation between CPUE and NINO3 is greater than the correlation between CPUE and SOI in both regions. CPUE lags NINO3 by 9–11 months in APR and 4 months in OCT. Thus, the effects of an El Niño event cause declines in CPUE for *Loligo opalescens* in Southern California 4 months later and in Monterey Bay 9–11 months later (long arrows). High correlation coefficients at a 10-month lag in Southern California (OCT) may be due to a second generation of market squid responding to changes in SST (shorter arrow).

all stations were averaged to create the February PDI (Fig. 6 lower right), and this PDI was then compared to the November recruitment of spawning adults (CPUE) to the fishery for the same year. Linear regression was not significant for 1999–2003 (r^2=0.522, P=0.1683). However, if 1999 was treated as an outlier because it lacked nearshore sampling sites where 76% of the paralarvae were captured subsequently, the regression explains 97.8% of the variance, and the F-value of the ANOVA ratio test for this regression is significant, P=0.007 (Fig. 7). From 1992 through 2002, SCB (36.2%) and SM (16.2%) represented nearly half of the landings for the state, and therefore this technique (regression of CPUE on PDI) could apply throughout the state.

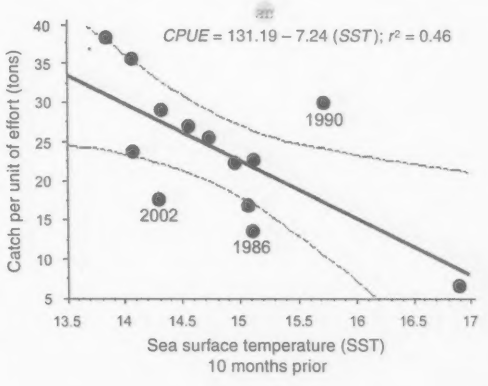

Figure 5

Linear regression and 95% confidence intervals for CPUE in November, the highest recruitment month, from SST of the previous January in the SM region. $CPUE$=131.19 – 7.24×SST; r^2=0.46, P=0.0033.

Discussion

We report landings, effort, and catch per unit of effort for *Loligo opalescens* in California for 1981–2003. It is important to reiterate that CPUE is an approximation of abundance in the fishery and fails to estimate biomass of squid in California waters. Vessels that attempt to cap-

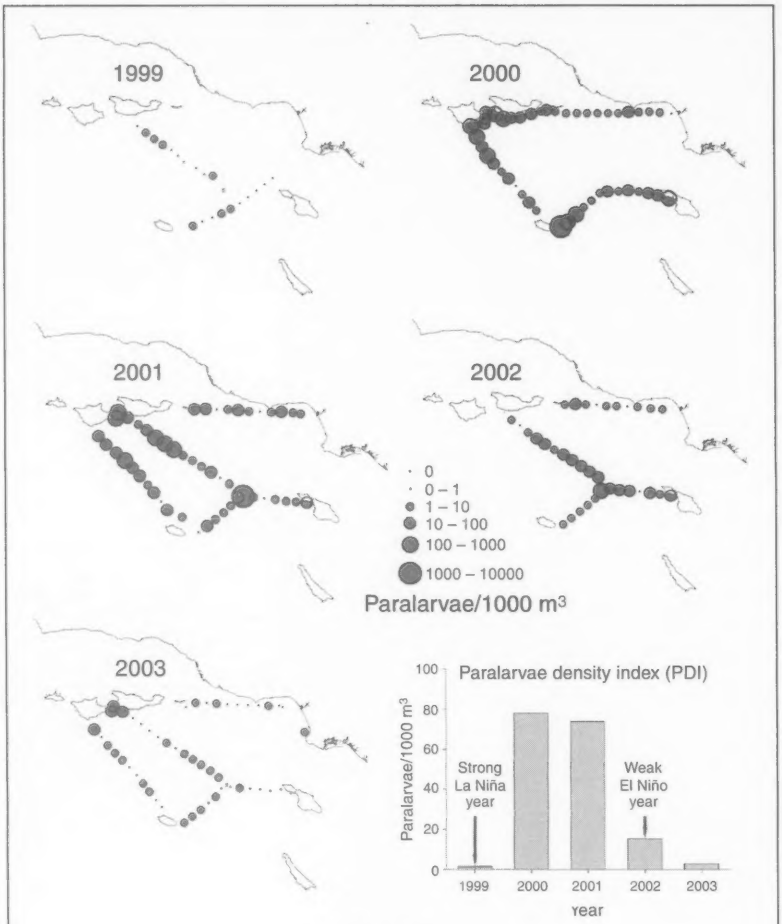

Figure 6

Density profiles (exponential bubble plot) for *Loligo opalescens* paralarvae in the Southern California Bight, February 1999–2003 (shaded area of Fig. 1). Size of circles corresponds to number of paralarvae/1000 m^3 seawater sampled. Data for 1999–2001 reprinted with permission from Springer-Verlag, originally in Zeidberg and Hamner (2002) Mar. Biol. 141(1):111–122. Data from all tows were averaged to obtain a paralarvae density index (PDI) for each year, lower right. 1999 La Niña (cold) and 2002 El Niño (warm) events are labeled above bars in the index. Note the lack of any sample sites within 8 km of shore or with >100 paralarvae/1000 m^3 in 1999.

ture squid and fail cannot be tracked with this method, and squid that are not harvested commercially are not accounted for in this report. *Loligo opalescens* reproduces by aggregating from small, foraging groups of hundreds of individuals to groups of millions of individuals. It is possible, therefore, that a large decrease in biomass can be masked by a larger percentage of the population aggregating in seemingly similar-size spawning masses. Such species are vulnerable to highly mobile fisheries (Oostenbrugge et al., 2002).

Trends in the fishery

The fishery for market squid (*Loligo opalescens*) has increased in all parts of the study area since 1983 because of an increase in demand for calamari internationally and because of the collapse of other fisheries both within and outside California waters. The majority of fishing activity has shifted from Monterey Bay to the Southern California Bight since the 1980s. Fishing activity in the bight experienced a second increase in

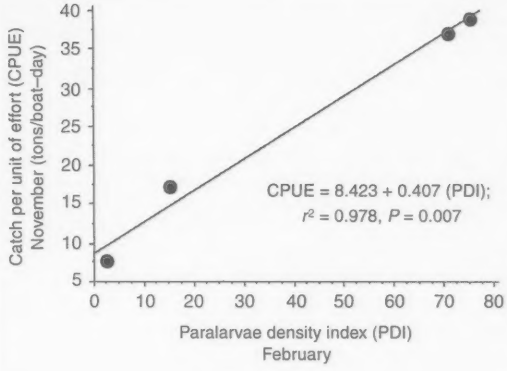

Figure 7

Stock-recruitment model: linear regression of catch per unit of effort (CPUE) for spawning adults in November on the February paralarvae density index (PDI) in the SM and SCB areas for 2000–2003.

the 1990s, reflecting fishery participants from Alaska, Washington, and Oregon. The most economically harmful trend has been the substantial decrease in landings during the second year of strong El Niño events, and the slight decrease in landings after weak ones.

The initial impetus of performing the spectral analysis was to determine if the squid were migrating to the spawning grounds in relation to a lunar or tidal signal. It is important to note that the spectral analysis with CPUE and landings data (not shown) did not show that squid recruit to spawning sites in a fortnightly cycle. There was no 14-day period in any area. Spectral analysis demonstrated periodicities for CPUE of *Loligo opalescens* on scales ranging from days to years. The most common periods for all areas were annual. Varying from 315 to 390 days, annual cycles made up more than half of the top ten signals in the analysis. The 4.5-year cycle corresponds well with the El Niño events of 1982–83, 1987, 1992, and 1997–98 (Hayward et al., 1999). In each of these cases the CPUE anomalies were negative (Zeidberg, 2003). The longest period was 7.5 years in the MB and CC areas. There were evident leaps in the mean CPUE based on mean CPUE ±5 months in MB at mid-1988 and the end of 1995, when out-of-state fishermen began to harvest squid in California (Zeidberg, 2003). Although these leaps may correspond to changes in the biomass of the squid, they are more likely due to enhancements in the capacity of the fishery to capture squid as acoustic and communication technology has improved. The 3.7-year period is probably a statistical harmonic of the 7.5-year period.

Paralarvae density index (PDI) can predict CPUE

Zeidberg and Hamner (2002) have sampled the SCB and SM areas for *Loligo opalescens* paralarvae since 1999 and we used that data to create a paralarvae density index (PDI). CPUE appears to be a better indicator of stock abundance than landings data for squid (Sakurai et al., 2000). Adults recruiting to the fishery in November, measured in CPUE, can be predicted by linear regression from the PDI of February. A regression of the CPUE data from the PDI data for 1999–2003 is not significant, but if 1999 is treated as an outlier the remaining four points (2000–03) create a regression that explains 97.8% of the variance. Our 1999 sampling of paralarvae may not be representative of the fishery because it was the first sampling year and the sampling sites were located farther offshore than those sampled in 2000–03. In 1999 there were no sites within 7.4 km of shore, where 76% of the paralarvae were captured in the following four years of sampling. Despite these caveats, this method could provide the first opportunity to manage California's market squid fishery according to scientifically gathered biological indicators and with very few of the inherent assumptions needed for many other types of forecasting (Mangel et al., 2002). As the years of logbook data accumulate, estimates of CPUE will be more closely related to the actual biomass of the species. By the end of February, we can have a prediction for the CPUE for the following year's adult recruitment. Paralarvae may be the best stage of the life cycle for a fishery prediction because juveniles can escape trawls, fewer assumptions need to be made than with estimates from spawning females (Macewicz et al., 2004), and there is sufficient time (6–9 months) to develop predictions. These predictions could help managers set catch limits and aid fishermen in deciding how to invest in gear for the following season.

In addition to our paralarvae sampling, CalCOFI has sampled the waters of California for zooplankton in a manner similar to ours since 1949. Paralarval distributions for *Loligo opalescens* have been described from these data (Okutani and McGowan, 1969). The greatest difference between the two sampling efforts is the number of stations that are in close proximity to land. The majority of the paralarvae (76%) captured by Zeidberg and Hamner (2002) were at stations less than 8 km from shore, but there is only one CalCOFI station at this proximity to land. After reviewing their surveys and models of larval dispersal (Franks, 1992; Botsford et al., 2001; Siegel, 2003), we predict that a PDI calculated from CalCOFI samples will be substantially lower than ours, but given the long time period of the CalCOFI sampling program, any significant correlations could be more powerful statistically than ours. Furthermore, fishermen could be employed to perform bongo tows for paralarvae in proximity to shore to complement CalCOFI data. If the CalCOFI bongo net data were sorted for *Loligo opalescens* paralarvae, and fishermen collected paralarvae nearshore, Monterey Bay and southern California CPUE could be predicted months in advance. Separate management of the two regions would be necessary given the time lag of recruitment (APR and OCT).

Comparison of fishery data with physical data

We found a correlation between CPUE of the largest recruitment month with SST buoy data from 10 months earlier in the SM area only. There may be physical features specific to this area that increase the correlation between spawning recruitment and SST. For example, SM is a small area, it is close to the buoy, most of the area is sandy bottom, and it contains the Redondo Canyon. Thus if further attempts to match physical oceanography to the biology of a pelagic species were to occur, the Santa Monica Bay could be the most ideal location. But this correlation between CPUE of the largest recruitment month with SST in the SM area may be a seasonal effect because the regression is significant for SST only and not an SST anomaly. Furthermore, we caution that the significance of the correlation between CPUE and SST in SM may be a type-I error because it was the only significant test of the 30 tests run with an alpha level of 0.05. The size of the recruitment event was not strongly related to small deviations from average monthly SST; thus the timing of squid recruitment to spawning grounds in APR and OCT may be tied to annual fluctuations of prey availability and correlations with temperature may be coincidental. The 10-month lag corresponds to the egg-laying date of 9-month-old squid. The lack of a greater number of correlations may be due to the small spatial resolution of the buoy data and the enormous variability of SST data due to mesoscale oceanographic features in the large fishery areas. In some areas the nearest buoy was quite distant from the fishery zone.

To address the spatial distance of spawning grounds from buoys, we compared SSTs derived from satellite AVHRR images with CPUE. AVHRR data were collected from just the shelves and slopes of the six fishery areas because these are the most important areas for the growth of hatchlings and juveniles. Cross-correlation time series analyses were significant at 5–10 month lags (Table 3), but this significance did not translate into any predictive capabilities with linear regression.

Similarly, cross-correlations of CPUE with SOI and NINO3 were significant at a 10-month lag in Monterey Bay and a 4-month lag in the Southern California Bight. Thus the Monterey fishery (10% of landings) is offset by six months (roughly one short cohort) from the SCB fishery. The correlation coefficients for NINO3 were greater than those of SOI, corroborating the idea that the direct influence of the coastal waves ("oceanic teleconnection") is the main source of the changes in the hydrographic and ecological features of the California Current system (Huyer and Smith, 1985; Rienecker and Mooers, 1986; Lynn et al., 1995; Chavez, 1996; Ramp et al., 1997) rather than the ENSO (El Niño Southern Oscillation)-related changes of atmospheric circulation ("atmospheric teleconnection") (Simpson, 1983; Simpson, 1984a, 1984b; Mysak, 1986; Breaker and Lewis, 1988; Breaker et al., 2001; Schwing et al., 2002).

Loliginid life cycles and future management of squid fisheries

The correlation between SST and CPUE in the following season may have resulted from the unique development pattern of teuthids. The use of CPUE as an index of abundance of the population (Sakurai et al., 2000), in combination with studies of squid growth in relation to SST (Jackson and Domeier, 2003), could explain large fluctuations in landings data from year to year. In terms of bottom-up forcing, individual squid health and the resulting population size result from a combination of prey availability and metabolic rates. Squids grow exponentially in the first two months of life and then logarithmically until senescence. In rearing tanks and given a constant food supply, loliginids also grow faster in warmer temperatures (Yang et al., 1986; Forsythe et al., 2001) as their metabolic rates increase (O'Dor, 1982). Grist and des Clers (1998) predicted that annual fluctuations in SST that cause differential growth in squids can lead to younger cohorts hatched in warm temperatures and surpassing in size older cohorts born in colder seasons. Thus in October, a large 6-month-old squid that hatched in April and developed in warm water may spawn with a smaller 9-month-old squid that hatched in the cold waters of January.

However, in the California system and possibly in other upwelling systems the situation is more complex than in rearing tanks. For example, Jackson and Domeier (2003) demonstrated that due to the influences of El Niño and La Niña cycles and upwelling, the mean mantle length of *Loligo opalescens* is shortest when larvae are hatched in the warmest temperatures and longest when hatched in cold waters. Mantle length is also positively correlated with the upwelling index. In the ocean, squid do not have a constant food supply. The high productivity and cold temperatures caused by upwelling and La Niña combined to create a period of rich food resources and lower metabolic rates for squid, probably enhancing the recovery of the fishery in 1999. During the El Niño event the squids were small and less abundant because they had a high metabolic rate due to increased temperatures and were exposed to lower levels of available prey due to decreased ocean productivity. Seasonal maxima of phytoplankton in Monterey Bay occur in summer; but in the southern part of the Southern California Bight productivity peaks in winter (Nezlin et al., 2002). These differences may be an indicator of why the fishery operates in Monterey Bay from April to November, coinciding with the upwelling season, and in the Southern California Bight from November to May, coinciding with less stratification of the water column and more mixing due to winter storms and colder air temperatures.

Lowry and Carretta (1999) corroborated the temperature-induced plasticity of mantle length (ML) from beaks of squid in California sea lion (*Zalophus californianus*) scats and spewings. MLs of squid prey were half the size during El Niño years on San Clemente and Santa Barbara islands. However, at San Nicholas Island during El Niño events, there were both small- and regular-

size squid prey; this finding may indicate that the squid stock moved offshore to find productive waters. Alternatively, San Nicholas sea lions may have been feeding on squids from Baja California. Zeidberg and Hamner (2002) suggested the possibility of a northern shift of the squid population in El Niño years, as has been found for most zooplankton (Colebrook, 1977).

However, the growth plasticity and fluctuating reproductive success for *Loligo opalescens* should not be underestimated. The possibility remains that the huge fluctuations in squid landings during strong ENSO events is due to the entire biomass of market squid waning and waxing rather than to population migrations away from traditionally fished spawning grounds. Triennial groundfish surveys demonstrate that market squid experienced a coast-wide population decrease, not a poleward migration during the 1997–98 El Niño.[6]

With the exception of El Niño years, the fishery increased its landings each year until 2000. However, it remains unknown if the capacity of the fishery is close to reaching the total biomass of squid in California. The California sardine (*Sardinops sagax*) fishery collapsed in the 1960s, and a twenty-year moratorium was required before there was recovery to a fraction of prior spawning biomass (Wolf, 1992). Whether over-fishing or large scale, multidecadal climatic regime shifts caused this collapse is matter of debate (Chavez et al., 2003), but without an effective management plan, squid will continue to be fished because of market demand. Markets are driven by economic forces and traditionally do not control themselves in a biologically sustainable manner. A full recovery of the squid fishery occurred from 1998 to 2000 and thus spanned four generations of squid given a 6–9 month lifecyle; for the California sardine (with a 6-8 year lifecycle), a proportionally similar recovery period would be 24–32 years (Parrish[7]).

In 1998–99 the fishery for *Loligo opalescens* decreased to low levels during the El Niño event, then recovered to record levels in the following years. This was most likely due to the plasticity of squid development in relation to water temperature and upwelling and the short (4–6 month) life span of squid. One should not assume that the ability of this species to recover from environmental stress like El Niño applies also to the recent anthropogenic stresses associated with increasing fishery capacity. It remains to be seen if the large decline in southern California landings in the last five years (119,780–24,449 tons/year) is due to the small El Niño of 2002–03, the climate-regime shift in 1998, overfishing, or some other factor such as increased water stratification due to global warming. Although the short-lived squid may not be able to recover from overexploitation in short order, the huge number of long-lived birds, fish, and marine mammals (Morejohn et al., 1978; Lowry and Carretta, 1999) that depend on squid as a key forage species may not be able to recover rapidly from lack of management foresight. The recent establishment of the marine reserve system in the Channel Islands eliminates 13% of key squid fishing grounds. This ecosystem-based management approach may assist in protecting not only the squid but also their predators.

[7] CDFG (California Department of Fish and Game). 2005. Final market squid fishery management plan. Website: http://www.dfg.ca.gov/mrd/msfmp/index.html [Accessed on 6 June 2005.]

[7] Parrish, R. 2005. Personal commun. Fisheries and Marine Ecosystems Program, Pacific Fisheries Environmental Laboratory, 1352 Lighthouse Ave. Pacific Grove, CA 93950-2097.

Acknowledgments

This research was funded by a California Fish and Game award (no. FG7334MR) and a Coastal Environmental Quality Initiative Program grant (no. 783828-KH-19900) and was supported in part by the David and Lucile Packard Foundation through the Monteray Bay Aquarium Research Institute. Bruce Robison, Rich Ambrose, Peggy Fong, and Dick Zimmer provided thoughtful reviews. Andrea Steinberger assisted with data management.

Literature cited

Agnew, D. J., J. R. Beddington, and S. L. Hill.
2002. The potential use of environmental information to manage squid stocks. Can J. Fish. Aquat. Sci. 59:1851–1857.

Agnew, D. J., S. Hill, and J. R. Beddington.
2000. Predicting the recruitment strength of an annual squid stock: *Loligo gahi* around the Falkland Islands. Can J. Fish. Aquat. Sci. 57:2479–2487.

Aristegui, J., P. Tett, A. Hernandez-Guerra, G. Basterretxea, M. F. Montero, K. Wild, P. Sangra, S. Hernandez-Leon, M. Canton, J. A. Garcia-Braun, M. Pacheco, and E. D. Barton.
1997. The influence of island-generated eddies on chlorophyll distribution: a stufy of mesoscale variation around Gran Canaria. Deep Sea Res. 44:7–96.

Bakun, A.
1973. Coastal upwelling indices, west coast of North America, 1946–1971, 103 p. NOAA Tech. Rep. NMFS SSRF-671.

Botsford L. W., A. Hastings, and S. D. Gaines.
2001. Dependence of sustainability on the configuration of marine reserves and larval dispersal distance. Ecol. Lett. 4(2):144–150.

Bray N. A., A. Keyes, and W. M. L. Morawitz.
1999. The California Current system in the Southern California Bight and Santa Barbara Channel. J. Geophys Res 104 C4:7695–7714.

Breaker, L. C., and P. A. W. Lewis.
1988. A 40–50 day oscillation in sea-surface temperature along the central California coast. Estuar. Coast. Shelf Sci. 26:395–408.

Breaker, L. C., P. C. Liu, and C. Torrence.
2001. Intraseasonal oscillations in sea surface temperature, wind stress, and sea level off the central California coast. Cont. Shelf Res. 21(6-7):727–750.

Brink, K. H., R. C. Beardsley, J. Paduan, R. Limeburner, M. Caruso, and J. G. Sires.
2000. A view of the 1993–1994 California Current based on surface drifters, floats, and remotely sensed data. J. Geophys. Res. Oceans. 105(C4):8575–8604.

Caddy, J. F., and P. G. Rodhouse
1998. Cephalopod and groundfish landings: evidence for ecological change in global fisheries? Rev. Fish Biol. Fish. 8:431–444.
Chavez, F. P.
1996. Forcing and biological impact of onset of the 1992 El Nino in central California. Geophys. Res. Let. 23(3):265–268.
Chavez, F. P., J. Ryan, S. E. Lluch-Cota, and M. Niquen-C.
2003. From anchovies to sardines and back: multidecadal change in the pacific ocean. Science 299:217–221.
Colebrook, J. M.
1977. Annual fluctuations in biomass of taxonomic groups of zooplankton in the California Current 1955–59. Fish. Bull. 75:357–368.
DiGiacomo, P. M., and B. Holt.
2001. Satellite observations of small coastal ocean eddies in the Southern California Bight. J. Geophys. Res. 106 (C10):22,521–22,543.
Falkowski, P. G., D. Ziemann, Z. Kolber, P. K. Bienfang.
1991. Role of eddy pumping in enhanced primary production on the ocean. Nature 352:55–58.
Forsythe, J. W., L. S. Walsh, P. E. Turk, and P. G. Lee.
2001. Impact of temperature on juvenile growth and age at first egg-laying of the Pacific reef squid *Sepioteuthis lessoniana* reared in captivity. Mar. Biol. 138:103–112.
Franks, P. J. S.
1992. Sink or swim: accumulation of biomass at fronts. Mar. Ecol. Prog. Ser. 82:1–12.
Graham, W. M., and J. L. Largier.
1997. Upwelling shadows as nearshore retention sites: the example of northern Monterey Bay. Cont. Shelf Res. 17:509–532.
Grist, E. P. M., and S. des Clers.
1998. How seasonal temperature variations may influence the structure of annual squid populations. IMA J. of Math. Appl. Med. Biol. 15:187–209.
Harms, S., and C. D. Winant.
1998. Characteristic patterns of the circulation in the Santa Barbara Channel. J. Geophys. Res. V103, C2:3041–3065.
Hayward T. L., T. R. Baumgartner, D. M. Checkley, R. Durazo, G. Gaxiola-Castro, K. D. Hyrenbach, A. W. Mantyla, M. M. Mullin, T. Murphree, F. B. Schwing, P. E. Smith, M. J. Tegner.
1999. The state of the California Current in 1998–1999: Transition to cool-water conditions. Calif Coop Oceanic Fish Invest Rep 40:29–62.
Hernandez-Trujillo, S.
1999. Variability of community structure of Copepod related to El Niño1982–83 and 1987–88 along the west coast of Baja California Peninsula, Mexico. Fish. Oceanog. 8:284–295.
Hickey B. M., E. L. Dobbins, and S. E. Allen.
2003. Local and remote forcing of currents and temperature in the central Southern California Bight. J. Geophys. Res. Oceans 108(C3):3081–3084.
Huyer, A., and R. L. Smith.
1985. The signature of El Niño off Oregon in 1982–83. J. Geophys. Res. 90:7133–7142.
Jackson, G. D., and M. L. Domeier.
2003. The effects of an extraordinary El Niño/La Niña event on the size and growth of the squid *Loligo opalescens* off Southern California. Mar. Biol. 142:925–935.
Leos, R. R.
1998. The biological characteristics of the Monterey Bay squid catch and the effect of a two-day-per-week fishing closure. CalCOFI Reports 39:204–211.
Loukashkin, A. S.
1976. On biology of market squid, *Loligo opalescens*, a contribution toward the knowledge of its food habits and feeding behavior. CalCOFI Reports 18:109–111.
Lowry, M. S., and J. V. Carretta.
1999. Market squid (*Loligo opalescens*) in the diet of California sea lions (*Zalophus californianus*) in southern California (1981–1995). CalCOFI Reports 40:196–207.
Lynn, R. J., F. B. Schwing, T. L. Hayward.
1995. The effect of the 1991–1993 ENSO on the California Current system. CalCOFI Reports 36:57–71.
Macewicz, B. J., J. R. Hunter, N. C. H. Lo, E. L LaCasella.
2004. Fecundity, egg deposition, and mortality of market squid (*Loligo opalescens*). Fish. Bull. 102:306–327.
Mangel, M., B. Marinovic, C. Pomeroy, and D. Croll.
2002. Reqiuem for Ricker: unpacking MSY. Bull. Mar. Sci. 70:763–781.
Morejohn, G. V., J. T. Harvey, and L. T. Krasnow.
1978. The importance of *Loligo opalescens* in the food web of Marine vertebrates in Monterey Bay, Calif. Fish Game Fish Bull. 169:67–98.
McInnis, R. R., and W. M. Broenkow.
1978. Correlations between squid catches and oceanography conditions in Monterey Bay, Calif. Fish Game Fish Bull. 169:161–170.
Mysak, L. A.
1986. El Niño, interannual variability and fisheries in the northeast Pacific Ocean. Can. J. Fish. Aquat. Sci. 43:464–497.
Nezlin, N. P., W. M. Hamner, and L. D. Zeidberg.
2005. Influence of El Niño 1997–1998 on the Pelagic Ecosystem off California: remote sensed analysis. *In* California and the World Ocean '02 (O. T. Magoon, H. Converse, B. Baird, B. Jines, and M. Miller-Henson, eds.), p. 1233–1252.
Nezlin, N. P., and B. L. Li.
2003. Time series analysis of remote-sensed chlorophyll and environmental factors in the Santa Monica-San Pedro Basin off Southern California. J. Mar. Syst. 39:185–202.
O'Dor, R. K.
1982. Respiratory metabolism and swimming performance of the squid *Loligo opalescens*. Can J. Fish. Aquat. Sci. 39:580–587.
Okutani T., and J. A. McGowan.
1969. Systematics, distribution and abundance of the epiplanktonic squid (Cephalopoda, Decapoda) larvae of the California Current April, 1954–March, 1957. Bull. Scripps Inst. Oceanog. 14:1–90.
Oostenbrugge, J. A. E., J. J. Poos, W. L. T. van Densen, and M. A. M. Machiels.
2002. In search of a better unit of effort in the coastal liftnet fishery with lights for small pelagics in Indonesia. Fish. Res. 59:43–56.
Pauly, D., V. Christensen, J. Dalsgaard, R. Froese, and F. Torres Jr.
1998. Fishing down marine food webs. Science 279: 860–863.
Ramp, S. R., J. L. McClean, C. A. Collins, A. J. Semtner, and K. A. S. Hays.
1997. Observations and modeling of the 1991–1992 El Niño signal off central California. J. Geophys. Res. 102(C3):5553–5582.

Ravier, C., and J. M. Fromentin.
2001. Long-term fluctuations in the eastern Atlantic and Mediterranean bluefin tuna population. ICES J. Mar. Sci. 58:1299–1317.
Rienecker, M. M., and C. N. K. Mooers.
1986. The 1982–1983 El Niño signal off northern California. J Geophys. Res. 91:6597–6608.
Roberts, M. J., and W. H. H. Sauer.
1994. Environment: the key to understanding the South African chokka squid (*Loligo vulgaris* reynaudii) life cycle and fishery? Antarctic Science 6:249–258.
Robin, J. P., and V. Denis.
1999. Squid stock fluctuations and water temperature: temporal analysis of English Channel Loliginidae. J. Appl. Ecol. 36:101–110.
Rogers-Bennett, L.
2000. Review of some California fisheries for 1999: market squid, dungeness crab, sea urchin, prawn, abalone, groundfish, swordfish and shark, ocean salmon, nearshore finfish, Pacific sardine, Pacific herring, Pacific mackerel, reduction, white seabass, and recreational. CalCOFI Rep. 41:8–26.
Rocha, F., A. Guerra, R. Prego, U. Piatkowski.
1999. Cephalopod paralarvae and upwelling conditions off Galician waters (NW Spain). J. Plank. Res. 21:21–33.
Sakurai, Y., H. Kiyofuji, S. Saitoh, T. Goto, and Y. Hiyama.
2000. Changes in inferred spawning areas of *Todarodes pacificus* (Cephalopoda: Ommastrephidae) due to changing environmental conditions. ICES J. Mar. Sci. 57:24–30.
Schwing, F. B., T. Murphree, L. deWitt, and P. M. Green.
2002. The evolution of oceanic and atmospheric anomalies in the northeast Pacific during the El Niño and La Niña events of 1995–2001. Prog. Oceanog. 54(1–4):459–491.
Siegel, D. A., B. P. Kinlan, B. Gaylord, and S. D. Gaines.
2003. Lagrangian descriptions of marine larval dispersion. Mar. Ecol. Prog. Ser. 260:83–96.
Simpson, J. J.
1983. Large-scale thermal anomalies in the California Current during the 1982–1983 El Niño. Geophys. Res. Let. 10:937–940.
1984a. El Niño-induced onshore transport in the California current during 1982–1983. Geophys. Res. Let. 11(3):241–242.
1984b. A simple model of the 1982–1983 Californian "El Nino". Geophys. Res. Let. 11(3):243–246.
Vojkovich, M.
1998. The California fishery for market *squid (Loligo opalescens)*. CalCOFI Rep. 39:55–61.
Waluda, C. M., P. N. Trathan, and P. G. Rodhouse.
1999. Influence of the oceanographic vriability on recruitment in the *Illex argentinus* (Cephalopoda: Ommastrephidae) fishery in the South Atlantic. Mar. Ecol. Prog. Ser. 183:159–167.
Waluda, C. M., P.G. Rodhouse, G. P. Podesta, P. N. Trathan, and G. J. Pierce.
2001. Surface oceanography of the inferred hatching grounds of *Illex argentinus* (Cephalopoda: Ommastrephidae) and influences on recruitment variability. Mar. Biol. 139:671–679.
Watson, R., and D. Pauly.
2001. Systematic distortions in world fisheries catch trends. Nature 414:534–536.
Wing, S. R., J. L. Largier, and L. W. Botsford.
1995. Settlement and transport of benthic invertebrates in an intermittent upwelling region. Limnol. Oceanog. 40(2):316–329.
Wolf, P.
1992. Recovery of the Pacific sardine and the California sardine fishery. CalCOFI Reports 33:76–86.
Yang, W. T., R. F. Hixon, P. E. Turk, M. E. Krejci, W. H. Hulet, and R. T. Hanlon.
1986. Growth, behavior, and sexual maturation of the market squid, *Loligo opalescens*, cultured through the life cycle. Fish. Bull. 84:771–798.
Zar, J. H.
1984. Biostatistical analysis, 2nd ed., 718 p. Prentice Hall, Englewood Cliffs, NJ.
Zeidberg, L. D., and W. M. Hamner.
2002. Distribution of squid paralarvae, *Loligo opalescens* (Cephalopoda: Myopsida), in the Southern California Bight in the three years following the 1997 El Niño. Mar. Biol. 141:111–122.
Zeidberg, L. D.
2003. The early life history and fishery of the California market squid, *Loligo opalescens*. Ph.D. diss., 136 p. Univ. California Los Angeles, Los Angeles, CA.
Zeidberg, L. D., W. Hamner, K. Moorehead, and E. Kristof.
2004. Egg masses of *Loligo opalescens* (Cephalopoda: Myopsida) in Monterey Bay, California following the El Niño event of 1997–1998. Bull. Mar. Sci. 74:129–141.

Variability in supply and cross-shelf transport of pink shrimp (*Farfantepenaeus duorarum*) postlarvae into western Florida Bay

Maria M. Criales[1]
John D. Wang[2]
Joan A. Browder[3]
Michael B. Robblee[4]
Thomas L. Jackson[3]
Clinton Hittle[4]

[1] Rosenstiel School of Marine and Atmospheric Science, MBF
University of Miami
4600 Rickenbacker Causeway
Miami, Florida 33149
E-mail address (for M. M. Criales): mcriales@rsmas.miami.edu

[2] Rosenstiel School of Marine and Atmospheric Science, AMP
University of Miami
4600 Rickenbacker Causeway
Miami, Florida 33149

[3] NOAA Fisheries, Southeast Fisheries Science Center
75 Virginia Beach Drive
Miami, Florida 33149

[4] United States Geological Survey
Center for Water and Restoration Studies
3110 SW 9th Avenue
Ft Lauderdale, Florida 33315

Abstract—The variability in the supply of pink shrimp (*Farfantepenaeus duorarum*) postlarvae and the transport mechanisms of planktonic stages were investigated with field data and simulations of transport. Postlarvae entering the nursery grounds of Florida Bay were collected for three consecutive years at channels that connect the Bay with the Gulf of Mexico, and in channels of the Middle Florida Keys that connect the southeastern margin of the Bay with the Atlantic Ocean. The influx of postlarvae in the Middle Florida Keys was low in magnitude and varied seasonally and among years. In contrast, the greater postlarval influx occurred at the northwestern border of the Bay, where there was a strong seasonal pattern with peaks in influx from July through September each year. Planktonic stages need to travel up to 150 km eastward between spawning grounds (northeast of Dry Tortugas) and nursery grounds (western Florida Bay) in about 30 days, the estimated time of planktonic development for this species. A Lagrangian trajectory model was developed to estimate the drift of planktonic stages across the SW Florida shelf. The model simulated the maximal distance traveled by planktonic stages under various assumptions of behavior. Simulation results indicated that larvae traveling with the instantaneous current and exhibiting a diel behavior travel up to 65 km and 75% of the larvae travel only 30 km. However, the eastward distance traveled increased substantially when a larval response to tides was added to the behavioral variable (distance increased to 200 km and 85% of larvae traveled 150 km). The question is, when during larval development, and where on the shallow SW Florida shelf, does the tidal response become incorporated into the behavior of pink shrimp.

Manuscript submitted 16 September 2003 to the Scientific Editor's Office.

Manuscript approved for publication 30 June 2005 by the Scientific Editor.

Fish. Bull. 104:60–74 (2006).

Patterns of recruitment of coastal species are highly variable, mainly because of the complex interaction of biotic and abiotic factors across the different life history stages. These factors include but are not limited to reproductive dynamics, larval dispersal and behavior, physiological tolerances, and the hydrometeorological regime in which their life stages develop (e.g., Shanks, 1995; Cowen, 2002). The commercially valuable tropical penaeid shrimps that use different habitats during their life cycle (offshore spawning grounds and estuarine nursery habitats) have to cope with a large suite of physical processes and stimuli (Rothlisberg et al., 1995, 1996). The pink shrimp (*Farfantepenaeus duorarum*) of Dry Tortugas is one of the most economically and ecologically important species in southwest Florida. The pink shrimp supports an important year-round fishery of about 4000 metric tons in an area of 10,000 km^2 between Dry Tortugas and Key West (Iversen et al., 1960; Klima et al., 1986). The Tortugas fishery is directly dependent on young shrimp that migrate from inshore nursery areas onto the offshore fishing grounds (Sheridan, 1996; Browder et al., 2002). Recruitment shows no relationship to spawning size; therefore harvest fluctuations are apparently due to environmental conditions rather than fishing operations (Nance and Patella, 1989). To effectively manage this species, it is necessary to have accurate information on the processes linking nursery and spawning ground populations.

Pink shrimp population dynamics are affected by physical processes and environmental conditions occurring in the southwestern (SW) Florida Shelf of the Gulf of Mexico, the Atlantic coastal zone, and the Florida Bay. Early research on gonad development (Cummings, 1961), distribution of larval stages (Jones et al., 1970), and analysis of length frequency distributions of fishery stock data (Iversen et al., 1960; Roberts, 1986) indicated that the center of spawn-

ing is northeast of the Dry Tortugas. If gravid females spawn northeast of the Dry Tortugas, larvae need to travel up to 150 km to reach the main nursery ground in western Florida Bay. Females spawn on the continental shelf at about 30 m of depth, where larvae develop, passing through several changes in feeding habitats, behavior, and physical stages (nauplii, zoeae, myses) (Dobkin, 1961; Ewald, 1965; Jones et al., 1970). Postlarvae undergo between three and eight additional planktonic stages before settlement. Larvae develop rapidly, needing only about 30 days to become postlarvae ready to settle to the bottom (Ewald, 1965; Dobkin, 1961). Planktonic stages (larvae and postlarvae) approach the coast and postlarvae enter the nursery grounds of Florida Bay at about 9–10 mm total length (Tabb et al., 1962; Allen et al., 1980; Criales et al., 2000). Larval development and ocean hydrodynamics must be tightly linked to successfully bring these planktonic stages to their coastal nursery grounds.

Mechanisms of transport used by planktonic stages of penaeid shrimps are highly variable, depending on the species, different environmental conditions, oceanic physical processes, and complexity of larval behaviors (e.g., Dall, 1990; Rothlisberg et al., 1995, 1996; Wenner et al., 2005). Physical oceanographic processes significantly affect the transport of planktonic stages from spawning to nursery grounds (Yeung and Lee, 2002; Criales et al., 2003). Two main immigration routes have been hypothesized for pink shrimp postlarvae entering Florida Bay: 1) postlarvae may drift south-southeast downstream with the Florida Current and enter Florida Bay through the tidal channels of the Lower and Middle Florida Keys (Rehrer et al., 1967; Munro et al., 1968), and 2) postlarvae may move northeast across the SW Florida shelf and enter the Bay at its northwestern boundary (Jones et al., 1970; Criales and Lee, 1995). The most widely recognized pathway for postlarvae to reach Florida Bay up-to-now has been by transport up the Atlantic side through the tidal channels of the Middle Florida Keys (Munro et al., 1968; Criales and McGowan, 1994; Criales et al., 2003). The favorable Ekman transport generated by the southeastern winds along the west-east oriented coast, and coastal countercurrent flow generated by cyclonic eddies provide favorable onshore transport mechanisms along the Florida Keys coast (Criales and Lee, 1995; Lee and Williams, 1999). In contrast, larval transport across the broad, shallow SW Florida Shelf has not been well studied and questions exist about the feasibility of this pathway. Subtidal frequency flows are weak in the SW Florida shelf and mainly in the alongshore (north-south) direction as a direct response to wind events (Koczy et al., 1960; Weisberg et al., 1996; Lee et al., 2001). Tidal currents are strong mainly in the cross-shelf direction (Wang, 1998; Smith, 2000). Freshwater discharges from the Everglades affect a broad area of the SW Florida shelf (Lee et al., 2001; Jurado, 2003). Isopleths less than 32 are typically confined to the region between Cape Sable and Cape Romano, and from 32 to 36 extend from near Cape Romano to the vicinity of Dry Tortugas in a highly variable annual pattern (Lee et al., 2001; Johns and Szymanski[1]).

For tropical penaeid shrimps that undergo larval development offshore, but whose nursery grounds are inshore, migratory behavior is a key factor for their advection to nursery grounds (Dall et al., 1990; Shanks, 1995). The simplest migratory behavior is vertical movement, and three types of vertical migrations are known to mediate horizontal transport of larvae: ontogenic, diel, and tidal (for reviews see Sponaugle et al., 2002). For some Australian penaeid species (banana prawn [*Fenneropenaeus merguiensis*], grooved tiger prawn [*Penaeus semisulcatus*], and eastern king prawn [*Melicertus plebejus*]) it has been shown that early planktonic stages (protozoeae and myses) perform diel vertical migration cued by light and that later in development (as postlarvae) the migration is cued by tides (Rothlisberg, 1982; Rothlisberg et al., 1983, 1995) and there is no cross-shelf displacement of larvae during the 15 days of diel behavior. Previous studies of pink shrimp in South Florida have clearly indicated ontogenic behavior for pink shrimp; postlarvae have a higher degree of mobility than earlier protozoeae and myses (Temple and Fischer, 1965; Eldred et al., 1965; Jones et al., 1970; Criales and Lee, 1995). On the other hand, diel behavior is not so well determined. Although protozoeae, myses and postlarvae were more abundant at the surface during the night than during the day, day and night differences have not been statistically significant in any of these previous studies. The effect of diel, tidal, or ontogenic combinations of behavior on cross-shelf transport from South Florida spawning grounds to western Florida Bay nursery grounds has not previously been explored. The postlarvae of many penaeid shrimps, including pink shrimp, are known to synchronize vertical migration with the tides at the entrance to estuarine nursery grounds (for reviews see Garcia and Le Reste 1981, Dall et al., 1990). This process is known as selective tidal stream transport (STST) (Forward and Tankersley, 2001). Penaeid postlarvae ascend in the water column during the flood and sit on the bottom during the ebb to maximize up-estuary movement (e.g., Rothlisberg et al., 1995). This behavior has been shown for pink shrimp postlarvae inside Florida Bay (Tabb et al., 1962; Roessler and Rehrer, 1971), but not along the border of the bay with the Gulf of Mexico. When during the life cycle and where on the shelf this tidal behavior begins and what the environmental cues are—these questions remain unanswered.

The purpose of our research was 1) to determine patterns of supply of pink shrimp postlarvae into Florida Bay through two distinct regions, 2) to define the most important transport route for planktonic stages from the Dry Tortugas into Florida Bay, 3) to examine alternative behavioral responses of larvae and postlarvae, and 4) to propose a recruitment mechanism for

[1] Johns, E., and D. Szymanski. 2003. Mixing it up in Florida Bay. Florida Bay News, summer 2003:1–3.

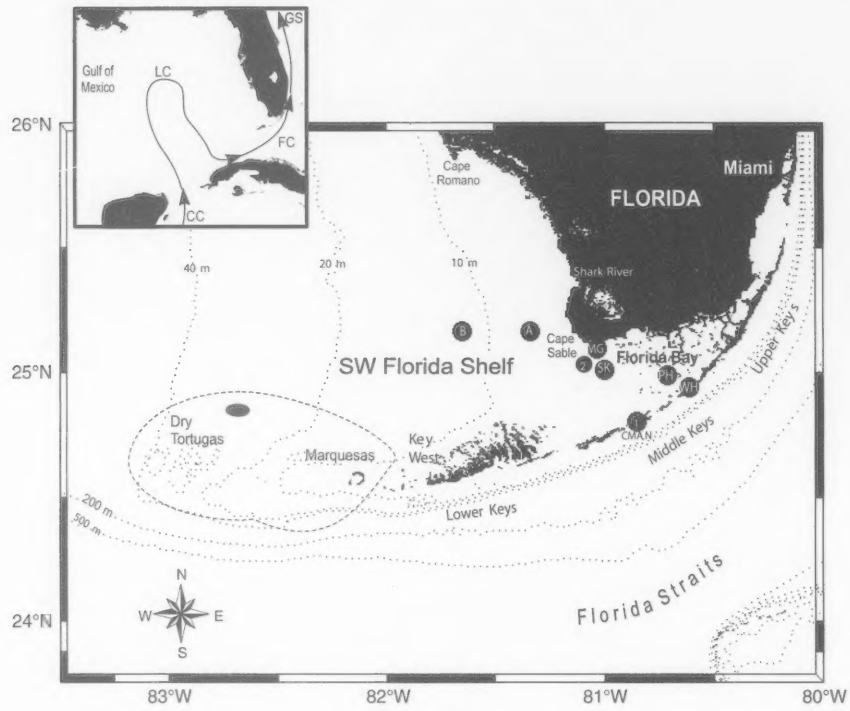

Figure 1

Map of the study area (with bathymetry) showing the channel net sampling stations at the northwestern and southeastern borders of the nursery grounds of Florida Bay, ADCP moorings, and CMAN and COMP stations. The Tortugas fishing grounds (area enclosed by dashed line) includes the center of spawning for *Farfantepenaeus duorarum* (filled ellipse). Northwestern stations: MG=Middle Ground and SK=Sandy Key; Florida Key stations: WH=Whale Harbor and PH=Panhandle; A and B=onshore and offshore ADCP moorings respectively; 1=Long Key CMAN station; 2=NW Florida Bay COMP station. Small map at the left corner indicates major currents in the Gulf of Mexico and off the coast of Florida. CC=Caribbean Current; LC=Loop Current; FC=Florida Current; GS=Gulf Stream.

pink shrimp across the SW Florida shelf that combines the effect of hydrodynamics with larval behavior. Four modes of behavior-related transport were simulated under hydrodynamic conditions occurring on the SW Florida shelf in order that the resulting distances traveled under each condition might be contrasted.

Material and methods

Pink shrimp postlarvae were collected in two regions of Florida Bay to evaluate postulated hypotheses of eastern and western gateways and pathways of larval transport into the bay. The two study sites consisted of two large channels connecting northwestern Florida Bay with the SW Florida shelf of the Gulf of Mexico (Sandy Key Channel [SK], and Middle Ground [MG]); and of more confined tidal channels in the Middle Florida Keys that connect the Bay with the Atlantic Ocean (Whale Harbor [WH], and Panhandle Key [PH]) (Fig. 1). Adjacent mud banks that are occasionally exposed at low tide and over-topped at higher tide stages define these channels. The averaged depth, tidal flow, and cross sectional area of the four channels are summarized in Table 1 to show the different levels of water flow through these pathways. Channels depths are similar, but western channels (Middle Ground and Sandy Key) have higher tidal flows and larger cross sectional areas than the Florida Keys channels (Table 1). Tidal fluctuations are primarily semidiurnal at all stations and have weaker diurnal constituents (Smith, 1998, 2000). Acoustic Doppler velocity meters (ADVMs) that measure continuous velocity and depth (tide and stage) and associated CTD instruments that measure conductivity and temperature were installed at each channel in January 2002. A boat-mounted acoustic Doppler current profiler (ADCP) was used to calculate total discharge across the cross-section of the channel during monthly sampling (Hittle et al., 2001).

Postlarvae were collected monthly in each channel during two nights around the new moon from January 2000 to December 2002. At the PH station sampling began in June 2000 after the original site (Captain Key channel) was abandoned because it had insufficient water flow for effective sampling. Two moored subsurface channel nets (net 1 and net 2) of 0.75-m^2 opening, 1-mm mesh size, and 500-μm mesh in the codend were suspended with floats at 0.5 m depth. Nets were deployed each night before dusk and removed shortly after dawn each day. General Oceanic flowmeters (2030R16, Low Speed Rotor, Miami, FL) were mounted in the mouth of the nets and the volume of water filtered through the nets was calculated for each net. *Farfantepenaeus duorarum* postlarvae were sorted, identified, and preserved in 90% ethanol. The raw catch in each sample was standardized to numbers of postlarvae per 1000 m^3 of water filtered. The average number of postlarvae over the two sampling nights was used as the mean monthly concentration for each net. The average of monthly postlarval concentration for each region (northwestern Florida Bay *vs.* Florida Keys) was compared by using a nonparametric two-way analysis of variance (ANOVA) (Anderson, 2001).

Three 12-hour experiments were conducted in summer 2002 in the SK channel to document the behavioral response of pink shrimp postlarvae to ebb and flood tides. Consecutive pairs of night (i.e. dark) flood and dark-ebb plankton samples were taken hourly from 19:00 to 07:00 h from 9 to 10 July (new moon), 23 to 24 July (full moon), and 8 to 9 August (new moon). In addition, plankton samples were taken for 10 consecutive hours daily on 8 August to verify the response of postlarvae to light. The nonparametric Kruskal-Wallis test and analysis of variance (ANOVA) were used to determine differences in concentration of postlarvae between dark-ebb and dark-flood periods.

To evaluate the possible effect of environmental variables on larval supply to Florida Bay and the pattern of seasonality in postlarval concentrations, available time series of winds and sea surface temperature (SST) on the coastal shelf were examined in relation to our time series of monthly measured larval concentrations. In particular we were looking for a pattern that might help to determine the reason for the marked summer peak in the concentration of postlarvae at the western border of Florida Bay. Time series of hourly winds and sea surface temperature (SST) for the 3-year sampling period were obtained from the Coastal Marine Automated Network (CMAN) station at Long Key, and from the Coastal Ocean Monitoring and Prediction System (COMP) station in NW Florida Bay (Fig. 1). Temperature and wind time series from the Long Key CMAN station and the NW Florida Bay COMP station were highly correlated with each other (r^2=0.9; P<0.01). The longer Long Key time series were used for coastal SST and wind analysis. Wind speed and direction over the Keys, as measured at CMAN sites, are highly coherent (Peng et al., 1999) and useful for explaining currents on the SW shelf (Lee and Williams 1999). Monthly averages of wind vectors and SST were calculated from hourly CMAN time series data (years 2000 to 2002) to examine the effect of winds and SST on the monthly postlarval collections.

Table 1

Mean cross section depth, peak tidal flow, and cross section area of the four channels sampled for pink shrimp (*Farfantepenaeus duorarum*) postlarvae at the northwestern border of Florida Bay, Middle Ground (MG) and Sandy Key (SK), and at the southeastern edge in the Middle Florida Keys, Whale Harbor (WH), and Panhandle Key (PH). Area was calculated at zero (m) of mean sea level.

Station	Depth (m)	Peak tidal flow (m^3/sec)	Cross area (m^2)
MG	3.0	1420	2723
SK	3.1	570	1345
WH	3.3	280	407
PH	2.0	30	74

Time series of current data from two established stations with moored ADCPs and temperature and salinity sensors were used to drive our transport model. Initially, these data were examined to determine whether prevailing currents alone could explain the transport of larvae from the Tortugas spawning grounds to Florida Bay nursery grounds. These stations also were a source of salinity data used in one set of simulations. These stations were located on the inner SW shelf of the Gulf of Mexico, about 30 km from our MG station (Lee et al., 2001) (Fig. 1). This array monitored coastal currents as part of the Florida Bay Circulation and Exchange Study (Lee et al., 2001). The ADCP moorings were located at depths of 6.4 m (mooring A=onshore) and 11.6 m (mooring B=offshore) and recorded data every 30 minutes for a 3-year period (A=21 September 1997 to 15 October 2000; B=22 September 1997 to 17 October 2000). The two ADCP moorings were about 30 km apart. Lee et al. (2001) reported insignificant differences between currents in the vertical for cross-shelf transport in the shallow SW Florida shelf. Wind and current vectors were resolved into cross-shelf (u=east [+] and west [–]) and alongshore (v=north [+] and south [–] constituents). The east-west and north-south displacement of current and wind constituents (half-hour current data and the hourly wind data) was the product of each current and wind constituent by the respective time interval. Correlation analysis was conducted on currents and wind time series.

A harmonic analysis was conducted on the three-year ADCP raw data to define tidal constituents and current magnitude. Period (Pi) and tidal excursion (Ti) were calculated for each constituent from amplitudes (Ai) and frequencies of the constituents as follows:

$$Ti = AiPi/\pi.$$

A simple Lagrangian trajectory model was developed to estimate the drift of planktonic stages. The model used the observed currents at ADCP moorings A and B to calculate trajectories. Because of the lack of information on spatial current variations and the difficulty of extrapolating vertical current profiles from one depth and bottom relief to other conditions, a simple two-dimensional (horizontal) simulation model was used. For the computations we selected the highest bin from the ADCP that had good data throughout the tidal cycle at each station. This bin typically was 1 m below the mean water level at that location and was the highest bin not affected by instrument sidelobe interference. Because instantaneous bottom currents were closely aligned in direction with surface currents and because magnitudes were only 25% lower, the tidal currents were barotropic and we used, therefore, the surface currents to estimate the largest possible distance traveled.

The larval transport was calculated with the equation

$$dx_i/dt = u_i,$$

where x_i = position vector of the larvae;
t = time; and
u_i = the local current velocity.

An Euler (forward in time) integration rule was used to numerically solve this equation. Because only two ADCPs (A and B) provided the current data for this large region, no attempt was made to extrapolate a current field from them. Simulations were run by using current meters A and B independently and by assuming that the current field was spatially homogeneous. The trajectories therefore were two-dimensional in the horizontal plane and the result was identical to a progressive vector diagram. Comparison between the two sets of trajectories (A and B) provided an estimate of the possible variability. The model was used to explore the potential transport of planktonic stages under various assumptions of behavior controlled by environmental cues: 1) a behavioral response to salinity and light, 2) a diel behavior, 3) a diel and tidal behavior throughout the planktonic phase, and 4) an ontogenic change that began with diel behavior and added a tidal behavior at the 15th day. All four hypotheses of larval behavior in relation to transport were simulated in order that their effects on distance traveled could be compared and contrasted. In all simulations, we assumed that larvae traveled only at night. We also assumed that the source of the pink shrimp larvae was located immediately northeast of the Dry Tortugas about 150 km from western Florida Bay (Cummings, 1961; Jones at al., 1970; Roberts, 1986). The program simulated distances traveled by particles for a period of 30 days (e.g., days 1–30, 31–60, 61–90, etc.), a period that corresponds to the estimated developmental period for pink shrimp from the time of hatching to the postlarval stage when larvae are ready for settlement (Dobkin, 1961; Ewald, 1965).

Results

Patterns of postlarval supply, SST, and winds

The monthly influx of postlarvae through the Middle Florida Keys channels (WH and PH) exhibited a highly variable temporal pattern from year to year. Postlarvae were observed every month through the three years (Fig. 2A). Peaks of postlarvae through the Middle Keys channels occurred in May, July, August, and October 2000; in January, July, and October 2001; and in January, March, June, and September 2002. In contrast, the monthly influx of postlarvae through the northwestern stations (SK and MG) showed a strong seasonal pattern with one distinct high peak centered in summer from July through September for each year of the 3-year period (Fig. 2B). The number of postlarvae entering through northwestern Florida Bay was much higher than through the Keys stations. The mean concentration of postlarvae per station over the 3-year period indicated that concentrations of postlarvae entering northwestern Florida Bay through SK and MG channels were about eight times greater than through the Florida Keys channels of WH and PH (Fig. 3). Results from a two-way ANOVA indicated that there was a significant effect of site (northwestern stations *vs.* Florida Key stations) and month on the supply of postlarvae entering Florida Bay (Table 2).

Winds showed a seasonal pattern; the spring and summer were dominated by weak southeasterly winds and the fall and winter, by strong northerly winds (Fig. 2, C–D). The monthly average alongshore showed a weak northward constituent in spring–summer of each year (Fig. 2C). The monthly average cross-shelf winds were consistently negative (toward the west) and showed no seasonality (Fig. 2D). The average temperature over the three-year time series was 26.1°C, and winter temperatures in 2000–01 were lower than in 2001–02 (Fig. 2E). In summer, during the period of peak postlarval immigration through the northwestern stations (MG and SK), the alongshore wind constituent was mainly northward, the cross-shelf wind was westward, and the SST was above average during the three-year period (Fig. 2, A–E). Postlarval concentrations at the northwestern stations were correlated with SST and alongshore winds (Fig. 2, B–E; Table 3). Postlarval concentrations at the Florida Keys stations (WH and PH) were not correlated with either winds or SST.

Subtidal and tidal currents at the SW Florida shelf

Advective displacement derived from two ADCP velocity records indicated that the net current is primarily in the alongshore direction (Fig. 4, A and B). The alongshore flow from onshore mooring A was northward, had a total mean velocity of 0.0062 m/sec, and a total water displacement of 589.3×10^3 m over the three years (Fig. 4A). The cross-shelf flow was westward, had a mean velocity of −0.0005 m/sec, and a total water displacement of -289.7×10^3 m. The alongshore flow from offshore moor-

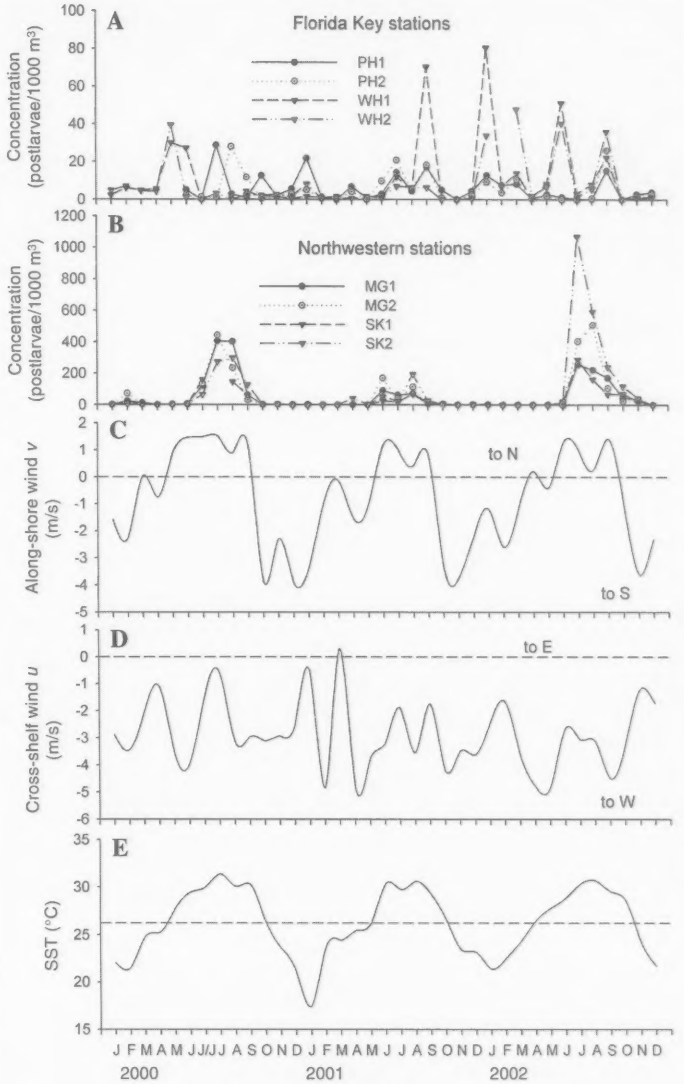

Figure 2

Monthly time series of pink shrimp (*Farfantepenaeus duorarum*) postlarval concentrations, winds, and sea-surface temperature: (**A**) mean concentration of pink shrimp postlarvae at the Florida Key stations of Whale Harbor (WH) and Panhandle (PH); (**B**) mean concentration of pink shrimp postlarvae at the northwestern Florida Bay stations of Middle Ground (MG) and Sandy Key (SK); concentrations of two nets are depicted as 1 and 2; (**C**) alongshore winds (v); (**D**) cross-shelf winds (u); (**E**) sea-surface temperature (SST). Winds and SST data are from Long Key CMAN station.

ing B was southward, had a mean velocity of −0.0038 m/sec and a total water displacement of -364.7×10^3 m (Fig. 4B). The cross-shelf flow was eastward, had a mean speed of 0.0015 m/sec, and a total water displacement of 145.5×10^3 m and a resultant southeastward current. The alongshore winds measured at Long Key were southward and had a total water displacement of 16.1×10^3 m, and the cross-shelf winds were westward and had a total

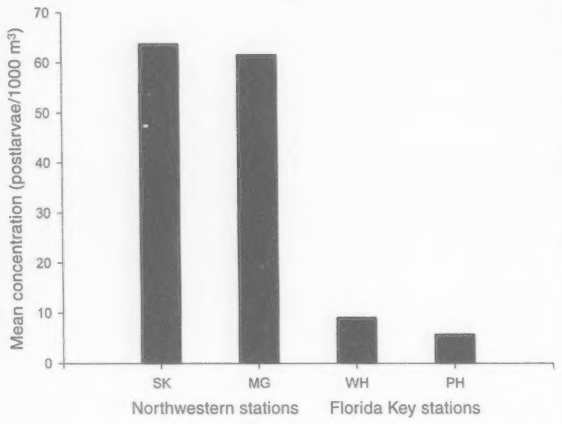

Figure 3

Mean concentration of pink shrimp (*Farfantepenaeus duorarum*) postlarvae over a three-year period at each sampling station: northwestern Florida Bay stations—Middle Ground (MG) and Sandy Key (SK); Florida Key stations—Whale Harbor (WH) and Panhandle (PH).

Table 2

Results of a nonparametric two-way ANOVA of the effect of site and month on pink shrimp (*Farfantepenaeus duorarum*) postlarvae entering Florida Bay. $P<0.05$ is indicated with an asterisk. SS=sum of squares; MS=mean of squares.

Factor	df	SS	MS	*F*	*P*
Month	80	756.7	9.5	5.6	0.007*
Site	1	65.9	65.9	39.3	0.002*
Month × site	1	1191.5	1191.5	711.3	0.007*
Error	461	772.2	1.7		

Table 3

Correlation coefficients of pink shrimp (*Farfantepenaeus duorarum*) postlarval concentrations with sea surface temperature (*SST*), cross-shelf wind (*U*), and alongshore wind (*V*) at the four sampling stations of MG= Middle Ground, SK= Sandy Key, WH= Whale Harbor and PH= Panhandle. Environmental data are from Long Key CMAN station. Significant correlations ($P<0.05$) are indicated with an asterisk.

	SST	*U*	*V*
MG	0.82*	−0.025	0.67*
SK	0.73*	0.11	0.57*
WH	0.15	0.16	0.36
PH	−0.17	0.14	−0.09

water displacement of -86.3×10^3 m (Fig. 4C). The subtidal currents in this region are very weak as also observed by other investigators (Koczy et al., 1960; Rehrer et al., 1967). Correlation coefficients between winds and currents in the alongshore direction (v) were significant for both onshore and offshore currents time series (Table 4). Correlation coefficients between winds and currents in the cross-shelf direction were higher in the onshore than in the offshore data series. This analysis indicated that prevailing currents, overall, were not favorable to passive transport of larvae from the Tortugas to western Florida Bay.

A harmonic analysis of the 3-year ADCP data showed that semidiurnal tidal constituents (M_2, S_2, K_2, and N_2, see Table 5 for explanation of abbreviations) are dominant on the SW Florida shelf. M_2 was the strongest tidal constituent and its east-west constituent explained 95% of the total current variance. The east-west amplitude of the M_2 constituent was 0.32 m/s for both moorings, and the north-south was 0.07 m/s for mooring A and 0.04 m/s for mooring B. The east-west amplitude (0.32 m/s) was much stronger than the long-term averaged subtidal cross-shelf constituent at both stations (0.001 m/s). The east-west tidal excursion of the M_2 constituent was similar for both moorings, but a few meters larger on the offshore station (Table 5). This result indicates that it is reasonable to consider that there are similar tidal excursions on the SW shelf up to 50 km.

Ebb versus flood catches

Concentration of postlarvae collected hourly over a complete dark portion of a tidal cycle showed clearly that dark-ebb catches were negligible (<10%) by comparison with dark-flood catches (>90%) (Fig. 5, A–C). Hourly concentrations of postlarvae collected on the dark flood were 92.7% from 9 to 10 July, 90.2% from 23 to 24 July, and 86.9% from 8 to 9 August 2002. A nonparametric Kruskal-Wallis test showed significant differences in catches of postlarvae between dark-ebb and dark-flood periods (Kruskal-Wallis: $H=15.5$, $n=36$, $P<0.001$; (ANOVA: $F=18.6$; $P<0.001$). Samples taken during the day on 8 August confirmed the hypothesis that postlarvae are present mostly at night in the water column (Table 6). A total of 18 postlarvae (31.5 postlarvae/1000 m^3) were captured during 10 consecutive daylight hours, against 2657 (3702.5 postlarvae/1000 m^3) captured during 10 consecutive hours of darkness. Although concentrations of postlarvae tend to increase with the tidal current, these differences were not significant (Kruskal-Wallis: $H=10.3$, $n=36$, $P=0.5$). From 9 to 10 July, no postlarvae were captured during the hours of highest current speed (2:00 to 3:00 h), which coincided with high rain and winds (Fig. 5A). It is not clear whether these factors caused a change of behavior in the postlarvae or a malfunction of the net. From 23 to 24 July, concentration of postlarvae on the dark flood followed the cur-

rent speed; highest catches occurred at the maximum speed and lowest catches at the minimum speed (Fig. 5B). From 8 to 9 August, the highest peak of postlarvae occurred at the end of the dark-flood period when the current had decreased in speed (Fig. 5C).

Transport simulations

Results of channel net sampling showed that the greatest postlarval influx occurred at the northwestern border of the bay, where there was a strong seasonal pattern with maxima from July through September each year. Postlarval concentrations at the northwestern stations were correlated with the alongshore winds and with surface temperature but did not correlate with the cross-shelf winds. However, postlarvae need to travel up to 150 km across the shelf to reach their nursery grounds.

Cross-shelf transport mechanisms were explored by using a Lagrangian trajectory model that simulated the maximum distance traveled by planktonic stages moving at night for a 30-day period. Four scenarios of transport were modeled under different assumptions of behavior:

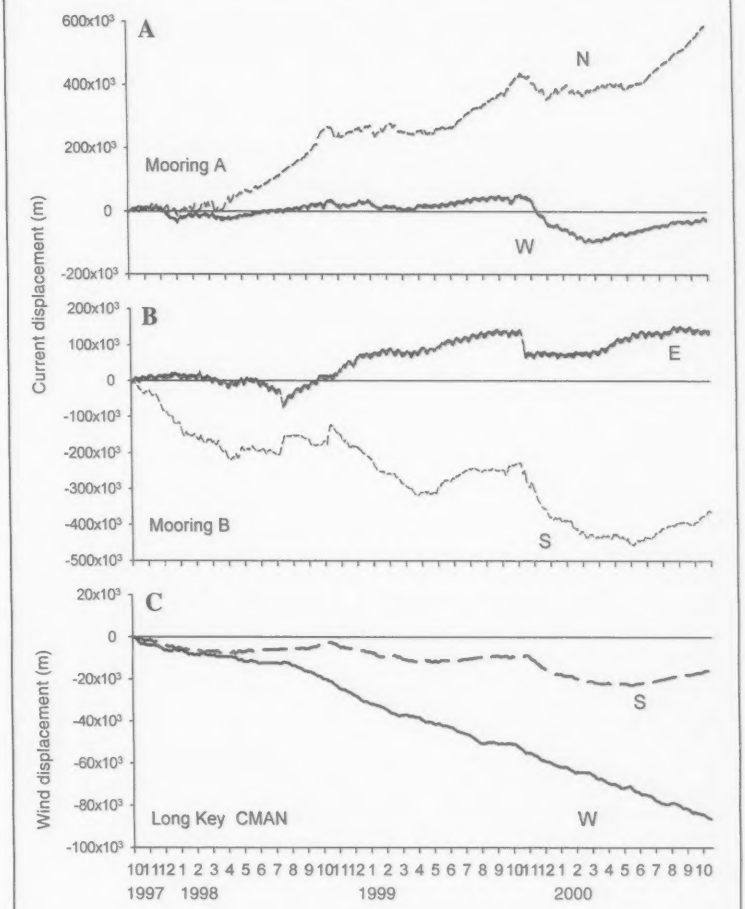

Figure 4

Time series of current and wind displacement, October 1997–October 2000. Current data are from two ADCPs located at the SW Florida shelf, and wind data are from Long Key CMAN station; (**A**) onshore ADCP mooring A, (**B**) offshore ADCP mooring B; see ADCP locations in Figure 1. (**C**) Wind displacement. Alongshore constituents are represented by interrupted lines (N=north [+], S=south [−]) and cross-shelf by continuous lines (E=east [+], W=west [−]).

Scenario 1 With the assumption that planktonic stages (larvae and postlarvae) of pink shrimp respond to light and salinity changes (Hughes 1969a, 1969b), the first simulation postulates that larvae and postlarvae move horizontally with a vertical migratory behavior cued by changes in salinity. Larvae and postlarvae swim to the surface at night when an increase in salinity is detected and remain near the bottom when the salinity decreases.

Onshore mooring The maximum distance traveled in the cross-shelf direction was 98 km eastward and 70% of larvae traveled up to 30 km (Fig. 6A). The average eastward distance in all simulations was 22 km. The maximum displacement occurred in fall-winter. Alongshore distances were as much as 25 km northward (70% of larvae) and 15 km southward (30%) (Fig. 6, A and B).

Offshore mooring The maximum distances traveled in the cross-shelf direction was 100 km (84% of larvae traveled 40 km). Alongshore distances were as much as 15 km northward (70%) and 20 km southward (30%) (Fig. 6, C and D).

Scenario 2 The second simulation assumes that planktonic stages travel at night using the instantaneous current.

Onshore mooring Distances traveled in the cross-shelf direction reached a maximum of 68 km and 75% of larvae traveled only 30 km eastward (Fig 6A). The average eastward distance in all simulations was 15 km. The maximum displacement occurred in spring-summer (May to September 1998) during the first year and in fall-winter (October 1999 to February 2000) during the second and third year. Distances recorded in the alongshore direction were as far as 40 km northward (48% of larvae) and 30 km southward (52%) (Fig. 6, A and B).

Offshore mooring Maximum distance traveled in the cross-shelf direction reached 60 km eastward and 80% of larvae traveled less than 30 km. Distances recorded in the alongshore direction were as far as 40 km northward (51%) and 40 km southward (49%) (Fig. 6, C and D).

Scenario 3 Under the assumption that pink shrimp larvae and postlarvae migrate vertically in a tidal cycle, the third simulation postulates that larvae and postlarvae swim in the water column near the surface at night during the flood tide and remain near the bottom during the ebb tide. In this simulation it is assumed that planktonic stages move by using the eastward current (flood tide) during the postulated 30 days of larval development.

Onshore mooring The maximum distance traveled in the cross-shelf direction was 200 km eastward and 86% of the larvae exceeded 150 km. The average eastward distance in all simulations was 132 km. The maximum larval displacement occurred from December 1999 through March 2000. Distance traveled in the alongshore direction was 45 km northward (70%) and 5 km southward (30%) (Fig. 6, A and B).

Offshore mooring The maximum larval displacement in the cross-shelf direction was 200 km eastward and 85% of the larvae reached 150 km. The maximum eastward displacement occurred in fall and in winter. Distance traveled in the alongshore direction was as much as 40 km northward (82%) and 5 km southward (18%). The maximum distance traveled was recorded in March–April and June 2000 (Fig. 6, C and D).

Scenario 4 In this simulation, it is assumed that there is a change in behavior for pink shrimp larvae—an assumption similar to the one taken in simulations for some Australian penaeid species (Rothlisberg, 1982; Rothlisberg et al., 1995, 1996). Early larval stages (protozoea and myses) migrate vertically in a diel cycle and there is no cross-shelf displacement during the first 15 days of development. Later in development, postlarvae migrate by using tidally induced behavior superimposed on the diel behavior for the remaining 15 days of planktonic development, and the eastward current (flood tide).

Onshore mooring The maximum displacement of larvae in the cross-shelf direction was 100 km eastward

Table 4

Correlation coefficients of wind and current components. *U* and *V* are the east-west and north-south components respectively. Nearsurface currents are from onshore (A) and offshore (B) ADCP moorings over the SW Florida shelf. Wind data are from Long Key CMAN station. Significant correlations ($P<0.05$) are indicated with an asterisk.

	Mooring A		Mooring B	
	onshore		offshore	
	U-current	*V*-current	*U*-current	*V*-current
U-wind	−0.25*	−0.22*	−0.10	−0.06
V-wind	0.26*	0.55*	0.12	0.60*

Table 5

Harmonic analysis results conducted on three years of ADCP data (September 1997–October 2000). Moorings were located at the SW Florida shelf: A (onshore) and B (offshore) moorings. *U* and *V* are the east-west and north-south tidal consistuents, respectively. Explained variance of constituent *U* was 95% and of *V* was 50% (for A), and 96% and 29% (for B), respectively. M2=semidiurnal lunar; S2= semidiurnal solar; N2=semidiurnal larger lunar elliptic; K1-diurnal lunisolar; M1=diurnal smaller lunar elliptic; O1=diurnal principal lunar; K2=semidiurnal lunisolar.

			Tidal constituent *U*		Tidal constituent *V*	
	Tidal constituent	Period (h)	Amplitude (m/sec)	Tidal excursion (m)	Amplitude (m/sec)	Tidal excursion (m)
A	M2	12.42	0.321	4561.7	0.070	993.5
	N2	12.66	0.056	810.8	0.013	191.5
	S2	12.00	0.100	1368.2	0.017	239.3
	K1	23.93	0.049	1332.9	0.015	408.7
	M1	24.84	0.005	139.5	0.001	31.3
	O1	25.82	0.039	1139.1	0.010	289.9
	K2	11.97	0.025	345.6	0.010	135.8
B	M2	12.42	0.323	4593.0	0.038	539.4
	N2	12.66	0.057	828.3	0.007	105.9
	S2	12.00	0.105	1439.7	0.009	129.3
	K1	23.93	0.052	1434.4	0.008	213.9
	M1	24.84	0.003	93.9	0.002	54.1
	O1	25.82	0.043	1278.1	0.002	68.0
	K2	11.97	0.023	319.5	0.005	63.1

and 86% of larvae reached 80 km. The average eastward distance traveled in simulations was 66 km. The maximum distances traveled in the alongshore direction was 25 km northward (70% of larvae) and 10 km southward (30%). The maximum distance traveled was recorded in March–April and June 2000 (Fig. 6, A and B).

Offshore mooring The maximum displacement of larvae in the cross-shelf direction was 90 km eastward and 85% of larvae reached 80 km. Distance traveled in the alongshore direction reached 20 km northward (86% of larvae) and 5 km southward (14%) (Fig. 6, C and D).

Discussion

The monthly influx of pink shrimp postlarvae entering Florida Bay through its northwestern border showed a strong seasonal pattern of annual high peaks in summer over the 3-year period. Postlarval concentrations were correlated with alongshore winds and sea surface temperature. Alongshore winds were seasonal, with a weak northward constituent in spring–summer of each year changing to a strong southward in fall and winter. This seasonal pattern agrees with the general circulation described for the SW Florida shelf, highly dependent on synoptic-scale winds, coupled with a strong seasonality and strong tidal currents (e.g., Weisberg et al., 1996; Wang, 1998; Smith, 2000; Lee et al., 2001). Although tidal currents seem to be the main vehicle of eastward transport for planktonic stages, alongshore winds may be fundamental for moving larvae northward along the SW Florida shelf by avoiding a drift with the Florida Current or with the cyclonic circulation of the gyres that form southwest of the Dry Tortugas (Lee et al., 1994; Fratantoni et al., 1998). Under these circumstances larvae may reach Florida Bay by the shortest route in summer using tidal currents and winds across the shallow SW Florida shelf and entering Florida Bay by its northwestern border. The summer seasonality of postlarval immigration may also be amplified by the seasonality of spawning because higher temperatures induce higher spawning activity (Cripe, 1994) and consequently more recruits to enter the Bay during favorable onshore conditions.

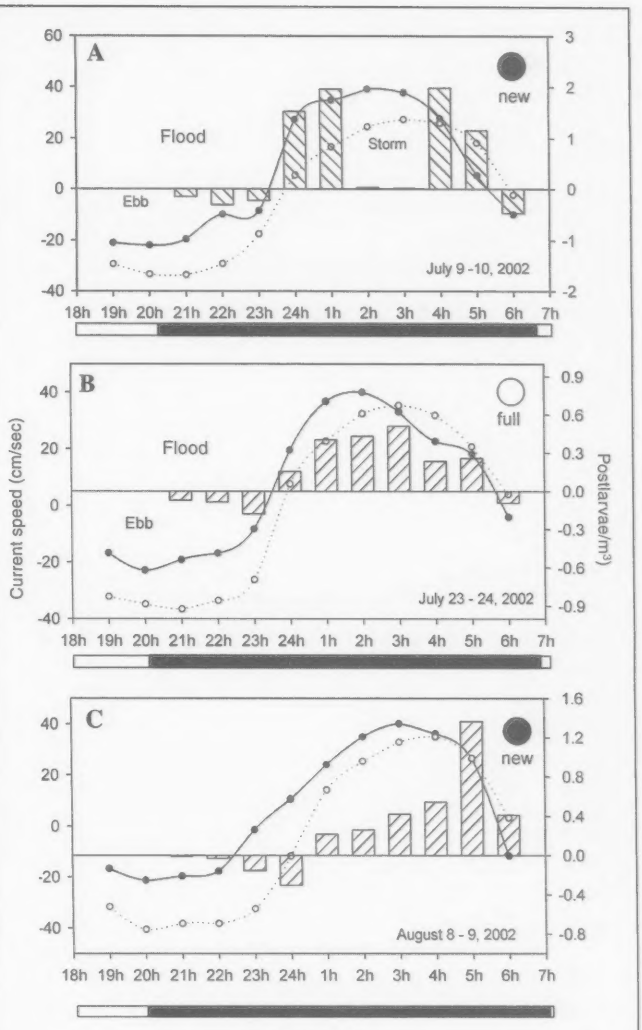

Figure 5

Hourly concentration of pink shrimp (*Farfantepenaeus duorarum*) postlarvae at Sandy Key station (SK) during a complete dark (night) tidal cycle conducted during (**A**) new moon, 9–10 July 2002, (**B**) full moon, 23–24 July 2002, and (**C**) new moon, 8–9 August 2002. Right *y*-axis indicates concentration of postlarvae/m^3; left *y*-axis is tidal current speed (cm/sec) measured by acoustic Doppler velocity meter (filled circle and solid line) and by flowmeter (empty circles and interrupted line). Positive values in the *y*-axes indicate transport into Florida Bay (flood), and negative values transport out of the Bay (ebb). Horizontal bars on the bottom indicate hours of darkness versus light.

Another alternative explanation for the summer larval immigration is that larvae may take advantage of a distinct annual tidal cycle produced in summer every year as a result of the interaction of the periods of the diel vertical migration and the tidal constituent (S_2, K_1) with the annual cycle of the length of the night (Criales et al., 2005). Larvae moving vertically in the water column with a diel behavior can be transported up to 70 km onshore in summer because the eastward current of the tidal constituents matches the diel cycle over extended intervals in the shorter summer nights

Table 6

Data from ebb-flood experiment conducted at Sandy Key (SK) station during 20 consecutive hours. E=ebb, F=flood, L=light, D=dark. VWF = volume of water filtered.

Date	Collection time	Tide stage	Light vs. dark	VWF (m^3)	Number of postlarvae	Concentrations (postlarval m^3)
08/08/2002	11:00	E	L	395.8	7	17.7
08/08/2002	12:00	E	L	535.3	2	3.7
08/08/2002	13:00	F	L	1360.1	0	0.0
08/08/2002	14:00	F	L	1262.3	0	0.0
08/08/2002	15:00	F	L	971.3	8	8.2
08/08/2002	16:00	F	L	531.2	1	1.9
08/08/2002	17:00	F	L	0.0	0	0.0
08/08/2002	18:00	F	L	0.0	0	0.0
08/08/2002	19:00	E	L	450.6	0	0.0
08/08/2002	20:00	E	L	575.6	0	0.0
08/08/2002	21:00	E	D	530.9	5	9.4
08/08/2002	22:00	E	D	477.6	14	29.3
08/08/2002	23:00	E	D	60.7	7	115.4
08/09/2002	0:00	E	D	263.3	87	330.4
08/09/2002	1:00	F	D	648.6	141	217.4
08/09/2002	2:00	F	D	944.3	247	261.6
08/09/2002	3:00	F	D	1164.1	491	421.8
08/09/2002	4:00	F	D	977.5	529	541.2
08/09/2002	5:00	F	D	737.8	1006	1363.6
08/09/2002	6:00	F	D	315.1	130	412.5

(Criales et al., 2005). Therefore, pink shrimp and other fish and invertebrate species that use tidal currents for transport with a daily vertical behavior may take advantage of this annual tidal cycle to improve their chances of reaching coastal nursery habitats.

The monthly influx of postlarvae through the Middle Florida Keys channels exhibited a highly variable seasonal pattern from year to year and from station to station. This section of the Keys coastal waters is frequented by coastal cyclonic eddies that originate at the Dry Tortugas and move downstream at 5–17 km/day along the edge of the shelf at intervals of 1 to 3 months (Fratantoni et al., 1998; Yeung et al., 2001). For planktonic stages, these eddies may serve as a delivery mechanism from offshore spawning grounds to the southeastern border of Florida Bay, allowing an onshore transport by the coastal countercurrent flow generated by the cyclonic circulation (Lee et al., 2001; Yeung et al., 2001; Criales et al., 2003). Episodic, mesoscale events associated with boundary current fronts and eddies may cause high variability in transport (Lee et al., 1994; Limouzy-Paris et al., 1997; Yeung and Lee, 2002). This variability was reflected in the influx of pink shrimp postlarvae through Middle Keys channels (Criales et al., 2003). The influx of postlarvae at WH and PH channels in the present study was also highly variable and there was no correlation with winds or sea surface temperature. Therefore, we hypothesized that the high variability in postlarval influx detected at the Florida Keys channels reflects the temporal and spatial variability associated with the passage of coastal eddies.

Simulations of transport based on current observations indicated that passive larvae could not consistently be advected the estimated 150 km eastward across the shelf between spawning and nursery grounds in 30 days. This is true primarily because of the weak eastern current and the reversing nature of tides. In contrast, planktonic stages (larvae and postlarvae) moving at night with the eastward current (flood tide) can consistently travel 100 to 200 km in 30 days. Hypothetically, 85% of the larvae can be transported far enough from the known spawning grounds of Dry Tortugas to the nursery grounds in western Florida Bay in 30 days. Previous works conducted inside Florida Bay (Tabb et al., 1962; Roessler and Rehrer, 1971) and our own data obtained along the western border of Florida Bay demonstrated the ability of pink shrimp postlarvae to respond to the dark flood tide and to distinguish between day and night. Over 90% of postlarvae were caught in the dark flood period and only a few postlarvae were caught during daylight hours. This behavior needs to be investigated for early larval stages to define the exact age at which larvae begin reacting to change in tides and to environmental cues that trigger the vertical movement in relation to tidal stage. For other penaeid

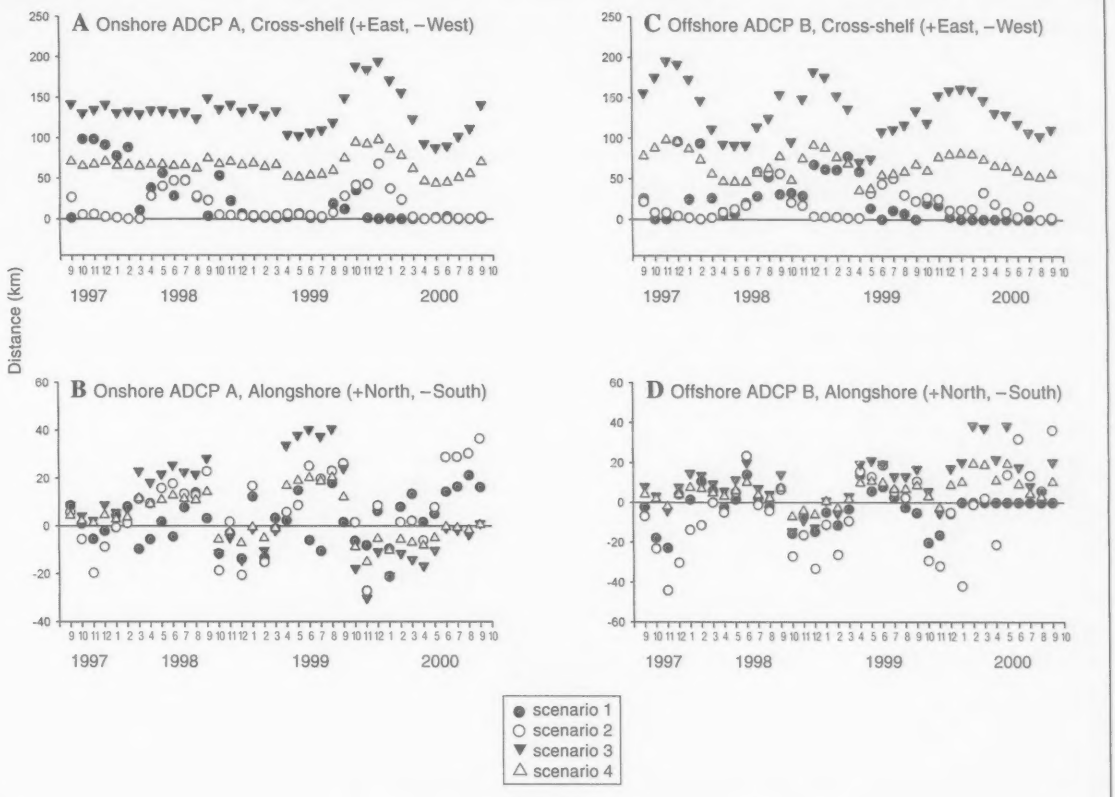

Figure 6

Outputs of transport simulations of pink shrimp (*Farfantepenaeus duorarum*) planktonic stages (larvae and postlarvae) developed from *in situ* current observations and under different scenarios of larval behavior. Each point represents 30 days of travel from September 1997 to October 2000; (**A** and **B**) outputs from onshore ADCP A currents, cross-shelf and alongshore constituents, respectively; (**C** and **D**) outputs from offshore ADCP B currents, cross-shelf and alongshore constituents, respectively. Scenario 1 (filled circles) = planktonic stages migrating with the instantaneous current and a diel behavior (at night) cued by changes in salinity; scenario 2 (empty circles) = planktonic stages migrating with the instantaneous current and a diel behavior (at night); scenario 3 (filled triangles) = planktonic stages migrating with a diel (at night) and a tidal (eastward current) behavior; scenario 4 (empty triangles) = planktonic stages migrating by an induced ontogenic change of behavior (a diel behavior during the first 15 days and a tidally induced behavior (eastward current) superimposed on the diel behavior (at night) for the remaining 15 days).

species (*Fenneropenaeus merguiensis, Penaeus plebejus,* and *Penaeus semisulcatus*) in the Gulf of Carpentaria, Australia, an ontogenic change in behavior has been documented for planktonic stages (Rothlisberg, 1982; Rothlisberg et al., 1995. 1996; Condie et al., 1999). Results of these studies showed that during the first two weeks of planktonic development, larvae migrate vertically in a diel cycle; later in development, the vertical migration is tidally induced. Under those conditions there was little or no systematic cross-shelf displacement of larvae during the first two weeks; afterward, cross-shelf displacement occurred rapidly (Rothlisberg et al., 1995; 1996). Simulation of transport for pink shrimp larvae using this ontogenic change of behavior indicated that planktonic stages can be transported up to 100 km eastward and 85% of larvae reach 80 km. If this behavior applies to pink shrimp, the location of the spawning grounds needs to be reconsidered in favor of areas closer to Florida Bay. Alternatively, the behavior of early planktonic stages may have been underestimated. Results of this research indicated once again the extreme importance of defining larval behavior and including behavior in dispersal models.

The cue(s) that penaeid postlarvae use to migrate in the water column during the flood tide and to return to the bottom on the ebb tide are not completely understood and could be species specific. Hughes (1969a, 1972) demonstrated in laboratory experiments that

pink shrimp postlarvae react to changes in salinity by changing swimming direction. Postlarvae were more active in the water column with increases in salinity, and this finding implies a shoreward displacement with the flood tide. Similar responses to salinity changes have been found for postlarvae of *Farfantepenaeus californiensis, Farfantepenaeus brevirostris, Litopenaeus stylirostris,* and *Litopenaeus vannamei* from the Mexican Pacific (Mair, 1980). The importance of a salinity cue for transport has been questioned for other penaeid species that inhabit hypersaline estuaries (southeast African, western Australia) in which penaeid postlarvae would need to move against a salinity gradient (Penn, 1975; Forbes and Benfield, 1986; Rothlisberg et al., 1995). Our simulations of transport guided by salinity changes indicated that planktonic stages could travel distances in the range of only 30 km in 30 days. This result may indicate that salinity is not the only environmental factor controlling long cross-shelf migrations of pink shrimp. However, Hughes (1969a, 1969b) in early experiments suggested that a salinity cue could apply to postlarvae near the nursery grounds. Changes in water pressure have been proposed as the only environmental factor that triggers the vertical migration of postlarval shrimps in the Gulf of Carpentaria, Australia (Penn, 1975; Forbes and Benfield, 1986; Rothlisberg et al., 1995). Laboratory experiments and numerical models have shown that tiger shrimps (*Penaeus semisulcatus* and *Penaeus esculentus)* larvae switch behavior when the change in water pressure with tides becomes a significant fraction of the total pressure (Rothlisberg et al., 1996; Condie et al., 1999; Vance and Pendrey[2]). This behavior only occurred in larvae above a certain size. However, it still remains to be determined whether, in a natural ecological context, the rates of relative changes of pressure are consistent with the tidal cycle periodicity and are detectable at absolute amounts in order to permit a behavioral response.

By means of simulations of transport, we have identified a potential STST mechanism for planktonic pink shrimp to migrate the estimated 150 km in 30 days from spawning to nursery grounds over the Florida shelf. Organisms inhabiting coastal ecosystems dominated by tides have the potential to control their cross-shelf movement through STST (Shanks, 1995). The extent of the transport depends on the speed of the tidal current and the time that organisms spend in the water column. Success in reaching the nursery grounds depends upon the stage in larval or postlarval development when the tidal behavior is added. A dependence on tidal currents for the entire larval transport period was postulated for *Melicertus latisultacus* in Western Australia (Penn, 1975). The shrimp *Lucifer faxoni* is the only species for which a STST mechanism across the shelf has been shown (Woodmansee, 1966). Strong tidal currents and several coastal sources of fresh water define the spawning grounds of the wide and shallow SW Florida shelf (Lee et al., 2001; Jurado, 2003). Under these conditions, parts of the SW Florida shelf may behave as an estuary in which planktonic pink shrimp may easily recognize tides by means of endogenous behavior or environmental variables.

From this study we determined that the greatest influx of postlarval pink shrimp occurred at the northwestern border of Florida Bay in summer. Postlarvae entering Florida Bay through the channels of the Middle Florida Keys occurred at a much lower magnitude and there were only sporadic peaks and no apparent seasonality in influx. The transport mechanism of planktonic stages of pink shrimp across the SW Florida shelf seems to depend heavily on semidiurnal tides and larval behavior, and much less on seasonal winds. The response of postlarvae to the tidal currents was clearly observed at the western margin of Florida Bay. Such behavior needs to be explored in early stages to define the age at which larvae begin to respond to tides, the location on the Florida shelf at which this response occurs, and the specific environmental cues linked to such behavior. With this information, more realistic simulations of transport can be made with a complete hydrodynamic model that would incorporate spatial and vertical variations in currents. Depending on the resulting transport, the location of spawning grounds may be better defined, leading to better protection of this valuable fishery resource. Information on recruitment variability and key environmental factors affecting larval transport are essential to accurately interpret stock assessments, maintain the ecological integrity of both spawning grounds and nursery grounds, and to effectively manage the pink shrimp fishery.

Acknowledgments

We are especially grateful to Thomas Lee and Elizabeth Williams (RSMAS, University of Miami), Elizabeth Johns, Ryan Smith, Shailer Cummings, and Nelson Melo (NOAA/AOML, Miami), and Ned Smith (Harbor Branch Oceanographic Institute) for providing ADCP data and valuable comments; to William Richards (NMFSC/NOAA Miami) and Robert Cowen (RSMAS, University of Miami) for their constructive comments and support; to Hernando Cardenas (NMFSC) for his assistance sorting plankton samples; to Andre Daniels (USGS, Miami), for his valuable support of fieldwork; and to the personnel involved in collecting and managing data from C-MAN and COMP stations. This research was funded by the NOAA South Florida Ecosystem Resto-

[2] Vance D. J., and R. C. Pendrey. 2001. Vertical migration behaviour of postlarval penaeid prawns: a laboratory study of the effect of tide, water depth and day/night. *In* The definition of effective spawning stocks of commercial tiger prawns in the Northern prawn fishery and king prawns in the eastern king prawn fishery-behaviour of postlarval prawns, p. 28–52. Fisheries Research and Development Corporation (FRDC) Final Report (Project 97/108), 68 p. CSIRO Marine Research Laboratories, P.O. Box 120, Cleveland, Qld. 4163, Australia.

ration Prediction and Modelling (SFERPM) program through a cooperative agreement between Southeast Fisheries Science Center, USGS and CIMAS, RSMAS, University of Miami, and the DOI Critical Ecosystems Studies Initiative of the Everglades Restoration Program. The sampling that supported this research was conducted pursuant to National Park Service Permit no. EVER-2003-SCI-0109 and Florida Fish and Wildlife Conservation Commission Special Activity License no. 03SR-502.

Literature cited

Allen, D. M., J. H. Hudson, and T. J. Costello.
1980. Postlarval shrimp (*Penaeus)* in the Florida Keys: species, size, and seasonal abundance. Bull. Mar. Sci. 30:21–33.

Anderson, M. J.
2001. A new method for non-parametric multivariate analysis of variance. Aust. Ecol. 26: 32–46.

Browder, J. A., Z. Zein-Eldin, M. M. Criales, M. B. Robblee, S. Wong, T. L. Jackson, and D. Johnson.
2002. Dynamics of pink shrimp (*Farfantepenaeus duorarum)* recruitment potential in relation to salinity and temperature in Florida Bay. Estuaries 25:1355–71.

Condie S. A., N. R. Loneragan, and D. J. Die.
1999. Modelling the recruitment of tiger prawns *Penaeus esculentus* and *P. semisulcatus* to nursery grounds in the Gulf of Carpentaria, northern Australia: implications for assessing stock-recruitment relationships. Mar. Ecol. Prog. Ser. 178:55–68.

Cowen, R. B.
2002. Larval dispersal and retention and consequences for population connectivity. *In* Coral reef fishes: dynamics and diversity in a complex ecosystem (P. Sale, ed.), p. 149–170. Academic Press, London.

Criales, M. M., M. J. Bello, and C. Yeung,
2000. Diversity and recruitment of penaeoid shrimps at Bear Cut, Biscayne Bay, Florida. Bull. Mar. Sci. 67:773–788.

Criales, M. M., and T. N. Lee.
1995. Larval distribution and transport of penaeoid shrimps during the presence of the Tortugas Gyre in May–June1991. Fish. Bull. 93:471–482.

Criales, M. M., and M. F. McGowan.
1994. Horizontal and vertical distribution of penaeidean and caridean larvae and micronektonic shrimps in the Florida Keys. Bull. Mar. Sci. 54:843–856.

Criales, M. M., J. Wang, J. A. Browder, and M. B. Robblee.
2005. Tidal and seasonal effect of transport of pink shrimp postlarvae. Mar. Ecol. Prog. Ser. 286:231–238.

Criales, M. M., C. Yeung, D. Jones, T. L. Jackson, and W. J. Richards.
2003. Variation of oceanographic processes affecting the size of pink shrimp (*Farfantepenaeus duorarum*) postlarvae and their supply to Florida Bay. Estuar. Coast. Shelf Sci. 57 (3): 457–468.

Cripe, G. M.
1994. Induction of maturation and spawning of pink shrimp, *Penaeus duorarum*, by changing water temperature, and survival and growth of young. Aquaculture 128:255–260.

Cummings, D. C.
1961. Maturation and spawning of pink shrimp, *Penaeus duorarum* Burkenroad. Trans. Am. Fish. Soc. 90: 462–468.

Dall, W., B. J. Hill, P. C. Rothlisberg, and D. J. Staples.
1990. The biology of Penaeidae. Adv. Mar. Biol. 27, 489 p.

Dobkin, S.
1961. Early development stages of pink shrimp, *Penaeus duorarum*, from Florida waters. Fish. Bull. 61: 321–349.

Eldred, J. W., G. T. Martin, and E. A. Joyce Jr.
1965. Seasonal distribution of penaeid larvae and postlarvae of the Tampa Bay area, Florida. Fl. Board Conserv. Mar. Res. Lab., Tech. Ser. 44, 47 p.

Ewald, J. J.
1965. The laboratory rearing of pink shrimp, *Penaeus duorarum* Burkenroad. Bull. Mar. Sci. 15(2):436–449.

Forbes, A. T., and M. C. Benfield.
1986. Tidal behaviour and post-larval penaeid prawns (Crustacea: Decapoda: Penaeidae) in a southeast African estuary. J. Exp. Mar. Biol. Ecol. 102:23–34.

Forward, R. B., and R. A. Tankersley.
2001. Selective tidal-stream transport of marine animals. Oceanog. Mar. Biol. 39:305–353.

Fratantoni, P. S., T. N., Lee, G. P. Podesta, and F. Müller-Karger.
1998. The influence of Loop Current perturbations on the formation and evolution of Tortugas eddies in the southern Straits of Florida. J. Geophys. Res. 103:24759–79.

Garcia, S., and L. Le Reste.
1981. Life cycles, dynamics, exploitation and management of coastal penaeid shrimp stocks. FAO Tech. Paper 203, 215 p. FAO, Rome.

Hittle, C., E. Patino, and M. Zucker.
2001. Freshwater flow from estuarine creeks into northeastern Florida Bay. USGS Water-Resources Invest. Rep. 01-4164, 32 p.

Hughes, D. A.
1969a. Responses to salinity change as a tidal transport mechanism of pink shrimp, *Penaeus duorarum* Burkenroad. Biol. Bull. 136:45–53.
1969b. Evidence for the endogenous control of swimming in pink shrimp, *Penaeus duorarum*. Biol. Bull. 136:398–404.
1972. On the endogenous control of tide-associated displacements of pink shrimp, *Penaeus duorarum* Burkenroad. Biol. Bull. 142:271–280.

Iversen, F. S., A. E. Jones, and C. P. Idyll.
1960. Size distribution of pink shrimp, *Penaeus duorarum*, and fleet concentrations on the Tortugas fishery grounds. U.S. Fish. Wild. Ser. Spec. Sci. Rep. 356: 1–62.

Jones, A. C., D. E. Dimitriou, J. J. Ewald, and J. H. Tweedy.
1970. Distribution of early developmental stages of pink shrimp, *Penaeus duorarum*, in Florida water. Bull Mar. Sci. 20:634–661.

Jurado, J. L.
2003. The dynamics of diatom blooms and silicon cycling in coastal waters of the southwestern Florida shelf and northwestern Florida Bay. Ph.D. diss, 268 p. Univ. Miami, Miami, FL.

Klima E. F., G. A. Matthews, and F. J. Patella.
1986. Synopsis of the Tortugas pink shrimp fishery, 1960-1983, and the impact of the Tortugas Sanctuary. North Am. J. Fish. Manag. 6:301–310.

Koczy, F. F., M. O.Rinkel, and S. J. Niskin.
1960. The current patterns on the Tortugas shrimp grounds. Proc. Gulf Carib. Fish. Inst. 12th Annual Sess., Nov. 1959:112–125.

Lee, T. N. M. E. Clarke, E. Williams, A. F. Szmant, and T. Berger.
1994. Evolution of the Tortugas Gyre and its influence on recruitment in the Florida Keys. Bull. Mar. Sci. 54:621–646.

Lee, T. N, E. Johns, D. Wilson, E. Williams, and N. P. Smith.
2001. Transport processes linking south Florida coastal ecosystems. *In* Linkages between ecosystems in the South Florida hydroscape (J. Porter and K. Porter, eds.), p 309–342. CRC Press, Boca Raton, FL.

Lee, T. N., and E. Williams.
1999. Mean distribution and seasonal variability of coastal currents and temperature in the Florida Keys with implications for larval recruitment. Bull Mar. Sci. 64:35–56.

Limouzy-Paris, C., H. C. Graber, D. L. Jones, A. W. Röpke, and W. J. Richards.
1997. Translocation of larval coral reef fishes via submesoscale spin-off eddies from the Florida Current. Bull. Mar. Sci. 60: 966–83.

Mair, J. McD.
1980. Salinity and water-type preferences of four species of postlarval shrimps (*Penaeus)* from west Mexico. J. Exp. Mar. Biol. Ecol. 45:69–82.

Munro, J. L., A. C. Jones, and D. Dimitriou.
1968. Abundance and distribution of the larvae of the pink shrimp (*Penaeus duorarum*) on the Tortugas Shelf of Florida, August 1962–October 1964. Fish. Bull. 67:165–181.

Nance, E. F., and F. J. Patella.
1989. Review of the Tortugas shrimp fishery from May 1987 to January 1989. NOAA Tech.Memo., NMFS-SEFC-238, 11 p.

Peng, G., C. N. K. Mooers, and H. Graber.
1999. Coastal winds in South Florida. J. Appl. Meteor. 38:1740–1757.

Penn, J. W.
1975. The influence of tidal cycles on the distribution pathway of *Penaeus latisulcatus* Kishinouye in Shark Bay, Western Australia. J. Mar. Freshw. Res. 26:93–102.

Rehrer, R., A. C. Jones, and M. A. Roessler.
1967. Bottom water drift on the Tortugas Grounds. Bull. Mar. Sci. 17:562-575.

Roberts, T. W.
1986. Abundance and distribution of pink shrimp in and around the Tortugas Sanctuary, 1981–1983. North Am. J. Fish. Manag. 6:311–327.

Roessler M. A., and G. Rehrer.
1971. Relation of catches of postlarval pink shrimp in Everglades National Park, Florida, to the commercial catches on the Tortugas Grounds. Bull. Mar. Sci. 21 (4):790–805.

Rothlisberg, P. C.
1982. Vertical migration and its effect on dispersal of penaeid shrimp larvae in the Gulf of Carpentaria, Australia. Fish. Bull. 80:541–554.

Rothlisberg, P. C., J. A. Church, and C. Fandry.
1995. A mechanism for near-shore density and estuarine recruitment of post-larval *Penaeus plebejus* Hess (Decapoda, Penaeidae). Estuar. Coast. Shelf Sci. 40: 115–138.

Rothlisberg, P. C., J. A. Church, and A. M. G. Forbes.
1983. Modelling advection of vertically migrating shrimp larvae. J. Mar. Res. 41:511–538.

Rothlisberg, P. C., P. D. Craig, and J. R. Andrewartha.
1996. Modelling penaeid prawn larval advection in Albatross Bay, Australia: defining the effective spawning population. Mar. Freshw. Res. 47:157–168.

Shanks, A. L.
1995. Mechanisms of cross-shelf dispersal of larval invertebrates and fish. *In* Ecology of marine invertebrate larvae (L. R. McEdward, ed.), p. 323–367. CRC Press, Inc., Boca Raton, FL.

Sheridan, P.
1996. Forecasting the fishery for pink shrimp *Penaeus duorarum*, on the Tortugas Grounds, Florida. Fish. Bull. 94:743–755.

Smith, N. P.
1998. Tidal and long-term exchanges through channels in the Middle and Upper Florida Keys. Bull. Mar. Sci. 62:199–211.
2000. Transport across the western boundary of Florida Bay. Bull. Mar. Sci. 66:291–304.

Sponaugle, S., R. K. Cowen, A Shanks, S. G. Morgan, J. M. Leis, J. Pineda, G. W. Boehlert, M. J. Kingsford, K.C. Linderman, C. Grimes, and J. L. Munro.
2002. Predicting self-recruitment in marine populations biophysical correlations and mechanisms. Bull. Mar. Sci. 70(1) suppl.:341–375.

Tabb, D. C., D. L Dubrow, and A. E. Jones.
1962. Studies on the biology of pink shrimp *Penaeus duorarum* Burkenroad, in Everglades National Park, Florida. Fla. Board Conser. Tech. Ser. 37:1–32.

Temple, R., and C. C. Fischer.
1965. Vertical distribution of the planktonic stages of penaeid shrimp. Inst. Mar. Sci. Publ. 10:59–67.

Wang, J. D.
1998. Subtidal flow patterns in western Florida Bay. Estuarine Coast. Shelf Sci. 46:901–915.

Weisberg, R. H., B. D. Black, and J. Yang.
1996. Seasonal modulation of the West Florida continental shelf circulation. J. Geophys. Res. 23:2247–2250.

Wenner, E. L., D. M. Knott, C. A. Barans, S. Wilde, J. O. Blanton, and J. Amft.
2005. Key factors influencing transport of white shrimp (*Litopenaeus setiferus*) postlarvae into the Ossabaw Sound system, Georgia, USA. Fish. Ocean. 14(3)175–194.

Woodmansee, R. A.
1966. Daily vertical migration of *Lucifer*. Planktonic numbers in relation to solar and tidal cycles. Ecology 47:847–850.

Yeung, C., D. L. Jones, M. M. Criales, T. L. Jackson, and W. J. Richards.
2001. Influence of coastal eddies and counter-currents on the influx of spiny lobster, *Panulirus argus*, postlarvae into Florida Bay: influence of eddy transport. Mar. Freshw. Res. 52:1217–32.

Yeung, C., and T. L. Lee.
2002 Larval transport and retention of the spiny lobster, *Panulirus argus*, in the coastal zone of the Florida Keys, USA. Fish. Oceanog. 11:86–309.

Biology and assessment of the painted sweetlips (*Diagramma pictum* (Thunberg, 1792)) and the spangled emperor (*Lethrinus nebulosus* (Forsskål, 1775)) in the southern Arabian Gulf

Edwin M. Grandcourt
Thabit Z. Al Abdessalaam
Ahmed T. Al Shamsi
Franklin Francis

Marine Environment Research Centre
Environmental Research and Wildlife Development Agency
Corniche Road
P. O. Box 45553
Khalidiya
Abu Dhabi, United Arab Emirates
E-mail address (for E. M. Grandcourt): egrandcourt@erwda.gov.ae

Abstract—The population biology and status of the painted sweeplips (*Diagramma pictum*) and spangled emperor (*Lethrinus nebulosus*) in the southern Arabian Gulf were established by using a combination of size-frequency, biological, and size-at-age data. Transverse sections of sagittal otoliths were characterized by alternating translucent and opaque bands that were validated as annuli. Comparisons of growth characteristics showed that there were no significant differences ($P>0.05$) between sexes. There were well defined peaks in the reproductive cycle, spawning occurred from April to May for both species, and the mean size at which females attained sexual maturity was 31.8 cm fork length (L_F) for *D. pictum* and 27.6 cm (L_F) for *L. nebulosus*. The mean sizes at first capture (21.1 cm L_F for *D. pictum* and 26.4 cm L_F for *L. nebulosus*) were smaller than the sizes for both at first sexual maturity and those at which yield per recruit would be maximized. The range of fishing-induced mortality rates for *D. pictum* (0.37–0.62/yr) was substantially greater than the target (F_{opt}=0.07/yr) and limit (F_{limit}=0.09/yr) estimates. The range of fishing-induced mortality rates for *L. nebulosus* (0.15/yr to 0.57/yr) was also in excess of biological reference points (F_{opt}=0.10/yr and F_{limit}=0.13/yr). In addition to growth overfishing, the stocks were considered to be recruitment overfished because the biomass per recruit was less than 20% of the unexploited levels for both species. The results of the study are important to fisheries management authorities in the region because they indicate that both a reduction in fishing effort and mesh-size regulations are required for the demersal trap fishery.

Manuscript submitted 29 December 2003 to the Scientific Editor's Office.
Manuscript approved for publication 11 July 2005 by the Scientific Editor.
Fish. Bull. 104:75–88 (2006).

The painted sweetlips (*Diagramma pictum* (Thunberg, 1792)), is a member of the family Haemulidae and is widely distributed throughout the Indo-West Pacific, from the Red Sea and East Africa to Japan and New Caledonia (Randall et al., 1997). Adults are found in shallow coastal waters and coral reefs down to a depth of 80 m, and juveniles are often found in weedy areas (Smith and McKay, 1986). The diet of this species consists of benthic invertebrates and fishes (Sommer et al., 1996). It is a relatively large tropical species attaining 100 cm fork length and 6 kg in total weight (Torres, 1991); consequently it is exploited throughout its range with a variety of gears, including handlines, traps, and nets (Fischer and Bianchi, 1984). *Diagramma. pictum* has a gonochoristic reproductive mode and spawning occurs annually with one clear seasonal peak (Breder and Rosen, 1966).

Fishes of the family Lethrinidae are abundant in the coastal tropical and subtropical Indo-Pacific (Young and Martin, 1982). The spangled emperor (*Lethrinus nebulosus* (Forsskål, 1775)), is distributed throughout the Indo-West Pacific from the Red Sea and East Africa to southern Japan and Samoa. It is found in a variety of habitats including coral reefs, sea grass beds and mangroves from near shore to a depth of 75 m (Randall, 1995). Adults are either solitary or are found in small schools, and juveniles form large schools in shallow, sheltered sandy areas. The diet of this species is mainly composed of mollusks, crustaceans, polychaete worms, and echinoderms (Fischer and Bianchi, 1984).

As with other representatives of the family Lethrinidae, *L. nebulosus* is a protogynous hermaphrodite, and sexual transformation from female to male occurs over a wide range of sizes (Young and Martin, 1982; Ebisawa, 1990). Lethrinids are considered to have long spawning seasons, running from spring to at least early fall, with spring and fall peaks. Spawning occurs after dark for most species in aggregations along the inner or outer edge of the fringing reef (Johannes, 1981). *Lethrinus nebulosus* is a large tropical species reaching 80.0 cm total length and 8.4 kg total weight (Randall, 1995) and is exploited throughout its range with a variety of gears (Fischer and Bianchi, 1984).

Both species form an important part of fisheries landings in the southern Arabian Gulf, where they are mainly caught with dome-shaped wire traps that have a hexagonal mesh of approximately 3.5 cm in diameter. Traps are either set individually or in strings from traditional wooden dhows, sets are made to a maximum depth of 40 m, and vessels fish an

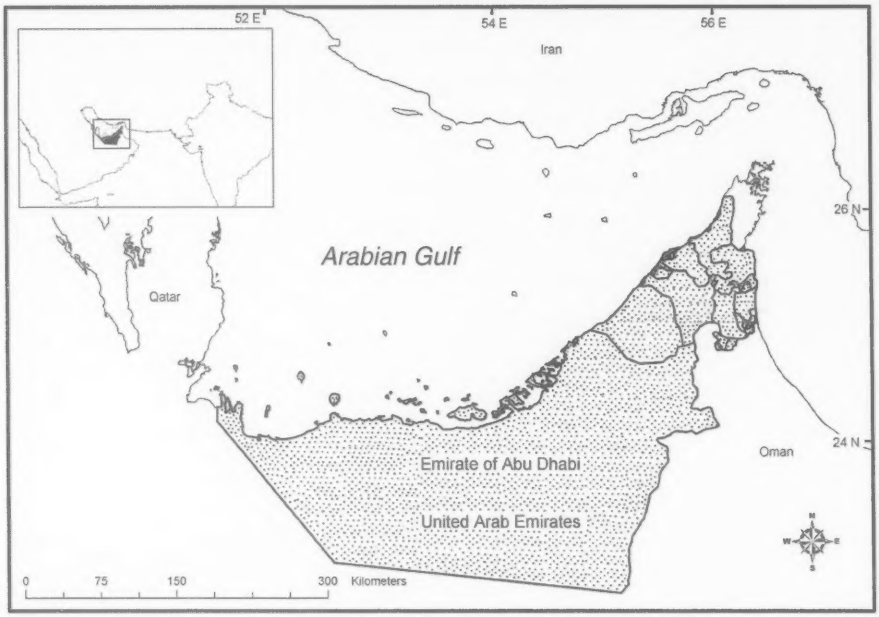

Figure 1

Study site (stippled area) showing the location of the Emirate of Abu Dhabi, off the coast of which data were collected for the painted sweetlips (*Diagramma pictum*) and spangled emperor (*Lethrinus nebulosus*) from commercial catches.

average of 210 traps each. Collection of catch-and-effort data for the fisheries of the Emirate of Abu Dhabi in the United Arab Emirates was initiated in 2001. However, many species, including *D. pictum* and *L. nebulosus*, are recorded to the family level, and therefore the use of statistical catch-at-age methods can not be used for conducting assessments at the species level. Landings of haemulids (predominantly *D. pictum*) and lethrinids (predominantly *L. nebulosus*), totaled 719 and 2911 metric tons, respectively, in the Emirate of Abu Dhabi during 2003 (Grandcourt et al.[1]). Despite the limited time scale for which catch and effort data are available, there has been an overall increase in fishing effort and catches since 2001.

Many of the fish populations in the Arabian Gulf have been heavily exploited (Samuel et al., 1987), and fishing effort may have already been above optimum levels for most demersal species (Siddeek et al., 1999). The expansion of the fishing fleet of the United Arab Emirates and the lack of appropriate data on most stocks underscore the need to assess the fisheries resources of the region. The goal of this study was to evaluate the status of *D. pictum* and *L. nebulosus* and to provide biological reference points and other pertinent information required for management. Specific objectives included establishing key demographic parameters by using validated age estimates, identifying reproductive characteristics and conducting yield-per-recruit analyses for the selected study species.

Materials and methods

Study site and sampling protocol

Size-frequency data were collected from commercial catches made off the coast of the Emirate of Abu Dhabi in the United Arab Emirates (Fig. 1) between September 2000 and March 2003. Fish were selected at random from landings and fork length (L_F) was recorded to the nearest cm by using a measuring board. Monthly target sample sizes were 500 individuals per species.

Biological data was collected from specimens purchased from commercial catches between June 2002 and May 2003. Samples were obtained from 30 individuals of each species from a representative size range during the last week of each month. Standard length (L_S), fork length (L_F), and total length (L_T) were recorded to the nearest mm by using a measuring board. Whole wet weight was measured with an electronic balance and recorded to the nearest g. The sex of a fish was determined by macroscopic examination of the gonad, which

[1] Grandcourt, E. M., F. Francis, A. Al Shamsi, K. Al Ali, and S. Al Ali. 2004. Annual fisheries statistics for Abu Dhabi Emirate 2003, 87 p. Environmental Research and Wildlife Development Agency, P.O. Box 45553, Government of Abu Dhabi, United Arab Emirates.

was removed and subsequently weighed to 0.1 g with an electronic balance.

Sagittal otoliths were extracted, cleaned in water, dried, and stored in seed envelopes. One of each pair of sagittae was weighed to 0.1 mg, burnt on a hotplate until it changed to a dark brown color, and embedded in epoxy resin. Transverse sections through the nucleus (of approximately 200–300 μm thickness) were obtained by using a twin blade saw. Sections were mounted on glass slides and examined with a low-power microscope and transmitted light.

Age and growth

The number of opaque bands in transverse sections was recorded in addition to the optical characteristics of the outer margin (opaque or translucent). The proportion of samples with opaque or translucent margins was calculated for each month and used to infer the timing and periodicity of increment formation. The age at which the first opaque band formed was calculated as the time between the mean birth date and the time of formation of opaque bands. Subsequently, the absolute age was calculated as the age at formation of the first band plus the number of opaque bands outside the first band and the time between the formation of the last band and capture. In order to establish the relationship of the timing of opaque zone formation with trends in sea water temperature, time series data were converted by using the scaling process given in Newman and Dunk (2003).

Growth was investigated by fitting the von Bertalanffy growth function (von Bertalanffy, 1938) to size-at-age data using standard nonlinear optimization methods. The model was fitted to pooled data and each sex separately. The von Bertalanffy growth function is defined as follows:

$$L_t = L_\infty\,(1 - e^{-k\,(t-t_0)}),$$

where L_t = length at time t;
L_∞ = the asymptotic length;
k = the instantaneous growth coefficient; and
t_0 = the hypothetical time at which length is equal to 0.

Growth curves were compared between sexes for each species by using the analysis of residual sums of squares method of Chen et al. (1992).

The growth performance index Φ' (Gayanilo and Pauly, 1997) was calculated in order to provide a basis for the comparison of growth characteristics in terms of length:

$$\Phi' = \Phi - 2/3\,\log_{10}(a),$$

where $\Phi = \log_{10}(k) + 0.67\,\log_{10}(W_\infty)$ and $W_\infty = aL_\infty{}^3$.

The constant, a, was derived from length-weight relationships and k and L_∞ were obtained from the von Bertalanffy growth function.

Parameters of the length-weight relationship were obtained by fitting the power function $W = aL_F{}^b$ to length and weight data where W is the total wet weight, a is a constant determined empirically, L_F is the fork length, and b is close to 3.0 for species with isometric growth. Ratios of total length (L_T) to fork length (L_F) were also calculated for each species.

Reproduction

The mean size at first sexual maturity was estimated for females by fitting the logistic function to the proportion of mature fish in 2-cm (L_F) size categories. The mean size at first maturity was taken as that at which 50% of individuals were mature. Gonadosomatic indices, calculated by expressing gonad weight as a proportion of total body weight, were plotted against the sample period by month to establish the timing and seasonality of spawning. The mean birth date was estimated from patterns in reproductive indices.

Population sex ratios were examined by using χ^2 goodness-of-fit tests. Independent tests were conducted to determine whether sex ratios differed significantly from unity for whole samples and for size and age categories within samples. The probability level was set at 0.05 (α=0.05) and Yates's correction factor was used on account of there being only one degree of freedom for each comparison. Juvenile retention was calculated as the proportion of fish in aggregated size-frequency samples below the mean size at first sexual maturity.

Mortality and selectivity

Size-at-age data were used to construct age-length keys following the method of Ricker (1975) and these were used to convert aggregated length-frequency data into age-frequency distributions. The number of fish above the age at which fish were fully recruited to the fishery was calculated as a proportion of the total number of fish. The annual instantaneous rate of total mortality (Z) was subsequently determined with the age-based catch curve method (Beverton and Holt, 1957). The natural logarithm of the number of fish in each age class was plotted against the corresponding age, and Z (±95% CI) was estimated from the descending slope of the best fitting line by using least-squares linear regression. Initial ascending points representing fish that were not fully recruited to the fishery were excluded from the analyses.

The annual instantaneous rate of total mortality was also estimated with the length-converted catch method of Pauly (1983). Pooled length-frequency samples were converted into relative age-frequency distributions by using parameters of the von Bertalanffy growth function. The natural logarithm of the number of fish in each relative age group divided by the change in relative age was plotted against the relative age, and Z (±95% CI) was estimated from the descending slope of the best fitting line with least-squares linear regression. The estimates of Z from age-based and length-

converted catch curves were compared by using a modified *t*-test (Sokal and Rohlf, 1995).

Backwards extrapolation of the length-converted catch curves was used to estimate the probability of capture data. Selectivity curves were generated by fitting a logistic function to the plot of the probability of capture against size, from which values of the parameters L_{50}, L_{75}, and the size at which fish were fully recruited to the fishery (L_{100}) were obtained.

Estimates of the annual instantaneous rate of natural mortality (M) were obtained for each species with the empirical equation derived by Hoenig (1983). Maximum age estimates of 31 years for *D. pictum* and 21 years for *L. nebulosus* from the literature (Loubens, 1980; Edwards and Shaher, 1991) were used because the maximum ages and sizes obtained in our study were considerably lower than other reported values.

The annual instantaneous rate of fishing-induced mortality (F) was calculated by subtracting the natural mortality rate (M) from the total mortality rate (Z) derived from age-based catch curves ($F=Z-M$). The calculation was also made for the upper and lower 95% confidence intervals for estimates of Z in order to derive a range of fishing mortality rate estimates. The exploitation rate (E) was calculated as the proportion of the fishing mortality in relation to total mortality ($E=F/Z$).

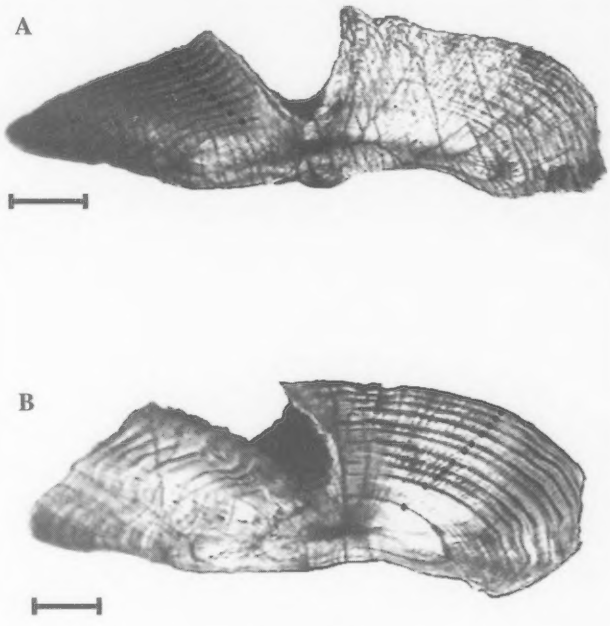

Figure 2

Photomicrographs of transverse sections through the sagittal otoliths of (**A**) *Diagramma pictum*, 56.0 cm L_F and (**B**) *Lethrinus nebulosus*, 45.7 cm L_F. Dots show opaque zones (scale bar=1 mm).

Assessment of the fishery

Relative yield and biomass-per-recruit analyses were used to assess the fishery. Growth (k and L_∞), mortality (M), and selectivity (L_{50}) parameters were used as model inputs, and knife-edge selection was assumed. The Beverton and Holt (1966) yield-per-recruit (YPR) model modified by Pauly and Soriano (1986) was used to estimate the sizes at maximum yield per recruit (L_{max}) and to predict the effects of increasing the mean size at first capture (L_{50}) to the mean size at first sexual maturity (L_{mat}) and that at which yield per recruit would be maximized (L_{max}). Estimates of exploitation rates representing 1) a marginal increase of relative yield per recruit which is 0.1 of its value at the origin ($E_{0.1}$) and 2) maximum yield (E_{max}) were also derived from the model. The exploitation rates corresponding to F_{opt} and F_{limit} (E_{opt} and E_{limit}) were calculated and used to estimate the relative biomass per recruit for each species for L_{50}, L_{mat}, and L_{max} from relative biomass-per-recruit curves. Precautionary target (F_{opt}) and limit (F_{limit}) biological reference points were calculated as 0.5 and 2/3 M, respectively, and used to infer resource status by direct comparison with the fishing mortality rates established for the study species.

Results

Age and growth

Alternating translucent and opaque growth increments were observed in transverse sections of the sagittal otoliths of *D. pictum* and *L. nebulosus* when viewed with transmitted light under low-power magnification (Fig. 2). For both species, one growth increment consisting of an opaque and translucent zone was formed on an annual basis. Opaque bands formed in the summer months between May and September in association with increasing sea water temperatures (Fig. 3); conversely translucent zones were deposited in the autumn and winter (October to February) in association with decreasing sea water temperatures.

The maximum age estimates determined from counts of opaque bands were 13 and 14 years for *D. pictum* and *L. nebulosus*, respectively. Size-at-age relationships were asymptotic in form and there was considerable individual variability in growth (Fig. 4) (parameters of the von Bertalanffy growth function are given in Table 1). A comparison of the growth characteristics between sexes revealed that there were no significant differences in parameter estimates for both species ($P=0.125$, df=319 for *D. pictum* and $P=0.878$, df =324 for *L. nebu-*

losus). Values of the growth performance index Φ' for growth in length were 2.81 for *D. pictum* and 2.80 for *L. nebulosus*.

The length-weight relationship provided a good fit to length and weight data for *D. pictum* ($W=1\times10^{-5}\times L^{2.99}$) ($r^2=0.994$) and *L. nebulosus* ($W=3\times10^{-5}\times L^{2.88}$) ($r^2=0.992$). Ratios of total length (L_T) to fork length (L_F) were 1.11:1.0 for *D. pictum* and 1.07:1 for *L. nebulosus*.

Reproduction

The mean size at first sexual maturity (L_{mat}) for *D. pictum* was 30.7 cm L_F for males (24.3–37.2 cm 95% CI) and 31.8 cm L_F for females (24.3–38.9 cm 95% CI). Those for *L. nebulosus* were 28.6 cm L_F (23.7–33.8 cm 95% CI) and 27.6 cm L_F (19.6–35.6 cm 95% CI) for males and females, respectively.

There was a peak in the gonadosomatic index for both *D. pictum* and *L. nebulosus* females in April, the main spawning period lasted until the end of May (Fig. 5), and the mean birth date was estimated as 1 May. There was a significant ($P<0.05$) female bias in the overall sex ratios (male to female) of 1:2.8 for *D. pictum* and 1:2.6 for *L. nebulosus*. The results of chi-square goodness-of-fit tests conducted for the sex ratios in both age and size categories revealed that the female bias was consistent across all categories for *L. nebulosus* although the bias was removed in the oldest age and largest size classes of *D. pictum* (Tables 2 and 3).

The proportion of fish in aggregated size-frequency samples that were below the mean size at first sexual maturity for females (juvenile retention rate) was 35.1% for *D. pictum* and 10.9% for *L. nebulosus*.

Mortality and selectivity

Modal age groups in age-frequency distributions derived from age-length keys and size-frequency data were 3 years for *D. pictum* and 5 years for *L. nebulosus* (Fig. 6). The proportion of fish above the age at which fish were fully recruited was 13.8% and 45.7% for *D. pictum* and *L. nebulosus*, respectively. There were no significant differences between the total mortality rate estimates derived from age-based and length-converted catch curves for *D. pictum* ($t=0.81$, $P=0.43$, 15 df) and *L. nebulosus* ($t=0.03$, $P=0.98$, 11 df) (Fig. 7). Fishing mortality rates were in excess of the natural mortality rates, accounting for 79% and 64% of the total mortality for *D. pictum* and *L. nebulosus*, respectively (Table 4).

The selectivity range derived from plots of the probability of capture at size was 25.0 cm for *D. pictum* (18.0–43.0 cm) and 34.0 cm for *L. nebulosus* (13.0–47.0 cm) (Fig. 8). Values of the sizes where the probability of capture was 50% (L_{50}), 75% (L_{75}), and 100% (L_{100}) are given in Table 5. For both species, fish were recruited

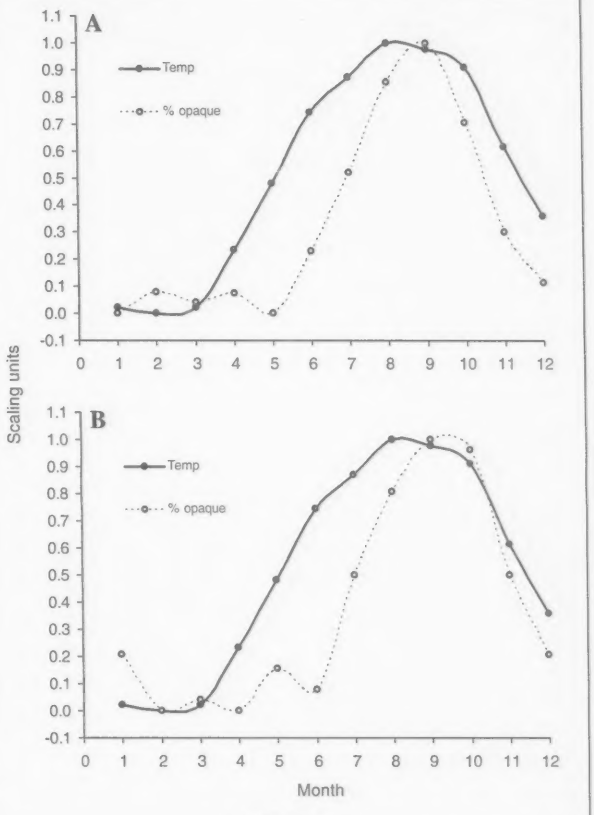

Figure 3

The proportion of otoliths with opaque outer margins for (**A**) *Diagramma pictum* ($n=348$) and (**B**) *Lethrinus. nebulosus* ($n=343$) and monthly sea temperatures off the Emirate of Abu Dhabi. Note that the values have been converted to a standardized scale to enable comparison of the trends.

Table 1

Parameters of the von Bertalanffy growth function, coefficients of determination (r^2), and sample sizes (n) for *Diagramma pictum* and *Lethrinus nebulosus* in the southern Arabian Gulf.

	D. pictum			*L. nebulosus*		
	Males	Females	All	Males	Females	All
k	0.29	0.23	0.24	0.10	0.11	0.11
L_∞ cm (L_F)	60.6	63.8	63.0	69.9	65.2	66.2
t_0 (yr)	−1.2	−1.5	−1.4	−3.3	−2.9	−3.0
r^2	0.86	0.83	0.84	0.91	0.88	0.79
n	81	244	325	86	244	330

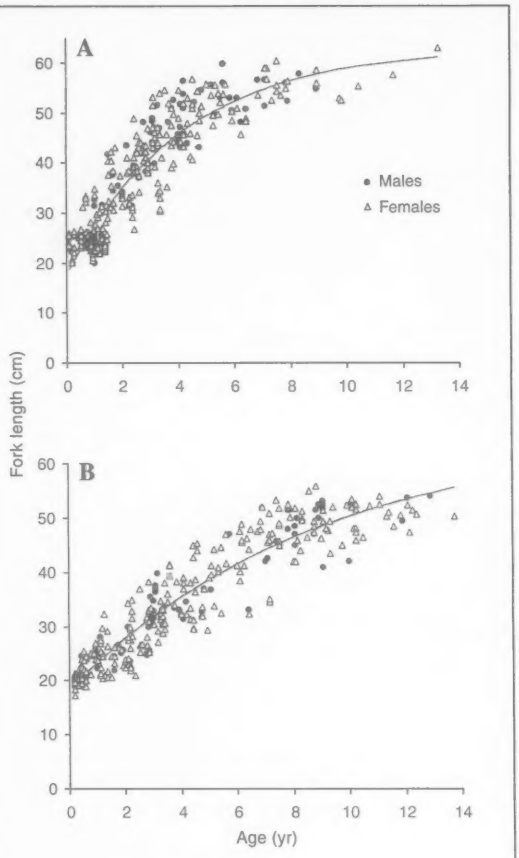

Figure 4

The von Bertalanffy growth function fitted to size-at-age relationships for (**A**) *Diagramma pictum* and (**B**) *Lethrinus nebulosus*.

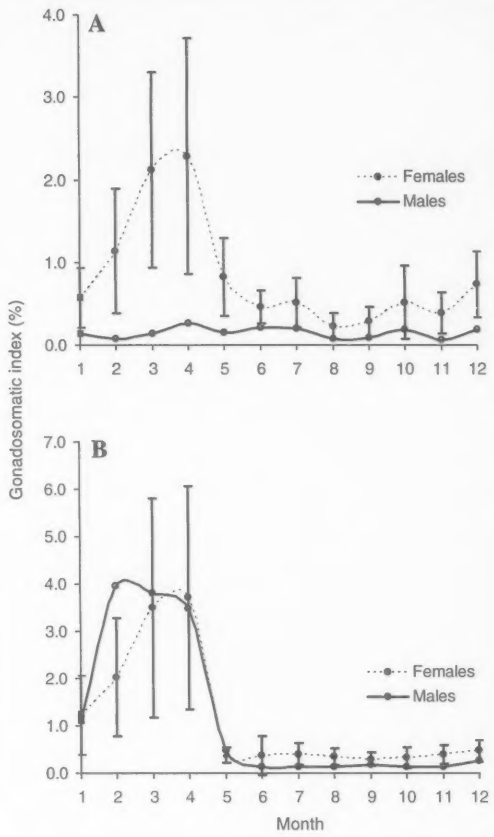

Figure 5

Mean monthly gonadosomatic indices (±SE) for (**A**) *Diagramm pictum* (n=359) and (**B**) *Lethrinus nebulosus* (n=360).

Table 2

Results of chi-square goodness-of-fit tests on sex ratios within age categories for *Diagramma pictum* and *Lethrinus nebulosus* (* significant at α=0.05).

Age category (yr)	No. of males	No. of females	Chi-square (total)	*P*
D. pictum				
0–2	29	130	64.2	<0.01*
3–5	38	91	21.8	<0.01*
6–13	16	29	3.8	>0.05
L. nebulosus				
0–2	34	93	27.4	<0.01*
3–6	29	88	29.8	<0.01*
7–14	27	69	18.4	<0.01*

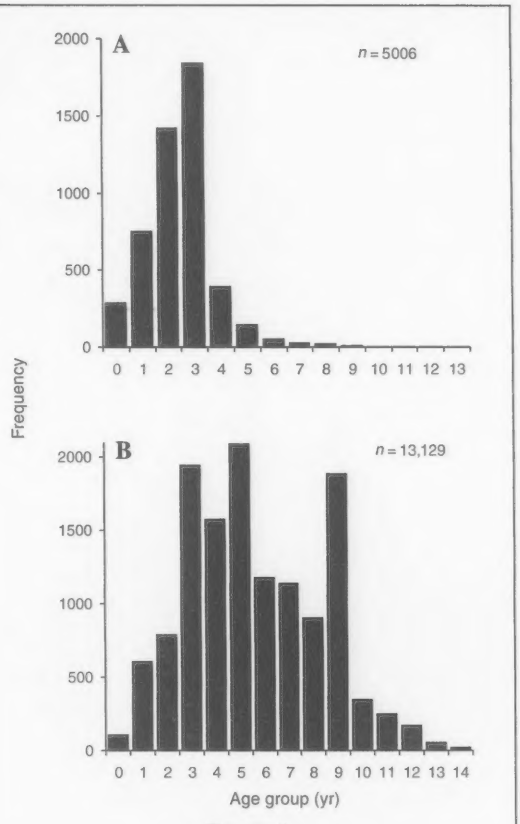

Figure 6

Age-frequency distributions for (**A**) *Diagramma pictum* and (**B**) *Lethrinus nebulosus* derived from age-length keys and size-frequency data.

to the fishery at a mean size (L_{50}) which was smaller than the mean size at which first sexual maturity was attained (L_{mat}).

Assessment of the fishery

The size at which yield per recruit would be maximized (L_{max}) was 44.4 cm (L_F) for *D. pictum* and 36.9 cm (L_F) for *L. nebulosus*. For both species, these values were considerably greater than the mean size at first capture and the mean size at first sexual maturity (Fig. 9).

The exploitation rate for *D. pictum* (0.79/yr) was greater than that which would maximize yield per recruit (0.57/yr) at the existing mean size at first capture (Table 6). Furthermore, the same yield per recruit could be achieved at a much lower exploitation rate and at an increased relative biomass per recruit (Fig. 10). The yield-per-recruit function also indicated that an increase in the size at first capture to that which would

Table 3

Results of chi-square goodness-of-fit tests on sex ratios within size categories for *Diagramma pictum* and *Lethrinus nebulosus* (*=significant at α=0.05).

Size category (cm L_F)	No. of males	No. of females	Chi-square (total)	*P*
D. pictum				
20–34	26	128	67.6	<0.01*
35–49	41	93	20.2	<0.01*
50–64	27	43	3.7	>0.05
L. nebulosus				
15–29	40	121	40.8	<0.01*
30–44	41	89	17.7	<0.01*
45–54	26	73	22.3	<0.01*

Table 4

Mortality and exploitation rates (±95 CI) for *Diagramma pictum* and *Lethrinus nebulosus*.

	D. pictum	*L. nebulosus*
Total mortality rate/yr (Z)		
(Age-based catch curve)	0.63 (0.50–0.75)	0.56 (0.35–0.77)
(Length-converted catch curve)	0.69 (0.58–0.79)	0.56 (0.53–0.60)
Natural mortality rate/yr (M)	0.13	0.20
Fishing mortality rate/yr (F)	0.50 (0.37–0.62)	0.36 (0.15–0.57)
Exploitation rate/yr (E)	0.79	0.64

Table 5

Probability of capture (selectivity) for *Diagramma pictum* and *Lethrinus nebulosus*.

Probability of capture	*D. pictum* cm (L_F)	*L. nebulosus* cm (L_F)
50% (L_{50})	21.1	26.4
75% (L_{75})	30.7	35.1
100% (L_{100})	40.3	43.8

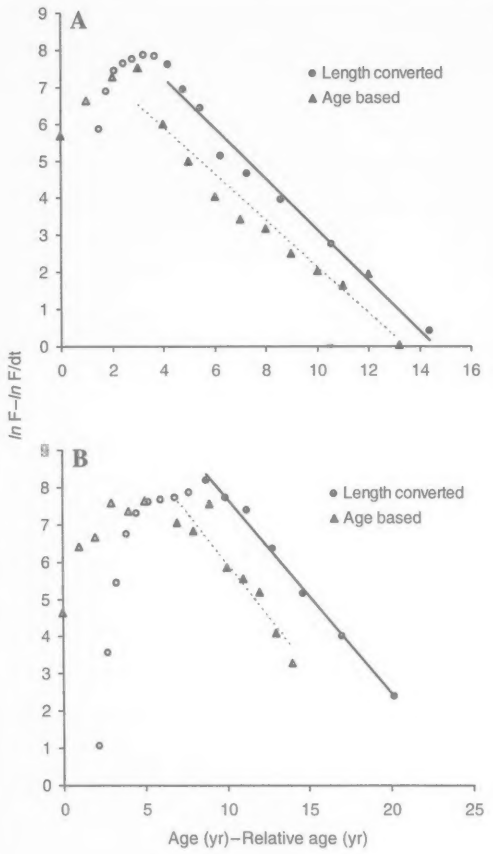

Figure 7

Age-based catch curves (ln$F$ against *Age*) and length-converted catch curves (ln F/dt against *Relative age*) for *Diagramma pictum* (**A**) and *Lethrinus nebulosus* (**B**). Dashed and solid lines show the regression equation ($y=bx+a$) fitted to data for age-based and length-converted catch curves, respectively. Only solid points are included in the regressions.

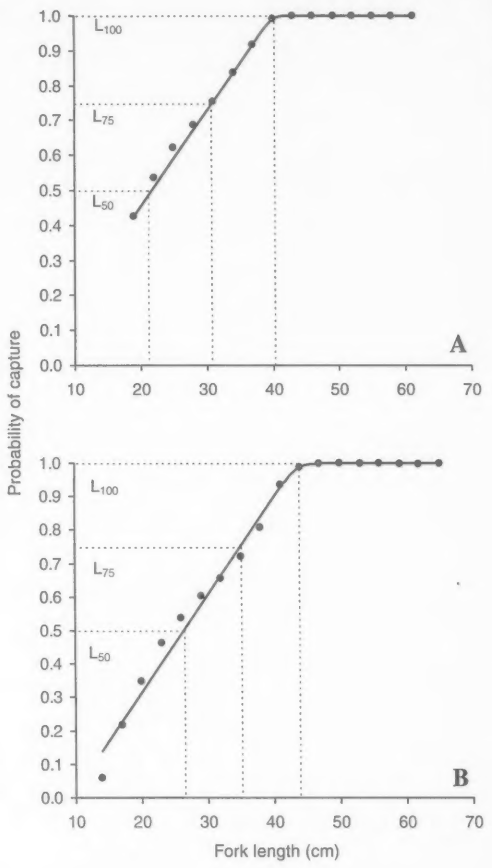

Figure 8

Selectivity curves for (**A**) *Diagramma pictum* and (**B**) *Lethrinus nebulosus*, showing the mean size at first capture at probabilities of 0.5 (L_{50}), 0.75 (L_{75}), and the size at which fish are fully recruited to the fishery (L_{100}).

Table 6

Exploitation rates ($E_{0.1}$ and E_{max}) at the existing size at first capture (L_{50}), the size at first capture at sexual maturity (L_{mat}) and the size at first capture at maximum yield per recruit (L_{max}) for *Diagramma pictum* and *Lethrinus nebulosus*.

Exploitation rate	*D. pictum*			*L. nebulosus*		
	L_{50}	L_{mat}	L_{max}	L_{50}	L_{mat}	L_{max}
$E_{0.1}$ (/yr)	0.50	0.56	0.75	0.51	0.56	0.75
E_{max} (/yr)	0.57	0.65	0.81	0.63	0.65	0.86

maximize yield per recruit would be associated with a substantial increase in yield at the current level of exploitation. An increase in the size at first capture to that at which sexual maturity occurs (L_{mat}) was also predicted to be associated with an increase in yield, although to a lesser degree (Fig. 10).

The relative biomass per recruit for *D. pictum* at the current exploitation rate was less than 10% of that at the theoretical unexploited level. An increase in the mean size at first capture to that which would maximize yield per recruit was predicted to be associated with a small increase in biomass per recruit. Changes in the exploitation rate were predicted to have a greater impact on biomass per recruit, which was estimated to be above 50% of the unexploited level at the optimum exploitation rate (E_{opt}) (Table 7).

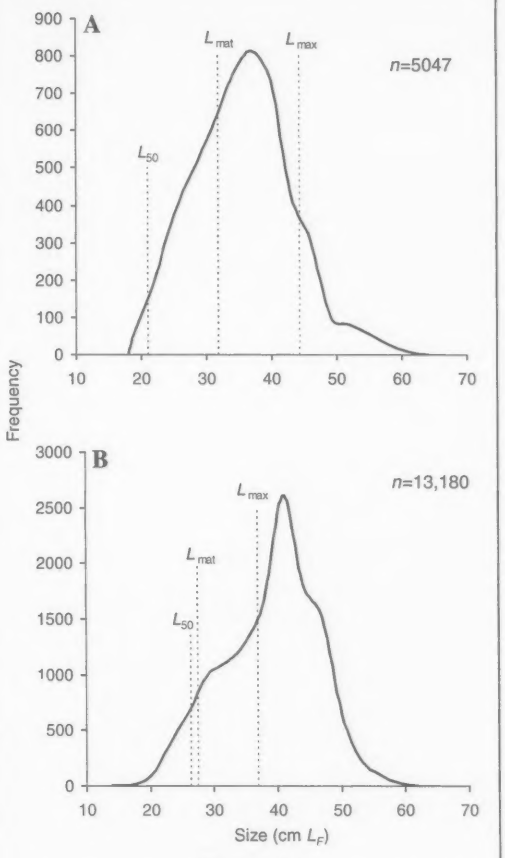

Figure 9

Aggregated length-frequency distributions for (**A**) *Diagramma pictum* and (**B**) *Lethrinus nebulosus* showing the mean sizes at first capture (L_{50}), sexual maturity (L_{mat}), and the size at first capture which would maximize yield per recruit (L_{max}).

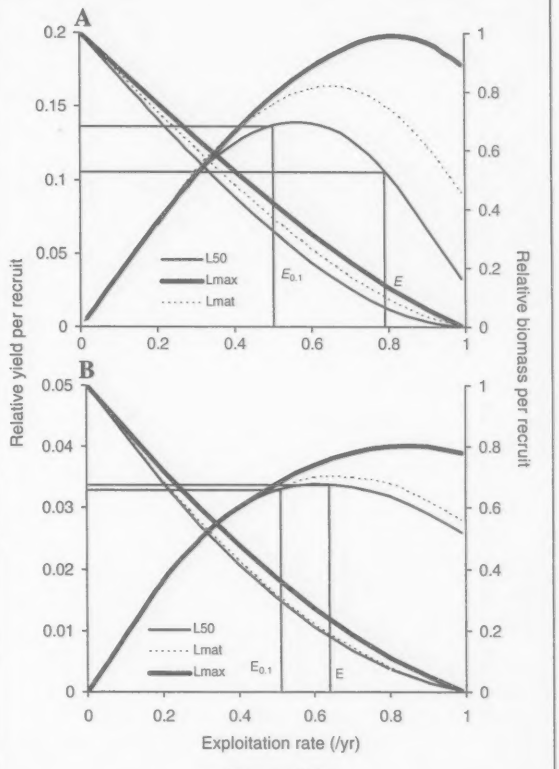

Figure 10

Relative yield and respective biomass-per-recruit curves (descending lines) for (**A**) *Diagramma pictum* and (**B**) *Lethrinus nebulosus* showing the existing exploitation rate (E) and the exploitation rate at which the slope of the yield-per-recruit curve is 0.1 of its value at the origin ($E_{0.1}$). Curves show the effect of increasing the existing mean size at first capture (L_{50}) to the mean size at first sexual maturity (L_{mat}) and the size which would maximize yield per recruit (L_{max}).

Estimates of precautionary target and limit exploitation rates (E_{opt} and E_{limit}) for *D. pictum* were 0.34 and 0.40, respectively.

The exploitation rate for *L. nebulosus* (0.64/yr) was marginally greater than that which would maximize yield per recruit (0.63/yr) at the existing mean size at first capture (Table 6). The yield-per-recruit function indicated that an increase in the size at first capture to that which would maximize yield per recruit would be associated with an increase in yield at the current level of exploitation. An increase in the size at first capture to that at which sexual maturity occurs (L_{mat}) was also predicted to be associated with an increase in yield, although to a lesser degree (Fig. 10).

The relative biomass per recruit for *L. nebulosus* at the current exploitation rate was less than 20% of that

Table 7

Relative biomass per recruit at precautionary exploitation rates (E_{opt} and E_{limit}) at the existing size at first capture (L_{50}), the size at first capture at sexual maturity (L_{mat}), and the size at first capture at maximum yield per recruit (L_{max}) for *Diagramma pictum* and *Lethrinus nebulosus*.

Exploitation rate	Relative biomass per recruit					
	D. pictum			*L. nebulosus*		
	L_{50}	L_{mat}	L_{max}	L_{50}	L_{mat}	L_{max}
E_{opt} (/yr)	0.52	0.55	0.60	0.50	0.51	0.53
E_{limit} (/yr)	0.44	0.48	0.53	0.39	0.40	0.45

at the theoretical unexploited level. An increase in the mean size at first capture to that which would maximize yield per recruit was predicted to be associated with a small increase in biomass per recruit. Changes in the exploitation rate were predicted to have a greater impact on biomass per recruit, which was estimated to be above 50% of the unexploited levels at the optimum exploitation rate (E_{opt}) (Table 7). Estimates of precautionary target and limit exploitation rates (E_{opt} and E_{limit}) for *L. nebulosus* were 0.33 and 0.43, respectively. For both *D. Pictum* and *L. nebulosus*, the exploitation rates predicted from the yield per recruit function ($E_{0.1}$ and E_{max}) were equal to or in excess of values where F=M (0.5) for all sizes at first capture.

The range of fishing mortality rates estimated for *D. pictum* (0.37–0.62/yr) was substantially greater than both the target (F_{opt}=0.07/yr) and limit (F_{limit}=0.09/yr) biological reference points. The range of fishing mortality rates for *L. nebulosus* (0.15/yr to 0.57/yr) were also in excess of the biological reference points for this species (F_{opt}=0.10/yr and F_{limit}=0.13/yr).

Discussion

Age and growth

The formation of alternating translucent and opaque growth zones in fish otoliths has been associated with a variety of factors, including seasonal variations in water temperature, photoperiod, feeding, and reproduction (Moe, 1969; Reay, 1972; Panella, 1980; Manickchand-Heileman and Phillip, 2000). Although the mechanisms of growth-increment formation are poorly understood, the deposition of the opaque zone in tropical species generally occurs in the spring and summer months during periods of accelerated growth, whereas the translucent zone is formed when there is reduced metabolic activity (Beckman and Wilson, 1995). The formation of opaque and translucent zones in the sagittal otoliths of *D. pictum* and *L. nebulosus* determined in our study follows this generalized pattern.

The southern Arabian Gulf exhibits marked seasonal variability in oceanographic characteristics; sea water temperatures can exceed 34°C in summer and fall to 21°C in the winter (Sheppard et al., 1992). The close association of the formation of opaque zones with increasing seawater temperature indicates that temperature could be the principal environmental signal stimulating the deposition of these growth zones. Other allied variables, such as productivity and subsequent food availability, may also be associated with seasonal growth-rate oscillations and the formation of growth increments. The validation of the annual periodicity of increment formation adds to a growing body of evidence (Fowler, 1995) and dismisses the misconception that annuli do not form in the otoliths of reef fish due to a lack of seasonality in the tropics (e.g., Sparre and Venema, 1992). Nevertheless, the edge analysis method used should ideally be conducted over a 2-year cycle and could have been more rigorous with the use of larger sample sizes and by conducting the analyses for individual ages. Furthermore, it is important to distinguish between the validation of increment periodicity and absolute age (Campana, 2001). Although our study has provided empirical evidence for an annual pattern of increment formation, the absolute age of the study species remains to be validated. Validation of the absolute age could be achieved through independent means such as a mark-recapture study and the chemical marking of juvenile fish of known age.

The maximum number of opaque bands counted for *D. pictum* in the present study (13) was considerably less than the maximum age of 31 years estimated by Loubens (1980) for this species in New Caledonia. Likewise, our longevity estimate of 14 years for *L. nebulosus* was less than that of Mathews and Samuel (1991) (20 years) and of Edwards and Shaher (1991) (21 years) for this species in the northern Arabian Gulf and Gulf of Aden, respectively. Our longevity estimates therefore were most likely to have been underestimated owing to the absence of fish close to the maximum reported sizes for these species.

A method of validating growth parameters involves the comparison of growth performance indices (Φ') in terms of growth in length with other estimates obtained for the same or a similar species (Gayanilo and Pauly, 1997). Values of Φ' for *D. pictum* available from other studies have ranged from 2.88 (Loubens, 1980) to 3.24 (Baillon and Kulbicki, 1988), and an estimate of 3.07 has been obtained for this species in the Gulf of Aden (Edwards et al., 1985). The estimate obtained in our study (2.81) compares with the lower end of this range. Values of Φ' for *L. nebulosus* have ranged from 2.55 (Kuo and Lee, 1986) to 3.41 (Baillon, 1991), and an estimate of 2.87 obtained for this species in the northern Arabian Gulf in the waters off Kuwait (Baddar, 1987) compares well with our estimate of 2.80. Although the growth parameters in our study would appear to be of the right order (by comparison), improvements in our estimates could have been made by the addition of larger specimens close to the maximum size for both species.

Despite its widespread use, the von Bertalanffy growth function may not be suitable for hermaphroditic populations (Appeldoorn, 1996). Growth analyses have shown distinct differences in the sizes of equal-age males and females of protogynous species (Moe, 1969; Nagelkerken, 1979; Garratt et al., 1993), and experiments have shown what are considered to be growth accelerations leading to sex change (Ross et al., 1983). Failure to account for growth spurts in yield models can result in significant over estimation of both maximum yield and optimal effort (Bannerot et al., 1987). Although *L. nebulosus* is a protogynous hermaphrodite (Young and Martin, 1982; Ebisawa, 1990), the results of the analysis of residual sums of squares in our study indicated that there are no differences in the growth characteristics between sexes and that the use of growth parameters from pooled data would therefore be justified in yield-per-recruit analyses.

Reproduction

Simulation models and evidence of the effects of fishing have shown that protogynous species are far more vulnerable to fishing pressure than comparable gonochoristic stocks (Huntsman and Schaaf, 1994). For protogynous species, in which males tend to be larger than females on average, there are indications that size-selective fishing mortality may result in the differential loss of larger males (Sadovy, 1996) and the possibility that insufficient males remain in the reproductive population to fertilize eggs from all females (Koenig et al., 1996). In this context, *L. nebulosus* may be particularly vulnerable to such effects because the female-biased sex ratios were consistent throughout all the age categories and size classes. The overall female bias and removal of the bias in the oldest and largest age category for *D. pictum* is generally representative of the sexual structure of a protogynous population. Given these characteristics, histological confirmation of the reproductive mode of this species should be considered.

The well-defined spawning period of *D. pictum* and *L. nebulosus* between April and May supports the view that seasonal reproductive cycles are common among tropical fishes (Robertson, 1990; Montgomery and Galzin, 1993; Sadovy, 1996). There were high levels of juvenile retention for *D. pictum* (35.1%) because fish were recruited to the fishery before the mean size at which sexual maturity occurred, indicating a need to increase the mesh size of traps.

Mortality and selectivity

Estimates of natural mortality derived from other studies of *D. pictum* range from 0.43/yr (Edwards et al., 1985) to 0.67/yr (Baillon and Kulbicki, 1988). The comparatively low value of M obtained in our study (0.13/yr) can be attributed to the difference in methods used, but errors in other estimates from the empirically derived formula of Pauly (1980) may have occurred because the relationship has tended to overestimate M, especially for slow growing species (e.g., Ralston, 1987; Russ et al., 1998). Similarly, our value of the instantaneous natural mortality rate for *L. nebulosus* (0.20/yr) was lower than other estimates that range from 0.279/yr (Edwards et al., 1985) to 1.18/yr (Baillon, 1991). Although estimates of M derived from the Hoenig (1983) relationship have been shown to provide a reasonable approximation of M in tropical demersal fishes (Hart and Russ, 1996; Newman et al., 1996), errors in this parameter were potentially the greatest source of error in our assessment.

Upward bias in estimates of the total mortality rate (Z) may have occurred if larger fish were less vulnerable to the fishing gear or if adult fish underwent migrations, for example. A survey of the biomass of demersal species in the Arabian Gulf waters of the United Arab Emirates showed that there were no seasonal changes in the abundance of *L. nebulosus* and the haemulid *Plectorhinchus sordidus* (Shallard[2]). This finding indicates that ontogenetic or spawning-associated migrations would unlikely be altering the size and age composition and subsequent estimates of Z for the species investigated. Although size-specific selectivity cannot be discarded as a possible explanation for the small proportion of larger and older fish in size-frequency and biological samples, the impact of fishing on the size and age structure of the respective populations is considered a more likely reason for these observations and is likely to be the probable cause given the historic absence of regulation in the trap fishery.

Because the size at first capture (21.1 cm L_F) was considerably smaller than the size at which yield per recruit would be maximized (44.4 cm L_F) for *D. pictum*, an increase in the mesh size for the trap fishery should be considered by management authorities especially given the high rate of juvenile retention for this species. The same is applicable for *L. nebulosus* with a mean size at first capture of 26.4 cm L_F and size at maximum yield per recruit of 36.9 cm L_F.

Assessment of the fishery

The use of yield-per-recruit models may be particularly restrictive for fast growing tropical species with high rates of natural mortality because the curves may not reach a maximum within a reasonable range of fishing mortality values (Gayanilo and Pauly, 1997). Although the species examined in our study were relatively slow growing and had low rates of natural mortality, failure of the yield-per-recruit model may still have occurred at the upper end of the fishing mortality range.

Gulland (1970) suggested that in an optimally exploited stock, fishing mortality should be about equal to natural mortality, resulting in an exploitation rate of 0.5/yr. However, exploitation rates should be very conservative for relatively long-lived reef fish (Newman and Dunk, 2003), especially given that potential yields may be over estimated by a factor of 3–4 where $F=M$ (Beddington and Cooke, 1983). With a range from 0.5 to 0.86/yr, the exploitation rates derived from yield-per-recruit analyses ($E_{0.1}$ and E_{max}) are considered to have overestimated the associated fishing mortality rates.

The relative yield-per-recruit analyses indicated that an increase in the size at first capture of *D. pictum* and *L. nebulosus* to that which would maximize yield per recruit would be associated with increases in yields at the existing exploitation rates. However, the existing exploitation rate for *D. pictum* (0.79/yr) was greater than that which would maximize yield per recruit (E_{max}=0.57/yr). Although the exploitation rate for *L. nebulosus* (0.64/yr) was comparable to that which would maximize yield per

[2] Shallard, B. 2003. Distribution and abundance of demersal fish stocks in the UAE, 211 p. Technical Report 1. Fish Resources Assessment Survey Project of Abu Dhabi and UAE Waters. Bruce Shallard and Associates and Environmental Research and Wildlife Development Agency, P.O. Box 45553, Government of Abu Dhabi, United Arab Emirates.

recruit (0.63/yr), given that E_{max} was probably overestimated, the results indicate that growth overfishing is also occurring for this species.

The specified precautionary target (F_{opt}=0.5.M) and limit (F_{limit}=2/3.M) values are considered to be more appropriate biological reference points in light of the constraints of the yield-per-recruit model. The range of fishing mortality rates estimated for *D. pictum* (0.37–0.62/yr) was substantially greater than both the target (F_{opt}=0.07/yr) and limit (F_{limit}=0.09/yr) biological reference points, and the existing exploitation rate (0.79/yr) was more than double the optimum level (0.34/yr). The range of fishing mortality rates for *L. nebulosus* (0.15/yr to 0.57/yr) were also in excess of the biological reference points for this species (F_{opt}=0.10/yr and F_{limit}=0.13/yr) and the exploitation rate (0.64/yr) was approximately double the optimum target level (0.33/yr). This result clearly indicates growth overfishing for both species and, in combination with the results of the yield-per-recruit analyses, demonstrates that effort reductions are also required in the fishery because target reference points cannot be achieved by modification of the gear-selectivity characteristics alone.

A critical limitation of the yield-per-recruit model is the assumption that there is no relationship between the size of the spawning stock biomass and recruitment (Buxton, 1992). Even if the size at first capture is less than the size at first sexual maturity, the stock size may approach zero at high levels of fishing mortality in spite of predictions of high levels of yield per recruit. It is therefore important to consider the size of the spawning stock biomass across the range of fishing mortality rates when interpreting results. The relative biomass per recruit of *D. pictum* and *L. nebulosus* at the estimated fishing mortality rates was particularly low at less than 10% and 20%, respectively, of unexploited levels. If the critical spawning stock biomass is between 20% and 50% of the unexploited levels, as suggested by King (1995), recruitment overfishing is likely to be occurring for both species. This is most clearly seen in the age structure for *D. pictum*, for which only 13.8% of the total number of fish were above the age at which fish were fully exploited by the gear (ages 4–13 years). For this species, the majority of the yield was derived from the newly recruited age class representing fish that had just become fully vulnerable to the gear.

The relative biomass per recruit at the exploitation rates that were equivalent to F_{opt} corresponded to 52% and 51% of the theoretical unexploited biomass levels for *D. pictum* and *L. nebulosus*, respectively. The associated levels of fishing mortality are therefore considered appropriate target reference points, given the present fisheries policy which is aimed at resource conservation and stock rebuilding. Accordingly, the results of our study are important to fisheries management authorities in the region because they indicate that both a substantial reduction in fishing effort and an increase in mesh-size of traps are currently necessary for the previously unregulated demersal trap fishery.

Acknowledgments

We are very grateful to Sultan Al Ali, Khaled Al Ali, John Hoolihan, and Kunath Gopalan for their assistance with data collection and Abdulla Aboubaker for helping with data entry. Howard Choat and Will Robbins assisted in the training of technicians in otolith processing. The comments of the anonymous reviewer helped considerably in improving the manuscript. This study was funded by the Government of the United Arab Emirates through the Environmental Research and Wildlife Development Agency's Marine Environment Research Centre.

Literature cited

Appeldoorn, R. S.
1996. Model and method in reef fishery assessment. *In* Reef fisheries (N. V. C. Polunin and C. M. Roberts, eds.), p. 219–248. Chapman and Hall, London.

Baddar, M. K.
1987. A preliminary study of the population dynamics of sheiry, the starry pigface bream, *Lethrinus nebulosus*. Kuwait Bull. Mar. Sci. 9:215–220.

Baillon, N.
1991. Otolithometrie en milieu tropical: application à trois espèces du lagon de Nouvelle-Caledonie. ORSTOM, Inst. Fr. Rech. Sci. Dév. Coop., Trav. Doc. 113, 296 p.

Baillon, N., and M. Kulbicki.
1988. Aging of adult tropical reef fish by otoliths: a comparison of three methods on *Diagramma pictum*. *In* Proceedings of the sixth international coral reef symposium, Townsville, Australia, 8th–12th August 1988 (J. H. Choat, ed.), p. 341–346. 6th International Coral Reef Symposium Executive Committee, Townsville, Queensland, Australia.

Bannerot, S. P., W. W. Fox, and J. E. Powers.
1987. Reproductive strategies and the management of snappers and groupers in the Gulf of Mexico and the Caribbean. *In* Tropical snappers and groupers: biology and fisheries management (J. J. Polovina and S. Ralston, eds.), p. 561–603. Westview Press, Boulder, CO.

Beckman, D. W., and C. A. Wilson.
1995. Seasonal timing of opaque zone formation in fish otoliths. *In* Recent developments in fish otolith research (D. H. Secor, J. M. Dean, and S. E. Campana eds.), p. 27–43. Univ. South Carolina Press, Colombia, SC.

Beddington, J. R., and J. G. Cooke.
1983. The potential yield of fish stocks. FAO Fish. Tech. Pap. 242, 47 p. FAO, Rome.

Beverton, R. J. H., and S. J. Holt
1957. On the dynamics of exploited fish populations, 533 p. Chapman and Hall, London.
1966. Manual of methods for fish stock assessment, part II. Tables of yield function. Fisheries Biology Technical Paper 38, 67 p. FAO, Rome.

Breder, C. M., and D. E. Rosen.
1966. Modes of reproduction in fishes, 941 p. T.F.H. Publications, Neptune City, NJ.

Buxton, C. D.
1992. The application of yield-per-recruit models to two South African sparid reef species, with special consideration to sex change. Fish. Res. 15:1–16.

Chen, Y. D., D. A. Jackson, and H. H. Harvey.
1992. A comparison of von Bertalanffy and polynomial functions in modelling fish growth data. Can. J. Fish. Aquat. Sci. 49:1228–1235.

Campana, S. E.
2001. Accuracy, precision and quality control in age determination, including a review of the use and abuse of age validation methods. J. Fish. Biol. 59:197–242.

Ebisawa, A.
1990. Reproductive biology of *Lethrinus nebulosus* (Pices: Lethrinidae) around the Okinawan waters. Nippon Suisan Gakkaishi 56 (12):1941–1954.

Edwards, R. R. C., A. Bakhader, and S. Shaher.
1985. Growth, mortality, age composition and fishery yields of fish from the Gulf of Aden. J. Fish. Biol. 27:13–21.

Edwards, R. R. C., and S. Shaher.
1991. The biometrics of marine fishes from the Gulf of Aden. Fishbyte 9(2):27–29.

Fischer, W., and G. Bianchi.
1984. FAO species identification sheets for fishery purposes. Vol. II: Western Indian Ocean (Fishing Area 51), 257 p. Prepared and printed with the support of the Danish International Development Agency (DANIDA). FAO. Rome.

Fowler, A. J.
1995. Annulus formation in the otoliths of coral reef fish—a review. *In* Recent developments in fish otolith research (D. H. Secor, J. M. Dean, and S. E. Campana, eds.), p. 45–63. Univ. South Carolina Press, Colombia, SC.

Garratt, P. A., A. Govender, and A. E. Punt.
1993. Growth acceleration at sex change in the protogynous hermaphrodite *Chrysoblephus puniceus* (Pisces: Sparidae). S. Afr. J. Mar. Sci. 13:187–193.

Gayanilo, F. C. Jr., and D. Pauly.
1997. FAO–ICLARM stock assessment tools. Reference manual, 262 p. FAO. Rome.

Gulland, J. A.
1970. The fish resources of the ocean. FAO Fisheries Technical Paper 97, 425 p. FAO, Rome.

Hart, A. M., and G. R. Russ.
1996. Response of herbivorous fish to crown of thorns starfish *Acanthaster planci* outbreaks. III: Age, growth, mortality and maturity indices of *Acanthurus nigrofuscus*. Mar. Ecol. Prog. Ser. 136:25–35.

Hoenig, J. M.
1983. Empirical use of longevity data to estimate mortality rates. Fish. Bull. 82:898–902.

Huntsman, G. R., and W. E. Schaaf.
1994. Simulation on the impact of fishing on reproduction of a protogynous grouper, the graysby. N. Am. J. Fish. Manag. 14:41–52.

Johannes, R. E.
1981. Words of the lagoon, 320 p. Univ. Calif. Press, Los Angeles, CA.

King, M.
1995. Fisheries biology, assessment and management, 341 p. Blackwell Science Ltd., London.

Koenig, C. C., F. C. Coleman, L. A. Collins, Y. Sadovy, and P. L. Collin.
1996. Reproduction in gag (*Mycteroperca microlepis*) (Pices: Serranidae) in the eastern Gulf of Mexico and the consequences of fishing spawning aggregations. *In* Biology, fisheries and culture of tropical groupers and snappers (F. Arreguin-Sanchez, J. L. Munro, M. C. Balgos, and D. Pauly, eds.), p. 307–323. ICLARM Conf. Proc. 48.

Kuo, C. L., and S. S. Lee.
1986. Age and growth of common porgy, *Lethrinus nebulosus* (Forsskål) in shelf waters off northwest Australia. J. Fish. Soc. Taiwan. 3:39–57.

Loubens, G.
1980. Biologie de quelques espèces de poissons du lagon Néo-Calédonien. III. Croissance. Cah. Indo-Pac. 2:101–153.

Manickchand-Heileman, S. C., and D. A. Phillip.
2000. Age and growth of the yellow edge grouper, *Epinephelus flavolimbatus*, and the yellowmouth grouper, *Mycteroperca interstitialis*, off Trinidad and Tobago. Fish. Bull. 98:290–298.

Mathews, C. P., and M. Samuel.
1991. Growth, mortality and length-weight parameters for some Kuwaiti fish and shrimp. Fishbyte 9(2):30–33.

Moe, M. A.
1969. Biology of the red grouper, *Epinephelus Morio*, (Valenciennes) from the eastern Gulf of Mexico. Florida Dept. Nat. Resour. Mar. Res. Lab., Prof. Pap. Ser. 10:1–95.

Montgomery, W. L., and R. Galzin.
1993. Seasonality in gonads, fat deposits and condition of tropical surgeonfishes (Teleostei: Acanthuridae). Mar. Biol. 115:529–536.

Nagelkerken, W. P.
1979. Biology of the graysby, *Epinephelus cruentatus*, of the coral reef of Curaçao. Stud. Fauna Curaçao other Carib. Islands 186, 118 p.

Newman, S. J., and I. J. Dunk.
2003. Age validation, growth, mortality, and additional population parameters of the goldband snapper (*Pristipomoides multidens*) off the Kimberley coast of northwestern Australia. Fish. Bull. 101:116–128.

Newman, S. J., D. McB. Williams, and G. R. Russ.
1996. Age validation, growth and mortality rates of the tropical snappers (Pices: Lutjanidae), *Lutjanus adetii* (Castelnau, 1873) and *L. quinquelineatus* (Bloch, 1790) from the Central Great Barrier Reef, Australia. Mar. Freshw. Res. 47(4):575–584.

Panella, G.
1980. Growth patterns in fish sagittae. *In* Skeletal growth of aquatic organisms (D. C. Rhoads and R. A. Lutz, eds.), p. 519–560. Plenam Press, New York, NY.

Pauly, D.
1980. On the interrelationships between natural mortality, growth parameters and mean environmental temperature in 175 fish stocks. J. Cons. Int. Explor. Mer 39:175–199.
1983. Length-converted catch curves: a powerful tool for fisheries research in the tropics (part 1). Fishbyte 1(2):9–13.

Pauly, D., and M. L. Soriano.
1986. Some practical extensions to Beverton and Holt's relative yield-per-recruit model. *In* The first Asian fisheries forum (J. L. Maclean, L. B. Dizon, and L. V. Hosillo, eds.), p. 491–496. Asian Fisheries Society, Manila, Philippines.

Randall, J. E.
1995. Coastal fishes of Oman, 439 p. Univ. Hawaii Press, Honolulu, HI.

Randall, J. E., G. R. Allen, and R. C. Steene.
1997. Fishes of the Great Barrier Reef and Coral Sea, 507 p. Univ. Hawaii Press, Honolulu, HI.

Ralston, S.
1987. Mortality rates of snappers and groupers. *In* Tropical snappers and groupers: biology and fisheries management (J. J. Polovina and S. Ralston eds.), p. 375–404. Westview Press, Boulder, CO.
Reay, P. J.
1972. The seasonal pattern of otolith growth and its application to back-calculation studies in *Ammodytes tobianus*. J. Cons. Int. Explor. Mer 34:485–504.
Ricker, W. E.
1975. Computation and interpretation of biological statistics of fish populations, 382 p. Bull. Fish. Res. Board Can. 191.
Robertson, D. R.
1990. Differences in the seasonalities of spawning and recruitment of some small neotropical reef fishes. J. Exp. Mar. Biol. Ecol. 144:49–62.
Ross, R. M., G. S. Losey, and M. Diamond.
1983. Sex change in coral reef fish:dependence of stimulation and inhibition on relative size. Science 221:574–575.
Russ, G. R., D. C. Lou, J. B. Higgs, and B. P. Ferreira.
1998. Mortality rate of a cohort of the coral trout, *Plectropomus leopardus*, in zones of the Great Barrier Reef Marine Park closed to fishing. J. Mar. Freshw. Res. 49:505–11.
Sadovy, Y. J.
1996. Reproduction of reef fishery species. *In* Reef fisheries (N. V. C. Polunin and C. Roberts, eds.), p. 15–59. Chapman and Hall, London.
Samuel, M., C. P. Mathews, and A. S. Bawazeer.
1987. Age and validation of age from otoliths for warm water fishes from the Arabian Gulf. *In* Age and growth of fish (R. C. Summerfelt and G. E. Hall, eds.), p. 253–265. IOWA State Univ. Press, Ames, IA.
Sheppard, C., A. Price, and C. Roberts.
1992. Marine ecology of the Arabian region. Patterns and processes in extreme tropical environments, 347 p. Academic Press. London.
Siddeek, M. S. M., M. M. Fouda, and G. V. Hermosa Jr.
1999. Demersal fisheries of the Arabian Sea, the Gulf of Oman and the Arabian Gulf. Estuar. Coastal Shelf Science 49 (suppl. A):87–97.
Smith, M. M., and R. J. McKay.
1986. Haemulidae. *In* Smiths' sea fishes (M. M. Smith and P. C. Heemstra, eds.), p. 564–571. Springer-Verlag, Berlin.
Sokal, R. R., and F. J. Rohlf
1995. Biometry. The principles and practice of statistics in biological research. 3rd ed., 887 p. W. H. Freeman and Co., New York, NY.
Sommer, C., W. Schneider, and J. M. Poutiers.
1996. FAO species identification field guide for fishery purposes. The living marine resources of Somalia, 376 p. FAO, Rome.
Sparre, P., and S. C. Venema.
1992. Introduction to tropical fish stock assessment. Part 1. FAO Fisheries Technical Paper No. 306.1, rev. 1, 376 p. FAO, Rome.
Torres, F. S. B., Jr.
1991. Tabular data on marine fishes from Southern Africa. Part I. Length-weight relationships. Fishbyte 9(1):50–53.
von Bertalanffy, L.
1938. A quantitative theory of organic growth. Hum. Biol. 10:181–213.
Young, P. C., and R. B. Martin.
1982. Evidence for protogynous hermaphroditism in some lethrinid fishes. J. Fish. Biol. 21:475–84.

A catch-free stock assessment model with application to goliath grouper (*Epinephelus itajara*) off southern Florida

Clay E. Porch
Anne-Marie Eklund
Gerald P. Scott
Southeast Fisheries Science Center
National Marine Fisheries Service, NOAA
75 Virginia Beach Drive
Miami, Florida 33149-1099
E-mail address: clay.porch@noaa.gov

Abstract—Many modern stock assessment methods provide the machinery for determining the status of a stock in relation to certain reference points and for estimating how quickly a stock can be rebuilt. However, these methods typically require catch data, which are not always available. We introduce a model-based framework for estimating reference points, stock status, and recovery times in situations where catch data and other measures of absolute abundance are unavailable. The specific estimator developed is essentially an age-structured production model recast in terms relative to pre-exploitation levels. A Bayesian estimation scheme is adopted to allow the incorporation of pertinent auxiliary information such as might be obtained from meta-analyses of similar stocks or anecdotal observations. The approach is applied to the population of goliath grouper (*Epinephelus itajara*) off southern Florida, for which there are three indices of relative abundance but no reliable catch data. The results confirm anecdotal accounts of a marked decline in abundance during the 1980s followed by a substantial increase after the harvest of goliath grouper was banned in 1990. The ban appears to have reduced fishing pressure to between 10% and 50% of the levels observed during the 1980s. Nevertheless, the predicted fishing mortality rate under the ban appears to remain substantial, perhaps owing to illegal harvest and depth-related release mortality. As a result, the base model predicts that there is less than a 40% chance that the spawning biomass will recover to a level that would produce a 50% spawning potential ratio.

Manuscript submitted 30 April 2004 to the Scientific Editor's Office.
Manuscript approved for publication 14 July 2005 by the Scientific Editor.
Fish. Bull. 104:89–101 (2006).

The last decade has witnessed considerable interest in the so-called precautionary approach to resource management, where human activities are curtailed to prevent further environmental degradation without the burden of proving that these activities are to blame. Fisheries applications of the precautionary approach typically hinge on the notion that fishing pressure should be reduced in a predetermined fashion as certain "limit" reference points are approached (FAO, 1995; Caddy, 1998; Restrepo et al., 1998). In the United States, the Magnuson-Stevens Fishery Conservation and Management Act (Public Law 94-265) mandates the development of fishery management plans (FMPs) that specify criteria for determining when a stock is overfished and the remedial measures necessary to ensure a timely recovery. The National Standard Guidelines developed by the National Marine Fisheries Service to implement the Act require each FMP to include an "MSY control rule" that comprises two reference points, known as the maximum fishing mortality threshold (MFMT) and the minimum stock size threshold (MSST). When the abundance of the stock dips below the MSST, special provisions must be made to rebuild the stock to the level that would support the maximum sustainable yield within a time frame that is as short as possible and that is commensurate with the intrinsic productivity of the stock and the needs of the fishing community.

Many modern stock assessment methods provide the machinery for determining limit reference points as well as for appraising where the stock is in relation to them and how quickly it can be rebuilt. However, these methods typically require data on total catch or absolute abundance, which are not always available. In the case of goliath grouper (*Epinephelus itajara*), for example, a recent review panel concluded that the catch statistics were unreliable and not useful for assessment purposes (Anon.[1]). Several *ad hoc* control rules have been developed to accommodate such "data-poor" situations. One of the more common is simply to define the MSST in terms of historical indices of abundance that supposedly represent a desirable stock condition (Annala, 1993; Cadrin et al., 2004). An advantage of this type of approach is that it is model-free, and nothing is assumed concerning the recovery rate of the stock. Being model-free, however, is a disadvantage with respect to the requirements of the Magnuson-Stevens Act, inasmuch as the recovery time cannot be estimated. Moreover, there may be other types of information that could influence the perception of the status of the stock, and it would be useful to integrate that information formally into the assessment.

[1] Anon. 2003. Goliath grouper data workshop report. SEDAR3-DW-1, 11 p. South Atlantic fishery Management Council, 1 Southpark Circle, Charleston SC 29406.

The purpose of this article is to introduce a model-based framework for estimating reference points, stock status, and recovery times in situations where catch data and other measures of absolute abundance are unreliable. The specific estimator developed in this study is essentially an age-structured production model recast in terms relative to pre-exploitation levels. A Bayesian estimation scheme is adopted to allow the incorporation of pertinent auxiliary information such as might be obtained from meta-analyses of similar stocks or anecdotal observations. The approach is applied to the population of goliath grouper off southern Florida, which is believed to have been severely depleted during the 1980s and has been protected from all harvest since 1990 (GMFMC[2]).

Materials and methods

Population dynamics model

The study period begins when the stock is believed to be near virgin levels, such that the relative abundance N of each age class a at the beginning of the first year is given by

$$N_{a,1} = \begin{cases} 1 & a = a_r \\ N_{a-1,1} e^{-M_{a-1}} & a_r < a < A \\ N_{A-1,1} e^{-M_{A-1}} / (1 - e^{-M_A}), & a = A \end{cases} \quad (1)$$

where a_r = the youngest age class in the analysis;
A = a "plus-group" representing age classes A and older; and
M = the natural mortality rate.

The relative abundance at the beginning of subsequent years (y) is modeled by the recursion

$$N_{a,y} = \begin{cases} r_y & a = a_r \\ N_{a-1,y-1} e^{-F_{y-1} v_{a-1} - M_{a-1}} & a_r < a < A \\ N_{A-1,y-1} e^{-F_{y-1} v_{a-1} - M_{a-1}} + & \\ N_{A,y-1} e^{-F_{y-1} v_A - M_A}, & a = A \end{cases} \quad (2)$$

where r_y = the annual recruitment to age class a_r relative to virgin levels;
F = the fishing mortality rate on the most vulnerable age class; and
v_a = the relative vulnerability of the remaining age classes (which implicitly includes factors such as gear selectivity, size limit regulations, and the fraction of the stock exposed to the fishery).

Relative recruitment (r) is modeled as a first-order lognormal autoregressive process,

$$r_y = \mu_r e^{\varepsilon_y}$$
$$\varepsilon_y = \rho_r \varepsilon_{y-1} + \eta_{r,y}, \quad (3)$$

where μ_r = the median expectation
ρ_r = the correlation coefficient; and
η = normal-distributed random variates having mean 0 and standard deviation σ_r (ostensibly representing the effect on recruitment of fluctuations in the environment).

The median is modeled by the Ricker or Beverton-Holt spawner-recruit functions recast in terms of the maximum lifetime reproductive rate α and relative spawning biomass s:

$$\mu_r = \begin{cases} s_{y-a_r}^{\alpha^{1-s_{y-a_r}}} & \text{Ricker} \\ \dfrac{\alpha s_{y-a_r}}{1+(\alpha-1)s_{y-a_r}} & \text{Beverton and Holt} \end{cases} \quad (4)$$

$$s_y = \sum_{a=a_r}^{A} E_a e^{-(F_y v_a + M_a) t_s} N_{a,y} \Big/ \sum_{a=a_r}^{A} E_a e^{-M_a t_s} N_{a-1},$$

where E = an index of the per-capita number of eggs produced by each age class (E); and
t_s = the fraction of the year elapsed at the time of spawning.

The shapes of these two curves are essentially the same as the conventional relationships (Fig. 1); however their domain is implicitly limited to the interval $0 \le s \le 1$ (see Appendix 1 for a derivation).

The fishing mortality rate on the most vulnerable age class F is also modeled as a first-order lognormal autoregressive process,

$$F_y = \mu_F e^{\delta_y}$$
$$\delta_y = \rho_F \delta_{y-1} + \eta_{F,y}, \quad (5)$$

where μ_F = the median level;
ρ_F = the correlation coefficient; and
η = normal-distributed random variates having mean 0 and standard deviation σ_F.

The median annual is generally assumed to be proportional to an index of fishing effort f:

$$\mu_F = \phi f_y, \quad (6)$$

[2] GMFMC (Gulf of Mexico Fishery Management Council). 1990. Amendment number 2 to the fishery management Plan for the reef fish fishery of the Gulf of Mexico, 31 p. Gulf of Mexico Fishery Management Council. 3018 North US Highway 301, Suite 1000, Tampa, FL 33619.

where ϕ can vary among three eras of exploitation: a "prehistoric" period, during which little data are available; a "modern" period, when presumably there are some data on abundance or mortality rates; and a "future" period, when fishing mortality rates are controlled (input). The absence of data during the "prehistoric era" generally precludes the estimation of annual deviations in recruitment (ε) or fishing mortality rate (δ) during that period.

The average weight or fecundity of the plus group is expressed as a function of the average age of the plus-group. Initially, it is assumed that the age composition of the plus-group is in equilibrium consistent with Equation 1, in which case the average age of the plus-group at the beginning of the first year is approximately

$$\bar{a}_{A,1} = A + \frac{e^{-M_A}}{1-e^{-M_A}}. \quad (7)$$

Subsequently, the age of the plus-group is updated as

$$\bar{a}_{A,y+1} = \frac{AN_{A-1,y}e^{-F_y v_{A-1} - M_{A-1}} + (\bar{a}_{A,y}+1)N_{A,y}e^{-F_y v_A - M_A}}{N_{A,y+1}}. \quad (8)$$

Reference points

Equations 1–4 describe the relative dynamics of a population apart from its absolute abundance. As such they are suitable for developing management plans where the fishing mortality rate is controlled directly (e.g., by reducing effort) and the biomass reference points are expressed on a relative scale. When the virgin spawning biomass itself is used as the reference point, the estimated value of s_y is a direct measure of the status of the stock. For example, if the management goal is to maintain spawning biomass at or above 50% of the virgin level, then estimates of s below 0.5 may trigger some action to reduce fishing pressure.

A related reference point is the equilibrium spawning potential ratio (Goodyear, 1993), defined as the expected lifetime fecundity per recruit at a given F (ψ_F) divided by the expected lifetime fecundity in the absence of fishing (ψ_0):

$$p = \frac{\psi_F}{\psi_0}$$
$$\psi_F = \sum_{a=0}^{A} E_a e^{-(F_a+M_a)t_s} e^{-\sum_{i=0}^{a-1} Fv_i + M_i}. \quad (9)$$

As shown in Appendix 2, the corresponding equilibrium level of relative spawning biomass (denoted by a tilde) may be computed as

$$\tilde{s}_p = \begin{cases} 1 + \dfrac{\log_e p}{\log_e \alpha} & \text{Ricker} \\ \dfrac{\alpha p - 1}{\alpha - 1} & \text{Beverton and Holt} \end{cases} \quad (10)$$

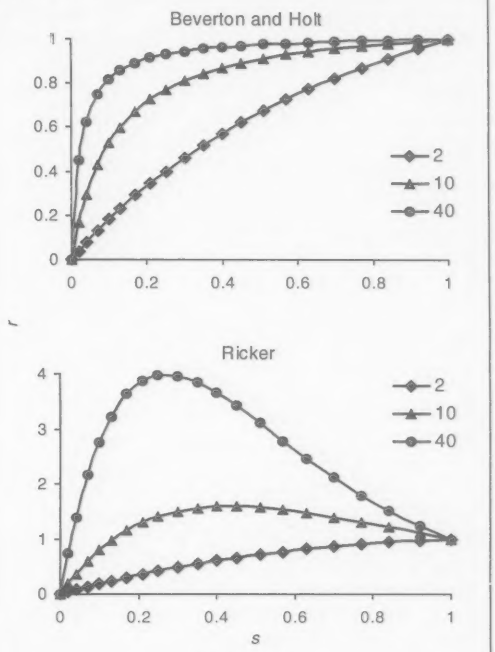

Figure 1

Examples of scaled Beverton-Holt and Ricker spawner-recruit relationships for various values of α (maximum lifetime fecundity). The labels s and r refer to relative spawning biomass and relative recruitment, respectively.

Note that $\tilde{s}_p$ is independent of the vulnerability vector v. Accordingly, MSST definitions based on $\tilde{s}_p$ will have the desirable property of being insensitive to changes in fishery behavior.

Other management plans employ reference points such as F_{max} or $F_{0.1}$, which are based on the yield per recruit statistic

$$\left(\frac{Y}{R}\right) = \sum_{a=0}^{A} w_a F v_a \frac{1-e^{-(Fv_a+M_a)}}{Fv_a+M_a} e^{-\sum_{i=0}^{a-1} Fv_i + M_i}, \quad (11)$$

where w_a is some measure related to the average weight of the catch. Inasmuch as there are no terms involving the absolute abundance of the stock, the calculation of such statistics poses no special problems for the relative framework presented in the present study. Prescriptions based on the maximum sustainable yield (MSY) are slightly more complicated because equilibrium yield is the product of equilibrium recruitment $\tilde{R}$ and equilibrium yield per recruit:

$$\tilde{Y} = \tilde{R}_F \sum_{a=0}^{A} w_a F v_a \frac{1-e^{-(Fv_a+M_a)}}{Fv_a+M_a} e^{-\sum_{i=0}^{a-1} Fv_i + M_i}. \quad (12)$$

However, the fishing mortality rate that maximizes Equation 12 also maximizes Equation 12 divided by the virgin recruitment R_0 (a constant). Thus, F_{MSY} may be obtained from

$$\max_F \left\{ \frac{F\tilde{s}_p}{p} \sum_{a=0}^{A} w_a v_a \frac{1-e^{-(Fv_a+M_a)}}{Fv_a+M_a} e^{-\sum_{i=0}^{a-1} Fv_i+M_i} \right\}. \quad (13)$$

where $\tilde{s}_p/p$ has been substituted for $\tilde{R}_F/R_0$.

The values of p and $\tilde{s}_p$ corresponding to F_{max} , $F_{0.1}$, or F_{msy} may be calculated by means of Equations 9 and 10, respectively. Note however, that p is no longer the target value specified by management, but a derivative of the targeted values of F. This means that MSST definitions based on $\tilde{s}_{max}$, $\tilde{s}_{0.1}$, and $\tilde{s}_{msy}$ will vary somewhat with the behavior of the fishery. In some cases this could lead to risk prone situations where the perception of stock status changes simply because the fishery targets different age groups (i.e., the definition of MSST changes rather than the abundance of the resource). In the case of MSY, a more stable alternative is to define the MSST in terms of a "spawn at least once" policy where mature animals are regarded as fully vulnerable to the fishery and immature animals area regarded as invulnerable.

Parameter estimation

The equations above include numerous "unknowns" representing the processes of reproduction, mortality, and growth. In the case of "data-poor" stocks like goliath grouper, there are insufficient data to estimate all of these unknown parameters with an acceptable level of precision. However, it is often possible to increase the precision of the estimates through the use of Bayesian prior probability densities constructed to reflect expert opinion (e.g., Wolfson et al., 1996; Punt and Walker, 1998) or based on meta-analyses involving similar species (e.g., Liermann and Hilborn, 1997; Maunder and Deriso, 2003).

The Bayesian approach to estimation seeks to develop a "posterior" probability density for the parameters Θ that is conditioned on the data D, $P(\Theta \mid D)$. By application of Bayes rule it is easy to show that

$$P(\Theta \mid D) \propto P(D \mid \Theta) P(\Theta). \quad (14)$$

where $P(D \mid \Theta)$ is the sampling density (likelihood function); and $P(\Theta)$ is the prior density (in this case the analyst's best guess of the probability density for Θ).

Estimates for Θ may be obtained by integrating the posterior (the classical Bayes moment estimator; cf. Gelman et al., 1995)

$$\bar{\theta}_j = \int \theta_j P(D \mid \Theta) P(\Theta) d\theta_j, \qquad \theta_j \in \Theta \quad (15)$$

or by minimizing its negative logarithm (the highest posterior density estimator; Bard, 1974)

$$\min_{\Theta} \left\{ -\log_e P(D \mid \Theta) - \log_e P(\Theta) \right\}. \quad (16)$$

In the present model, a prior needs to be specified for the parameters reflecting recruitment (α and ε_y), mortality (M, ϕ, δ_y, v_a), fecundity (E_a), and growth in weight (w_a). It is assumed in the present study that the parameters are statistically independent with respect to prior knowledge, such that the joint prior is merely the product of the marginal priors for each parameter. The exceptions are the process error functions for the annual recruitment and fishing mortality rate deviations, ε_y and δ_y. These are assumed to be autocorrelated lognormal variates with negative- log density functions of the form

$$-\log P(\varepsilon) = \frac{1}{2\sigma_r^2} \left[\varepsilon_1^2 + \sum_y (\varepsilon_{y+1} - \rho_r \varepsilon_y)^2 \right] + \log \sigma_r, \quad (17)$$

where ρ_r = the correlation coefficient; and
σ_r^2 = the variance of $\log_e \eta_r$.

For stability reasons, it is assumed that $\varepsilon_0 = 0$.

It is possible, at least in principle, to conduct an assessment based on prior specifications alone. However, it may be difficult to develop sufficiently informative priors for some of the parameters, particularly for the fishing mortality rates. The preferred approach, of course, is to condition the estimates on data. With the present model it is assumed that catch data are either unavailable or unreliable, otherwise a standard age-structured production model (cf. Restrepo and Legault, 1998) would be more appropriate. However, time series of catch-per-unit-of-effort data or fishery-independent surveys are often available even when total catches are not. To the extent that changes in these data (c) are proportional to changes in the abundance of the population as a whole (N), they may be modeled as

$$\begin{aligned} c_{i,y} &= q_i \sum_a v_{i,a} N_{a,y} e^{-(F_y v_a + M_a) t_i} e^{\gamma_{i,y}} \\ \gamma_{i,y} &\sim Normal(0, \sigma_{c,i}), \end{aligned} \quad (18)$$

where i indexes the particular survey time series;
q = the proportionality coefficient scaling the time series to the relative abundance of the population;
t_i = the fraction of the year elapsed at the time of the survey;
$\sigma_{c,i}$ = the standard deviation of the fluctuations in $\log_e c_i$ owing to observation errors or changes in the distribution of the stock; and
v_a and $v_{i,a}$ = the relative vulnerability of each age class to the fishery and the i^{th} survey, respectively.

The corresponding negative logarithm of the sampling density is

$$-\log P(c \mid \Theta) = \sum_i \sum_y \left\{ \frac{1}{2\sigma_{c,i}^2} \left(\log_e(c_{i,y}) - \log_e \left(q_i \sum_a v_{i,a} N_{a,y} e^{-(F_y v_a + M_a)t_i} \right) \right)^2 + \log \sigma_{c,i} \right\}. \quad (19)$$

Anecdotal observations may be treated in similar fashion. For example the perceptions of constituents on the abundance of the resource relative to virgin levels (n) can be modeled as

$$n_y = \frac{\sum_a \lambda_a N_{a,y} e^{-(F_y v_{i,a} + M_a)\Delta}}{\sum_a \lambda_a e^{-M_a \Delta} e^{-\sum_{i=0}^{a-1} M_i}} e^{\gamma_{n,y}} \quad (20)$$

$$\gamma_{n,y} \sim Normal(0, \sigma_n).$$

Here $\lambda_{,a}$ is the relative contribution of each age class in forming the perception of total abundance (e.g., fishermen may never encounter very young fish), Δ is the time of the year most reflective of the period upon which the perceptions were based (e.g., the peak of the fishing season), and σ_n is the standard deviation of the fluctuations in $\log_e n_y$.

It is not generally possible to obtain consistent estimates for all of the elements of the covariance matrix **V** (i.e., ρ_F, σ^2_F, ρ_r, σ^2_r, $\sigma^2_{c,i}$ and σ^2_n). In the case of survey data, the variances associated with sampling variability are often estimated extraneous to the population model (e.g., during the standardization procedure). However, there may be additional variance owing to fluctuations in the distribution of the stock in relation to the survey area (IWC, 1994). To accommodate such possibilities, the survey variance parameters are modeled as

$$\sigma^2_{c,i,y} = \chi^2_{c,i,y} + \beta_{c,i}\sigma^2$$
$$\sigma^2_{n,y} = \chi^2_{n,y} + \beta_n \sigma^2, \quad (21)$$

where the $\chi^2_{c,i,y}$ and $\chi^2_{n,y}$ = the annual observation variances (estimated outside the model);

σ^2 reflects some overall process variance (estimated within the model); and

β = constant multipliers (usually fixed by the analyst based on a careful consideration of the inherent variability of the underlying processes).

The recruitment variance and correlation coefficient are generally inestimable without a good index of recruitment and may have to be fixed to some moderate values (say σ_r=0.4 and ρ=0.5).

Table 1

Anecdotal reports from nine individuals concerning the abundance of adult-size goliath grouper (*Epinephelus itajara*) in 1990 in relation to their abundance in the 1950s (expressed as percent reduction).

Interviewee	Method	% reduction
1	diver	60
2	angler	70
3	diver	75
4	angler	90
5	diver	90
6	diver	95
7	diver	95
8	diver	97
9	diver	98

The model outlined above was implemented by using the nonlinear optimization package AD Model Builder (version 4.5, Otter Research Ltd., Sidney, Canada), which provides facilities for estimating the mode and shape of the posterior distribution. Confidence intervals for the probability of recovery were generated directly from the posteriors approximated by the likelihood profile method (the accuracy of which was checked by replicating the prior distributions without data and by comparing the modes of the posterior with the HPD estimates). For some quantities confidence limits were computed by using normal approximations centered at the HPD estimate with variances obtained by inverting the Hessian matrix. This approach reduced computing time considerably, but the approximations were poor for confidence intervals broader than 80 percent owing to the thick tails and skewed nature of the posterior distributions.

Application to goliath grouper

Goliath grouper are large, long-lived predators found predominantly in the tropical western Atlantic and Caribbean Sea. They are among the least wary of reef fishes, easily approached by spearfishers and readily caught in traps or by hook and line gear. Not surprisingly, they have declined considerably throughout much of their range (Sadovy and Eklund, 1999). Although there are few data on the historic abundance of these animals in southern Florida, anecdotal reports suggest that they were much more abundant during the 1950s and 60s than they are now (Table 1). Concerns of overfishing prompted regulators in the U.S. to impose a moratorium on the harvest of goliath grouper that has remained in effect since 1990. To date, the duration of the moratorium has not been specified owing to the paucity of information on their potential recovery rates.

Spawner-recruit relationship There does not appear to be any reliable information on the nature of the

spawner-recruit relationship for any grouper species. A Beverton and Holt model was assumed in this study because it is difficult to envision a mechanism for the strong density dependence in mortality rates required by the Ricker model. A prior for the value of α (Fig. 2) was constructed from a subset of the values collected by Myers et al. (1999) that corresponds to larger, highly fecund fishes with long life spans (the 'periodic' strategists of Rose et al., 2001).

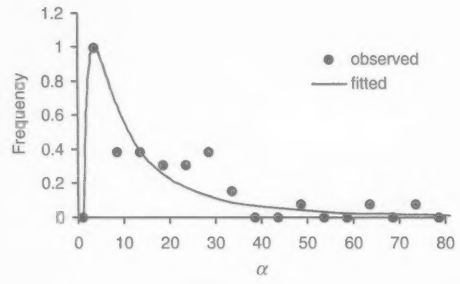

Figure 2

Lognormal prior for the maximum lifetime fecundity parameter (α) derived from the values in Myers et al. (1999) that correspond to species categorized as periodic strategists by Rose et al. (2001). The lognormal density was fitted to the values of α–1 (with median 9.8 and log-scale variance 1.31) and then was shifted 1 unit to provide a prior for α.

Fecundity and growth To date there are insufficient data for estimating a fecundity-at-age relationship for goliath grouper. We followed Legault and Eklund[3] and substituted the weight at age relationship:

$$E_a = \begin{cases} 0 & a < 6 \\ w_a = 1.31 \times 10^{-5} l^{3.056} & a \geq 6 \end{cases} \qquad (22)$$
$$l = 200.6\left(1 - e^{-0.126(a+0.49)}\right)$$

where w = weight in kg; and
l = length in cm expressed as a von Bertalanffy function of age (see Bullock et al., 1992).

Natural mortality The maximum observed age of 37 years (Sadovy and Eklund, 1999) suggests a value for M of about 0.11/yr according to the method of Hoenig (1983). Legault and Eklund[5] suggested a plausible range of 0.037 yr to 0.19/yr (midpoint 0.11) based on an analysis of the fraction surviving to various maximum ages. To reflect this uncertainty, a lognormal prior with a median of 0.11 and CV of 0.4 was used (Fig. 3A).

Fishing mortality rate and relative vulnerability A large fraction of the recreational landings of goliath grouper appear to come from the Ten Thousand Islands area in Southwest Florida, where most of the animals caught have been between the ages of one and five years. However, large animals were often targeted by commercial and recreational fishermen in other areas. Accordingly, we assumed the vulnerability of goliath grouper generally increased with age according to the sigmoid-shaped logistic curve

$$v_a = \frac{1}{1 + e^{-(a - a_{50})/d}}. \qquad (23)$$

Estimates for the parameters a_{50} and d were obtained by fitting the curve (weighted by cumulative mortality at age) to the relative frequency of ages in two different data sets. The first data set included mostly juveniles animals between the ages of 0 and 5, obtained during creel censuses of recreational catches in the Ten Thousand Islands area of the Everglades National Park (see Porch et

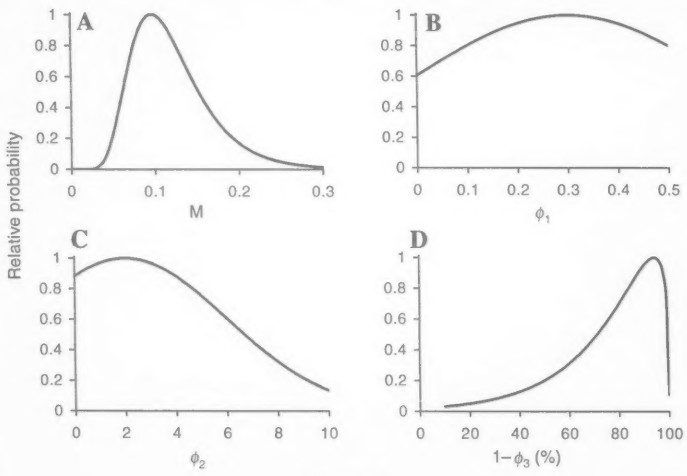

Figure 3

Priors for the mortality rate parameters: (**A**) lognormal prior for natural mortality rate, (**B**) truncated normal prior for proportionality factor ϕ_1, (**C**) truncated normal prior for multiplier ϕ_2 (**D**) gamma prior for percent reduction in F associated with the 1990 harvest ban. The upper and lower boundaries for each parameter are as given on the horizontal axes.

[3] Legault, C. M., and A.-M. Eklund. 1998. Generation times for Nassau grouper and jewfish with comments on M/K ratios. Sustainable Fisheries Division Contribution SFD-97/98-10A, 5 p. Southeast Fisheries Science Center, 75 Virginia Beach Drive, Miami, Florida 33149.

al.[4]). The second data set included mostly adult animals obtained opportunistically from recreational and commercial catches in the eastern Gulf of Mexico (Bullock et al., 1992). The SEDAR stock assessment review panel based their advice on models that used the former selection curve (Kingsley[5]); however the effect of using the latter curve was examined as a sensitivity analysis. The two curves are contrasted in Fig. 4A.

The fishing mortality rate on the most vulnerable age class was modeled as follows:

$$F_y = \begin{cases} \phi_1 f_y & 1900 \le y \le 1979 \\ \delta_y \phi_2 F_{1979}, & 1980 \le y < 1990 \\ \phi_3 \overline{F}_{1980-89} & 1990 \le y \end{cases} \quad (24)$$

where f_y = a time series of historical effort; and
ϕ_1, ϕ_2, ϕ_3, δ_y are parameters to be estimated.

In the present study, effort was assumed to track the U.S. Census[6] for the number of people living in South Florida coastal counties between 1900 and 1980. From 1980 to 1989 this assumption was no longer required owing to the availability of several time series of relative abundance (see below). Instead, interannual variations in fishing mortality were modeled according to Equation 5 with median $\phi_2 F_{1979}$, log-scale variance σ_F^2=0.15 and correlation coefficient ρ_F=0.5, which essentially amounts to a mild constraint on year-to-year changes in F. The nonzero correlation coefficient is intended to reflect the momentum in effective fishing effort from one year to the next that arises from a combination of market demands and the tendency of many fishermen to target only the species they are most adept at catching. Even so, the relatively large variance term admits substantial interannual variations if the data warrant them. Moreover, runs with ρ_F=0.0 (no year-to-year momentum) did not produce substantially different results.

The effect of the harvest moratorium was modeled as a percentage ϕ_3 of the average fishing mortality rate in the 1980–89 period. Relatively uninformative priors were used for ϕ_1 and ϕ_2 (Fig. 3, B and C). A somewhat more informative prior with bounds between 0.01 and 0.5 was used for ϕ_3, based on the opinions of members of the SEDAR panel (Fig. 3D).

Survey information Porch and Eklund (2004) have developed relative indices of abundance from two visual surveys: the personal observations of a professional spearfisher (DeMaria[7]) and a volunteer fish-monitoring program administered by the Reef Education and Environmental Foundation (REEF 2000). In addition, Cass-Calay and Schmidt[8] have standardized catch rate data collected in the Ten Thousand Islands area by the Everglades National Park (ENP). The two visual surveys are assumed to reflect the abundance of mature fish ages 6 and older (based on diver reports of size). The ENP catch rate index, on the other hand, is assumed to reflect the relative abundance of juveniles with relative vulnerabilities given by the dome-shaped gamma function (normalized to a maximum of 1):

$$v_{ENP,a} = \left(\frac{a}{a_{100\%}} e^{1-a/a_{100\%}} \right)^{cv^{-2}-1}, \quad (25)$$

where $a_{100\%}$ = the most vulnerable age; and
CV = the coefficient of variation.

Estimates for $a_{100\%}$ (3.47) and CV (0.34) were obtained by fitting the mortality-weighted gamma curve to the frequency of ages 0 –7 in the Ten Thousand Islands data mentioned earlier (for more detail see Porch et al.[4]). The resulting curve is shown in Figure 4B.

Anecdotal impressions of stock status Johannes et al. (2000) pointed out that local fishermen often disagree with the conclusions drawn by scientists in data-poor situations and suggest that many times additional data will prove the fishermen correct. As mentioned earlier, expert judgements about the relative abundance of a stock can be treated as data or represented by a "prior." We collected information on the value of s at the time moratoriums began (1990) by interviewing fishermen and divers who had been active in southern Florida since the early 1960s or before. Specifically, interviewees were asked to state their perception of the percent reduction in goliath grouper populations from the time they began diving to the time the moratorium on catch was imposed (1990). The average percent reduction reported for large goliath (approximately age 6 and older) was 86% (standard deviation of about 13%, Table 1). This information was modeled as data in accordance with Equation 20.

[4] Porch, C. E., A-M. Eklund and G. P. Scott. 2003. An assessment of rebuilding times for goliath grouper. Sustainable Fisheries Division Contribution SFD-2003-0018. Southeast Fisheries Science Center, 75 Virginia Beach Drive, Miami, Florida 33149. 26 p.

[5] Kingsley, M. C. S., ed. 2004. The Goliath Grouper in southern Florida: assessment review and advisory report. Report prepared for the South Atlantic Fishery Management Council, the Gulf of Mexico Fishery Management Council, and the National Marine Fisheries Service, 17 p. South Atlantic fishery Management Council, 1 Southpark Circle, Charleston SC 29406.

[6] Population of Florida Counties by Decennial Census: 1900 to 1990, 4 p. 1995. Compiled and edited by Richard L. Forstall. Population Division, U.S. Bureau of the Census. Washington, DC 20233

[7] DeMaria, D. 2004. Personal. observ. P.O. Box 420975, Summerland Key, FL 33042.

[8] Cass-Calay, S. L., and T. W. Schmidt. In review. Standardized catch rates of juvenile goliath grouper, *Epinephelus itajara*, from the Everglades National Park Creel Survey, 1973–1999.

Results

The model was able to fit the ENP index of juvenile goliath grouper very well but could not reconcile the conflicting trends indicated by the DeMaria and REEF indices for adult goliath grouper (Fig. 5). The estimated trends in spawning biomass were rather uncertain (Fig. 6A), but nevertheless indicated a rapid decline to about 5% of virgin levels by the time the harvest ban was imposed in 1990, followed by a significant increase. The estimates of fishing mortality were also somewhat uncertain, but generally indicated a gradual increase in fishing mortality to moderate levels during the 1970s followed by a rapid increase during the 1980s (Fig. 6B). The harvest moratorium was estimated to have been about 83% effective in reducing fishing mortality, nevertheless losses owing to human activities (e.g., illegal harvest and release mortality of animals caught at depth) were still estimated to be substantial (F =0.05/yr). If, in accordance with the Gulf of Mexico Management Council's generic Sustainable Fisheries Act amendment, the limit reference point is taken to be the equilibrium spawning biomass corresponding to a spawning potential ratio of 50%, then the model indicates that current fishing mortality rates are near $F_{50\%}$ and that there is less than a 50% chance the stock will recover within 15 years (Fig. 7).

Sensitivity runs were conducted to examine the implications of 1) dropping one or more of the indices, 2) increasing the assumed minimum age represented in the REEF and DeMaria indices from 6 to 10, 3) assuming that the historical period began in 1950 rather than 1900 and using the anecdotal information as a tuning index and (4) using the alternate fishery selection curve that was fitted to the data from Bullock et al. (1992), where adult animals were much more vulnerable to the fishery than were juveniles. Of these, the results were most sensitive to removal of the DeMaria index—the projected trends being much more optimistic (Fig. 8). This is because the DeMaria index indicates that the adult population increased rapidly during the first few years of the harvest ban, but then suffered a set back in 1999 and has since leveled off. In contrast, the REEF index indicates that the population continued to increase during that time. Thus, when the DeMaria index is removed, the model allows for a faster postmoratorium increase in the adult population by estimating a low fishing mortality rate of about 0.01/yr (i.e., a harvest ban that is 97% effective). The fishing mortality rate estimates for the 1980s are also lower without the DeMaria index inasmuch as the DeMaria index indicates a more precipitous decline during that time than the ENP index (the REEF index does not begin until 1994).

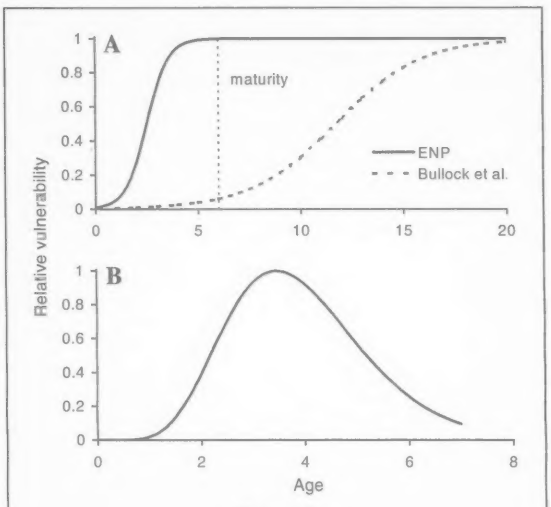

Figure 4

Selection curves used to represent the vulnerability of goliath grouper (*Epinephelus itajara*) to (**A**) the overall fishery and (**B**) Everglades National Park anglers. The logistic curves shown in (A) were fitted to either age-composition data derived from the Everglades National Park (ENP) creel census or opportunistic samples from offshore fishing trips (Bullock et al., 1992).

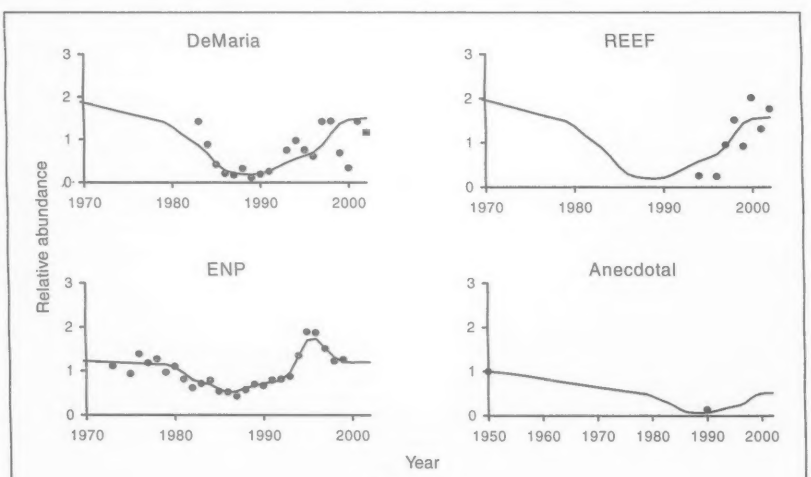

Figure 5

Base model fitted to the four indices of abundance for goliath grouper (*Epinephelus itajara*) in southern Florida.

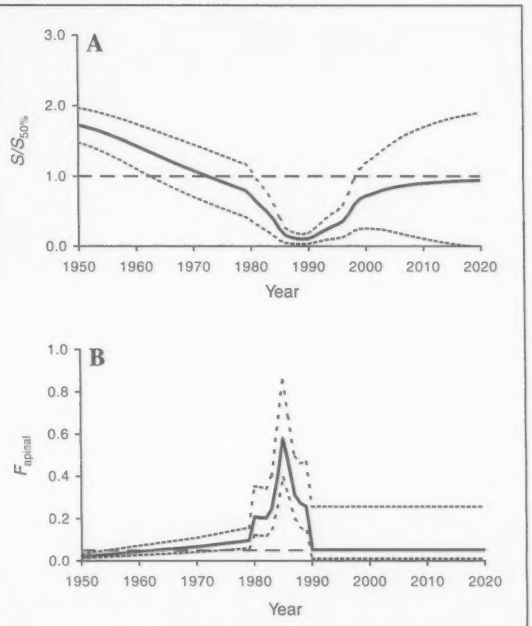

Figure 6

Base model predictions of (**A**) spawning biomass of goliath grouper (*E. itajara*) in southern Florida in relation to the equilibrium level associated with a spawning potential ratio of 50%, $s/s_{50\%}$, and (**B**) the apical fishing mortality rate on goliath grouper (*E. itajara*), F_{apical}. The lines with small dashes represent approximate 80% confidence limits and the dashed horizontal lines represent the levels associated with an SPR of 50%.

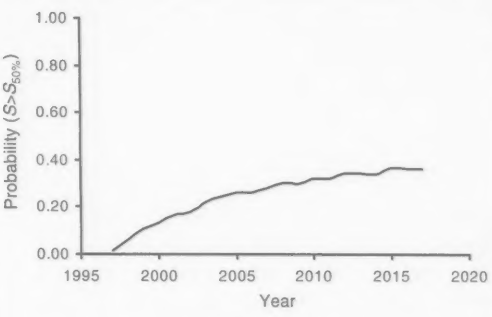

Figure 7

Predicted probability that the stock of goliath grouper (*E. itajara*) in southern Florida will have recovered to levels exceeding the equilibrium spawning biomass associated with a spawning potential ratio of 50%.

The sensitivity run with the alternate selection curve also produced more optimistic results (Fig. 8). Inasmuch as the model now attributes most of the fishing mortality to age classes well beyond the age at first maturity (see Fig. 4), the spawning stock biomass is estimated to have been reduced to a lesser extent (to about 10% of virgin levels by 1990 as compared to 5%). Thus, other things being equal, recovery requires less time. The level of $F_{50\%}$ increased with the alternate selection curve because fewer age classes are affected by fishing.

Discussion

All of the model formulations examined depicted the same qualitative patterns: escalating fishing mortality rates and rapidly declining spawning biomass, particularly during the 1980s, followed by a sharp decrease in fishing mortality and strong recovery in spawning biomass after the 1990 harvest ban. These trends are remarkably consistent with the anecdotal observations shown in Table 1 and Figure 5 as well as with the expert testimony given during the SEDAR stock assessment review. The estimated rapid increase in fishing mortality during the 1980s appears to reflect a real increase in effort that occurred due to elevated demand and selling prices (Sadovy and Eklund, 1999), as well as the widespread use of the LORAN-C navigational system (which made it easier for fishermen to relocate productive offshore shipwrecks). Thus, it seems safe to conclude that the population was overfished at the time the harvest ban was imposed and is currently undergoing a substantial recovery. Less clear is the extent to which the population has recovered since the harvest ban.

Using the base model, we estimated that the harvest ban has reduced fishing pressure by more than 50%, but probably less than 90% (Fig. 9). Thus, there is a strong chance that the current fishing mortality rate, although greatly reduced as compared to the 1980s, remains greater than $F_{50\%}$ (i.e., above 0.05/yr). This in turn translates into less than a 40% chance that the population will recover to levels above $s_{50\%}$ within the next 15 years. Several fishermen have testified that the harvest ban is probably less than 90% effective because goliath grouper are still taken illegally in places and because animals caught and released in deeper water often do not survive[7]; therefore this result does not appear unrealistic.

More optimistic results, implying a 70% to 80% chance of recovery within 15 years, were obtained when the DeMaria index was excluded or when selection was oriented more towards older animals. There does not appear to be a strong *a priori* case for excluding the DeMaria index in favor of the REEF and ENP indices. Although the coverage is rather limited, the trends of the DeMaria index are consistent with those of the ENP index (with a suitable time lag) and with anecdotal accounts of the trends in other areas.[7] The issue of selection is more vexing. It can be argued that the age-composition data from the ENP creel census adequately reflects the composition of the juvenile catch inasmuch

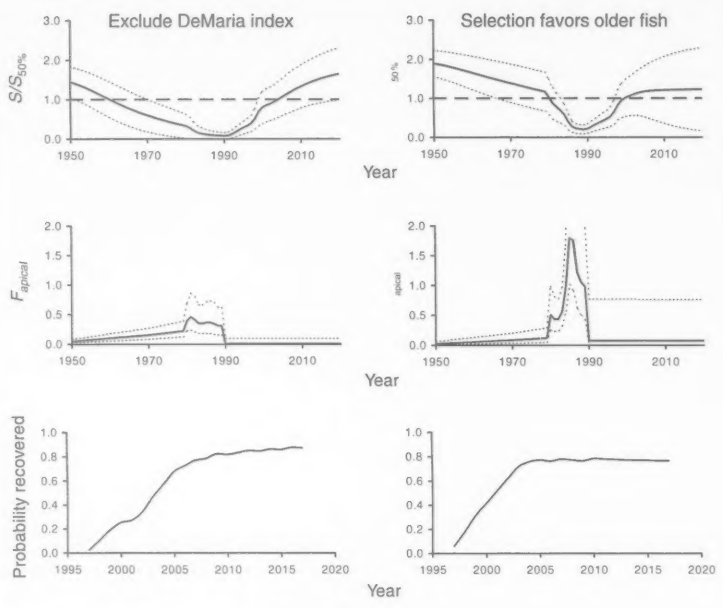

Figure 8

Trends in relative spawning biomass ($s/s_{50\%}$), apical fishing mortality rate (F), and the probability of recovery ($s>s_{50\%}$) for two sensitivity runs—one excluding the DeMaria index (left) and the other with the selection curve favoring older fish (right).

as it comes from the center of juvenile abundance; however most adults were caught outside this area of abundance. Thus, the relative contribution of juveniles and adults to the overall catch is unclear and the directional bias in the fitted logistic selection curve is uncertain.

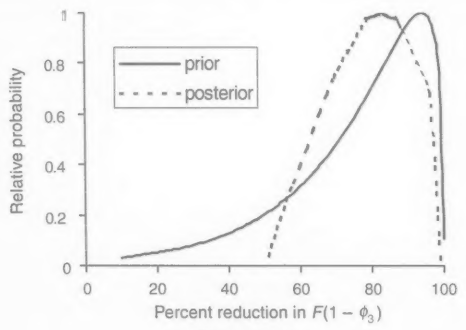

Figure 9

Posterior and prior distributions for the effectiveness of the 1990 harvest ban in reducing the fishing mortality rate F on southern Florida goliath grouper (*E. itajara*) populations (in relation to the fishing mortality rate levels observed during the 1980s).

The only other age composition information that has come to light comes from the study by Bullock et al (1992), which was not designed to provide a random sample of the catch and is probably biased towards larger animals caught on offshore wrecks. In principle, one could reflect this uncertainty more formally either by developing a prior for the selectivity parameters or else by weighting the results from the two selection models. The scientists on the SEDAR stock assessment review panel based their advice on the selection curve derived from the ENP data,[7] which is equivalent to placing negligible weight on the curve derived from the Bullock et al. (1992) data; however they recognized the selection curve as an important source of uncertainty that is difficult to address without adequate data.

It is important to emphasize that the Bayesian approach adopted in the present study allows one to explicitly model the uncertainty about parameters such as M, for which no data may exist, but a prior distribution covering the plausible range of values may be specified. There is, of course, the potential for introducing bias when one or more of the priors are based on expert opinion or otherwise subjective information. However, the same sorts of bias can be introduced by conducting sensitivity analyses where the unknown parameters are fixed to various values selected by the analysts. Furthermore, if unbiased data are in short supply, analyses

based on completely uninformative priors will be useless for generating advice because the range of plausible outcomes is too large. Accordingly, we view the use of subjective priors primarily as a vehicle for providing more realistic limits on uncertainty and prefer to express the model outcomes in terms of probability statements. For example, the point estimate from the base model indicated that the population would never recover to $s_{50\%}$ because the fishing mortality rate under the harvest ban was still slightly above $F_{50\%}$. However, consideration of the uncertainty led to the conclusion that the chance of recovering to $s_{50\%}$ within 15 years was nearly 40%.

Some sources of uncertainty have not been adequately accounted for in the above assessment. For example, the relationship between fecundity and age is unknown. We used weight-at-age as a proxy for the relative fecundity-at-age in our analysis, but it is often the case that fecundity increases with age faster than weight. If this is true for goliath grouper, then our projections would be too optimistic. It should also be remembered that the results apply strictly to the goliath grouper population in southern Florida. It is believed that the center of abundance for the population in U.S. waters is off southern Florida, particularly in the Ten Thousand Islands area, but goliath grouper are known to have occurred throughout the coastal waters of Gulf of Mexico and along the east coast of Florida, and on up through the Carolinas. Inasmuch as goliath grouper are not highly migratory, it is possible it may take some additional time for the species to fully occupy its historical range, thus delaying the overall recovery of the U.S. population.

The primary advantage of the catch-free assessment model proposed in the present study is that it does not require knowledge of the total number of removals. In this light it is worth noting that 623 of the 905 stocks included in the 2000 annual report to Congress on the Status of Fisheries were listed as having unknown status, often because catch data were either unavailable or deemed unreliable. Thus we expect the proposed method will become increasingly useful as fishery scientists are asked more and more to develop FMPs for poorly monitored fisheries. The fact that the model estimates the population's relative abundance, rather than its absolute abundance, is of little consequence when, as is often the case, adjustments to the target fishing mortality rate or catch quota are made in relation to the levels in previous years (Caddy, 2004). Moreover, certain biases tend to cancel out when dimensionless quantities like relative abundance are used. If, for example, only a consistent fraction of the population were sampled, then the absolute estimates of abundance would be biased but the relative estimates would not (Prager et al., 2003).

The greatest drawback of the catch-free method is probably its inability to provide direct estimates of the equilibrium catch levels associated with particular reference points (e.g., MSY). This situation could perhaps be ameliorated by obtaining estimates of absolute abundance from a comprehensive short-term survey covering the entire range of the animal, in which case the relative outputs from the model (including relative catch) could be appropriately scaled. Alternatively, a long-term monitoring program at select sites located throughout the known range of the animal could be established to detect changes in relative abundance under various closely monitored trial levels of catch.

Acknowledgments

The present paper benefitted greatly from the scrutiny given to a related document[6] by members of the SEDAR stock assessment review panel (R. Allen, L. Barbieri, J. Brodziak, M. Cufone, D. DeMaria, M. Kingsley, D. Murie, M. Murphy, J. Neer, J. Rooker, R. Taylor, E. Toomer, and J. Wheeler). S. Turner, L. Brooks, and two anonymous reviewers also gave helpful comments on the manuscript. S. Cass-Calay and T. Schmidt secured the goliath grouper length-composition data from the Everglades National Park creel survey; J. Brusher and J. Schull provided the age-length data from their sampling program in the Ten Thousand Islands area.

Literature cited

Annala, J.
1993. Fishery assessment processes in New Zealand's ITQ system. *In* Proceedings of the international symposium on management strategies for exploited fish populations, 21–24 October 1992, Anchorage Alaska (G. Kruse, D. M. Eggers, R. J. Marasco, C. Pautzke, and T. J. Quinn II, eds.), p. 791–806. Alaska Sea Grant College Program, Univ. Alaska, Fairbanks, AL.

Bard, Y.
1974. Nonlinear parameter estimation. Academic Press, San Diego, CA, 341 p.

Bullock, L. H., M. D. Murphy, M. F. Godcharles, and M. E. Mitchell.
1992. Age, growth, and reproduction of jewfish *Epinephelus itajara* in the eastern Gulf of Mexico. Fish. Bull. 90:243–249.

Caddy, J. F.
1998. A short review of precautionary reference points and some proposals for their use in data poor situations. FAO Fish. Tech. Pap. 379, 30 p. FAO, Rome.
2004. Current usage of fisheries indicators and reference points, and their potential application to management of fisheries for marine invertebrates. Can. J. Fish. Aquat. Sci. 61:1307–1324.

Cadrin, S. X., J. A. Boutillier, and J. S. Idoine.
2004. A hierarchical approach to determining reference points for Pandalid shrimp. Can. J. Fish. Aquat. Sci. 61:1373–1391.

FAO (Food and Agricultural Organization).
1995. Precautionary approach to fisheries. FAO Fish. Tech. Pap. 350, 210 p. FAO, Rome.

Gelman, A., J. B. Carlin, H. S. Stern, and D. B. Rubin.
1995. Bayesian data analysis, 526 p. Chapman and Hall, London.

Goodyear, C. P.
1993. Spawning stock biomass per recruit in fisheries

management: foundation and current use. *In* Risk evaluation and biological reference points for fisheries management (Smith, S. J., J. J. Hunt, and D. Rivard, ed.), p. 67–81. Can Spec. Publ. Fish. Aquat. Sci 120.

Hoenig, J. M.
1983. Empirical use of longevity data to estimate mortality rates. Fish. Bull. 82:898–903.

IWC (International Whaling Commission).
1994. Report of the Scientific Committee, Annex D. Report of the sub-committee on management procedures. Rep. Int. Whal. Comm. 44:74–92.

Johannes, R. E., M. M. R. Freeman, and R. J. Hamilton.
2000. Ignore fishers' knowledge and miss the boat. Fish Fish. 1:257–271.

Liermann, M., and R. Hilborn.
1997. Depensation in fish stocks: a hierarchic Bayesian meta-analysis. Can. J. Fish. Aquat. Sci. 54: 1976–1984.

Maunder, M. N., and R. B. Deriso.
2003. Estimation of recruitment in catch-at-age models. Can. J. Fish. Aquat. Sci. 60:1204–1216.

Myers, R. A., K. G. Bowen, and N. J. Barrowman.
1999. Maximum reproductive rate of fish at low population sizes. Can. J. Fish. Aquat. Sci. 56: 2404-2419.

Porch, C. E., and A.-M. Eklund.
2004. Standardized visual counts of goliath grouper off South Florida and their possible use as indices of abundance. Gulf Mex. Sci. 22:155–163.

Prager, M. H., C. E. Porch, K. W. Shertzer, and J. F. Caddy.
2003. Targets and limits for management of fisheries: A simple probability-based approach. N. Am. J. Fish. Manag. 23:349–361.

Punt, A. E., and T. I. Walker.
1998. Stock assessment and risk analysis for the school shark (*Galeorhinus galeus*) off southern Australia. Mar. Freshw. Res. 49:719–731.

Restrepo, V. R., and C. M. Legault.
1998. A stochastic implementation of an age-structured production model. *In* Fishery stock assessment models (F. Funk, T. J. Quinn II, J. Heifetz, J. N. Ianelli, J. E. Powers, J. F. Schweigert, P. J. Sullivan, and C.-I. Zhang. eds.), p. 435–450. Alaska Sea Grant College Program Report No. AK-SG-98-01, Univ. Alaska, Fairbanks, AL.

Restrepo, V. R., G. G. Thompson, P. M. Mace, W. L. Gabriel, L. L. Low, A. D. MacCall, R. D. Methot, J. E. Powers, B. L. Taylor, P. R. Wade, and J. F. Witzig.
1998. Technical guidance on the use of precautionary approaches to implementing National Standard 1 of the Magnuson-Stevens Fishery Conservation and Management Act. NOAA Technical Memo. NMFS-F/SPO-31, 54 p. National Technical information Center, 5825 Port Royal Road, Springfield, VA 22161.

Rose, K. A., J. H. Cowan, K. O. Winemiller, R. A. Myers, and R. Hilborn.
2001. Compensatory density dependence in fish populations: importance, controversy, understanding and prognosis. Fish Fish. 2:293–327.

Sadovy, Y., and A-M. Eklund
1999. Synopsis of biological data on the Nassau grouper, *Epinephelus striatus* (Bloch, 1792), and the jewfish, *E. itajara* (Lichtenstein, 1822). NOAA Tech. Report NMFS 146, 65 p.

Wolfson, L. J., J. B. Kadane, and M. J. Small.
1996. Bayesian environmental policy decisions: two case studies. Ecol. Appl. 6:1056–1066.

Appendix 1: reparameterized spawner-recruit relationships

The number of young fish recruiting to a population (R) is often related to the aggregate fecundity of the spawning stock (S) by using one of two functional forms:

$$R = \begin{cases} aSe^{-bS} & \text{Ricker} \\ \dfrac{abS}{b+S}. & \text{Beverton and Holt} \end{cases} \quad \text{(A.1)}$$

The parameter a is the slope of the curve at the origin and the parameter b controls the degree of density dependence. Notice that the domain of both functions extends from zero to infinity, whereas in practice there must be some limitation on S and R even in the absence of fishing owing to environmental constraints (call them S_0 and R_0, respectively). This being so, we obtain

$$a\frac{S_0}{R_0} = \begin{cases} e^{bS_0} & \text{Ricker} \\ 1+S_0/b. & \text{Beverton and Holt} \end{cases} \quad \text{(A.2)}$$

The ratio S_0/R_0 represents the maximum expected lifetime fecundity of each recruit and a represents the survival of recruits in the absence of density dependence. Accordingly, the product $\alpha = aS_0/R_0$ may be interpreted as the maximum possible number of recruits produced by each spawner over its lifetime (Myers et al., 1999).

The dimensionless character of α makes it useful for interspecies comparisons, or for borrowing values from species with similar life history strategies. Solving for b in terms of α one obtains

$$b = \begin{cases} \log_e \alpha / S_0 & \text{Ricker} \\ S_0/(1-\alpha). & \text{Beverton and Holt} \end{cases} \quad \text{(A.3)}$$

Substituting Equation A.3 into Equation A.1 gives

$$R = \begin{cases} aS\alpha^{-S/S_0} & \text{Ricker} \\ \dfrac{aS_0}{1+(\alpha-1)S/S_0} & \text{Beverton and Holt} \end{cases} \quad \text{(A.4)}$$

and, since $a = \alpha R_0/S_0$,

$$R = \begin{cases} R_0 \dfrac{S}{S_0} \alpha^{1-S/S_0} & \text{Ricker} \\ R_0 \dfrac{\alpha S/S_0}{1+(\alpha-1)S/S_0}. & \text{Beverton and Holt} \end{cases} \quad \text{(A.5)}$$

Dividing through by R_0 and defining s as S/S_0 gives Equation 4.

Appendix 2: formula for equilibrium spawning biomass

The spawning potential ratio (p) is defined as the number of spawners produced by each recruit at equilibrium with a given fishing mortality rate F divided by the number of spawners per recruit under virgin conditions (F=0). This may be written

$$p = \frac{\psi_F}{\psi_0} = \frac{\tilde{S}_F/\tilde{R}_F}{\tilde{S}_0/\tilde{R}_0} = \frac{\tilde{S}_F/S_0}{\tilde{R}_F/\tilde{R}_0} = \tilde{s}/\tilde{r}, \quad \text{(A.6)}$$

where the tilde signifies equilibrium values.

At equilibrium we also obtain from Equation 4

$$\tilde{r} = \begin{cases} \tilde{s}\alpha^{1-\tilde{s}} & \text{Ricker} \\ \dfrac{\alpha\tilde{s}}{(1+\tilde{s}(\alpha-1))}. & \text{Beverton and Holt} \end{cases} \quad \text{(A.7)}$$

Dividing both sides of Equation A.7 by $\tilde{r}$, substituting p for Equation A.6, and solving for $\tilde{s}$ gives Equation 10.

Fish assemblages found in tidal-creek and seagrass habitats in the Suwannee River estuary

Troy D. Tuckey

Florida Fish and Wildlife Conservation Commission
Florida Wildlife Research Institute
Apalachicola Field Laboratory
East Point, Florida 32328
Present address: School of Marine Science
Virginia Institute of Marine Science
College of William and Mary
P.O. Box 1346, Route 1208 Greate Road
Gloucester Point, Virginia, 23062
E-mail address: tuckey@vims.edu

Mark Dehaven

Department of Agriculture and Consumer Services
Division of Aquaculture
11350 SW 153rd Ct.
Cedar Key, Florida 32625

Abstract—Fish assemblages were investigated in tidal-creek and seagrass habitats in the Suwannee River estuary, Florida. A total of 91,571 fish representing 43 families were collected in monthly seine samples from January 1997 to December 1999. Tidal creeks supported greater densities of fish (3.89 fish/m^2; 83% of total) than did seagrass habitats (0.93 fish/m^2). We identified three distinct fish assemblages in each habitat: winter–spring, summer, and fall. Pinfish (*Lagodon rhomboides*), pigfish (*Orthopristis chrysoptera*), and syngnathids characterized seagrass assemblages, whereas spot (*Leiostomus xanthurus*), bay anchovy (*Anchoa mitchilli*), silversides (*Menidia* spp.), mojarras (*Eucinostomus* spp.), and fundulids characterized tidal-creek habitats. Important recreational and commercial species such as striped mullet (*Mugil cephalus*) and red drum (*Sciaenops ocellatus*) were found primarily in tidal creeks and were among the top 13 taxa in the fish assemblages found in the tidal-creek habitats. Tidal-creek and seagrass habitats in the Suwannee River estuary were found to support diverse fish assemblages. Seasonal patterns in occurrence, which were found to be associated with recruitment of early-life-history stages, were observed for many of the fish species.

Manuscript submitted 20 July 2004 to the Scientific Editor's Office.

Manuscript approved for publication 19 July 2005 by the Scientific Editor.

Fish. Bull. 104:102–117 (2006).

The Suwannee River estuary, located on the gulf coast of Florida, is relatively pristine and supports commercial and recreational fisheries. It is an unusual estuary, with an orientation along the open coastal shoreline, and its habitats include oyster bars, mudflats, seagrasses, tidal creeks, and an extensive salt marsh (Comp and Seaman, 1985). In other estuaries of the United States, fish assemblages, species abundance, and habitat associations within estuaries have been studied extensively. Particular attention has focused on estuaries as nursery habitats for young-of-the-year (YOY) fishes that use seagrasses, tidal-creeks, and marshes during their early-life stages (Shenker and Dean, 1979; Bozeman and Dean, 1980; Livingston, 1984; Cowan and Birdsong, 1985; Gilmore, 1988; McGovern and Wenner, 1990; Baltz et al., 1993; Peterson and Turner, 1994; Rooker et al., 1998). In addition, comparisons between different habitats within estuarine systems have been conducted to evaluate the value of each habitat as a nursery (Weinstein and Brooks, 1983; Sogard and Able, 1991; Rozas and Minello, 1998; Paperno et al., 2001). Aside from basic species-composition studies of marsh fishes (Kilby, 1955; Nordlie, 2000) and fishes that inhabit shallow waters near Cedar Key (Reid, 1954), only one recent study (Tsou and Matheson, 2002) has investigated the distribution patterns of fishes in the Suwannee River estuary. Tsou and Matheson (2002) found that the nekton community structure for the Suwannee River estuary had a strong seasonal pattern that was consistent among years and followed patterns for water temperature and river discharge. They found assemblages that were associated with warm and cold seasons, and wet and dry seasons, but they did not examine habitat specific assemblages (Tsou and Matheson, 2002). For proper management of fishery resources, it is beneficial to have detailed, current information concerning the status of all life-history stages and associated habitats of species that reside in the area, as well as information concerning species interactions and associated food webs. Although human development in the Suwannee River estuary is not a current threat, the potential withdrawal of freshwater from the Suwannee River for human consumption is a possibility and could impact fish assemblages found in the estuary (Tsou and Matheson, 2002).

This article describes habitat-specific assemblages by examining the fish fauna collected in seagrass habi-

tats with those collected in tidal-creek habitats in the Suwannee River estuary. We performed comparisons of monthly collections of fish found along tidal-creek shorelines and those found in seagrass habitats to define fish assemblages and incorporated abiotic parameters as potential factors influencing the assemblages. We also compared length distributions of species in each habitat to examine the success of YOY recruitment and the subsequent influence of YOY recruitment on fish assemblages in order to understand the nursery function of each habitat.

Methods

Study location

This study took place in the Suwannee River estuary, which lies along the gulf coast of Florida, extending from just north of the Suwannee River to Cedar Key (Fig. 1). The Suwannee River empties directly into the Gulf of Mexico forming an unusual open estuary that stretches 13 kilometers north of the river mouth, southeastward to the islands of Cedar Key, and extends approximately 8 kilometers offshore (Leadon[1]). The Suwannee River estuary is shallow (water depth <2.2 m below mean sea level), and has semidiurnal tides with a tidal range of 0.7 m. The shoreline is relatively undeveloped; the city of Cedar Key (pop. 898) along the southeastern edge of the estuary and the small town of Suwannee approximately 4.8 kilometers inland along the Suwannee River are the only populated areas. The remainder of the coastline, consisting of the Lower Suwannee and Cedar Keys National Wildlife Refuges and the Cedar Key State Preserve, is owned by the public.

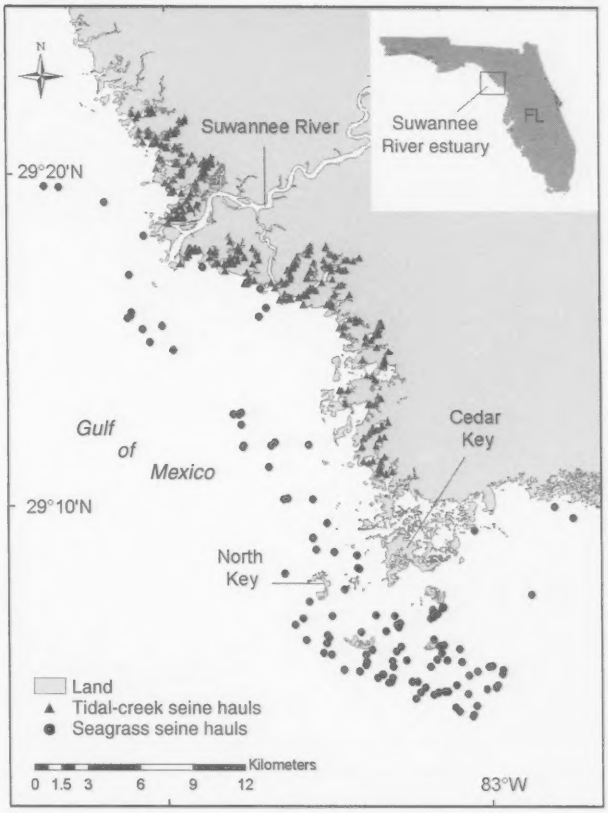

Figure 1

Study area showing location of tidal-creek and seagrass seine hauls in the Suwannee River estuary, located on the gulf coast of Florida.

Study design

Randomly selected sites were sampled monthly within tidal-creek and seagrass habitats from January 1997 through December 1999. Juvenile and small adult fish from each site were collected using a 21.3-m × 1.8-m nylon seine with 3.2-mm mesh and a center bag measuring 1.8-m × 1.8-m × 1.8-m. Sampling methods depended on the habitat sampled, and all seines were deployed during daylight hours.

Collections in tidal creeks consisted of six hauls per month in 1997 and increased to nine hauls per month in 1998 and 1999. Tidal creeks consisted of soft mud, deep channels, oyster bars, and steep banks. Shoreline vegetation included saltmarsh cord grass (*Spartina alterniflora*) and needle rush (*Juncus roemerianus*) near the creek mouths and changed to a variety of freshwater marsh grasses and terrestrial vegetation upstream. The seine was set from a boat in a semicircular pattern along the shoreline, retrieved onshore, and sampled an average area of 68 m^2 per haul. Shoreline areas inundated with vegetation were not sampled if the water depth was greater than 0.5 m in order to reduce the interference of vegetation during sample collections. Sampling in tidal-creeks was limited to the shoreline because the water was too deep in the channels to deploy the seine. In addition, despite the importance of oyster bar habitat, oyster bars located inside tidal creeks were not sampled because they interfered with the proper deployment of the seine.

Seagrass habitats generally surrounded the major islands near Cedar Key, including North Key and nearby islands (Fig. 1). In addition, vegetated patches extended from North Key northwestward to the mouth of the Suwannee River and were present in shallow areas approximately three kilometers west of the Suwannee River (Fig. 1). Dominant seagrass species in the Suwannee River estuary included turtle grass (*Thalassia testudi-*

[1] Leadon, C. J. 1979. Unpubl. manuscr. Environmental effects of river flows and levels in the Suwannee River subbasin below Wilcox and the Suwannee River estuary, Florida, 59 p. Suwannee River Water Management District Interim Report, 9225 County Road 49, Live Oak, FL 32060.

num), manatee grass (*Syringodium filliforme*), and shoal grass (*Halodule wrightii*). Percent coverage was estimated visually, or if water clarity was insufficient to visually inspect the bottom, bottom samples were collected at 3-m intervals during deployment of the seine. For analytical purposes, areas sampled had to contain at least ten percent seagrass to be considered seagrass habitat. Samples were classified as "vegetated" or "unvegetated" after sampling; and monthly collections varied from one to seven hauls per month depending on seagrass coverage. Seagrass habitats were sampled by pulling the seine into the current or wind, whichever was strongest. We kept the opening of the net at a constant width by maintaining tension on a 15.5-m line that was attached between each end pole of the seine while the seine was hauled for a distance of 9.1 m. The distance covered by the seine was measured by a weighted line from the starting point. The net was retrieved by bringing the end poles together and pulling the net at an angle around a vertical pole that closed the wings of the net and forced the catch into the bag. A typical seine haul over seagrass habitat covered approximately 140 m^2.

In the field, all fish were identified to the lowest possible taxon, counted, and released. Up to 40 individuals of species of special interest (important to the commercial or recreational fishery) and 10 individuals of all other species were measured to the nearest millimeter standard length (SL). For quality-control purposes, three specimens of each species collected were returned to the laboratory so that species identification could be confirmed. At each site, Secchi depth and water depth were measured, and water temperature (°C), salinity, dissolved oxygen level (mg/L), and pH were measured by using a Hydrolab Surveyor3® water-quality instrument (Hach Environmental, Loveland, CO).

Data analysis

Multivariate analyses were used to compare fish community structures along tidal-creek shorelines to those found in seagrass habitats (Field et al., 1982). Average monthly abundance estimates (number of fish divided by the number of hauls) were calculated separately for each fish species in each habitat type. Average monthly abundance estimates were then converted to percent composition to correct for bias introduced by the two different net-deployment methods and for the different levels of effort in each habitat. Fishes that were not identified to species were eliminated (<0.1% of total fish collected) except where species complexes, such as silversides (*Menidia* spp.), mojarras (*Eucinostomus* spp. <50 mm SL), menhaden (*Brevoortia* spp.), and minnows (*Notropis* spp.) were substituted. Species complexes were used when meristic characters for juveniles were insufficient to distinguish between two or more possible species (*Eucinostomus* spp. and *Notropis* spp.) or where there was possible hybridization (*Menidia* spp. and *Brevoortia* spp.).

Fish-community comparisons based on percent species composition by habitat and month were conducted by using algorithms in PRIMER (Plymouth Routines in Multivariate Ecological Research, vers. 5, Plymouth Marine Laboratory, UK) for the study of community structure (Clarke and Warwick, 1994). To identify fish assemblages, hierarchical agglomerative cluster analysis was performed with the Bray-Curtis similarity matrix calculated on fourth-root transformed percentage data. The fourth-root transformation reduced the dominance of abundant species and increased the influence of less abundant species in the community analysis. The cluster analysis was run on one matrix consisting of all transformed fish abundance estimates collected in tidal-creek and seagrass habitats combined.

To identify species that were responsible for the patterns observed in the cluster analysis, similarity and dissimilarity percentage breakdowns were conducted by using the SIMPER procedure in PRIMER (Clarke, 1993). Average similarities between assemblages were analyzed to determine the contribution of each species to the overall similarity. This procedure reduced the number of species required to explain the patterns observed in the cluster diagram and allowed for a simplified interpretation of the species assemblages. The higher the similarity value, the more alike samples were within assemblages. Alternatively, dissimilarity values were examined to identify species that were characteristic of a particular assemblage. Species that have high average dissimilarity values and low standard deviations are those that contribute consistently to samples within their group, with the result that they can be used to distinguish between groups.

The relationship between environmental variables and fish community structure was examined by using the BIO-ENV procedure. A Spearman rank correlation test was used to compare ranked values from the aforementioned biota similarity matrix to ranked values from an environmental similarity matrix, which was created from environmental variables measured in this study. Comparisons were based on normalized Euclidean distance. The environmental variables used to create the environmental similarity matrix included pH, water temperature, salinity, water depth, and Secchi depth. Dissolved oxygen was strongly correlated with water temperature and was therefore not included in the analysis because it would produce results similar to those produced by water temperature. Abiotic variables were standardized by subtracting each mean and dividing by the standard error to remove any bias associated with the different measurement scales.

The influence of recruitment of YOY fishes in defining fish assemblages was examined. By relating increases in abundance of species that were identified to be important contributors through the SIMPER procedure to decreases in their average length in both habitats, we were able to identify the timing of juvenile recruitment. Length-frequency distributions showed that the seine continued to catch larger individuals and therefore the decrease in average length was not due to a decrease

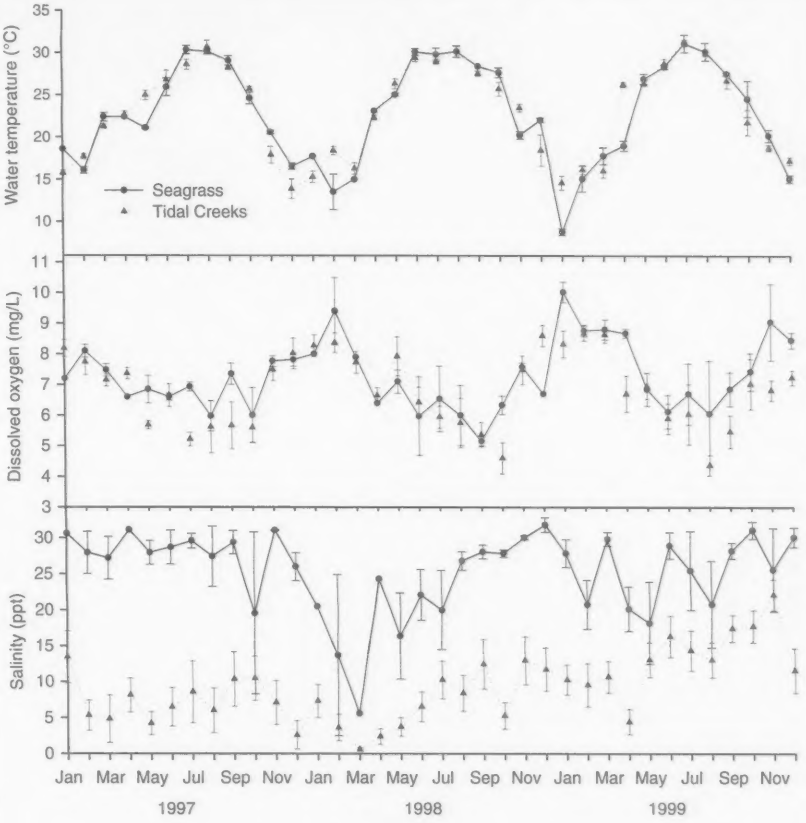

Figure 2

Monthly mean values (± standard error) for water temperature, dissolved oxygen, and salinity from January 1997 to December 1999. Circles represent values measured in seagrass habitats; triangles represent values measured in tidal-creek habitats.

in the number of larger fish. The mean length of each species in each sample was calculated by habitat, and differences in mean length were tested by using fish assemblages as the main factor in a one-way ANOVA. Multiple comparisons tests (Tukey's test) were then conducted to examine significant ANOVA results and these tests determined which assemblages contained fishes with significantly different lengths.

Results

Environmental conditions

The combination of water temperature, salinity, and water depth had the highest correlation (ρ_w=0.659) with the fish assemblages of any possible combination of measured abiotic variables. Seasonal patterns were observed for water temperature and dissolved oxygen, whereas salinity fluctuated in seagrass habitats and generally increased during 1999 in tidal-creek habitats (Fig. 2). Water temperatures ranged from 7.5° to 32.5°C (mean=23.0°C, SE=0.99) in the seagrass habitats and ranged from 10.3° to 33.3°C (mean=23.1°C, SE=0.91) in the tidal-creek habitats. Minimum values of dissolved oxygen coincided with the highest water temperatures in each habitat and ranged from 2.9 to 12.7 mg/L in the seagrass habitats and from 2.9 to 13.6 mg/L in the tidal-creek habitats. Salinity, however, was lower during all seasons in the tidal-creek habitats than in the seagrass habitats (Fig. 2). Mean salinity in the seagrass habitats was 27.1‰ (SE=0.91) and ranged from nearly fresh (1.3‰) to marine (34.8‰) depending on river discharge, whereas in the tidal creeks, mean salinity was 9.5‰ (SE=0.81) and ranged from 0.0‰ to 29.0‰. An unusually high period of rain during February and March of 1998 decreased salinity values in the tidal-creek and seagrass habitats.

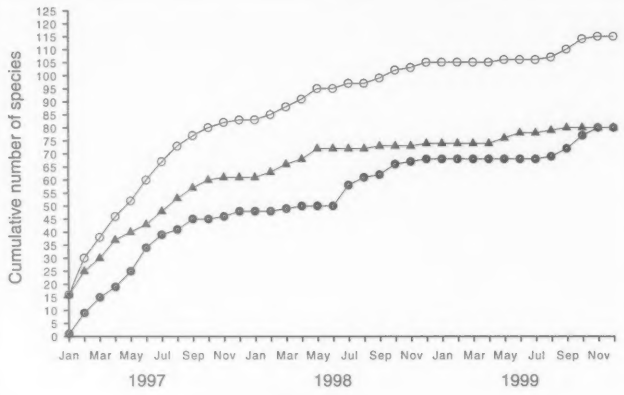

Figure 3

Cumulative number of species collected in both tidal-creek and seagrass habitats (open circles) and number of species collected in tidal-creeks (triangles) and seagrass habitats (filled circles) by year and month from January 1997 to December 1999.

Fish fauna

At the conclusion of the three-year study, 111 fish species and 4 additional species complexes had been collected. During the first year of the study, 61 species were collected in samples taken in tidal-creek habitats, and 48 species were collected in seagrass habitats (Fig. 3). Thirteen new species were added to the species list from tidal creek samples and 20 new species were added to the list from samples taken in seagrass habitats during 1998. During the final year of sampling only six additional species were collected in tidal creeks and 12 new species were collected in seagrass habitats. Overall, tidal creeks contained greater relative (uncorrected for gear efficiency) densities of fish (3.89 fish/m^2) compared with seagrass habitats (0.93 fish per m^2). In seagrass habitats, 15,395 individuals were collected in 118 samples that covered approximately 16,520 m^2 of seagrass habitat (Table 1). In tidal-creek habitats, a total of 76,176 individuals were collected from 288 samples that covered approximately 19,584 m^2 of tidal-creek shoreline habitat (Table 2). Thirty-five species were restricted to seagrass habitats, and another 35 species were collected only in tidal creeks. The remaining 45 species were collected in both habitats at least once during the study. Overall, twelve families were restricted to seagrass habitats: phycid hakes (Phycidae), toadfishes (Batrachiodidae), batfishes (Ogcocephalidae), flyingfishes (Exocoetidae), cardinalfishes (Apogonidae), barracudas (Sphyraenidae), wrasses (Labridae), combtooth blennies (Blenniidae), mackerels (Scombridae), triggerfishes (Balistidae), boxfishes (Ostraciidae), and porcupinefishes (Diodontidae; Table 1). Seven families were restricted to tidal-creek habitats: minnows (Cyprinidae), sunfishes (Centrarchidae), killifishes (Cyprinodontidae), gars (Lepisosteidae), eagle rays (Myliobatidae), pikes (Esocidae), and livebearers (Poeciliidae; Table 2).

Fish assemblages

A clear separation of fish assemblages was identified and indicated by two main branches that corresponded to fishes found in seagrass habitats and those found in tidal-creek habitats (Fig. 4). There were two months identified from seagrass samples (January 1997 and March 1998) that had a species composition that was more closely linked to samples taken from tidal creeks.

Seagrass habitats

Seasonal fish assemblages in seagrass habitats were evident during all three years of the study, which included winter–spring, summer, and fall assemblages (Fig. 4). The winter–spring assemblage consisted principally of pinfish (*Lagodon rhomboides*), pigfish (*Orthopristis chrysoptera*), dusky pipefish (*Syngnathus floridae*), southern puffer (*Sphoeroides nephelus*), and gulf pipefish (*Syngnathus scovelli*), which together accounted for more than 95% of the cumulative percent similarity. The summer assemblage had a higher average similarity value (43.67) than did the winter–spring assemblage (42.56) and consisted of more than 21 species. Eleven of these species—silver perch (*Bairdiella chrysoura*), *S. floridae*, bay anchovy (*Anchoa mitchilli*), *L. rhomboides*, *Eucinostomus* spp., spotted seatrout (*Cynoscion nebulosus*), *S. scovelli*, planehead filefish (*Monacanthus hispidus*), striped anchovy (*Anchoa hepsetus*), inshore lizardfish (*Synodus foetens*), and *O. chrysoptera*—accounted for more than 75% of the cumulative similarity of the summer assemblage. The fall assemblage had the high-

Table 1

Taxonomic list of individuals collected in seagrass habitats for each species by month and total number collected, all years combined.

Family	Species	Jan	Feb	Mar	Apr	May	Jun	Jul	Aug	Sep	Oct	Nov	Dec	Total
Dasyatidae	*Dasyatis sabina*	0	0	0	0	0	0	1	0	1	3	1	1	7
	Dasyatis say	0	0	0	0	0	2	0	0	0	0	0	0	2
Ophichthidae	*Myrophis punctatus*	0	0	0	1	0	0	0	0	0	0	0	0	1
Clupeidae	*Harengula jaguana*	0	0	0	0	0	0	6	230	0	162	0	0	398
	Brevoortia spp.	0	0	1	0	0	0	0	0	0	0	0	0	1
	Opisthonema oglinum	0	0	0	0	0	4	1	4	35	9	0	0	53
	Sardinella aurita	0	0	0	0	0	0	0	16	0	0	0	0	16
Engraulidae	*Anchoa hepsetus*	0	0	0	0	1	540	2	1	235	13	3	0	795
	Anchoa mitchilli	0	0	4	3	0	38	1567	3838	632	3504	53	0	9639
Ariidae	*Arius felis*	0	0	0	0	0	1	1	14	45	1	0	0	62
	Bagre marinus	0	0	0	0	0	0	0	0	1	0	0	0	1
Synodontidae	*Synodus foetens*	0	0	0	0	1	2	3	8	3	1	1	1	20
Gadidae	*Urophycis floridana*	0	0	0	0	0	0	0	0	0	0	0	6	6
Batrachiodidae	*Opsanus beta*	0	0	0	0	0	0	0	0	1	0	0	0	1
Ogcocephalidae	*Ogcocephalus radiatus*	0	0	0	1	0	0	0	0	0	0	0	0	1
Exocoetidae	*Hyporhamphus meeki*	0	0	0	0	1	7	2	0	0	0	0	0	10
Belonidae	*Strongylura marina*	0	0	0	0	0	1	3	1	0	0	0	0	5
Atherinidae	*Membras martinica*	0	10	0	0	1	10	49	21	13	15	3	0	122
	Menidia spp.	0	0	0	0	0	0	0	0	0	0	1	2	3
Syngnathidae	*Hippocampus erectus*	0	0	0	0	0	0	0	0	0	1	0	0	1
	Hippocampus zosterae	0	1	0	0	0	0	1	1	2	0	1	2	8
	Syngnathus floridae	2	7	1	9	2	34	33	53	48	26	52	38	305
	Syngnathus louisianae	0	0	0	1	0	3	4	2	1	4	3	0	18
	Syngnathus scovelli	0	3	6	4	0	11	32	4	9	10	13	13	105
Serranidae	*Mycteroperca microlepis*	0	0	0	0	0	0	0	0	0	1	0	0	1
	Centropristis striata	0	0	0	0	0	1	2	7	12	3	74	12	111
	Serraniculus pumilio	0	0	0	0	0	0	0	0	0	0	10	0	10
	Serranus subligarius	0	0	0	0	0	0	0	0	2	0	0	0	2
Apogonidae	*Astrapogon alutus*	0	0	0	0	0	0	0	0	0	1	0	0	1
Carangidae	*Caranx hippos*	0	0	0	0	0	0	0	0	0	2	0	0	2
	Chloroscombrus chrysurus	0	0	0	0	0	0	2	12	5	0	0	0	19
	Oligoplites saurus	0	0	0	0	0	7	2	2	4	2	0	0	17
	Selene vomer	0	0	0	0	0	0	0	0	0	2	0	0	2
Lutjanidae	*Lutjanus griseus*	0	0	0	0	0	0	0	1	0	1	0	0	2
	Lutjanus synagris	0	0	0	0	0	0	3	0	0	1	2	0	6
Gerreidae	*Eucinostomus gula*	0	0	0	0	0	0	0	0	6	6	4	1	17
	Eucinostomus harengulus	0	0	0	0	0	1	0	2	1	0	0	0	4
	Eucinostomus spp.	0	0	0	0	0	34	172	162	73	13	54	36	544
Haemulidae	*Haemulon plumieri*	0	0	0	0	0	0	1	6	11	4	3	7	32
	Orthopristis chrysoptera	1	0	6	26	738	30	38	0	8	4	0	1	852
Sparidae	*Diplodus holbrooki*	0	0	0	0	7	17	0	4	1	7	0	0	36
	Lagodon rhomboides	17	65	63	87	21	54	24	27	40	36	32	87	553
Sciaenidae	*Bairdiella chrysoura*	0	0	0	3	24	159	273	59	184	44	2	1	749
	Cynoscion arenarius	0	0	0	0	0	0	1	24	0	0	0	0	25
	Cynoscion nebulosus	0	0	0	0	0	4	70	37	10	6	1	0	128
	Leiostomus xanthurus	2	34	1	0	0	0	0	0	2	0	0	0	39
	Menticirrhus americanus	0	0	0	0	0	2	13	119	2	0	1	0	137

continued

Table 1 (continued)

Family	Species	Jan	Feb	Mar	Apr	May	Jun	Jul	Aug	Sep	Oct	Nov	Dec	Total
Sciaenidae (cont.)	*Menticirrhus saxatilis*	0	0	1	0	0	7	0	5	0	0	0	2	15
	Sciaenops ocellatus	0	0	0	0	0	0	0	0	0	0	9	0	9
Ephipidae	*Chaetodipterus faber*	0	0	0	0	0	0	2	12	2	0	0	0	16
Mugilidae	*Mugil cephalus*	0	5	1	0	0	0	0	0	0	0	0	0	6
	Mugil curema	0	0	0	1	0	0	0	0	0	0	0	0	1
Sphyraenidae	*Sphyraena borealis*	0	0	0	0	4	0	0	0	0	0	0	0	4
Labridae	*Halichoeres bivittatus*	0	0	0	0	0	0	0	3	0	0	0	0	3
	Lachnolaimus maximus	0	0	0	0	0	0	0	0	2	1	0	0	3
Blenniidae	*Chasmodes saburrae*	0	0	0	0	0	0	9	0	5	0	2	0	16
	Parablennius marmoreus	0	0	0	0	0	0	0	1	0	0	1	0	2
	Hypsoblennius hentzi	0	0	0	0	0	0	0	0	1	0	0	2	3
	Hypleurochilus geminatus	0	0	0	0	0	0	2	0	0	0	0	0	2
Gobiidae	*Gobionellus boleosoma*	0	0	0	0	0	0	9	0	0	0	0	0	9
	Gobiosoma bosc	0	0	0	0	0	0	29	0	0	0	1	0	30
	Gobiosoma longipala	0	0	0	0	0	0	0	0	0	1	0	0	1
	Gobiosoma robustum	0	0	0	2	0	0	7	2	0	1	0	1	13
	Microgobius gulosus	0	0	0	0	0	0	3	2	0	0	2	0	7
	Microgobius thalassinus	0	0	0	0	0	0	0	77	0	0	0	0	77
Scombridae	*Scomberomorus maculatus*	0	0	0	0	0	0	0	0	1	0	0	0	1
Triglidae	*Prionotus scitulus*	0	2	0	0	0	2	5	4	2	1	0	1	17
	Prionotus tribulus	0	0	0	0	0	0	0	2	0	0	1	0	3
Bothidae	*Paralichthys albigutta*	0	0	2	2	0	0	2	0	2	0	0	0	8
	Etropus crossotus	0	3	1	0	0	0	2	1	1	0	0	1	9
	Etropus microstomus	0	0	1	0	0	0	0	0	0	0	0	0	1
Cynoglossidae	*Symphurus plagiusa*	0	0	1	0	0	1	1	9	0	0	0	1	13
Soleidae	*Achirus lineatus*	0	0	0	0	0	0	1	7	0	0	0	0	8
	Trinectes maculatus	0	0	0	0	0	0	0	0	1	0	0	0	1
Balistidae	*Aluterus schoepfi*	0	0	0	0	0	1	1	2	0	1	0	0	5
	Monacanthus ciliatus	0	0	0	0	0	0	0	2	10	8	2	19	41
	Monacanthus hispidus	0	0	0	0	2	10	1	36	3	9	7	25	93
Ostraciidae	*Lactophrys quadricornis*	0	0	2	0	0	2	0	6	6	3	3	1	23
Tetraodontidae	*Sphoeroides nephelus*	0	0	2	16	4	2	2	2	1	4	2	2	37
Diodontidae	*Chilomycterus schoepfi*	0	1	2	0	4	2	0	11	5	10	5	9	49
Column total		22	131	95	156	810	989	2382	4839	1429	3921	349	272	15,395
Number of hauls		6	10	9	4	5	15	10	11	11	11	10	16	118

est average similarity level at 48.90, and nine species—*S. floridae*, *M. hispidus*, black seabass (*Centropristis striata*), *L. rhomboides*, *Eucinostomus* spp., fringed filefish (*Monacanthus ciliatus*), *S. scovelli*, striped burrfish (*Chilomycterus schoepfi*), and *S. nephelus*—accounted for more than 91% of the cumulative similarity. *Lagodon rhomboides* and *S. floridae* were characteristic of all three assemblages, and *Eucinostomus* spp., *S. scovelli*, and *M. hispidus* were important contributors to the summer and fall assemblages. Other abundant species from seagrass assemblages included southern kingfish (*Menticirrhus americanus*), rough silverside (*Membras martinica*), and gobiids, particularly green goby (*Microgobius thalassinus*) and naked goby (*Gobiosoma bosc*).

A significant drop in salinity during March 1998 corresponded to an alteration in the fish community collected in seagrass habitats. The species present in the seagrass habitats during March 1998 were more consistent with species collected in tidal creeks and included *A. mitchilli*, *Brevoortia* spp., and spot (*Leiostomus xanthurus*), none of which were collected in March of 1997 or 1999 in seagrass habitats. Samples collected during March 1997 and 1999 contained individuals more characteristic of seagrass habitats, such as *C. schoepfi*, *L. rhomboides*, *O. chrysoptera*, and *S. nephelus* in 1997 and scrawled cowfish (*Acanthostracion quadricornis*), *O. chrysoptera*, *L. rhomboides*, *S. floridae*, and *S. scovelli* in 1999.

Table 2

Taxonomic list of individuals collected in tidal-creeks for each species by month and total number collected, all years combined.

Family	Species	Jan	Feb	Mar	Apr	May	Jun	Jul	Aug	Sep	Oct	Nov	Dec	Total
Dasyatidae	*Dasyatis sabina*	0	0	6	1	1	0	0	0	1	1	3	0	13
Myliobatidae	*Rhinoptera bonasus*	0	0	0	0	3	0	0	0	0	0	0	0	3
Lepisosteidae	*Lepisosteus osseus*	0	0	0	0	0	2	2	1	0	0	0	0	5
	Lepisosteus platyrhincus	0	0	1	1	0	1	1	0	2	2	0	0	8
Ophichthidae	*Myrophis punctatus*	0	0	0	0	1	0	0	0	0	0	0	0	1
Clupeidae	*Harengula jaguana*	0	0	0	0	2	1	2	9	10	2	0	0	26
	Brevoortia spp.	15	139	93	400	394	7	5	0	0	0	0	1	1054
	Sardinella aurita	0	0	0	0	0	0	22	0	0	0	0	0	22
Engraulidae	*Anchoa hepsetus*	3	0	0	1	175	482	71	33	7	0	3	0	775
	Anchoa mitchilli	86	497	825	108	612	3298	10,329	6970	5776	7436	1637	2107	39,681
Cyprinidae	*Notemigonus crysoleucas*	0	2	1	0	0	0	0	0	0	0	0	0	3
	Notropis spp.	0	0	0	0	4	9	0	0	0	0	0	0	13
Ariidae	*Arius felis*	0	0	0	0	0	0	0	2	3	0	0	0	5
Esocidae	*Esox niger*	0	0	0	1	1	0	0	0	0	0	0	0	2
Synodontidae	*Synodus foetens*	0	0	0	3	7	0	0	0	1	0	3	1	15
Belonidae	*Strongylura marina*	0	0	0	2	4	1	8	1	1	1	0	0	18
	Strongylura notata	2	0	0	0	0	0	3	2	8	0	1	0	16
	Strongylura timucu	0	0	0	0	11	1	8	3	11	0	0	0	34
Cyprinodontidae	*Adinia xenica*	7	7	0	4	1	0	12	23	0	153	14	25	246
	Cyprinodon variegatus	4	0	0	1	0	0	0	0	0	0	2	3	10
	Lucania goodei	0	0	11	0	0	0	0	0	0	0	0	0	11
	Lucania parva	0	2	2	0	0	1	2	15	4	0	0	6	32
Fundulidae	*Fundulus confluentus*	2	0	0	0	0	0	0	0	0	1	0	3	6
	Fundulus grandis	33	39	6	28	9	30	21	127	9	39	170	218	729
	Fundulus majalis	29	12	24	7	0	18	0	42	3	10	13	65	223
	Fundulus seminolis	7	2	0	1	0	14	0	14	5	6	0	1	50
Poeciliidae	*Gambusia holbrooki*	6	0	59	2	4	1	0	1	12	4	1	7	97
	Heterandria formosa	0	1	0	0	0	0	0	0	0	1	0	0	2
	Poecilia latipinna	1	0	0	0	2	2	0	17	0	4	4	12	42
Atherinidae	*Membras martinica*	0	0	4	0	9	566	2286	28	114	7	1	0	3015
	Menidia spp.	383	429	201	265	145	695	982	571	814	602	749	358	6194
Syngnathidae	*Syngnathus floridae*	0	1	0	0	0	0	0	0	1	0	0	0	2
	Syngnathus louisianae	0	0	0	0	0	0	0	0	1	0	1	0	2
	Syngnathus scovelli	2	1	2	0	1	0	1	7	5	1	2	11	33
Serranidae	*Diplectrum bivittatum*	0	0	0	0	0	0	0	0	0	0	1	0	1
Centrarchidae	*Enneacanthus gloriosus*	0	0	2	0	0	0	0	0	0	0	0	0	2
	Elassoma zonatum	0	0	0	0	4	0	0	0	0	0	0	0	4
	Lepomis gulosus	0	1	1	0	0	0	0	0	0	0	0	0	2
	Lepomis macrochirus	0	0	0	0	0	0	0	0	1	0	0	0	1
	Lepomis marginatus	0	0	0	1	0	0	0	0	0	0	0	0	1
	Lepomis microlophus	0	0	0	0	1	0	0	0	0	0	0	0	1
	Lepomis punctatus	1	0	0	1	1	1	2	2	3	2	0	0	13
	Micropterus salmoides	0	0	3	1	14	4	0	5	8	2	0	0	37
Carangidae	*Chloroscombrus chrysurus*	0	0	0	0	0	0	1	3	15	2	0	0	21
	Oligoplites saurus	0	0	0	0	0	8	53	25	47	17	6	0	156
	Trachinotus falcatus	0	0	0	0	0	0	0	0	0	3	0	0	3

continued

Table 2 (continued)

Family	Species	Jan	Feb	Mar	Apr	May	Jun	Jul	Aug	Sep	Oct	Nov	Dec	Total
Lutjanidae	*Lutjanus griseus*	0	0	0	0	0	2	2	9	8	6	2	1	30
Gerreidae	*Eucinostomus gula*	1	0	0	0	0	0	0	4	7	25	49	3	89
	Eucinostomus harengulus	0	25	5	2	6	3	41	150	88	100	65	45	530
	Eucinostomus spp.	17	38	6	1	1	87	1035	1082	503	862	691	358	4681
Haemulidae	*Orthopristis chrysoptera*	0	0	0	0	0	0	0	2	0	0	0	0	2
Sparidae	*Archosargus probatocephalus*	7	1	1	0	1	1	0	1	0	0	1	0	13
	Lagodon rhomboides	87	231	146	142	67	114	111	85	38	29	53	10	1113
Sciaenidae	*Bairdiella chrysoura*	0	0	7	7	200	154	58	246	117	4	3	0	796
	Cynoscion arenarius	0	0	0	5	236	102	90	91	46	76	5	0	651
	Cynoscion nebulosus	3	1	1	0	5	11	21	53	62	23	36	2	218
	Leiostomus xanthurus	9526	2044	834	771	274	42	125	24	6	5	2	31	13,684
	Menticirrhus americanus	0	0	0	0	3	12	50	36	12	10	5	0	128
	Micropogonias undulatus	4	4	0	5	2	0	0	0	1	0	6	2	24
	Pogonias cromis	0	0	0	0	2	2	0	3	0	1	0	1	9
	Sciaenops ocellatus	26	28	20	15	3	7	4	1	1	48	105	65	323
Ephipipidae	*Chaetodipterus faber*	0	0	0	0	0	1	3	1	3	0	0	0	8
Mugilidae	*Mugil cephalus*	175	159	59	25	2	39	22	7	18	1	6	6	519
	Mugil curema	1	0	0	0	0	25	2	0	0	0	0	1	29
	Mugil gyrans	0	0	0	0	0	0	0	0	2	0	0	4	6
Gobiidae	*Bathygobius soporator*	0	0	0	4	0	0	2	1	18	5	6	3	39
	Gobionellus boleosoma	0	0	3	6	9	0	1	6	15	0	4	0	44
	Gobiosoma bosc	8	3	14	7	1	40	21	17	52	20	18	67	268
	Gobiosoma robustum	0	6	3	1	0	8	7	10	6	0	4	15	60
	Microgobius gulosus	5	23	7	5	4	7	0	25	5	8	3	14	106
	Microgobius thalassinus	0	0	0	0	0	0	1	1	1	0	1	0	4
Triglidae	*Prionotus scitulus*	0	0	0	0	0	1	0	0	0	0	0	0	1
	Prionotus tribulus	0	0	0	1	0	0	0	0	1	11	4	0	17
Bothidae	*Paralichthys albigutta*	5	1	0	0	0	2	0	0	1	0	0	0	9
	Paralichthys lethostigma	0	0	1	0	0	1	0	0	0	0	0	0	2
	Etropus crossotus	0	0	0	0	0	1	0	0	0	0	0	0	1
Cynoglossidae	*Symphurus plagiusa*	6	0	0	0	0	2	2	1	13	5	1	5	35
Soleidae	*Achirus lineatus*	0	0	0	0	0	2	4	9	10	8	2	0	35
	Trinectes maculatus	1	8	10	0	5	13	1	13	2	4	2	1	60
Tetraodontidae	*Sphoeroides nephelus*	0	0	0	1	6	0	0	0	0	4	0	1	12
Column total		10,453	3705	2358	1826	2233	5821	15,414	9779	7898	9551	3685	3453	76,176
Number of hauls		24	24	24	24	24	24	24	24	24	24	24	24	288

Recruitment of YOY fishes had an influence on defining fish assemblages in seagrass habitats. The winter–spring assemblage was dominated by YOY *L. rhomboides* and *O. chrysoptera* (Table 3), which had significantly shorter standard lengths than did the other assemblages (Table 4). The summer assemblage showed an increase in the number of species and an increase in their abundance, but there were no significant differences in length for YOY for any species between assemblages.

Tidal-creek habitats

Three fish assemblages (winter–spring, summer, and fall) were identified from samples taken in tidal-creek habitats and reflected similar seasonal patterns compared with fish assemblages identified from seagrass habitats (Fig. 4). The winter–spring assemblage had an average similarity level of 51.76 and consisted of *L. xanthurus*, *Menidia* spp., *A. mitchilli*, *L. rhomboides*, *M. cephalus*, and red drum (*Sciaenops ocellatus*). These six

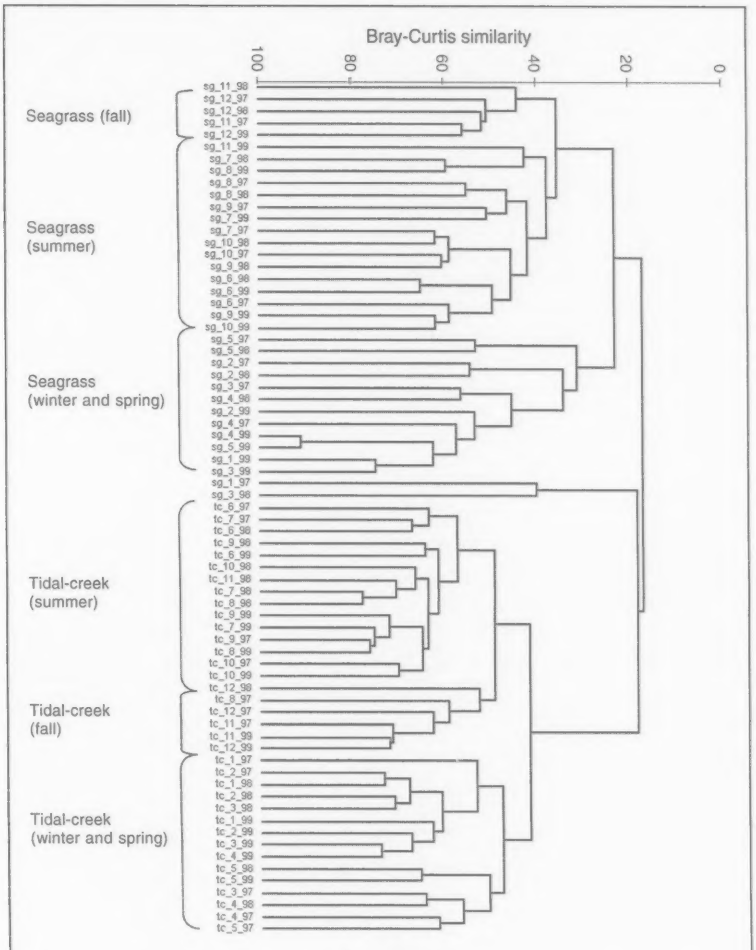

Figure 4

Results of cluster analysis for fish assemblages found in the Suwannee River estuary. SG=seagrass habitats, TC=tidal-creek habitats, 1=January, 2=February, etc., and the year is denoted by the last two digits of the year. For example, SG_1_97 corresponds to samples collected during January of 1997 in seagrass habitats. Note: Clusters are free to rotate at the point at which the lines branch.

species accounted for more than 68% of the cumulative similarity within the winter–spring assemblage. The summer assemblage had an average similarity level of 62.29 and was characterized by ten species that accounted for 70.65% of the cumulative similarity: *A. mitchilli*, *Menidia* spp., *Eucinostomus* spp., sand seatrout (*Cynoscion arenarius*), *B. chrysoura*, *C. nebulosus*, *L. rhomboides*, *E. harengulus*, *M. martinica*, and leatherjacket (*Oligoplites saurus*). The fall assemblage had an average similarity level of 60.36 and was characterized by *Eucinostomus* spp., *Menidia* spp., gulf killifish (*Fundulus grandis*), *A. mitchilli*, *E. harengulus*, diamond killifish (*Adinia xenica*), clown goby (*Microgobius gulosus*), and *M. cephalus*, which accounted for more than 67% of the cumulative similarity. Species tolerant of low salinity, such as *A. xenica*, marsh killifish (*Fundulus confluentus*), mosquitofish (*Gambusia holbrooki*), and least killifish (*Heterandria formosa*) were commonly collected in tidal creeks. There were 35 species collected, including groups such as cyprinids, cyprinodontids, poeciliids, lepisosteids, and centrarchids, which were restricted entirely to tidal creeks (Table 2).

Seasonal recruitment of juvenile fishes to tidal-creek habitats was evident and remained consistent throughout the study resulting in three clearly defined assemblages. Young-of-the-year *L. xanthurus* recruited to

Table 3

Results of SIMPER procedure showing the average percent dissimilarity (δ%) for important species between seagrass assemblages. δi is the average contribution of the ith species to the disssimilarity between groups; δi/SD(δi) is the ratio between the average contribution of the i^{th} species and the standard deviation of δi; Cum δi% is the cumulative contribution to the total dissimilarity. Species are listed in decreasing contribution to average dissimilarity.

Species	Average abundance		δi	δi/SD(δi)	δi%	Cumulative δi%
	winter–spring	summer				
Eucinostomus spp.	0.24	9.9	4.8	1.38	6.31	6.31
Lagodon rhomboides	10.75	1.83	4.5	1.69	5.91	12.22
Bairdiella chrysoura	1.01	12.76	4.38	1.25	5.75	17.97
Orthopristis chrysoptera	26.58	0.94	3.66	1.17	4.81	22.78
Monacanthus hispidus	0.09	1.89	3.25	1.22	4.27	27.05
Syngnathus floridae	1.2	3.88	3.24	1.1	4.25	31.3
Centropristis striata	0.01	1.82	2.68	0.99	3.52	34.82
Anchoa hepsetus	0.03	11.95	2.67	0.8	3.51	38.33
Syngnathus scovelli	0.8	1.13	2.48	1.36	3.25	41.58
Sphoeroides nephelus	1.24	0.19	2.27	1.2	2.99	44.57
Anchoa mitchilli	0.33	4.46	2.27	0.95	2.98	47.55
Chilomycterus schoepfi	0.18	0.46	2.12	1.07	2.78	50.33
	winter–spring	fall				
Anchoa mitchilli	0.33	478.1	10.87	2.32	13.31	13.31
Lagodon rhomboides	10.75	4.57	6.43	1.36	7.87	21.18
Orthopristis chrysoptera	26.58	1.33	4.73	1.05	5.79	26.97
Bairdiella chrysoura	1.01	8.26	3.39	1.58	4.15	31.12
Leiostomus xanthurus	0.67	0.14	3.26	0.61	3.99	35.11
Syngnathus scovelli	0.8	0.71	2.83	1.19	3.46	38.57
Syngnathus floridae	1.2	3.26	2.81	1.27	3.44	42.01
Eucinostomus spp.	0.24	5.38	2.68	1.24	3.28	45.29
Harengula jaguana	0	9.74	2.57	1.24	3.15	48.44
Sphoeroides nephelus	1.24	0.12	2.55	0.91	3.12	51.56
	summer	fall				
Anchoa mitchilli	4.46	478.1	6.13	1.98	9.30	9.30
Eucinostomus spp.	9.9	5.38	3.11	1.34	4.72	14.02
Bairdiella chrysoura	12.76	8.26	2.70	1.21	4.10	18.12
Anchoa hepsetus	11.95	0.48	2.36	0.98	3.59	21.71
Syngnathus floridae	3.88	3.26	2.35	1.05	3.56	25.27
Monacanthus hispidus	1.89	0.38	2.34	1.14	3.55	28.82
Harengula jaguana	2.79	9.74	2.15	1.25	3.27	32.09
Centropristis striata	1.82	0.64	2.06	1.01	3.13	35.22
Syngnathus scovelli	1.13	0.71	1.82	1.35	2.77	37.99
Lagodon rhomboides	1.83	4.57	1.75	1.08	2.65	40.64
Chilomycterus schoepfi	0.46	0.52	1.72	1.13	2.61	43.25
Cynoscion nebulosus	1.54	1.95	1.66	1.31	2.53	45.78
Monacanthus ciliatus	0.45	0.45	1.62	0.83	2.47	48.25
Orthopristis chrysoptera	0.94	1.33	1.62	1.04	2.46	50.71

Table 4

Results of ANOVA comparing standard length of each species between habitats and seasonal assemblages identified through PRIMER. * <0.05, **<0.01, ***<0.001.

Species	Factor	df	*F*	*P*	Tukey HSD
Bairdiella chrysoura	habitat	1	0.02	0.8750	
	season	2	0.38	0.6819	
Cynoscion nebulosus	habitat	1	2.74	0.1008	
	season	2	8.03	***	winter > summer
Lagodon rhomboides	habitat	1	6.61	*	tidal-creek > seagrass
	season	2	80.12	***	summer > fall > winter
Leiostomus xanthurus	habitat	1	6.84	*	
	season	2	29.87	***	summer > fall, winter
Mugil cephalus	habitat	1	1.23	0.2713	
	season	2	2.54	0.0862	
Orthopristis chrysoptera	habitat	1	2.96	0.0996	
	season	2	4.6	*	summer > winter
Sciaenops ocellatus	habitat	1	1.98	0.1633	
	season	2	6.28	**	summer, winter > fall

tidal creeks and dominated samples collected during January and February (Tables 2 and 5). Recruitment of YOY *L. rhomboides* and *C. arenarius* also contributed to the winter-spring species assemblage (Tables 4 and 5). The summer assemblage was influenced by recruitment of YOY *F. grandis* and *C. nebulosus*, which had significantly shorter standard lengths than they had in the winter-spring assemblage. The recruitment of *S. ocellatus* helped to characterize the fall assemblage. Emigration of larger individuals could also account for a decrease in mean length; however length-frequency plots showed that larger individuals remained vulnerable to the gear and that the reduction in mean length was due to recruitment of YOY fishes.

Discussion

Fishes collected in seagrass habitats in this study were similar to those found in other studies of seagrass habitats; resident species were present year-round and there were seasonal pulses of juveniles that used the seagrass habitats as a nursery (Reid, 1954; Livingston, 1982; Weinstein and Brooks, 1983). The assemblages we identified were the result of the staggered influx of YOY fishes of different species to seagrass habitats throughout the year. For example, YOY *L. rhomboides* and *O. chrysoptera* recruited during winter and spring, whereas other abundant species such as YOY *B. chrysoura* and *Eucinostomus* spp. entered the nursery during summer and fall. We found an increase in species abundance and species richness during summer and fall similar to that found by Reid (1954), who conducted his study near Cedar Key. The same pattern was evident in other estuarine systems (Cowan and Birdsong, 1985; Rooker et al., 1998), demonstrating that recruitment of many juvenile fish species to seagrass habitats during summer and fall allows the juveniles to use the protection provided by the growing seagrasses (Stoner, 1983) and to use the food resources found within them (Carr and Adams, 1973).

Early-life-history stages of species with commercial or recreational importance were found in each habitat, but seagrass habitats contained a greater variety of juveniles from offshore reef species than did tidal creeks. Along the southeastern United States, juveniles of many economically important species use a variety of habitats in estuaries as nurseries, including mangroves, oyster reefs, marshes, tidal creeks, and seagrass habitats (Coleman et al., 1999, Coleman, et al., 2000). In our study, YOY reef fish taxa, such as serranids, lutjanids, and haemulids, were more abundant in seagrass habitats than they were in tidal-creek habitats, except for gray snapper (*Lutjanus griseus*). Juveniles of several reef species (*C. striata*, *Mycteroperca microlepis*, *Serraniculus pumilio*, *Serranus subligaris*, and *Lachnolaimus maximus*) were found only in seagrass habitats. However, a complicating factor in our study was the elimination of oyster habitats from our sampling design. Oyster reefs are known to harbor juvenile *C. striata* and *M. microlepis* (Coleman et al., 2000) and they may have been under-estimated in our study because we did not sample these habitats. Other economically important species, such as *C. nebulosus*, also recruited to the seagrass habitats and are known to reside in them much of their life (Reid, 1954; McMichael and Peters, 1989; Mason and Zengel, 1996). These economically important species use seagrass habitats in the Suwannee River estuary as a nursery and eventually enter local fisheries. Consequently, the maintenance of healthy

Table 5

Results of SIMPER procedure showing the average percent dissimilarity (δ%) for important species between tidal-creek assemblages. δi is the average contribution of the i^{th} species to the disssimilarity between groups; δi/SD(δi) is the ratio between the average contribution of the i^{th} species and the standard deviation of δi; Cum δi% is the cumulative contribution to the total dissimilarity. Species are listed in decreasing contribution to average dissimilarity.

Species	Average abundance		δi	δi/SD(δi)	δi%	Cumulative δi%
	winter–spring	summer				
Leiostomus xanthurus	177.1	8.43	4.17	2.07	7.03	7.03
Anchoa mitchilli	4.93	243.61	3.83	2.4	6.46	13.49
Brevoortia spp.	10.87	0.74	2.65	1.42	4.46	17.95
Eucinostomus spp.	0.24	22.28	2.62	1.74	4.42	22.37
Cynoscion arenarius	1.62	3.02	1.94	1.77	3.26	25.63
Mugil cephalus	4.52	0.88	1.91	1.57	3.21	28.84
Membras martinica	0.04	21.61	1.9	1.10	3.19	32.03
Lagodon rhomboides	6.46	2.92	1.83	1.46	3.08	35.11
	winter–Spring	fall				
Leiostomus xanthurus	177.1	0.96	4.33	2.32	7.85	7.85
Eucinostomus spp.	0.24	24.63	4.03	2.63	7.30	15.15
Brevoortia spp.	10.87	0.03	2.58	1.41	4.68	19.83
Eucinsotomus herengulus	0.07	2.86	2.51	2.73	4.56	24.39
Fundulus grandis	1.26	12.02	2.19	1.72	3.97	28.36
Fundulus majalis	0.77	3.47	1.66	1.40	3.02	31.38
Adinia xenica	0.23	1.82	1.62	1.55	2.94	34.32
Cynoscion nebulosus	0.07	1.16	1.60	1.68	2.90	37.22
	summer	fall				
Fundulus grandis	1.16	12.02	2.59	2.34	4.84	4.84
Anchoa mitchilli	243.61	14.92	2.52	1.69	4.70	9.54
Sciaenops ocellatus	0.53	5.36	2.09	1.39	3.91	13.45
Eucinostomus spp.	22.28	24.63	1.89	1.27	3.53	16.98
Fundulus majalis	0.26	3.47	1.88	1.45	3.51	20.49
Bairdiella chrysoura	4.06	1.53	1.81	1.71	3.38	23.87
Adinia xenica	0.97	1.82	1.76	1.9	3.28	27.15
Cynoscion arenarius	3.02	0.87	1.7	1.78	3.18	30.33

seagrasses in this area is important to the preservation of these resources.

Tidal-creek habitats in the Suwannee River estuary provided resources for many species that had restricted distributions related to salinity tolerances and included taxa that were also found in the nearby seagrass habitats. We found recreationally important freshwater taxa, such as *Micropterus salmoides* and *Lepomis punctatus*, in tidal-creek habitats. Other groups restricted to tidal-creeks were those tolerant of low salinity and included the fundulids, poeciliids, and cyprinodontids. In addition, some economically valuable species were more abundant in tidal-creeks than in seagrass habitats, including *M. cephalus*, *C. arenarius*, *S. ocellatus*, and *L. griseus*. Tidal creeks also supported a greater density of fishes than did seagrass habitats—a density that could have resulted from habitat preferences, differential mortality between habitat types, or gear avoidance. Because the seine was set along the shoreline in tidal creeks, fishes were trapped between the seine and the shoreline, perhaps making them more vulnerable to the gear, whereas in seagrass habitats, the seine was pulled along the bottom with the end open prior to retrieval and fishes could have used the opening to escape.

The results of our study showed that there was a more consistent assemblage of fishes in tidal creeks, whereas

fish assemblages found in seagrass habitats had greater variability in the species present and in the abundance of those species. The more consistent assemblage of fishes found in tidal creeks could be explained by the persistence of vegetation throughout the year in tidal creeks, which may have contributed to reduced predation and may have provided direct or indirect sources of food. Vegetation coverage in seagrass habitats was seasonal and Strawn (1961) found that above-ground seagrass biomass declined during winter and increased during summer and fall. The increased complexity resulting from blade density and seagrass species heterogeneity offered by the growing seagrasses is known to affect fish abundance and composition (Stoner, 1983). The fish community structure in our study reflected this seasonal change; fewer fish species were present during winter and spring than in summer and fall. As seagrass biomass increased, fish species composition and total numbers also increased, resulting in greater variability within seagrass fish assemblages.

We found that the combination of water temperature, salinity, and water depth, more than any other combination of abiotic variables, helped to explain the fish community structure found in the Suwannee River estuary. Although water temperatures between the two habitats were similar, tidal creeks typically had soft mud sediments instead of sand and mud, marsh-grass species instead of submerged aquatic vegetation, deeper average depths, and lower salinity values. Water temperature has been shown to correlate with timing of recruitment for YOY fishes, which is ultimately related to adult spawning patterns (Subrahmanyam and Coultas, 1980; Nelson, 1998; Paperno, 2002). Because water temperatures were similar in each habitat, differences in fish-community structures were more likely related to salinity tolerances, factors that correlate with salinity and water depth. Water depth in the Suwannee River estuary varies seasonally; lowest water levels occur during winter (Strawn, 1961). The result is a confounding effect of water temperature and water depth that probably act in concert to limit distribution of fishes. A strong indicator that salinity may be the major abiotic factor that determines fish distributions, and ultimately species assemblages, was the low-salinity event during March 1998 that changed the seagrass fish assemblage to one more closely resembling a tidal-creek assemblage. If vegetation type were the primary factor controlling species assemblages in these habitats, tidal-creek species would remain in tidal-creeks and not invade seagrass habitats when salinity values changed to more favorable conditions. Therefore, varying salinities allowed different groups of fishes to use habitats according to their salinity tolerance (Wagner, 1999).

Nordlie (2003) examined 20 studies of estuarine salt marsh fish communities in eastern North America and characterized communities based on the life history patterns exhibited by the species. General life history categories were originally established by McHugh (1967) and included permanent residents, marine nursery, marine transients, diadromous, and freshwater transients. The 45 species that had overlapping distributions among habitats in our study were consistent with the classifications for marine nursery or marine transient species. Marine transient species do not require estuarine habitats for development, but venture into estuaries during periods of low rainfall, whereas marine nursery species require estuarine conditions for development. The two exceptions in our study (*Gobionellus bolesoma* and *M. gulosus*) were considered primary residents of saltmarsh communities, but were frequently found in estuaries.

We collected 80 fish species in tidal creeks in the Suwannee River estuary—more species than have been found in most other studies of tidal creeks—and this number could be related to the long-term duration of sampling. For example, Peterson and Turner (1994) observed 29 fish species inhabiting Louisiana marshes in a one-year study, whereas we found 51 additional species in our tidal-creek habitats. Similarly, Hettler (1989) found 35 species in a one-year study of saltmarsh fishes in North Carolina, and Weinstein (1979) recorded 61 species from his one-year study of the Cape Fear River, North Carolina. Furthermore, Cain and Dean (1976) found 51 species in a one-year examination of fishes in an intertidal creek in South Carolina. The first year of our study resulted in the collection of 61 species from tidal-creek habitats. It is likely that three years of sampling in our study increased our chances of collecting rare species, which resulted in the higher level of species richness.

Another reason for the high species diversity and abundance of fishes that we found in tidal creeks could be attributed to our sampling along the tidal-creek edge, which is known for its structural complexity (Montague and Wiegert, 1990) and importance as a foraging and refuge area (Baltz et al., 1993; Kneib and Wagner, 1994; Peterson and Turner, 1994). For example, Baltz et al. (1993) collected fishes in Louisiana marsh edges to look at the importance of the marsh-edge microhabitat and found that the 15 most abundant fishes were concentrated near the marsh edge and consisted mostly of early-life-history stages. They hypothesized that the fishes aggregated near the marsh edge to take advantage of the protection provided by the vegetation and the available food resources. Our sampling targeted the tidal-creek edge, and the gear we used selected for juveniles and small-adult species, which could explain the higher diversity than that seen in other studies. Another possibility is that our randomly chosen sampling sites covered a greater variety of microhabitats along tidal-creek shorelines than did the sampling of Weinstein (1979), Hettler (1989), and Peterson and Turner (1994), which could also explain the higher species richness. Despite differences in sampling methods, the collection of 80 fish species in tidal creeks appears to be unusual.

The withdrawal of fresh water from the Suwannee River would likely change the salinity regime in the Suwannee River estuary, which may in turn reduce species diversity in the region by reducing habitat availability to groups tolerant of low salinity. Furthermore, the high abundance of juvenile fishes that use low-salinity

tidal creeks as a nursery would be altered and the responses could vary on a species-specific basis (Tsou and Matheson, 2002). A decline in the amount of freshwater inflow into the tidal-creeks could lead to an overall shift towards a more saline environment and result in the expansion of seagrass habitats. However, Strawn (1961) showed that the distribution of seagrasses at Cedar Key was affected by water depth, water clarity, and the interaction of temperature and tides during winter months, making the prospect of seagrass expansion unlikely. Although a decrease in the amount of fresh water may result in an increase in water clarity through a reduction in dissolved nutrient input and reduced primary productivity, as has been seen in Apalachicola Bay, Florida (Livingston, 2003), the extreme low tides, cold temperatures, wave action, and sediment geochemistry in the Suwannee River estuary may negate the effects of increased light penetration (Koch, 2001). Therefore, a decrease in fresh water may result in an increase in high-salinity bare substrate that has been shown to be less suitable as a fish nursery than either seagrass or tidal-creek habitats (Sogard and Able, 1991; Rozas and Minello, 1998).

Tidal-creek and seagrass habitats in the Suwannee River estuary contained diverse fish communities that reflected seasonal changes associated with recruitment of YOY fishes. Many of these species are the targets of commercial and recreational activities, which support local economies. Although much of the land surrounding the Suwannee River estuary has been preserved, measures must be taken to ensure that the supply of fresh water from the Suwannee River is also preserved to maintain the integrity of the aquatic environment and the associated estuarine fish community.

Acknowledgments

We appreciate the effort of our coworkers at the Florida Marine Research Institute's Cedar Key Field Laboratory for assisting with the collection of data for this study and to Fred Vose and Cynthia Cooksey for the initial concept of this study. This paper benefitted from reviews by D. Nemeth, D. Adams, B. Winner, F. Vose, J. Whittington, K. Tisdel, R. McMichael, J. Leiby, J. Quinn, T. Tsou, and two anonymous reviewers. This project was supported in part by funding from the Department of the Interior, U. S. Fish and Wildlife Service, Federal Aid for Sport Fish Restoration Project number F-43, and Florida recreational fishing license revenues.

Literature cited

Baltz, D. M., C. Rakocinski, and J. W. Fleeger.
1993. Microhabitat use by marsh-edge fishes in a Louisiana estuary. Environ. Biol. Fish. 36:109–126.

Bozeman, E. L. Jr., and J. M. Dean.
1980. The abundance of estuarine larval and juvenile fish in a South Carolina intertidal creek. Estuaries 3:89–97.

Cain, R. L., and J. M. Dean.
1976. Annual occurrence, abundance and diversity of fish in a South Carolina intertidal creek. Mar. Biol. 36:369–379.

Carr, W. E. S., and C. A. Adams.
1973. Food habits of juvenile marine fishes occupying seagrass beds in the estuarine zone near Crystal River, Florida. Trans. Am. Fish. Soc. 102:511–540.

Clarke, K. R.
1993. Non-parametric multivariate analyses of changes in community structure. Austr. J. Ecol. 18:117–143.

Clarke, K. R., and R. M. Warwick.
1994. Change in marine communities: an approach to statistic analysis and interpretation, 144 p. National Environmental Research Council, UK.

Coleman, F. C., C. C. Koenig, A. Eklund, and C. B. Grimes.
1999. Management and conservation of temperate reef fishes in the grouper-snapper complex of the southeastern United States. Am. Fish. Soc. Symp. 23:233–242.

Coleman, F. C., C. C. Koenig, G. R. Huntsman, J. A. Musick, A. M. Eklund, J. C. McGovern, R. W. Chapman, G. R. Sedberry, and C. B. Grimes.
2000. Long-lived reef fishes: the grouper-snapper complex. Fisheries 25(3):14–21.

Comp, G. S., and W. Seaman Jr.
1985. Estuarine habitat and fishery resources of Florida. *In* Florida aquatic habitat and fishery resources, (W. Seaman jr., ed.), p. 337–436. Florida Chapter of the American Fisheries Society, Eustis, FL.

Cowan, J. H. Jr., and R. S. Birdsong.
1985. Seasonal occurrence of larval and juvenile fishes in a Virginia Atlantic coast estuary with emphasis on drums (Family Sciaenidae). Estuaries 8:48–59.

Field, J. G., K. R. Clarke, and R. M. Warwick.
1982. A practical strategy for analyzing multispecies distribution patterns. Mar. Ecol. Prog. Ser. 8:37–52.

Gilmore, R. G. Jr.
1988. Subtropical seagrass fish communities: population dynamics, species guilds and microhabitat associations in the Indian River Lagoon, Florida. Ph.D. diss., 199 p. Florida Inst. Technology, Melbourne, FL.

Hettler, W. F., Jr.
1989. Nekton use of regularly-flooded saltmarsh cordgrass habitat in North Carolina, USA. Mar. Ecol. Prog. Ser. 56:111–118.

Kilby, J. D.
1955. The fishes of two gulf coastal marsh areas of Florida. Tulane Stud. Zool. 2:175–247.

Koch, E. W.
2001. Beyond light: Physical, geological, and geochemical parameters as possible submersed aquatic vegetation habitat requirements. Estuaries 24:1-17.

Kneib, R. T., and S. L. Wagner.
1994. Nekton use of vegetated marsh habitats at different stages of tidal inundation. Mar. Ecol. Prog. Ser. 106:227–238.

Livingston, R. J.
1982. Trophic organization of fishes in a coastal seagrass system. Mar. Ecol. Prog. Ser. 7:1–12.
1984. The relationship of physical factors and biological response in coastal seagrass meadows. Estuaries 7:377–390.

2003. Trophic organization in coastal systems, 388 p. CRC Press, Boca Raton, FL.

Mason, W. T., Jr., and S. A. Zengel.
1996. Foods of juvenile spotted seatrout in seagrasses at Seahorse Key, Florida. Gulf Mex. Sci. 2:89–104.

McGovern, J. C., and C. A. Wenner.
1990. Seasonal recruitment of larval and juvenile fishes into impounded and non-impounded marshes. Wetlands 10:203–221.

McHugh, J. L.
1967. Estuarine nekton. *In* Estuaries (Lauff, G. H., ed.), p. 581–620. AAAS, Publ 83, Washington, D.C.

McMichael, R. H., Jr., and K. M. Peters.
1989. Early life history of spotted seatrout, *Cynoscion nebulosus* (Pisces: Sciaenidae), in Tampa Bay, Florida. Estuaries 12:98–110.

Montague, C. L., and R. G. Wiegert.
1990. Salt marshes. *In* Ecosystems of Florida (R. L. Myers and J. E. Ewel, eds.), p. 481–516. Univ. Central Florida Press, Orlando, FL.

Nelson, G. A.
1998. Abundance, growth, and mortality of young-of-the-year pinfish, *Lagodon rhomboides*, in three estuaries along the gulf coast of Florida. Fish. Bull. 96:315–328.

Nordlie, F. G.
2000. Patterns of reproduction and development of selected resident teleosts of Florida salt marshes. Hydrobiologia 434:165–82.
2003. Fish communities of estuarine salt marshes of eastern North American, and comparisons with temperate estuaries of other continents. Reviews Fish. Biol. Fisheries 13:281–325.

Paperno, R.
2002. Age-0 spot (*Leiostomus xanthurus*) from two estuaries along central Florida's east coast: comparisons of the timing of recruitment, seasonal changes in abundance, and rates of growth and mortality. Fl. Sci. 65:85–99.

Paperno, R., K. J. Mille, and E. Kadison.
2001. Patterns in species composition of fish and selected invertebrate assemblages in estuarine subregions near Ponce De Leon Inlet, Florida. Estuar. Coast. Shelf Sci. 52:117–130.

Peterson, G. W., and R. E. Turner.
1994. The value of salt marsh edge vs. interior as a habitat for fish and decapod crustaceans in a Louisiana tidal marsh. Estuaries 17:235–262.

Reid, G. K. Jr.
1954. An ecological study of the Gulf of Mexico fishes, in the vicinity of Cedar Key, Florida. Bull. Mar. Sci. Gulf Car. 4:3–94.

Rooker, J. R., S. A. Holt, M. A. Soto, and G. J. Holt.
1998. Postsettlement patterns of habitat use by sciaenid fishes in subtropical seagrass meadows. Estuaries 21:318–327.

Rozas L. P., and T. J. Minello.
1998. Nekton use of salt marsh, seagrass, and nonvegetated habitats in a South Texas (USA) estuary. Bull. Mar. Sci. 63:481–501.

Shenker, J. M., and J. M. Dean.
1979. The utilization of an intertidal salt marsh creek by larval and juvenile fishes: abundance diversity and temporal variation. Estuaries 2:154–163.

Sogard, S. M., and K. W. Able.
1991. A comparison of eelgrass, sea lettuce macroalgae, and marsh creeks as habitats for epibenthic fishes and decapods. Estuar. Coast. Shelf Sci. 33:501–519.

Stoner, A. W.
1983. Distribution of fishes in seagrass meadows: role of macrophyte biomass and species composition. Fish. Bull. 81:837–846.

Strawn, K.
1961. Factors influencing the zonation of submerged monocotyledons at Cedar Key, Florida. J. Wild. Manag. 25:178–189.

Subrahmanyam, C. B., and C. L. Coultas.
1980. Studies on the animal communities in two north Florida salt marshes Part III. Seasonal fluctuations of fish and macroinvertebrates. Bull. Mar. Sci. 30:790–818.

Tsou, T., and R. E. Matheson Jr.
2002. Seasonal changes in the nekton community of the Suwannee River estuary and the potential impacts of freshwater withdrawal. Estuaries 25:1372–1381.

Wagner, C. M.
1999. Expression of the estuarine species minimum in littoral fish assemblages of the lower Chesapeake Bay tributaries. Estuaries 22:304–312.

Weinstein, M. P.
1979. Shallow marsh habitats as primary nurseries for fishes and shellfish, Cape Fear River, North Carolina. Fish. Bull. 77:339–357.

Weinstein, M. P., and H. A. Brooks.
1983. Comparative ecology of nekton residing in a tidal creek and adjacent seagrass meadow: community composition and structure. Mar. Ecol. Prog. Ser. 12:15–27.

Abstract—Examination of 203 adult bluefish (*Pomatomus saltatrix*) from Long Island, New York, in 2002 and 2003 and 66 from the Outer Banks, North Carolina, in 2003 revealed the presence of dracunculoid nematodes (*Philometra saltatrix*) in the ovaries of female fish. Percent prevalence reached 88% in July and then decreased after the peak of the spawning season. Bluefish contained up to 100 parasites per fish. Infection was associated with a range of disorders, including hemorrhage, inflammation, edema, prenecrotic and necrotic changes, and follicular atresia, that may prevent proper development of oocytes and probably affect bluefish fecundity. Historical occurrences, life cycle, and geographical distribution of this nematode remain largely unknown, but may play important roles in recruitment processes of bluefish.

Prevalence, intensity, and effect of a nematode (*Philometra saltatrix*) in the ovaries of bluefish (*Pomatomus saltatrix*)

Lora M. Clarke
Marine Sciences Research Center
Stony Brook University
Stony Brook, New York 11794-5000
E-mail address: Lora.Clarke@msrc.sunysb.edu

Alistair D. M. Dove
Department of Microbiology and Immunology
Cornell College of Veterinary Medicine
c/o Marine Sciences Research Center
Stony Brook University, Stony Brook, New York 11794-5000

David O. Conover
Marine Sciences Research Center
Stony Brook University
Stony Brook, New York 11794-5000

Manuscript submitted 14 July 2004 to the Scientific Editor's Office.
Manuscript approved for publication 25 July 2005 by the Scientific Editor.
Fish. Bull. 104:118–124 (2006).

Factors influencing recruitment variability in marine fishes are often complex and poorly understood. Slight variations in mortality rates, growth rates, and stage durations in the early life stages can result in tenfold or greater fluctuations in abundance (Houde, 1987). Recruitment variation appears to be driven by a combination of factors, such as environmental and oceanographic processes (Munch and Conover, 2000), diet (Friedland et al., 1988; Marks and Conover, 1993; Juanes and Conover, 1995), growth and development (McBride and Conover, 1991; Hare and Cowen, 1997) and habitat use (Able et al., 2003). The importance of parasitism and disease has, however, seldom been considered.

In the Northwest Atlantic, the bluefish (*Pomatomus saltatrix*) is distributed from Florida to the Gulf of Maine and is both commercially and recreationally important. This highly migratory species has at least two distinct spawning seasons. The first occurs in the spring, from March to May, south of Cape Hatteras, North Carolina (NC) (Kendall and Walford, 1979; Collins and Stender, 1987) and the second occurs off the coast of New York (NY) from late June to August (Norcross et al., 1974; Sherman et al., 1984), peaking in July (Chiarella and Conover, 1990). Ichthyoplankton surveys have indicated that a third spawning event occurs south of Cape Hatteras, NC, in the autumn, but juveniles spawned during this time frame have rarely been captured (Collins and Stender, 1987).

During the collection of bluefish ovaries for another study, the nematode *Philometra saltatrix* Ramachandran, 1973 was detected in the ovaries of adult bluefish. Previous studies of *Philometra* spp. in other host species have indicated that their presence can have a negative effect on fecundity (Oliva et al., 1992; Hesp et al., 2002), implying that a more complete understanding of parasites may be important to understanding reproductive success. Although factors such as female size and condition are often considered in determining reproductive success, the role of parasitism is rarely investigated (Marshall et al., 1998; Marteinsdottir and Begg, 2002). The potential effect of this nematode on the reproductive

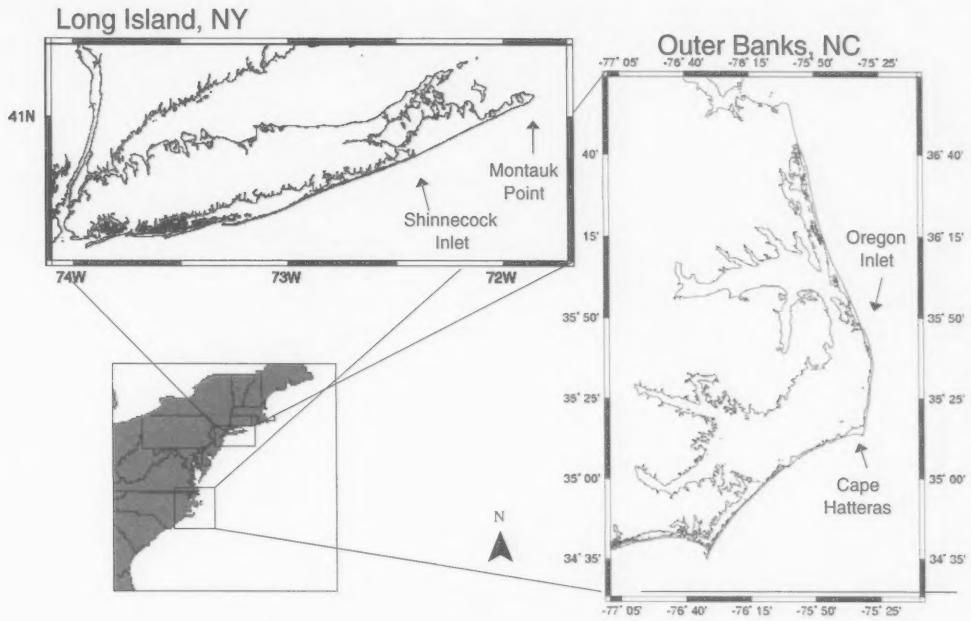

Figure 1

Map of the sampling area, Long Island, New York, and Outer Banks, North Carolina, where adult bluefish (*Pomatomus saltatrix*) were collected from commercial gill-netters, trawlers, and seafood markets in 2002–03 for examination of infestation by the nematode *Philometra saltatrix*.

potential and early life history success of bluefish is unknown. No information other than location of occurrence (Ramachandran, 1973) and a brief abstract describing the presence of philometrids in the heart of juvenile bluefish is available (Cheung et al.[1]). The purpose of this study is to investigate the prevalence, intensity, and effect of *Philometra saltatrix* in the ovaries of bluefish.

Materials and methods

Adult bluefish were collected from commercial gill-netters, trawlers, and seafood markets on Long Island, NY, and the Outer Banks, NC (Fig. 1). In NY, fish were caught off the southern coast of Long Island from Shinnecock Inlet to Montauk Point, approximately 1–15 km offshore. In NC, fish were caught approximately 1–40 km off the coast, and the majority of fish were caught 30–40 km east of Oregon Inlet.

Sampling dates were determined by the availability of fish through the local fishermen. In 2002, bluefish were sampled from mid-July through early October off the southern coast of Long Island, NY (80 females, 108 males). In 2003, fish were collected in NC in April (43 females, 21 males) and in NY from the end of June through September (123 females, 42 males).

Fork length (FL), fish weight, gonad weight, prevalence of both live and dead worms, total worm weight, and gonadosomatic indices (GSI) were recorded for each fish. Worms were often intertwined making it difficult to count the number of worms in each ovary; therefore, total worm weight per ovary was used as a proxy for intensity. Representative samples were fixed in a solution of 95% glacial acid and 5% formalin for identification. Initially, examinations of both male and female fish were conducted, but after preliminary evidence showed that nematodes were not present in the gonads of male fish, future examinations were restricted to female fish.

Haphazardly selected ovaries were preserved in 10% formalin and processed according to standard histological methods (Luna, 1968) to investigate pathologies associated with the parasite. Transverse sections were cut from the same region in the center of each ovary. These were examined under a light microscope and images were captured with a Spot Insight digital CCD and processed with ImagePro Plus software (Media Cybernetics, Silver Spring, MD).

[1] Cheung, P. J., R. F. Nigrelli, and G. D. Ruggieri. 1984. *Philometra saltatrix* infecting the heart of the 0-class bluefish, *Pomatomus saltatrix* (L.), from the New York coast. *In* S. F. Snieszko commemoration fish disease workshop, p. 27. Joint Workshop of Fish Health Section, AFS, and Midwest Disease Group, Little Rock, AR.

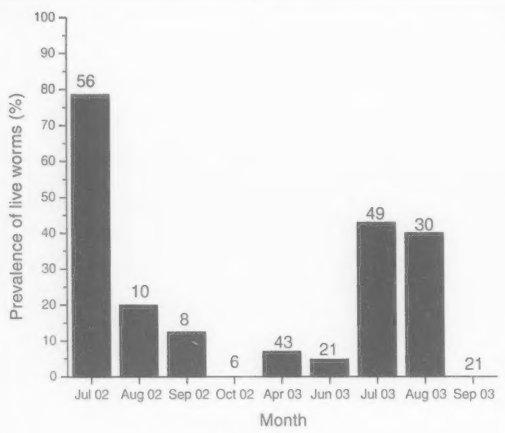

Figure 2

Monthly prevalence of live *Philometra saltatrix* in the ovaries of bluefish (*Pomatomus saltatrix*). Sample sizes are noted on the top of the bars.

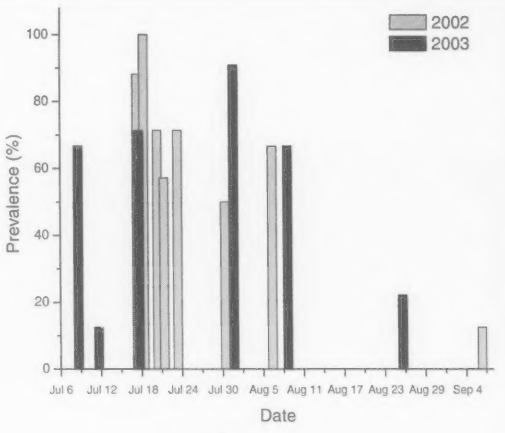

Figure 3

Daily prevalence of live *Philometra saltatrix* in the ovaries of bluefish (*Pomatomus saltatrix*) in 2002 and 2003.

Results

Description and location of worm

Philometra saltatrix was identified in the gonads of female fish ranging in size from 363 to 815 mm (FL) in both NC and NY samples. The majority of worms found in the ovaries were gravid females. Gravid female worms were visible macroscopically and most often visible even before the initiation of ovary dissection. Female worms reached a maximum of 150 mm in length and approximately 300 μm in width. Dead worms were present in all months sampled and were encapsulated by several melanised layers of fibrotic tissue. Approximately 20 juvenile male and female worms were identified in the ovary of a female fish in July 2003. These immature worms reached a maximum length of 2 mm. It should be noted, however, that not all fish were examined microscopically; therefore, it is possible that other male and juvenile worms were present in other hosts but not detected.

Prevalence and intensity

Bluefish in the western North Atlantic represent a single genetic stock (Graves et al., 1992), allowing us to combine data from New York and North Carolina to examine seasonal trends. Pooled by month of capture, the prevalence of infection varied seasonally during the two sampling years. In NC, prevalence of live nematodes was 7% in April, the spring spawning season (Fig. 2). Prevalence of live worms in NY in June was 4.8% and reached a maximum of 79% (2002) and 42% (2003) in July during the summer spawning season (Fig. 2). It is important to note that sampling in 2002 did not begin until mid-July but was conducted for the entire month in 2003. If only the second half of July is examined for both years, the prevalence is 79% and 83% for 2002 and 2003, respectively. This peak in prevalence was followed by a slow decrease in live worms until late August and early September after which time live worms were no longer detected.

Examination of prevalence by sampling day showed greater evidence of interannual variation. In the middle of July 2002, 100% of bluefish examined were infected with live *Philometra saltatrix,* whereas in 2003 the highest percentage of fish sampled that were infected was 91% (Fig. 3). Furthermore, in 2002 prevalence peaked in the middle of July, whereas in 2003 prevalence was highest at the end of the month. Additionally, live worms were detected until the end of August in 2002 but were detected two weeks later in 2003.

Intensity of parasite infection, as indicated by total live and dead worm weight per fish, reached a maximum 0.145 g (mean of 0.081 g ±0.1367) and was highest during the month of July in both years of the study (Fig. 4). Patterns of intensity were similar to those of prevalence; intensity was highest during the summer spawning season and then later decreased. One bluefish caught just south of Cape Hatteras, NC, in the beginning of May 2003 had the highest intensity observed with over 100 nematodes present (Fig. 5, A and B). This fish was not included in the data analysis because it was the only fish examined during that month, but this extreme instance of infection sets the upper bound on the level of observed intensity.

Binary logistic regression was used to test whether the presence or absence of the nematode was related to fork length (P=0.096), fish weight (P=0.292), or GSI (P=0.783), but no significant relationships were found.

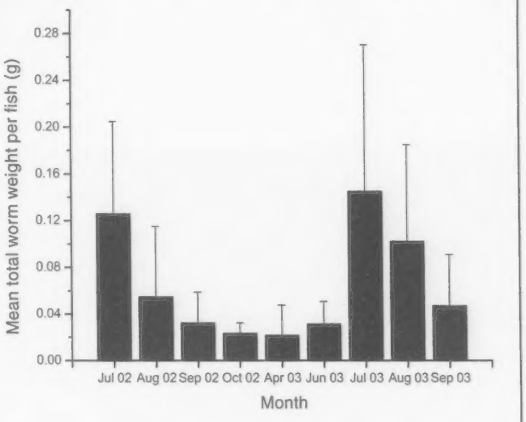

Figure 4

Monthly intensity of live and dead *Philometra saltatrix* in the ovaries of bluefish (*Pomatomus saltatrix*).

However, a significant positive correlation was found between intensity and fish weight (R= 0.169, P=0.000), intensity and fork length (R=0.221, P=0.003), and intensity and GSI (R=0.262, P=0.000). The Bonferroni method was applied to account for the multiple comparisons. Adjusted P-values are given.

Observations in adult males and YOY

Although not the target of this study, we also detected the presence of *Philometra saltatrix* in the pericardial cavity of one adult male bluefish collected in NC and three adult males in NY. Fish size ranged from 411 to 429 mm FL. Worms were not detected in the gonads of male fish.

Additionally, we detected worms in the pericardial cavity of three young of the year (YOY) bluefish caught in the Long Island Sound. Fish ranged in size from 140 to 185 FL.

Histopathology

Worms found in the ovary were surrounded by oocytes at various stages of development. The guts of these worms were most often filled with host erythrocytes. A diversity of pathological responses was noted, and significant variability was found among host individuals (Fig. 5). In many cases, infection was associated with interstitial hemorrhage in the connective tissues of the ovary. Occasionally, hemorrhage into the lumen of the ovary was also observed, but it was not clear whether this was caused by feeding activities of the worm or from tissue damage by other means. In many cases, moderate lymphocytic infiltration was observed in ovarian connective tissues. Some specimens showed marked edema in the perifollicular spaces. Prenecrotic changes, including pyknosis and cellular swelling, were observed in connective tissue cells, and necrosis of both connective tissue and oocytes (atresia) was observed in several instances. Granulomatous inflammation and fibrosis occurred in association with dead worms and, occasionally, atretic follicles. Fibrotic capsules surrounding dead worms were polylaminate and melanised and appeared to represent female worms that had expelled larvae and had subsequently died. Encapsulated worms that still contained larvae were also observed occasionally.

Discussion

Bluefish along the east coast of the United States appear to be heavily infected with the ovarian nematode *Philometra saltatrix*. Although many studies provide descriptions of various philometrid species, very few provide information about the prevalence, intensity, or effect of these nematodes. Ramachandran (1973) described the presence of several female and male worms in a single ovary but provided no information on pathological changes associated with infection.

Intensity and prevalence of *Philometra saltatrix* cycle seasonally and appear to be synchronous with the bluefish spawning cycle. Although live worms were detected from April to October, the levels of infection were higher in July than in any other month sampled and this timing is coincident with the peak of the summer spawning season off NY (Chiarella and Conover, 1990). The life cycle of *Philometra saltatrix* is unknown and, therefore, it is not clear whether initial infection coincides with the spawning season or if nematodes are acquired at an earlier time and reside in some other host tissue site before migrating to the ovaries during the spawning season, perhaps stimulated by hormonal cues from the host. Prevalence and intensity were much lower during the spring spawning season south of Cape Hatteras, NC. It is difficult to determine whether this was due to geographical differences or the limited sampling that month; it is possible that we missed the peak spawning period in 2003. The rapid decline in both prevalence and intensity after the summer spawning period indicates that *Philometra saltatrix* are released or migrate out of the host fish synchronously with the release of fish eggs. We speculate that the reproduction cycle of the nematode is closely matched to that of the host bluefish.

Other studies have reported that infection occurs after first host maturity and that female nematodes have only been observed in the gonads of females (Oliva et al., 1992; Hesp et al., 2002). Although not the focus of this study, the pericardial cavity was also found to be infected by *Philometra saltatrix* in adult males in NC and NY and in YOY bluefish in NY waters, in contradiction to these other findings. It is not clear if these YOY infections represent separate infections or if they are the same infections observed in adult females. Reviewing the reported lifecycle of other spirurid nematodes

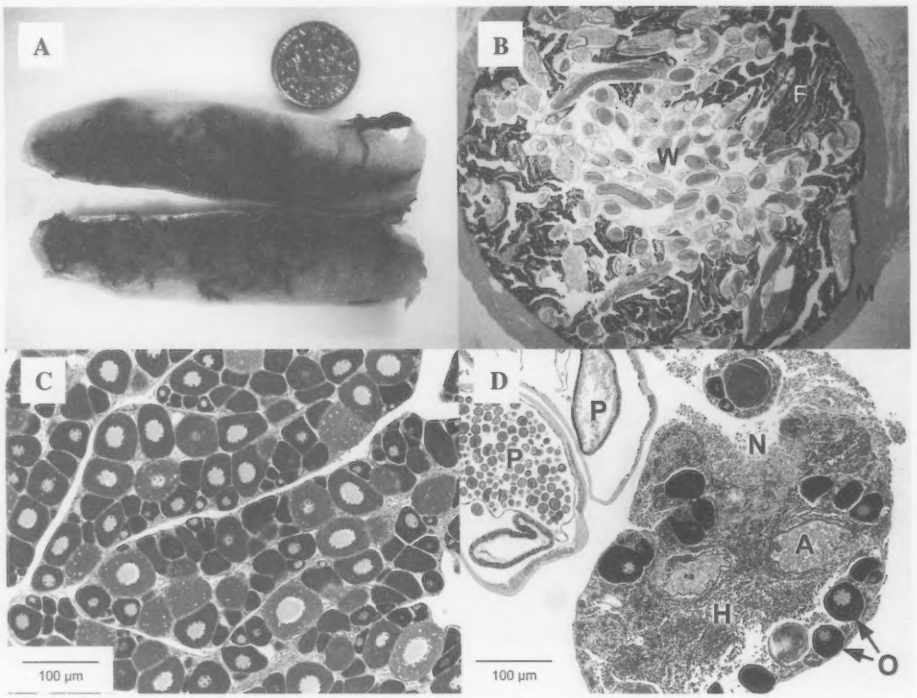

Figure 5

Observations associated with *Philometra saltatrix* infection in bluefish (*Pomatomus saltatrix*) ovaries. (**A**) Gross, bisected ovary from infected bluefish, showing heavy infection with *Philometra* (**B**) Low power view of transverse section (approximately 1.5 cm in diameter) of heavily-infected bluefish ovary. M=muscular capsule, F=ovarian follicles, W=nematodes in lumen of ovary, displacing oocytes. (**C**) Histological section of healthy ovarian tissue showing dense packing of healthy oocytes in various developmental stages, little connective tissue, and no cellular infiltrates. (**D**) Histological section of infected bluefish ovary, showing relatively fewer oocytes (O) and the presence of *Philometra* (P). In addition, there is severe interstitial hemorrhage (H) and necrosis (N) of ovarian tissue, with heavy cellular infiltration and atresia (A) of ovarian follicles.

and *Philometra* spp. (Williams and Jones, 1994), we speculate that nematode larvae are released at spawning time, pass through the copepod intermediate stage, and a second perhaps paratenic intermediate host (or perhaps pass through only one intermediate host), and infect YOY bluefish. It is important to note that most YOY bluefish larger than approximately 40 mm TL are piscivorous (Marks and Conover 1993); thus, it is possible that the infected YOY bluefish observed in this study were infected through a second intermediate host. The existence of a second intermediate fish host is supported by the observed positive relationship between host body size and parasite intensity. After initial infection, these worms reside in non-ovarian sites such as the pericardial cavity (as we observed), where they may remain quiescent until maturation of the host. At that time, worms may migrate through the tissues to the ovary for spawning and the completion of their life-cycle. This proposed life history would explain the ontogenetic and seasonal patterns of worm distribution that we observed and explain the rapid appearance of well-developed worms in the ovary at the onset of the spawning season.

The prevalence and intensity of infections we observed in bluefish were significantly higher than those reported in most other fish species. For example, intensity of infection in *Glaucosoma hebraicum* by *Philometra lateolabracis* ranged from 1 to 7 nematodes (mean of 2 nematodes) (Hesp et al., 2002), whereas prevalence of *Philometra margolisi* in the gonads of red grouper, *Epinephelus morio*, ranged from 14 to 28% depending on locality (Moravec et al., 1995) and prevalence of *Philometra lateolabracis* in *Parupeneus indicus* was 5.3% (intensity of 1–2 nematodes) (Moravec et al., 1988).

Although most studies indicate the occurrence of these nematodes to be lower than in bluefish, in a later study Moravec et al. (1997) reported prevalence of *Philometra margolisi* in the gonads of *Epinephelus morio* to be as high as 88% with an intensity of up to 84 nematodes. Additionally, although most studies report the absence of male worms (Hesp et al., 2002), we found up to 20 males in the ovary of one female fish. The high percentage of adult female bluefish that are infected may indicate that *Philometra saltatrix* are significantly affecting the reproductive success of bluefish.

Despite some studies showing deleterious effects of other parasites on fish ovaries (see for example, Adlerstein and Dorn, 1998), studies on the effects of philometrids on fish ovaries remain scarce. Indeed, in a recent review of histopathological assessments of gonadal tissue in wild fishes, Blazer (2002) made no mention of *Philometra* spp., despite the fact that it is probably the most common adult helminth observed in fish gonads. Annigeri (1962) described damage to ovaries of *Otolithus argenteus* by an unidentified philometrid, and Ramachandran (1975) mentioned necrosis in the ovaries of *Mugil cephalus* caused by *Philometra cephalus*. The infection of testes of pink snapper *Pagrus auratus* by *Philometra lateolabracis* resulted in partial or extensive atrophy of those gonads (Hine and Anderson 1981). Oliva et al. (1992) alluded briefly to lower fecundity in *Paralabrax humeralis* as a result of infection with *Philometra* but provided no data in support of this assertion. Hesp et al. (2002) studied the dynamics and effects of *P. lateolabracis* in the gonads of the Australian predatory marine fish *Glaucosoma hebraicum*, but did not observe significant pathological abnormalities associated with infection.

Histopathological changes associated with philometrid infection in bluefish were significant. The hemorrhaging, edema, inflammation, atresia, and necrosis observed most likely reduce oocyte number and quality, leading to lower fecundity. The presence of erythrocytes in the guts of nematodes indicates that the parasites were feeding on the blood of the host; this diversion of nutrients to the parasite may exacerbate the impacts of the worm on ovarian tissue. Furthermore, intense infections can reduce the effective volume of the ovary and thus lead to lower fecundity (Fig. 5, A and B).

The high prevalence, intensity, and pathological damage observed could be an important factor in recruitment variation in bluefish. Although modest interannual differences in prevalence and timing of infection were observed in this study (Fig. 4), *Philometra saltatrix* was not observed by researchers conducting studies of the GSI of bluefish from NY waters in the 1980s (Chiarella and Conover, 1990; Conover, personal observ.). Hence, it is possible that the abundance of *Philometra* may fluctuate greatly over long time scales. The reason for the current prevalence of the worm and its effect on bluefish recruitment is unknown. Future studies of this host-parasite system should seek to account for temporal variations of this kind.

Acknowledgments

We thank R. Knotoff and numerous other commercial fishermen from Shinnecock Inlet, NY, for helping us to obtain samples. B. Burns and J. Pearce of the NC Division of Marine Fisheries helped collect North Carolina bluefish. We thank R. Clarke, C. Knakal, and S. Abrams for laboratory and field assistance. We also thank two anonymous reviewers for helpful comments on the manuscript. Funding was provided by the Rutgers/NOAA Bluefish-Striped Bass Research Program and the New York State Department of Environmental Conservation.

Literature cited

Able K. W., P. Rowe, M. Burlas, and D. Byrne.
2003. Use of ocean and estuarine habitats by young-of-year bluefish (*Pomatomus saltatrix*) in the New York Bight. Fish. Bull. 101:201–214.

Adlerstein, S. A., and M. W. Dorn.
1998. The effect of *Kudoa paniformis* infection on the reproductive effort of female Pacific hake. Can. J. Zool. 76:2285–2289.

Annigeri, G. G.
1962. A viviparous nematode, *Philometra* sp., in the ovaries of *Otolithus argenteus* (Cuvier). J. Mar. Biol. Assoc. (India) 3:263–265.

Blazer, V. S.
2002. Histopathological assessment of gonadal tissue in wild fishes. Fish Physiol. Biochem. 26: 85–101.

Chiarella, L., and D. O. Conover.
1990. Spawning season and first year growth of adult bluefish (*Pomatomus saltatrix*) from the New York Bight. Trans. Am. Fish. Soc. 119:455–462.

Collins, M. R., and B. W. Stender.
1987. Larval king mackerel (*Scomberomorus cavalla*), Spanish mackerel, (*S. maculatus*) and bluefish (*Pomatomus saltatrix*) off the southeast coast of the United States, 1973–1980. Bull. Mar. Sci. 41:822–834.

Friedland, K. D., G. C. Garman, A. J. Bejda, A. L. Studholme, and B. Olla.
1988. Interannual variation in diet and condition in juvenile bluefish during estuarine residency. Trans. Am. Fish. Soc. 117:474–479.

Graves, J. E., J. R. McDowell, A. M. Beardsley, and D. R. Scoles
1992. Stock structure of the bluefish *Pomatomus saltatrix* along the mid-Atlantic coast. Fish Bull. 90 (4):703–710.

Hare, J., and R. K. Cowen.
1997. Size, growth, development, and survival of the planktonic larvae of *Pomatomus saltatrix*. Ecology 78:2415–2431.

Hesp, S. A., R. P. Hobbs, and I. C. Potter.
2002. Infection of the gonads of *Glaucosoma hebraicum* by the nematode *Philometra lateolabracis*: occurrence and host response. J. Fish Biol. 60:663–673.

Hine, P. M., and C. D. Anderson.
1981. Diseases of the gonads and kidneys of New Zealand snapper, *Chrysophrys auratus* Forster (F. Sparidae). *In* Wildlife diseases of the Pacific Basin and other countries (M. E. Fowler, ed.), p. 166–170. Academic Press, London.

Houde, E. D.
1987. Early life dynamics and recruitment variability. Am. Fish. Soc. Symp. 2:17–29.
Juanes, F., and D. O. Conover.
1995. Size-structured piscivory: advection and linkage between predator and prey recruitment in young-of-the-year bluefish. Mar. Ecol. Prog. Ser. 128:287–304.
Kendall, A. W. Jr., and L. A. Walford.
1979. Sources and distribution of bluefish, *Pomatomus saltatrix*, larvae and juveniles off the east coast of the United States. Fish. Bull. 77:213–227.
Luna, L. G.
1968. Manual of histological staining of the Armed Forces Institute of Pathology, 258 p. McGraw-Hill Book Company, New York, NY.
Marks, R., and D. O. Conover.
1993. Ontogenetic shift in the diet of young-of-the-year bluefish (*Pomatomus saltatrix*) during the oceanic phase of the early life history. Fish. Bull. 91:97–106.
Marshall, C. T., O. S. Kjesbu, N. A. Yaragina, P. Solemdal, O. Ulltang.
1998. Is spawner biomass a sensitive measure of the reproductive and recruitment potential of Northeast Arctic cod? Can. J. Fish. Aquat. Sci. 55:1766–1783.
Marteinsdottir, G., and G. A. Begg.
2002. Essential relationships incorporating the influence of age, size and condition on variables required for estimation of reproductive potential in Atlantic cod *Gadus morhua*. Mar. Ecol. Prog. Ser. 235:235–256
McBride, R. S., and D. O. Conover.
1991. Recruitment of young-of-the-year bluefish (*Pomatomus saltatrix*) to the New York Bight: variation in abundance and growth of spring and summer-spawned cohorts. Mar. Ecol. Prog. Ser. 78:205–216.
Moravec, F., P. Orecchia, and L. Paggi.
1988. Three interesting nematodes from the fish *Parupeneus indices* (Mullidae, Perciformes) of the Indian Ocean, including a new species, *Ascarophis parupenei* sp. N. (Habronematoidea). Folia Parasitol. 35:47–57.
Moravec, F., V. M. Vidal-Martinez, and L. Aquirremacedo.
1995. *Philometra margolisi* n.sp. (Nematoda, Philometridae) from the gonads of the red grouper, *Epinephelus morio* (Pisces, Serranidae), in Mexico. Can. J. Fish. Aquat. Sci. 52(suppl. 1) 161–165.
Moravec, F., V. M. Vidal-Martinez, J. Vargas-Vazquez, C. Vivas-Rodriguez, D. Gonzalez-Solis, E. Mendoza-Franco, R. Sima-Alvarez, and J. Guemez-Ricalde.
1997. Helminth parasites of *Epinephelus morio* (Pisces: Serranidae) of the Yucatan Peninsula, southeastern Mexico. Folia Parasitol. 44:255–266.
Munch, S. B., and D. O. Conover.
2000. Recruitment dynamics of bluefish, *Pomatomus saltatrix*, on the continental shelf from Cape Fear to Cape Cod, 1973–1995. ICES J. Mar. Sci. 57:393–402.
Norcross, J. J., S. L. Richards, W. H. Massmann, and E. B. Joseph.
1974. Development of young bluefish (*Pomatomus saltatrix*) and distribution of eggs and young in Virginian coastal waters. Trans. Am. Fish. Soc. 103:477–497.
Oliva, M. E., A. S. Bórquez, and A. N. Olivares.
1992. Sexual status of *Paralabrax humeralis* (Serranidae) and infection by *Philometra* sp. (Nematoda: Dracunculoidea). J. Fish Biol. 40:979–980.
Ramachandran, P.
1973. *Philometra saltatrix* sp. n., infecting the gonads of the common bluefish *Pomatomus saltatrix* (L.) off the New England coast of the United States. Zool. Anz. 191:325–328.
Ramachandran, P.
1975. *Philometra cephalus* sp. n. infecting the gonads of the striped mullet, *Mugil cephalus* L. from the Arabian Coast of Kerala, India, with a note on its pathology. Zool. Anz. 194:140–144.
Sherman, K., W. Smith, W. Morse, M. Berman, J. Green, and L. Ejsymont.
1984. Spawning strategies of fishes in relation to circulation, phytoplankton production, and pulses in zooplankton off the northeastern United States. Mar. Ecol. Prog. Ser. 18:1–19.
Williams, H., and A. Jones.
1994. Parasitic worms of fish, p. 139–146. Taylor and Francis Ltd., Bristol, PA.

Duration of unassisted swimming activity for spotted dolphin (*Stenella attenuata*) calves: implications for mother-calf separation during tuna purse-seine sets

Elizabeth F. Edwards

Southwest Fisheries Science Center
National Marine Fisheries Service
8604 La Jolla Shores Drive
La Jolla, California 92037
E-mail address: Elizabeth.Edwards@noaa.gov

Abstract—Size-related differences in power production and swim speed duration may contribute to the observed deficit of nursing calves in relation to lactating females killed in sets by tuna purse-seiners in the eastern tropical Pacific Ocean (ETP). Power production and swim-speed duration were estimated for northeastern spotted dolphins (*Stenella attenuata*), the species (neonate through adult) most often captured by the fishery. Power required by neonates to swim unassisted was 3.6 times that required of an adult to swim the same speed. Estimated unassisted burst speed for neonates is only about 3 m/s compared to about 6 m/s for adults. Estimated long-term sustainable speed is about 1 m/s for neonates compared to about 2.5 m/s for adults. Weight-specific power requirements decrease as dolphin calves increase in size, but power estimates for 2-year-old spotted dolphin calves are still about 40% higher than power estimates for adults, to maintain the same speed. These estimated differences between calves and adults are conservative because the calculations do not include accommodation for reduced aerobic capacity in dolphin calves compared to adults. Discrepancies in power production are probably ameliorated under normal circumstances by calves drafting next to their mothers, and by employing burst-coast or leap-burst-coast swimming, but the relatively high speeds associated with evasion behaviors during and after tuna sets likely diminish use of these energy-saving strategies by calves.

Manuscript submitted 15 February 2005 to the Scientific Editor's Office.

Manuscript approved for publication 25 July 2005 by the Scientific Editor.

Fish. Bull. 104:125–135 (2006).

Dolphin calves draft in echelon position next to their mothers for the first few weeks after birth and continue to return to drafting in echelon position frequently throughout at least their first year (Edwards[1]). "Echelon position' is the physical positioning of the calf within a few centimeters of the mother, near her mid-section, with fin motions reduced or absent (e.g., Norris and Prescott, 1961). This position takes advantage of the mother's flow field, reducing or effectively eliminating the energy cost to the calf of moving forward through the water (Weihs, 2004). Because drafting appears to be ubiquitous among dolphin calves, particularly during the neonate stage, it appears likely that drafting is an essential factor in maintaining physical association between calves and their mothers, especially when the calves are small.

In the eastern tropical Pacific Ocean (ETP) a situation occurs in which it becomes important to consider the consequences for calves of losing their drafting association with their mother. In this area, a tuna purse-seine fishery targets schools of large yellowfin tuna that associate closely with schools of dolphins, primarily the spotted dolphin (*Stenella attenuata*) (NRC, 1992). The associated schools of tunas and dolphins are located by a helicopter sent out from the purse-seine vessel and are subsequently captured through the actions of several high-powered speedboats, which are released from the purse-seiner to overtake and herd the associated animals into the closing arc of the purse-seine (NRC, 1992). Examination of the dolphins found dead in the net has revealed that 75% to 95% of the lactating females killed in the sets are not killed with an accompanying calf (Archer et al., 2004). This observed calf deficit is a potentially important factor in the lack of recovery of ETP dolphin populations despite over a decade of very low fishery mortality (Wade et al.[2]), but little is known about why or how the separation of mothers and calves occurs (Archer et al., 2004).

The chase, encirclement, and release procedure of purse-seine fishing operations tends to be relatively prolonged—chases averaging about 30 minutes, capture and confinement about 90 minutes, and postrelease swimming at least 90 minutes (Myrick and Perkins, 1995; Chivers

[1] Edwards, E. 2002. Behavioral contributions to separation and subsequent mortality of dolphin calves chased by tuna purse-seiners in the eastern tropical Pacific Ocean. National Oceanographic and Atmospheric Administration Administrative Report LJ-02-28, 33 p. Southwest Fisheries Science Center, 8604 La Jolla Shores Drive, La Jolla, CA 92037.

[2] Wade, P., S. Reilly, and T. Gerrodette. 2002. Assessment of the population dynamics of the northeastern offshore spotted and eastern spinner dolphin populations through 2002. National Oceanographic and Atmospheric Administration Administrative Report LJ-02-13, 58 p. Southwest Fisheries Science Center, 8604 La Jolla Shores Drive, La Jolla, CA 92037.

and Scott[3]). The set procedure also tends to induce relatively high, sustained swimming speeds in the dolphins. Swimming speeds of two spotted dolphins carrying velocity tags during and after tuna purse-seine sets in the ETP averaged 1.7–2.8 m/s during chase and 2.6–3.1 m/s after release, compared to undisturbed speeds of 1.2–1.9 m/s (Chivers and Scott[3]). Compared to adults, dolphin calves have smaller, less-coordinated muscles and lower aerobic capacity, especially at birth but persisting through the first year or more (Dolar et al., 1999; Dearoff et al., 2000; Noren et al., 2001; Noren et al., 2002; Eitner et al., 2003; Noren et al., 2004). Therefore, it appears possible that the observed calf deficit in the kill may result at least in part from energetics-related separation of calves from mothers during the chase or after release, as well as the inability of calves to maintain speed with adults while swimming alone.

The present study examines the possibility of energetics-related separation, by estimating the length of time (duration) during which spotted dolphin calves of different sizes ranging from neonate through two years of age can swim unassisted at various velocities. These velocity-durations are then compared to adult swimming capacities, in order to determine whether calves swimming without assistance may experience energy-based difficulty keeping up with adult dolphins during evasion from tuna purse-seine sets.

Materials and methods

Duration limits for unassisted swimming by spotted dolphin calves were calculated by combining estimates of mass-specific energy cost of steady, submerged, unassisted swimming by neonate through adult spotted dolphins, with reported swimming speed durations of adult dolphins of various species (Table 1). Swimming duration for adults was used because this information was not available for dolphin calves. The data were combined based on the assumption that the duration a given unit of dolphin muscle can sustain a given mass-specific energy cost is the same for both adults and calves within any species of dolphin. It is much more likely that swimming capacity of calves within any dolphin species is significantly lower than that of adults and that differences are particularly pronounced at birth (Dolar et al., 1999; Dearoff et al., 2000; Eitner et al., 2003; Noren et al., 2001, 2002, 2004), but the exact differences are unknown. The swimming duration estimates presented in this study therefore represent maximum durations. It is also possible that species differ in power production capacities, based on observations of blood chemistry differences between species (Ridgway and Johnston, 1965), but it is not unreasonable to assume that relative differences between species are maintained throughout the size ranges of individuals within a species, so that younger dolphins are probably less adept than adults in any particular species. Thus, although it is not yet possible to quantify differences between calf and adult swimming-duration capacities in *Stenella attenuata* in nature, they are likely greater than estimated in the present study, so that problems apparent from this study are likely greater during actual tuna purse-seine sets.

The energy cost of a steady, submerged, unassisted swimming rate was estimated in this study for velocities ranging from 1.5 to 6.0 m/s in order to encompass speeds from slow undisturbed swimming to the maximum likely to occur during attempted evasion from tuna purse-seine sets. Average velocities observed during tracking of dolphins before and after experimental sets varied from about 1.5 m/s m to about 3 m/s (Chivers and Scott[3]) but short term speeds attained during evasion maneuvers were likely to have exceeded these averages (Table 1). Total body energy costs were estimated first and then converted to mass-specific costs by dividing total estimated energy costs by the estimated total muscle weight of each size of modeled dolphin. Muscle-mass-specific measures are more appropriate than simply dividing by total body weight for comparisons between sizes because muscle fraction of body weight increases with body weight in *Stenella attenuata* in the ETP, from 35–40% in neonates to 55–60% in adults (Edwards, 1993).

Data sources

Total body energy costs were estimated for eight modeled *Stenella attenuata* ranging in size (age) from newborn through adult. Sizes were selected to emphasize changes during the early months (Table 2). Size-at-age to two years old was estimated from Hohn and Hammond (1985). Size of an adult reproductive female was estimated from Perrin and Reilly (1984). Total body wet weight, wetted surface area of body, fins, and flukes, maximum body diameter, and fraction of total body weight composed of muscle were estimated for each size of modeled dolphin by using regression equations developed from morphological measurements of ETP dolphins (Edwards 1993, Edwards[4]).

The morphological measurements were taken from 35 spotted dolphins ranging in size from 0.71 to 2.1 m total length (tip of rostrum to fluke notch). This size range encompasses all life-history stages (near-term fetus through mature adult) of the spotted dolphins found in the eastern tropical Pacific Ocean. Spotted dolphins are about 0.8 m total length at birth (Hohn and Hammond, 1985). Specimens included 22 females and 13 males (Edwards, 1993). Male specimens included

[3] Chivers, S., and M. Scott. 2002. Tagging and tracking of *Stenella* species during the 2001 Chase and Encirclement Stress Studies cruise. National Oceanographic and Atmospheric Administration Administrative Report LJ-02-33. 23 p. Southwest Fisheries Science Center, 8604 La Jolla Shores Drive, La Jolla, CA. 92037.

[4] Edwards, E. 2002. Energetics consequences of chase by tuna purse-seiners for spotted dolphins (*Stenella attenuata*) in the eastern tropical Pacific Ocean. National Oceanographic and Atmospheric Administration Administrative Report LJ-02-29, 32 p. Southwest Fisheries Science Center, 8604 La Jolla Shores Drive, La Jolla, CA 92037.

three fetuses, six immature, and four mature individuals. Female specimens included three fetuses, six immature, one mature resting, one mature lactating, and 11 mature pregnant individuals. All specimens were killed during tuna fishing operations in the eastern tropical Pacific Ocean. Two of the specimens were collected in February 1980, one in July 1983, nine in July 1985, two in August 1985, seventeen in December 1985, and four were collected without a date noted (Edwards, 1993). All specimens were processed according to the same procedures prior to dissection. Immediately after the sets, the dolphin specimens were brought on board the vessel and frozen whole in the brine wells of the vessel. The specimens were transported frozen to port and then transported frozen to the Southwest Fisheries Science Center. Specimens were kept frozen until thawed in fresh water (about 27°C) just prior to dissection. Not all measurements were made on all specimens; therefore sample sizes differ between the regression equations presented below.

Energetics model The energetics model used to estimate total body cost of swimming was taken from Edwards (1992, based on Magnuson, 1978), except that 1) new data were used to estimate dolphin body parameters and 2) the estimate of fin plus induced drag was replaced by the multiplier 3 (see below). The model used standard hydrodynamic equations and methods (Hoerner, 1965; Hertel, 1969; Webb, 1975) to estimate hydrodynamic drag on a fully submerged streamlined body of revolution moving steadily in turbulent flow. Body surface area was increased to specifically include the surface area of fins and flukes (Fish[5]), and drag estimates were increased to account for body and fin movements. Because energy to move forward (thrust energy) must exactly balance the drag experienced by a steadily swimming animal, estimating total drag energy is equivalent to estimating thrust energy, i.e., the energy cost to swim (Fish and Rohr, 1999).

Model formulation Total power (P_t, in watts) required to overcome drag during steady, submerged swimming (Hertel, 1969) by a modeled dolphin of a given total length (L, rostrum to fluke notch) was estimated as

$$P_t = P_c / (E_m E_p),$$

where P_c = mechanical power (in watts) required to overcome hydrodynamic drag;
E_m = muscle efficiency; and
E_p = "propeller efficiency" (efficiency of propulsion by flukes).

E_m was assumed to be 0.2 from studies of muscle efficiencies in terrestrial animals (e.g., Goldspink 1988), man (Alexander, 1983; quoting Dickinson, 1929) and dolphins (Fish, 1993, 1996). E_p was assumed to be 0.85 based on studies by Fish (1998), Webb (1975), and Yates (1983). P_c was estimated as a function of total hydrodynamic drag (D_t, in dynes) and velocity (V, in m/s) as

$$P_m = D_t V / 10^7,$$

where the factor 10^7 converts ($D_t V$) to watts.

Total drag was estimated as a function of drag due to body, fins, and movements of body parts as

$$D_t = 0.5\rho V^2 S_w C_{d3} = 1.5\rho V^2 S_w C_d,$$

where ρ = density of seawater (1.025 g/cm^3);
S_w = wetted surface area;
C_d = coefficient of total drag; and
3 = drag augmentation factor.

S_w includes surface area of body plus fins and flukes, where estimated planar area of fins was increased by 6% to account for the curvature of the fins, based on measurements of individual slices from fins and flukes from one small and one large dolphin, 1.32 m and 1.93 m in length, respectively (Edwards, unpubl. data). Drag augmentation factor generally varies between 3 and 5 (e.g., Lighthill, 1971; Fish, 1993) and was assumed equal to the value of 3 in the present study, based on studies of gliding vs. actively swimming dolphins (Skrovan et al., 1999). The factor 3 accounts for the increase over gliding drag caused by body movements during active swimming. Use of a squared relationship between V and D_t is supported by the observed relationship between total drag and velocity in free swimming *Tursiops truncatus* (Skrovan et al. 1999, Eq. 6). Use of a cubic relationship between V and P_t is supported by observations of swimming kinematics of *Tursiops truncatus* swimming between 1 and 6 m/s (Fish, 1993).

S_w (in cm^2) was estimated as

$$S_w = 0.299 L^{2.05},$$

based on measurements from 19 *Stenella attenuata* ranging in size from 0.71 to 2.01 m, where L is total length (in cm).

C_d was estimated from the formula for drag of submerged streamlined bodies of revolution moving at constant velocity (Hoerner, 1965; Hertel, 1969; Webb, 1975) as

$$C_d = C_f\left[1+\left(1.5(d/L)^{3/2}\right)+7\left((d/L)^3\right)\right],$$

C_f = the coefficient of friction drag; and
d = 0.12

where d = maximum body diameter (in cm) based on measurements from 24 *Stenella attenuata* ranging in size from 0.71 to 2.01 m.

C_f was estimated from the formula for submerged streamlined bodies of revolution moving at constant velocity in turbulent flow (e.g., Webb, 1975) as

[5] Fish, F. 2002. Personal commun. Liquid Life Laboratory, West Chester Univ. Pennsylvania, West Chester, PA.

Table 1

Reported duration of various swimming speeds for several species of dolphins.

Velocity (m/s)	Duration	Publication	Species
	Burst (seconds)		
11.2	leap	Rohr et al. (2002)	*Tursiops*
11.1	2	Lang (1975)	*Stenella*
10.6	2	Lang (1975)	*Stenella*
10.3	2	Lang (1975)	*Stenella*
9.7	leap	Rohr et al. (2002)	*Tursiops*
8.8	<2	Rohr et al. (2002)	*Delphinus*
8.8	leap	Rohr et al. (2002)	*Tursiops*
8.3	7.5	Lang (1975)	*Tursiops*
8.2	<3	Rohr et al. (2002)	*Tursiops*
8.2	<120	Au et al. (1988)	*Stenella*
8.0	7.6	Lang and Norris (1966)	*Tursiops*
8.0	<3	Rohr et al. (2002)	*Delphinus*
7.8	2	Lang (1975)	*Lagenor*
7.7	2–3	Lang and Prior (1966)	*Stenella*
7.5	leap	Lang (1975)	*Tursiops*
7.4	leap	Lang (1975)	*Tursiops*
7.3	leap	Au and Weihs (1980)	*Stenella*
6.8	10	Lang and Norris (1966)	*Tursiops*
6.7	1.4	Rohr et al. (2002)	*Delphinus*
6.7	<3	Rohr et al. (2002)	*Delphinus*
6.3	10	Lang and Norris (1966)	*Tursiops*
6.4	240	Au and Weihs (1980)	*Stenella*
6.2	<2	Rohr et al. (2002)	*Tursiops*
5.9	50	Lang and Norris (1966)	*Tursiops*
6.0	2	Rohr et al. (2002)	*Delphinus*
5.6	<10	Rohr et al. (2002)	*Tursiops*
5.3	6.6	Lang and Norris (1966)	*Tursiops*
	Maximum (minutes)		
4.7	11	Au and Perryman (1982)	*Stenella*
4.4	21	Au and Perryman (1982)	*Stenella*
4.2	<8.5	Rohr et al. (2002)	*Delphinus*
	Prolonged (hours–days)		
3.5	1 hour	Au and Perryman (1982)	*Stenella*
3.2	9.3 hour	Leatherwood and L. (1979)	*Stenella*
3.1	extended period	Lang and Norris (1966)	*Tursiops*
3.1	90 min	Chivers and Scott[3]	*Stenella*
3.0	1.5 hours	Au and Perryman (1982)	*Stenella*
2.8	15 min	Chivers and Scott[3]	*Stenella*
2.6	106 min	Chivers and Scott[3]	*Stenella*
2.1	days	Chivers and Scott[3]	*Stenella*
1.9	hours	Chivers and Scott[3]	*Stenella*
1.8	hours	Chivers and Scott[3]	*Stenella*
1.7	32 min	Chivers and Scott[3]	*Stenella*
1.6	4 days	Hui (1987)	*Delphinus*
1.6	hours–days	Chivers and Scott[3]	*Stenella*
1.5	hours	Chivers and Scott[3]	*Stenella*
1.2	hours	Chivers and Scott[3]	*Stenella*
1.2	<50 hours	Perrin et al. (1979)	*Stenella*

No. of animals	Length (m)	Weight (kg)	Swimming location	Swimming condition
3			tank	maximum observed leap velocity
1	1.86	52.7	lagoon	accelerating, 25 m course
1	1.86	52.7	lagoon	accelerating, 25 m course
1	1.86	52.7	lagoon	accelerating, 25 m course
3			tank	average maximum leap velocity
1			wild	maximum observed speed
3			tank	average leap velocity
1	1.91	89	lagoon	61 m course in 300 m lagoon
6	2.6	197	small tank	maximum speed, 8 m course
300			wild	evading helicopter
1	1.91	89	lagoon	61 m course; maximum speed observed
1	1.83	105	tank	5 or 8 m course
1	2.09	91	tank	accelerating, long narrow tank
1			captive	70 m circular pool; maximum speed
1	1.91	89	ocean	swimming in speedboat waves
1	1.91	89	ocean	swimming in speedboat waves
not specified			wild	during chase by speedboats
1	1.91	89	ocean	swimming in speedboat waves
"A school"			wild	average maximum observed speed
1	1.83	105	captive	mean high swim speed
1	1.91	89	lagoon	61 m course; maximum observed speed
not specified			wild	after escaping purse seine
6	2.6	197	tank	mean high swim speed
1	1.91	89	ocean	swimming in speedboat waves
41			wild	average maximum speed evading aircraft
4			wild	maximum speed after release
1	1.91	89	ocean	swimming in speedboat waves
school no. 5			wild	maximum observed speed and duration
school no. 5			wild	swimming with ocean swells
"A school"			wild	average maximum velocity evading aircraft
school			wild	average speed evading vessel
1	2.05		wild	average speed estimated from radiotag
1	1.91	89	ocean	swimming in speedboat waves
D230			wild	postrelease velocity
school no. 2			wild	average speed evading vessel
D230			wild	velocity during chase by seiner
D19			wild	postrelease velocity
12			wild	average speed, 1992, 1993
D230			wild	average nonchase velocity, night
D230			wild	average nonchase velocity, day
D19			wild	velocity during chase by senior
2	1.76	95	tank	small, shallow round tank
2			wild	average speed, 2001
D19			wild	average nonchase velocity, day
D19			wild	average nonchase velocity, night
26			wild	minimum distance traveled, radiotag

Table 2

Dolphin model parameters. See text for formulas and rationale.

Dolphin no.	Age	Total length (cm)	Body weight (kg)	Muscle weight (kg)	Wetted surface area (cm^2)	Maximum diameter (cm)	Fineness ratio
1	new born	85	6.40	2.62	2700	13.5	6.30
2	1 week	87	6.85	2.81	2832	13.8	6.29
3	1 month	90	7.58	3.18	3036	14.3	6.28
4	3 months	98	9.76	4.29	3615	15.7	6.24
5	6 months	110	13.76	6.33	4581	17.7	6.20
6	1 year	129	22.08	11.04	6351	21.0	6.14
7	2 years	154	37.37	20.18	9131	25.4	6.07
8	adult	190	69.73	41.84	14045	31.7	5.99

$$C_f = 0.072R^{-0.2},$$

where R is Reynold's number, estimated here as

$$R = LV / v,$$

where v = kinematic viscosity (=0.01 Stokes).

The calculations above generated estimates of the power required for a whole dolphin of a given size to swim at a given velocity (P_t, in watts). Power required per kilogram of wet weight muscle (P_m), for a given velocity was estimated as

$$P_m = P_t / M_m,$$

where M_m = total *muscle* mass (wet weight in kg), estimated from total *body* mass (M_t, wet weight in kg) as

$$M_m = -2.97M_t^{0.468}$$

based on ln-ln regression of measurements from a sample of 26 *Stenella attenuata* from the ETP ranging in size from 0.71 to 2.06 m. Total muscle was used rather than some portion of measured musculature because the complex and interconnected muscle and connective tissue of dolphins makes it difficult to isolate any particular portion as uniquely responsible for locomotion (Pabst, 1990). M_t was estimated from total length (L, in cm) as

$$M_t = 0.0000119L^{2.97}$$

based on ln-ln regression of measurements from a sample of 23 *Stenella attenuata* from the ETP ranging in size from 0.71 to 2.01 m.

Results

Model corroboration

Model estimates of the cost of swimming compared reasonably well with the cost of swimming in published reports for other species of dolphins swimming 1–6 m/s, in cases where the published reports can be appropriately compared with the present model. Although a number of studies present a variety of estimates of drag, thrust power, and metabolic power at various swimming speeds for a variety of dolphins (reviewed by Fish and Rohr, 1999), comparisons of present results with many of these earlier studies would be inappropriate because either the estimates were derived from completely different models from the one used in the present study or from generally similar models but where different assumptions were made about model parameters, such as propulsive efficiency, metabolic efficiency, drag formulation, and body structure (Edwards[4]). Only appropriately comparable published results are discussed in the present study.

All weight-specific measurements in the following paragraph refer to total body mass. At estimated optimum velocities ranging from about 1.2 m/s in neonate spotted dolphins to about 1.7 m/s in adults (Edwards[4]), model estimates are approximately 3 W/kg for all sizes of spotted dolphin, compared to measurements (derived under various methods) of about 2.5–5.5 W/kg for adults of various species of dolphins, either resting or swimming about 2 m/s (Hui, 1987; Worthy et al., 1987; Williams et al., 1992; Fish, 1993; Yadzi et al., 1999). Observed average total metabolic rates calculated from oxygen consumption by two *Tursiops* (average weight 162 kg), swimming 2 and 3 m/s, were approximately 2.5 and 3.7 W/kg (Yadzi et al., 1999), compared to model estimates of approximately 2.9 and 5.9 W/kg for an adult spotted dolphin (about 70 kg) swimming at the same speeds. Model estimates of thrust power output for an adult spotted dolphin (about 70 kg) also compared well with thrust power estimated as a function of velocity from videos of five *Tursiops* swimming between 1 and 6 m/s (Fish, 1993). Given an average adult *Tursiops* weight of 230 kg, average estimated thrust power for *Tursiops* swimming 1, 3, 5, and 6 m/s was 1, 3, 14, and 23 W/kg, compared to spotted dolphin model estimates of 1, 3, 13, and 21 W/kg, respectively. These comparisons refer to mechanical power output

only, because Fish's (1993) analysis does not include metabolic efficiency. Assuming the same metabolic efficiency of 0.2 for the *Tursiops* in Fish's study as used in the present model, an estimate of total power by his *Tursiops* swimming 6 m/s is 115 W/kg (i.e., 23×(1/0.2)), compared to the model estimate of about 125 W/kg for the adult spotted dolphin.

Mass-specific cost of swimming

Model estimates of mass-specific power requirements (watts per kilogram muscle, W/kg_m) for unassisted swimming by spotted dolphins in the ETP increase quickly with velocity, regardless of dolphin size, but increase much more quickly for smaller dolphins (Fig.1). Model results indicated that a neonate (85 cm) spotted dolphin must produce 3.6 times more power per kilogram of muscle than an adult swimming at the same speed. The factors are 3.5, 3.3, 2.8, 2.4, 1.8, and 1.4 times adult power for 87-, 90-, 98-, 110-, 129-, and 154-cm spotted dolphins. The factors do not vary with velocity because the relative differences between body dimensions in dolphins of different sizes remain constant regardless of swimming speed.

For example, at speeds typical of ETP dolphins attempting to evade speedboats during an impending tuna-purse-seine set or during escape from the net after release (about 3 m/s) (Chivers and Scott[3]), the model predicts that an 85-cm neonate swimming unassisted by its mother would require a muscle power of about 105 W/kg_m versus 30 W/kg_m for a 190-cm adult. The difference is still relatively marked even for two-year-old calves (154 cm), which would require an estimated 42 W/kg_m to maintain a steady submerged unassisted swim speed of 3 m/s, i.e., 1.4 times adult power requirements.

Velocity duration limits

Velocity duration limits for adults, drawn from literature sources, appear to range from a few seconds for burst speeds above about 5 m/s, to several minutes for maximum speeds of about 4 m/s, to hours at prolonged speeds below about 3.5 m/s (Table 1).

Estimated mass-specific muscle power required of adult spotted dolphins to achieve these speeds ranges from 208 W/kg_m for burst speeds of 6 m/s greater, to 67 W/kg_m for maximum sustainable speeds around 4 m/s, and 4–10 W/kg_m for prolonged duration speeds between 1 and 2 m/s (Fig.1).

If one assumes that these power-duration limits apply also to dolphin calf muscle, neonate dolphins (85 cm) for example, could generate a burst duration power of about 200 W/kg_m for a few seconds at unassisted swimming speeds of about 3.0 m/s, maximum duration power of about 70 W/kg_m for some minutes at about 2.2 m/s, and prolonged duration power of about 5–10 W/kg_m for hours at about 1.0 m/s (Fig.1). For two-year-old spotted dolphins (154 cm), estimated swimming duration limits were about 5 m/s for burst effort at 200 W/kg_m, about 3.5 m/s for maximum effort at 70 W/kg_m, and about 2 m/s for prolonged effort at 5–10 W/kg_m. Intermediate ages produced intermediate results.

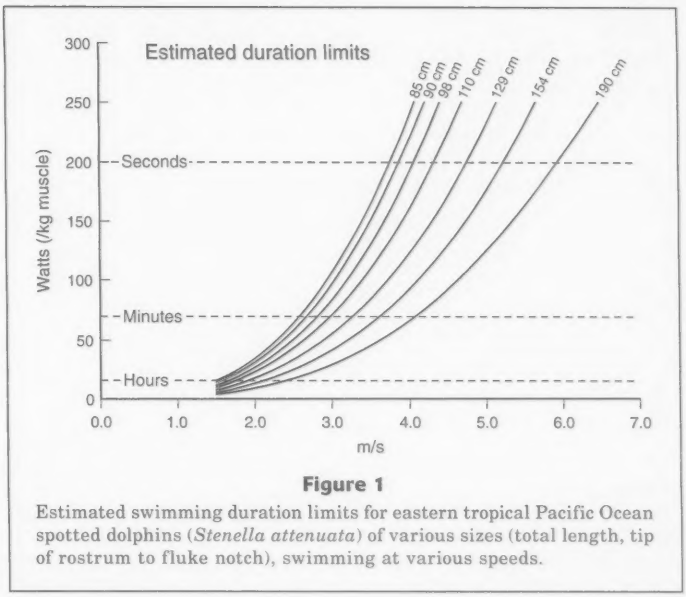

Figure 1

Estimated swimming duration limits for eastern tropical Pacific Ocean spotted dolphins (*Stenella attenuata*) of various sizes (total length, tip of rostrum to fluke notch), swimming at various speeds.

Discussion

Model results demonstrated clearly that swimming capability of dolphin calves is much lower than that of adults. The especially pronounced difference between neonates and adults appears a likely basis for development of the ubiquitous drafting behavior observed in both captive and wild neonates. Given the large difference in swimming capacities, it is difficult to imagine how small dolphin calves could maintain any long-term association with the mother without the hydrodynamic benefits of drafting, even under normal circumstances.

During the relatively fast-paced evasion swimming associated with tuna purse-seine sets in the ETP, it appears that spotted dolphin calves swimming unassisted are likely to have serious difficulty maintaining the same speed as adults—difficulties being especially pronounced for younger dolphins. It is also likely that the differences in swimming capacity presented in this study are underestimates because they do not include effects such as positive bouyancy (Cockroft and Ross, 1990; Mann and Smuts, 1999) and soft, flexible fins and flukes that are present for several hours after birth (McBride and Kritzler, 1951; Tavolga and Essapian,

1957; Wells, 1991). Other differences persist for weeks or months, including undeveloped musculature (Eitner et al., 2003) and uncoordinated swimming and respiratory movements (Tavolga and Essapian, 1957; Taylor and Saayman, 1972; Reiss, 1984; Cockroft and Ross, 1990; Peddemors, 1990; Herzing, 1997; Mann and Smuts, 1999). Aerobic capacity is also likely to be reduced throughout the first few months, and not likely to reach adult levels until two to three years of age (Dolar et al., 1999; Dearoff et al., 2000; Noren et al., 2001, 2002, 2004). The results presented in this study also do not include the added costs of increased drag due to swimming near the surface, and repeatedly piercing it, which will occur much more often during evasion of tuna sets than during normal swimming. These other effects increase the likelihood that dolphin calves, particularly the younger individuals, will have problems coping with the swimming conditions induced during tuna purse-seine sets.

Difficulties with unassisted swimming for dolphin calves may be ameliorated to some extent by employing drafting (Weihs, 2004), burst and coast (Au and Weihs, 1980), or leap-burst-coast swimming behaviors (or a combination of these behaviors) (Weihs, 2002). Theoretically, these strategies could significantly reduce the cost to calves of moving through the water. However, it is not clear that any of these energy-saving strategies will be consistently attainable by spotted dolphin calves during herd movements associated with evading or escaping sets by tuna purse-seiners in the ETP.

Drafting can only be sustained through respiratory leaps if mother and calf leave and reenter the water with equal speed and efficiency (Weihs, 2004). Because evasion of tuna purse-seine sets involves sustained high-speed swimming characterized by repeated full-body respiratory leaps from the water (Au and Wiehs, 1980), calves are likely to tire and lose coordination more quickly than adults, and the smallest calves will be the first to experience problems. These factors may have contributed to the observed failure of a neonate dolphin calf in the ETP to successfully maintain a drafting relationship with its assumed mother during a respiratory leap while attempting to evade a vessel (Weihs, 2004).

Once the drafting relationship is disrupted, the calf appears likely to fall behind because of its physical limitations, unless its mother alters her speed so that the calf can reestablish the drafting relationship. However, review of dolphin mother-calf behavior indicates that the mother is not likely to voluntarily leave other adults during attempted evasion of tuna purse-seine sets in the ETP (Edwards[1]). Thus, the faster or longer the chase or postrelease escape period (or combination of all three factors), and the younger the calf, the more likely it appears that the calf will become separated from its mother and be left behind during periods of fast swimming by the adults. Although fast swimming for a few minutes may not pose a great problem for many calves, longer periods appear increasingly likely to lead to significant calf loss in purse-seine operations. The duration of the high-speed period is at least as important as the speed maintained during the period, given the power-duration relationship. If fast swimming is concluded quickly, it is more likely that calves could achieve the required power during the short time required. As fast-swimming persists, power capacity decreases rapidly (Fig. 1), so that more and more calves are likely to be lost because they have exceeded their ability to keep up with the adults in their school.

Even under normal circumstances, burst and coast, or burst-leap-coast, swimming patterns are not likely to provide sustained benefits to free-swimming calves until they approach adult size, coordination, and swimming capacity, because the calves will still tire more quickly than their associated adults. In the case of tuna purse-seine set evasion, sustained use of these swimming patterns may not be employed even by adults because these behaviors become less efficient as swim speed increases (Weihs, 2002). Video studies of swimming behaviors of adult *Tursiops* have shown that burst and coast periods decrease with increasing drag and cease altogether if the drag is large (Skrovan et al., 1999). In a study of dolphin gaits, an adult *Tursiops* experiencing increased drag due to an instrument pack did not use burst and coast propulsion during horizontal swimming speeds and depths at which four other adult *Tursiops* (without instrument packs) did employ short periods of burst and coast swimming. Even animals swimming without instruments at 1.5–3.7 m/s incorporated only short periods of burst and coast, and glide periods rarely exceeded 2 seconds. At the speeds characteristic of tuna purse-seine sets, dolphins tend to swim steadily or employ burst-leap-coast swimming behaviors (Weihs, 2002, Au and Weihs, 1980). With their smaller power production capacities, calves will need to shift into leap-burst-coast mode at slower speeds than will adults (Weihs, 2002), and again will tire more quickly.

A potential shortcoming of the results presented in the present study is that the model produces absolute values from single calculations, without any associated statistics or sensitivity analyses. It is more likely that a range of values for morphological, physiological and behavioral characteristics occurs within real spotted dolphin populations in the ETP, so that a range of responses is much more likely than a single response for a given size, swimming speed, and duration of chase. Lack of statistical and sensitivity analyses can be a problem where responses tend to be subtle and therefore difficult to discern. However, the model results presented in this study with respect to estimated size-related differences in power production capacities of spotted dolphins in the ETP are far from subtle, and model results are reasonably similar to energy measures derived from observations on real dolphins indicating that these model results are not unrealistic. In general, results presented here imply that older calves may be able to swim unassisted as fast and for as long as their associated adults during or after most sets (or during and after most sets) by tuna purse-seine vessels in the ETP. The markedly smaller energy production

capacities of younger calves, particularly neonates and infants, compared to adults appears to be a reasonable factor contributing to mother-calf separation during or after sets by tuna vessels in the ETP.

Management and research implications

From these observations, it appears that energetic limitations may contribute significantly to the observed calf deficit in the retrieved purse-seine by facilitating mother-calf separation during purse-seine set activity. Separation risk appears to increase strongly with decreasing calf size and with increased speed and duration of evasion-related swimming. If separation is prolonged, subsequent mortality of milk-dependent calves appears likely due to predation or starvation because adoption by a surrogate mother is unlikely in the ETP (Edwards[1]). Examination of existing aerial photographs of spotted dolphins attempting to evade helicopters and research vessels, as well as directed future experiments in which aerial observations are conducted specifically to identify and monitor mother-calf pairs over time during various chase scenarios, would be very helpful in evaluating the extent to which calf size effects predicted here occur during relatively high-speed evasion behaviors by ETP spotted dolphin schools. Estimation of the rate at which dolphins of various ages are likely to encounter tuna purse-seine sets will be another important factor in relating the results of this analysis to potential calf loss during purse-seine sets.

Assuming that power limitations are a significant factor in calf loss during evasion of tuna purse-seine sets, management strategies that could be implemented to minimize calf loss include 1) avoiding setting on schools that contain calves, particularly young calves, 2) minimizing the speed or duration of chase, and 3) minimizing the length of time dolphins are retained in the net so that mothers and calves separated during the set may reunite more quickly, if possible. Minimizing the length of time in the net is already a desired fishery goal, related to minimizing cost and the potential for dolphin mortality in the net. Minimizing chase duration is also already a desired fishery goal, because shorter chases are both less expensive and tend to be more successful. Minimizing chase speed is not a realistic goal because it would likely lead to the escape of the dolphins and the targeted tuna. Thus, the only potential improvement that might be made under current conditions (i.e., while setting on dolphin calves is permitted) would be to concentrate effort on identifying and avoiding dolphin schools with calves, presumably by scrutinizing the school from the vessel's helicopter prior to initiating a set. This may or may not be possible, depending on the ability of observers in helicopters to spot calves from the air.

Given the model results presented here, it appears that further research and perhaps management actions should be implemented to better understand and reduce the risk of separation of mothers and calves during sets by tuna purse-seiners in the ETP.

Acknowledgments

This research was conducted under Section 304 (a)(1): Stress studies, of the 1997 International Dolphin Conservation Program Act amendments to the U.S. Marine Mammal Protection Act, and subsequent Congressional directives.

Literature cited

Alexander, R.
1983. Animal mechanics. Blackwell Scientific Publications, London, England.

Archer, F., T. Gerrodette, S. Chivers, and A. Jackson.
2004. Annual estimates of the unobserved incidental kill of pantropical spotted dolphin (*Stenella attenuata attenuata*) calves in the eastern tropical Pacific Ocean. Fish. Bull. 102:233–244.

Au, D., and W. Perryman.
1982. Movement and speed of dolphin schools responding to an approaching ship. Fish. Bull. 80:371–379.

Au, D., M. Scott, and W. Perryman.
1988. Leap-swim behavior of "porpoising" dolphins. Cetus 8:7–10.

Au, D., and D. Weihs.
1980. At high speeds dolphins save energy by leaping. Nature 284:548–550.

Cockroft, V., and G. Ross.
1990. Observations in the early development of a captive bottlenose dolphin calf. *In* The bottlenose dolphin (S. Leatherwood and R. Reeves, eds.), p. 461–478. Academic Press, San Diego, CA.

Dearoff, J., W. McLellan, R. Dillaman, D. Frierson, and D. Pabst.
2000. Precocial development of axial locomotor muscle in bottlenose dolphins (*Tursiops truncatus*). J. Morph. 244:203–215.

Dickinson, S.
1929. The efficiency of bicycle pedaling, as affected by speed and load. J. Phys. Lond. 76:242–255.

Dolar, M., P. Suarez, P. Ponganis, and G. Kooyman.
1999. Myoglobin in pelagic small cetaceans. J. Exp. Biol. 202:227–236.

Edwards, E.
1992. Energetics of associated tunas and dolphins in the eastern tropical Pacific Ocean: a basis for the bond. Fish. Bull. 90:678–690.
1993. Allometry of energetics parameters in spotted dolphin (*Stenella attenuata*) from the eastern tropical Pacific Ocean. Fish. Bull. 91:428–439.

Eitner, S., J. Dearoff, W. McLellan, and D. Pabst.
2003. Postural role of lateral axial muscles in developing bottlenose dolphins (*Tursiops truncatus*). Proc. R. Soc. Lond. B 271:909–918.

Fish, F.
1993. Power output and propulsive efficiency of swimming bottlenose dolphins (*Tursiops truncatus*). J. Exp. Biol. 185:179–183.
1996. Transitions from drag-based to lift-based propulsion in mammalian swimming. Am. Zool. 36:628-641.
1998. Comparative kinematics and hydrodynamics of odontocete cetaceans: morphological and ecological correlates with swimming performance. J. Exp. Biol. 201:2867–2877.

Fish, F., and J. Rohr.
1999. Review of dolphin hydrodynamics and swimming performance. Tech. Rept. 1801, 136 p. SPAWAR Systems Center, SSC San Diego, San Diego, CA.
Goldspink, G.
1988. Muscle energetics. *In* Mechanics and energetics of animal locomotion (R. Alexander and G. Goldspink, eds.), p. 57–81. Chapman and Hall, London, UK.
Hertel, H.
1969. Hydrodynamics of swimming and wave-riding dolphins. *In* The biology of marine mammals (H. Anderson, ed.), p. 31–63. Academic Press, New York, NY.
Herzing, D.
1997. The life history of free-ranging Atlantic spotted dolphins (*Stenella frontalis*): age classes, color phases, and female reproduction. Mar. Mamm. Sci. 13(4):576–595.
Hoerner, S.
1965. Fluid-dynamic drag, 460 p. Hoerner, 148 Busteed Drive, Midland Park, NJ.
Hohn, A., and P. Hammond.
1985. Early postnatal growth of the spotted dolphin, *Stenella attenuata*, in the offshore eastern tropical Pacific. Fish. Bull. 83:553–566.
Hui, C.
1987. Power and speed of swimming dolphins. J. Mamm. 68:126–132.
Lang, T.
1975. Speed, power, and drag measurements of dolphins and porpoises. *In* Swimming and flying in nature (T. Wu and C Brokaw, eds.), p. 553–572. Plenum Press, New York, NY.
Lang, T., and K. Norris.
1966. Swimming speed of a Pacific bottlenose porpoise. Science 151(3710):588–590.
Lang, T., and K. Pryor.
1966. Hydrodynamic performance of porpoises (*Stenella attenuatta*). Science 152:531–533.
Leatherwood, S., and D. Ljungblad.
1979. Nightime swimming and diving behavior of a radio-tagged spotted dolphin, *Stenella attenuata*. Cetology 34:1–6.
Lighthill, Sir J.
1971. Large-amplitude elongated-body theory of fish locomotion. Proc. R. Soc. Lond. B. 179:125–138.
Magnuson, J.
1978. Locomotion by scombroid fishes; hydromechanics, morphology and behavior. *In* Fish physiology, vol. 7 (W. Hoar and J. Randall, eds.), p. 240–313. Academic Press, New York, NY.
Mann, J., and B. Smuts.
1999. Behavioral development in wild bottlenose dolphin newborns (*Tursiops sp.*). Behavior 136:529–566.
McBride, A., and H. Kritzler.
1951. Observations on pregnancy, parturition, and postnatal behavior in the bottlenose dolphin. J. Mamm. 32.251–266.
Myrick, A., and P. Perkins.
1995. Adrenocortical color darkness as indicators of continuous premortem stress in chased and purse-seined male dolphins. Pathophys. 2:191–204.
NRC (National Research Council).
1992. Dolphins and the tuna industry, 176 p. Committee on Reducing Porpoise Mortality from Tuna Fishing, National Research Council. National Academy Press, Washington, D.C.
Noren, S., V. Cuccurulo, and T. Williams.
2004. The development of diving bradycardia in bottlenose dolphins (*Tursiops truncatus*). J. Comp. Physiol. B 174:139–147.
Noren, S., G. Lacave, R. Wells, and T. Williams.
2002. The development of blood oxygen stores in bottlenose dolphins (*Tursiops truncatus*): implications for diving capacity. J. Zool. Lond. 258:105–113.
Noren, S., T. Williams, D. Pabst, W. McLellan, and J. Dearoff.
2001. Development of diving in marine endotherms: preparing the skeletal muscles of dolphins, penguins, and seals for activity during submergence. J. Comp. Physiol. 171:127–134.
Norris, K., and J. Prescott.
1961. Observations on Pacific cetaceans of Californian and Mexican waters. Univ. Calif. Publ. in Zool. 63:291–402.
Pabst, A.
1990. Axial Muscles and Connective Tissues of the Bottlenose Dolphin. *In* The bottlenose dolphin (S. Leatherwood and R. Reeves, eds.), p. 51–67. Academic Press, San Diego, CA.
Peddemors, V.
1990. Respiratory development in a captive-born bottlenose dolphin. S. Afr. J. Zool. 5:178–184.
Perrin, W., W. Evans, and D. Holts.
1979. Movements of pelagic dolphins (*Stenella spp.*) in the eastern tropical Pacific as indicated by results of tagging operations, 1969–1976. NOAA Tech. Rept. NMFS SSRF-737, 14 p.
Perrin, W., and S. Reilly.
1984. Reproductive parameters of dolphins and small whales of the family Delphinidae. Rep. Int. Whal. Comm. (special issue 6):97–133.
Reiss, D.
1984. Observations on development of echolocation in young bottlenose dolphins. *In* Animal sonar (P. Natchtigall and P. Moore, eds.), p. 121–127. Plenum Press, New York, NY.
Ridgway, S., and D. Johnston.
1965. Blood oxygen and ecology of porpoises of three genera. Science 151:456–458.
Rohr, J., F. Fish, and J. Gilpatrick.
2002. Maximum swim speeds of captive and free-ranging delphinids: critical analysis of extraordinary performance. Mar. Mamm. Sci. 18(1):1–19
Skrovan, R., T. Williams, P. Berry, P. Moore, and R. Davis.
1999. The diving physiology of bottlenose dolphins (*Tursiops truncatus*) II. Biomechanics and changes in bouyancy at depth. J. Exp. Biol. 202:2749–2761.
Taylor, C., and G. Saayman.
1972. Social organization and behavior of dolphins and baboons. Ann. Cape Prov. Mus. Nat. Hist. 9(2): 11–49.
Tavolga, M., and F. Essapian.
1957. The behavior of the bottle-nosed dolphin (*Tursiops truncatus*): mating, pregnancy, parturition, and mother-infant behavior. Zoologica 42:11–31.
Webb, P.
1975. Hydrodynamics and energetics of fish propulsion. Bull. Fish. Res. Board Can. 190:1–158.
Weihs, D.
2002. Dynamics of dolphin porpoising revisited. Integr. Comp. Biol. 42:1071–1078.
2004. The hydrodynamics of dolphin drafting. J. Biol. 3(8):1–23.

Wells, R.
1991. Bringing up baby. Nat. Hist. August:56–62.
Williams, T., W. Friedl, M. Fong, R. Yamada, P. Sedivy, and J. Haun.
1992. Travel at low energetic cost by swimming and wave-riding bottle-nosed dolphins. Nature 355 (6363): 821–823.
Worthy, G., S. Innes, B. Braune, and R. Stewart.
1987. Rapid acclimation of cetaceans to an open-system respirometer. *In* Approaches in marine mammal energetics (A. Huntley, D. Costa, G. Worthy and M. Castellini, eds.), p. 115–126. Soc. Mar. Mamm. Spec. Publ. 1. Soc. Mar. Mamm., P.O. Box 368, Lawrence, KS 66044.
Yadzi, P., A. Kilian, and B. Culik.
1999. Energy expenditure of swimming bottlenose dolphins. Mar. Biol. 134:601–607.
Yates, G.
1983. Hydrodynamics of body and caudal fin propulsion. *In* Fish biomechanics (P. Webb and D. Weihs, eds.), p.177–213. Praeger Publishers, New York, NY.

Population structure and variance effective size of red snapper (*Lutjanus campechanus*) in the northern Gulf of Mexico*

Eric Saillant

John R. Gold

Center for Biosystematics and Biodiversity
Texas A&M University, TAMU-2258
College Station, Texas 77843-2258
E-mail address (for E. Saillant): esaillant@tamu.edu

Abstract—We assayed allelic variation at 19 nuclear-encoded microsatellites among 1622 Gulf red snapper (*Lutjanus campechanus*) sampled from the 1995 and 1997 cohorts at each of three offshore localities in the northern Gulf of Mexico (Gulf). Localities represented western, central, and eastern subregions within the northern Gulf. Number of alleles per microsatellite per sample ranged from four to 23, and gene diversity ranged from 0.170 to 0.917. Tests of conformity to Hardy-Weinberg equilibrium expectations and of genotypic equilibrium between pairs of microsatellites were generally nonsignificant following Bonferroni correction. Significant genic or genotypic heterogeneity (or both) among samples was detected at four microsatellites and over all microsatellites. Levels of divergence among samples were low ($F_{ST} \leq 0.001$). Pairwise exact tests revealed that six of seven "significant" comparisons involved temporal rather than spatial heterogeneity. Contemporaneous or variance effective size (N_{eV}) was estimated from the temporal variance in allele frequencies by using a maximum-likelihood method. Estimates of N_{eV} ranged between 1098 and >75,000 and differed significantly among localities; the N_{eV} estimate for the sample from the northcentral Gulf was >60 times as large as the estimates for the other two localities. The differences in variance effective size could reflect differences in number of individuals successfully reproducing, differences in patterns and intensity of immigration, or both, and are consistent with the hypothesis, supported by life-history data, that different "demographic stocks" of red snapper are found in the northern Gulf. Estimates of N_{eV} for red snapper in the northern Gulf were at least three orders of magnitude lower than current estimates of census size (N). The ratio of effective to census size (N_e/N) is far below that expected in an ideal population and may reflect high variance in individual reproductive success, high temporal and spatial variance in productivity among subregions or a combination of the two.

Manuscript submitted 17 July 2004 to the Scientific Editor's Office.

Manuscript approved for publication 25 July 2005 by the Scientific Editor.

Fish. Bull. 104:136–148 (2006).

Red snapper (*Lutjanus campechanus*) is a highly exploited marine fish found primarily on the continental shelf of the Gulf of Mexico (Hoese and Moore, 1977). Red snapper abundance in the northern Gulf of Mexico (hereafter, Gulf) has decreased by almost 90% in the past two decades (Goodyear and Phares[1]) owing to overexploitation by commercial and recreational fishermen, high juvenile mortality due to the shrimp-trawl fishery, and habitat change (Christman[2]; Gallaway et al., 1999). An important question for management and conservation of red snapper resources regards delineation of geographic stock structure. Should separate stocks exist, management of the fishery, including assessment and allocation, could be subdivided to avoid subregional over-exploitation and to maintain potentially adaptive genetic variation (Carvalho and Hauser, 1995; Hauser and Ward, 1998). A second important question for management is whether sufficient genetic resources exist to ensure long-term integrity of red snapper stocks. Preliminary estimates of the number of red snapper adults in the northern Gulf range from 7.8 to 11.7 million (Cowan[3]; Porch[4]), which may indicate *a priori* that sufficient genetic resources are available. However, recent studies in other, commercially exploited marine fishes have shown that genetic effective size (N_e) can be three–five orders of magnitude smaller than estimates of census size or N (Hauser et al., 2002; Turner et al., 2002). Briefly, N_e is defined as the number of individuals in an "ideal" population that would experience the same magnitude of genetic drift as the actual population (Hartl and Clark, 1989). N_e is an important biological parameter, in part because it reflects the relative effects of genetic drift and selection on nonneutral loci, and in part because it can indicate long-term risk of extinction from genetic factors (Turner et al., 2002). As long-term sustainability requires maintenance of sufficient genetic resources (Allendorf and Waples, 1996), populations (or stocks) with small N_e potentially may

* Contribution 133 from the Center for Biosystematics and Biodiversity, Texas A&M University, College Station, Texas 77843-2258.

[1] Goodyear, C. P., and P. Phares. 1990. Status of red snapper stocks of the Gulf of Mexico: report for 1990, 72 p. National Marine Fisheries Service, Southeast Fisheries Centre, Miami Laboratory, CRD 89/90-05, 75 Virginia Beach Drive, Miami, FL 33149-1099.

[2] Christman, M. C. 1997. Peer review of red snapper (*Lutjanus campechanus*) research and management in the Gulf of Mexico: statistics review, 51 p. Office of Science and Technology, National Oceanic and Atmospheric Administration, National Marine Fisheries Service, 1315 East-West Highway 9th Floor F/CS, Silver Spring, MD 20910.

[3] Cowan, J. H. 2004. Personal commun. Department of Oceanography and Coastal Sciences, Coastal Fisheries Institute, Louisiana State University, Baton Rouge, LA 70803.

[4] Porch, C. E. 2004. Personal commun. National Marine Fisheries Center, Southeast Fisheries Science Center, 75 Virginia Beach Drive, Miami, FL 33149.

suffer reduced capacity to respond to changing or novel environmental pressures (Frankham, 1995; Higgins and Lynch, 2001).

At present, red snapper resources in the northern Gulf are managed under a single-stock hypothesis (GMFMC[5,6]). This hypothesis is supported by a number of prior genetic studies that employed allozymes (Johnson[7]), mitochondrial (mt)DNA (Gold et al., 1997; Garber et al., 2004), and microsatellites (Gold et al., 2001b). In each study, genetic homogeneity was observed across sampling localities, leading to the inference that gene flow was sufficient to maintain statistically identical allele distributions across the sampling area. All of these studies, however, either involved individuals of mixed cohorts or were based on relatively small sample sizes. Alternatively, tag-and-release and ultrasonic tracking (Fable, 1980; Szedlmayer and Shipp, 1994; Szedlmayer, 1997) have indicated that adult red snapper are sedentary and exhibit high site fidelity (but see Patterson et al., 2001). In addition, Pruett et al. (2005) used nested-clade analysis of red snapper mtDNA sequences and found evidence of different temporal episodes of both range expansion and restricted gene flow due to isolation by distance. They suggested that the spatial distribution of red snapper in the northern Gulf had a complex history that likely reflected glacial advance and retreat, habitat availability and suitability, and that the latter (i.e., physical conditions, and habitat availability and suitability) could partially restrict gene flow among present-day red snapper.

Our objectives were to more rigorously assess genetic stock structure in the northern Gulf by employing a large sample size of individuals from discrete cohorts. We report allelic variation at 19 nuclear-encoded microsatellites sampled from each of two cohorts at three different localities in the northern Gulf. Genetic homogeneity among localities was tested and contemporaneous or variance effective size (N_{eV}) at each locality was estimated from the temporal variance in allele frequencies (Waples, 1989) by using a maximum likelihood method (Wang, 2001).

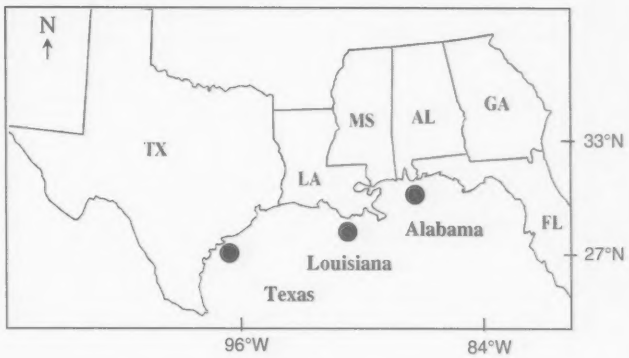

Figure 1

Sampling localities for adult red snapper (*Lutjanus campechanus*) in the northern Gulf of Mexico: northwestern Gulf (Texas), north-central Gulf (Louisiana), and northeastern Gulf (Alabama).

Materials and methods

Adult red snapper were sampled between 1999 and 2001 by angling 40–50 km offshore of Port Aransas (Texas), Port Fourchon (Louisiana), and Dauphin Island (Alabama). These localities represent western, central, and eastern subregions, respectively, within the northern Gulf (Fig. 1) but hereafter for convenience are referred to as Texas, Louisiana, and Alabama. Individual fish were aged by otolith-increment analysis (following Wilson and Nieland, 2001) and individuals belonging to the 1995 and 1997 cohorts were selected for genetic analysis. Sample sizes for the 1995 and 1997 cohorts at each locality were 203 and 211 (Texas), 286 and 272 (Louisiana), and 376 and 274 (Alabama). Tissue samples (heart and muscle) were removed from each fish and stored as described in Gold et al. (2001b). The genotype of all fish was determined at 19 microsatellites by using PCR primers and methods described in Gold et al. (2001b).

Summary statistics, including number of alleles, allelic richness (a measure of number of alleles independent of sample size), and unbiased gene diversity (expected heterozygosity) were computed for each microsatellite in each sample, with F-STAT, version 2.9.3 (Goudet, 1995). Homogeneity of allelic richness and gene diversity among samples was tested with Friedman rank tests. Departure of genotypic proportions from Hardy-Weinberg equilibrium expectations was measured within samples as Weir and Cockerham's (1984) *f*; probability of significance (P_{HW}) was assessed with a Markov-chain method (Guo and Thompson, 1992), as implemented in GENEPOP (Raymond and Rousset, 1995) and by using 5000 dememorizations, 500 batches, and 5000 iterations per batch. Genotypic disequilibrium between pairs of microsatellites within samples was tested by exact tests, as implemented in GENEPOP and by employing the same Markov-chain parameters as above. Sequential Bonferroni correction (Rice, 1989) was applied for all multiple tests performed simultaneously.

[5] GMFMC (Gulf of Mexico Fishery Management Council). 1989. Amendment number 1 to the Reef Fish Fishery Management Plan, 356 p. Gulf of Mexico Fishery Management Council, 2203 N. Lois Avenue, Suite 1100, Tampa, FL 33609.

[6] GMFMC (Gulf of Mexico Fishery Management Council). 1991. Amendment number 3 to the Reef Fish Fishery Management Plan, 17 p. Gulf of Mexico Fishery Management Council, 2203 N. Lois Avenue, Suite 1100, Tampa, FL 33609.

[7] Johnson, A. G. 1987. An investigation of the biochemical and morphometric characteristics of red snapper (*Lutjanus campechanus*) from the southern United States. Unpubl. manuscr., 26 p. National Marine Fisheries Service, Panama City Laboratory, 3500 Delwood Beach Road, Panama City, FL 32407-7499.

Homogeneity of allele and genotype distributions among samples was examined with exact tests; significance of probability values was assessed by a Markov-chain method, as implemented in GENEPOP and using the same Markov-chain parameters as above. The degree of differentiation between pairs of samples was estimated as Weir and Cockerham's (1984) θ, as implemented in F-STAT. Sequential Bonferroni correction (Rice, 1989) was applied for all multiple tests performed simultaneously. Spatial (geographic) differences among samples was assessed from multilocus data by estimating the likelihood that any given individual could be assigned to the sample locality from which it was drawn. The Bayesian method of Rannala and Mountain (1997), as implemented in GENECLASS vers. 2.0 (Piry et al., 2005), was used to "assign" sampled individuals to a locality; the probability that an individual belonged to a given locality was calculated by using the resampling algorithm in Paetkau et al. (2004) and was based on 1000 simulated individuals. A locality was excluded as a potential origin of a given individual if the probability of the individual belonging to that locality fell below a threshold level of 0.05.

Temporal changes in allele frequencies between the two cohorts were used to estimate variance effective size (N_{eV}) at each locality. This "temporal" method (Waples, 1989) estimates effective size from the temporal variance in allele frequencies over the time interval between sampling, thus providing a contemporaneous estimate of N_e. The pseudo-maximum-likelihood method described in Wang (2001) was used to obtain estimates and 95% confidence intervals of N_{eV} by using the program MLNE available at http://www.zoo.cam.ac.uk/ioz/software.htm#MLNE. The 95% confidence intervals were obtained as the range of support associated with a drop of two logarithm units of the likelihood function, as inferred from the likelihood distribution (Wang, 2001). We used the analytical method developed by Jorde and Ryman (1995, 1996) to account for effects of overlapping generations on temporal-method estimates of N_e. In a population with overlapping generations, the magnitude of temporal allele-frequency change is dependent in part on age-specific survivorship (l_i) and birth rate (b_i). Survivorship was calculated by assuming an equal probability (S) of surviving from one year class to the next and equal probability of survival of males and females. The value of S (0.56 for Texas and 0.604 for Louisiana and Alabama) was estimated by using age-structure data of red snapper to calculate age-specific survivorship ($l_i=S^{i-1}$) for each age class i. Birth rate was estimated by calculating mean individual (wet) weight at each age class, as an indicator of relative gamete contribution. Individual weights averaged across males and females within each age class were determined by using von Bertalanffy equations (Fischer et al., 2004) for red snappers at each locality; this mean value was then multiplied by l_i to obtain the proportional contribution of each age class to offspring (p_i); p_i values were then summed over k age classes. Mean individual weights at each age class were divided by

$$\sum_{i=1}^{k} p_i$$

to produce a standardized birth rate (b_i), corrected to reflect a nongrowing population with stable age structure, i.e.,

$$\sum_{i=1}^{k} l_i b_i = 1.$$

Both age-structure and individual (wet) weight data were from the commercial and recreational catch of red snapper in the northern Gulf were provided by D. Nieland of Louisiana State University. Resulting life-history tables were used to calculate a correction factor (C) for overlapping generations by using 100 iterations of Equation 5 in Jorde and Ryman (1996). The value C can be defined as a correction term that is determined by the particular values of l_i and b_i of the population under study. G, the mean generation length in years, was calculated by using Equation 10 in Jorde and Ryman (1996). Values of C and G obtained for each locality were subsequently used to correct estimates of N_e by $N_{ec} = N_e \times [C/G]$, where N_e is the pseudo-maximum-likelihood estimate of variance effective size obtained by following Wang (2001). C and G values, respectively, for the three localities were 10.1 and 6 (Texas), 12.1 and 6.1 (Louisiana), and 10.5 and 6.8 (Alabama).

Results

Summary statistics (number of alleles, allelic richness, gene diversity; and results of tests of HW equilibrium) for each sample are given in Appendix Tables 1 and 2. Number of alleles among all samples ranged from 4 to 7 at *Prs*260 to 20–23 at *Prs*248, and averaged (±SD) 11.67 ±5.15 (1995 cohort) and 11.30 ±5.02 (1997 cohort). Allelic richness generally paralleled the number of alleles. Gene diversity among all samples ranged between 0.178–0.238 (*Lca*20) and 0.898–0.915 (*Prs*257), and averaged (±SD) 0.597 ±0.224 (1995 cohort) and 0.602 ±0.217 (1997 cohort). No significant difference in allelic richness (P=0.35) or gene diversity (P=0.07) was detected.

Four of 114 tests of conformity to Hardy-Weinberg equilibrium expectations were significant following Bonferroni correction. These included two tests in the 1995 cohort (*Prs*275 in the Texas sample and *Prs*137 in the Alabama sample) and two tests in the 1997 cohort (*Lca*22 in the Texas sample and *Prs*229 in the Louisiana sample). F_{IS} values over all loci for all four samples ranged between 0.008 and 0.029 (Appendix Tables 1 and 2). A total of 21 of 1026 (pairwise) tests of genotypic disequilibrium were significant (P<0.05) after Bonferroni correction. All 21 involved different pairs of loci (i.e., only one out of six possible tests for a given pair combination was significant) except for *Lca*64 and *Prs*328 in the 1995 cohort from Alabama and the 1997 cohort from Texas, and *Lca*64 and *Prs*248 in both cohorts sampled from Texas.

Table 1

Probability of genic and genotypic homogeneity at 19 microsatellites among spatial and temporal samples of red snapper (*Lutjanus campechanus*) sampled from the northern Gulf of Mexico. Probability values are based on exact tests; significance was assessed via a Markov-chain method (cf text). Boldface indicates significance following sequential Bonferroni correction.

Microsatellite	Genic homogeneity	Genotypic homogeneity
*Lca*20	0.018	0.031
*Lca*22	**0.001**	0.005
*Lca*43	0.044	0.065
*Lca*64	0.109	0.127
*Lca*91	**0.000**	**0.001**
*Lca*107	0.416	0.292
*Prs*55	0.179	0.212
*Prs*137	0.706	0.788
*Prs*221	0.931	0.930
*Prs*229	0.024	0.047
*Prs*240	**0.000**	**0.000**
*Prs*248	0.101	0.154
*Prs*257	0.053	0.085
*Prs*260	0.098	0.111
*Prs*275	0.819	0.893
*Prs*282	0.050	0.063
Prs 303	0.014	**0.002**
*Prs*328	0.184	0.289
*Prs*333	0.137	0.113
Overall	**0.000**	**0.000**

Table 2

Pairwise F_{ST} values (upper diagonal) and probability that F_{ST}=0 (lower diagonal) for twelve samples (four cohorts×three localities) of red snapper (*Lutjanus campechanus*) from the northern Gulf of Mexico. Boldface indicates significance following sequential Bonferroni correction. TX=Texas; LA=Louisiana; AL-Alabama.

	TX 95	LA 95	AL 95	TX 97	LA 97	AL 97
TX 95	—	0.0012	0.0010	0.0013	0.0010	0.0020
LA 95	**0.002**	—	0.0006	0.0007	−0.0002	0.0009
AL 95	**0.001**	0.031	—	0.0008	−0.0001	0.0015
TX 97	**0.000**	0.013	**0.001**	—	0.0005	0.0002
LA 97	0.036	0.756	0.737	0.079	—	0.0006
AL 97	**0.000**	**0.000**	**0.000**	0.045	0.073	—

Table 3

Results of assignment tests (percentage of fish assigned to a given locality) based on red snapper (*Lutjanus campechanus*) sampled from three geographic localities in the northern Gulf of Mexico. TX=Texas; LA=Louisiana; AL=Alabama.

Origin of sample (sample size)	Highest likelihood of belonging to		
	TX	LA	AL
TX (414)	53.0	24.0	22.0
LA (558)	21.0	53.0	26.0
AL (651)	21.0	26.0	53.0

Table 4

Estimates of variance effective size (N_{eV}) and 95% confidence intervals for red snapper (*Lutjanus campechanus*) sampled at three geographic localities in the northern Gulf of Mexico. Estimates were generated using the pseudo-maximum-likelihood method of Wang (2001). Values are corrected for overlapping generations, following Jorde and Ryman (1995).

Locality	N_{eV}	95% low	95% high
Texas	1098	652	2706
Louisiana	>75,000	3275	>75,000
Alabama	1235	777	2515

Significant heterogeneity (exact tests) among samples in either allele or genotype distributions (or both) was found overall and, after Bonferroni correction, at four individual microsatellites (Table 1). Pairwise comparisons (exact tests) of allele and genotype distributions between samples paralleled one another and revealed that almost all of the genetic heterogeneity was due to the 1995 cohort from Texas and the 1997 cohort from Alabama (Table 2). This result indicated that the observed genetic heterogeneity is more temporal (between cohorts) than spatial (among localities). Temporal rather than spatial heterogeneity also was indicated by the nonsignificant exact tests among localities sampled in 1997 and by the average F_{ST} values among localities (both cohorts) of less than 0.001.

Results of assignment tests are given in Table 3. On average, 53% of the individuals were "assigned" (i.e., had the highest probability of belonging) to their original locality. This proportion was significantly higher (P<0.001) than that expected if multilocus genotypes were distributed randomly with respect to geographic location. However, the estimated probabilities of belonging to all three localities were higher than 0.05 for 96.4–99.8% of the individuals, indicating that none of the three localities could be rejected as a potential origin. In addition, for four individuals from the Alabama sample (0.6%), all three localities were excluded as the potential origin.

The pseudo-maximum-likelihood (temporal-method) estimates of variance effective size (N_{eV}), corrected for overlapping generations, and their 95% confidence intervals for all three localities are shown in Table 4.

Estimates for the samples from Texas (N_{eV}=1098) and Alabama (N_{eV}=1235) were essentially the same, falling well within the 95% confidence intervals of one another. An exact, maximum-likelihood estimate could not be generated for the sample from Louisiana because the value of N_{eV} with highest likelihood was >75,000 and the likelihood of higher values of N_{eV} could not be computed. This estimate is more than an order of magnitude greater than the N_{eV} estimates for the other two localities and is significantly higher than those based on 95% confidence intervals.

Discussion

Genetic population structure

Results obtained from pairwise exact tests indicated that the majority of genetic differentiation detected among the twelve spatial-temporal samples of red snapper was due to allele and genotype distributions in the 1995 cohort sampled from the northwestern Gulf (Texas) and in the 1997 cohort sampled from the northeastern Gulf (Alabama). In addition, exact tests among cohorts sampled in 1997 were nonsignificant and F_{ST} values among localities (both cohorts) averaged less than 0.001. These results indicate that the genetic differences observed in the present study are temporal (between cohorts within localities) and not spatial (among localities). A "hint" of spatial differentiation was suggested by assignment tests. A total of 53% of fish were reclassified (assigned) to their original locality, a proportion that differed significantly from that expected if genotypes were distributed randomly among localities. However, for 98% of the fish, none of the three localities could be unequivocally excluded as the locality of origin.

The above results are in general agreement with other, genetics-based studies of red snapper in the northern Gulf in that little to no significant geographic heterogeneity in genetic markers, ranging from allozymes to mtDNA to microsatellites, has been detected (Johnson[7]; Gold et al., 1997; Garber et al., 2004; Gold et al., 2001b). The one exception was a study by Bortone and Chapman[8] where significant heterogeneity in both temporal and spatial restriction-fragment patterns of the mitochondrially-encoded 16S ribosomal (r)RNA gene was reported. Bortone and Chapman[8] suggested that the observed genetic heterogeneity likely stemmed from nonrandom sampling where individuals related by descent had remained in close spatial proximity to one another. In general, the "consensus" inference has been that gene flow among present-day red snapper in the northern Gulf is sufficient to offset divergence by genetic drift of the (presumed) selectively neutral genetic markers assayed. Such gene flow could involve movement of adults (Patterson et al., 2001), hydrodynamic transport of pelagic eggs and larvae (Goodyear[9]), or both.

The foregoing notwithstanding, there are a number of caveats (discussed in Pruett et al., 2005) to the inference that significant gene flow occurs among present-day red snapper in the northern Gulf. Briefly, tag-and-recapture and ultrasonic-tracking studies (Fable, 1980; Szedlmayer and Shipp, 1994; Szedlmayer, 1997) have indicated that adult red snapper are largely sedentary and nonmigratory. Significant movement of adults in the northeastern Gulf was reported by Patterson et al. (2001), but movement *per se* was mostly unidirectional (west to east) and the average distance covered in roughly a year was only ~30 kilometers. Movement of (pelagic) red snapper eggs and larvae likely occurs, but neither egg nor larval type nor length of larval life are effective predictors of gene flow in marine fishes (Shulman and Bermingham, 1995) and larval exchange rates of marine species generally appear overestimated (Cowen et al., 2000). In addition, regardless of the life-history stage at which gene flow might occur in red snapper, movement across the continental shelf should be more-or-less linear and would be expected to follow a pattern of isolation by distance where fish from proximal localities are more similar genetically than fish from more distal ones. However, the correlations between genetic and geographic distance expected from isolation by distance have not been found (Gold et al., 1997; 2001b; this article). Finally, salient differences in geologic structure, habitat structure, and ecological conditions (Rezak et al., 1985; Gallaway et al., 1998), significant differences in salinity due to freshwater outflow from river systems in the northcentral Gulf (Morey et al., 2003), and the present-day occurrence during the summer months of a major hypoxic zone that extends out along the continental shelf from the Mississippi Delta westward (Rabalais et al.[10]; Ferber, 2001) potentially could serve as barriers to movement and gene flow.

Despite these caveats, the bulk of the genetics data has indicated essentially no difference among present-day red snapper sampled across the northern Gulf. This is consistent with the unit stock hypothesis and with the inference that observed genetic homogeneity is due to substantial gene flow. However, it is important to

[8] Bortone, S. A., and R. W. Chapman. 1995. Identification of stock structure and recruitment patterns for the red snapper, *Lutjanus campechanus*, in the Gulf of Mexico. Final report for Marfin Program Grant Number NA17FF0379-03, 39 p. Southeast Regional Office, National Marine Fisheries Service, 263 13th Avenue South, Saint Petersburg, FL 33701.

[9] Goodyear, C. P. 1995. Red snapper stocks in U.S. waters of the Gulf of Mexico, 171 p. National Marine Fisheries Service, SE Fisheries Center, Miami Laboratory, CRD 95/96-05, 75 Virginia Beach Drive, Miami, FL 33149-1099.

[10] Rabalais, N. N., R. E. Turner, D. Justic, Q. Dortch, and W. J. Wiseman. 1999. Characterization of hypoxia: topic I report for the integrated assessment on hypoxia in the Gulf of Mexico. NOAA Coastal Ocean Program Decision Analysis Series No. 15, 203 p. NOAA Coastal Ocean Program, 1305 East-West Hwy., N/SCI2 SSMC4, Silver Spring, MD 20910.

note the following. First, it is possible that gene flow among present-day red snapper in the northern Gulf is limited but there has been insufficient time for semi-isolated lineages to completely sort into monophyletic assemblages. Pruett et al. (2005), on the basis of results of nested-clade analysis of mtDNA haplotypes obtained from representative samples of the same cohorts (and localities) studied in the present study, hypothesized that semi-isolated assemblages of red snapper in the northern Gulf may exist over the short term, yet over the long term comprise a larger metapopulation tied together by periodic gene flow. Similarity in allele frequencies of genetic markers (such as used here and in previous studies of red snapper) presumed to be neutral to natural selection in theory could be maintained in such a metapopulation during periods when gene flow was limited or even absent. Second, all the genetic markers studied to date are presumed to be selectively neutral and to be affected primarily by the interaction(s) between gene flow and genetic drift. Genes affecting life-history and other traits that are influenced by natural selection need not necessarily follow the same pattern(s), and geographic differences in adaptively useful alleles at such genes can be maintained even in the face of substantial gene flow (Conover et al., 2005). It is thus not implausible that red snapper across the northern Gulf could differ in allele frequency at adaptively useful genes yet be homogeneous at selectively neutral ones.

Contemporaneous effective size (N_{eV}) and present-day demographic dynamics

Estimates of contemporaneous or variance effective size (N_{eV}) for the Texas and Alabama localities (~1100) were essentially the same, but were at least an order of magnitude less than the N_{eV} estimate (>75,000) for the Louisiana locality. These estimates reflect differences in effective population size under the assumption that no immigration into a locality has occurred during the study interval, an assumption at odds with the general absence of allele-frequency heterogeneity among localities as well as the low estimates of F_{ST} between pairs of samples. Short-term immigration (within the time interval of the study) could increase the variance in allele frequencies, thus resulting in an overestimate of N_{eV} (Wang and Whitlock, 2003); whereas longer-term immigration at a (more-or-less) constant rate from a source population would have the opposite effect. The observed differences among localities could thus reflect differences in effective sizes, differences in patterns and intensity of immigration, or both. Temporal variation in allele frequencies also could occur if only a fraction of potential spawners at a locality actually contributed to recruitment and if such "temporal" subpopulations differed in allele frequencies between years. Regardless, the differences in N_{eV} may indicate that different demographic dynamics currently exist among localities.

Wang and Whitlock (2003) recently extended previous maximum-likelihood methods to allow simultaneous estimation of N_{eV} and m (rate of migration), provided data from multiple loci were available and all sources of immigrants into a focal population were known. Because of the latter, we were able to generate estimates of N_{eV} and m only for the sample from the Louisiana locality (focal population), using the samples from the Texas and Alabama localities as source populations. Surprisingly, the estimate of N_{eV} for the Louisiana sample (4887, 95% confidence intervals of 1543 and 31,254) was at least ~15 times smaller than the estimate based on no migration; m was estimated to be 0.0097 (95% confidence intervals of <0.001 and 0.0355). Clearly, more extensive sampling across the northern Gulf is warranted to obtain estimates of N_{eV} and m at other localities and to place this finding into perspective.

Effective size (N_e)/census size(N) ratios

Estimates of N_{eV} for all three sample localities were two or more orders of magnitude less than the current, preliminary estimates of adult census size (7.8–11.7 million) across the northern Gulf (Cowan[3]; Porch[4]). Given that empirically derived N_e/N ratios from a variety of vertebrates are 0.10–0.11 on average (Frankham, 1995), this result is somewhat surprising in that red snapper have a long reproductive life-span and overlapping generations (Wilson and Nieland, 2001), life-history features that are expected to increase N_e/N by limiting variance in lifetime reproductive success among individuals (Jorde and Ryman, 1995; Waite and Parker, 1996). The issue is of importance in that census sizes of many commercially exploited marine fish populations are generally orders of magnitude larger than sizes where genetic resources might be lost (Franklin, 1980; Schultz and Lynch, 1997). However, species or populations with exceedingly small N_e/N ratios potentially could be in danger of losing genetic resources, resulting in reduced adaptation and population productivity (Hauser et al., 2002). In addition, low N_e/N ratios may explain in part why there often is a poor relationship between spawning stock size and recruitment (Hauser et al., 2002). To date, N_e/N ratios smaller than 10^{-3} have been found for four other exploited marine fish species (Hauser et al., 2002; Turner et al., 2002; Hutchinson et al., 2003; Gomez-Uchida and Banks[11]).

Factors that theoretically can lower genetic effective size with respect to census size include fluctuating adult number and year-class strength (Hedgecock, 1994; Vucetich et al., 1997), and variance in reproductive success. The latter can arise from biased sex ratio, high variance in male or female reproductive success, variance in productivity among habitats, or any combination of these factors (Nunney, 1996, 1999; Whitlock and Barton, 1997). Virtually any of these factors could lower N_e/N ratios in red snapper. Biased sex-ratio, however,

[11] Gomez-Uchida, D., and M. A. Banks. 2003. Oregon State Univ., Hatfield Marine Science Center, Department of Fisheries and Wildlife, 2030 SE Marine Sci. Dr. Newport, OR 97365.

seems unlikely, because the ratio of males and females across three years of red snapper catch data was 0.97 and did not differ significantly from unity (Nieland[12]).

Variation in population number and in year-class strength, alternatively, seems likely, given the annual differences in commercial and recreational landings and the annual differences in abundance of age-0 and age-1 red snapper, respectively (Schirripa and Legault[13]). Variance in reproductive success is far more difficult to assess but can include mating systems (Nunney, 1993) that lead to differences in reproductive success between males and females, and a "sweepstakes" process (Hedgecock, 1994) where size-dependent fecundity, combined with random but family-specific early mortality (Hauser et al., 2002), leads to a large variance in the number of (surviving) offspring per parent. The latter could be effected in red snapper by nonrandom removal of related subadults or juveniles either by localized overfishing or by shrimp trawling. Finally, variance in productivity among habitats across the northern Gulf can be inferred from subregional differences in red snapper growth rates (Fischer et al., 2004) and from subregional ecological differences (Gallaway et al., 1998) that distinguish the northeastern Gulf from the northwestern Gulf. Future ecological and behavioral studies to generate estimates of variance in individual reproductive success or variation in productivity among localities are clearly warranted.

Demographic stocks

The differences in variance effective size (N_{eV}) among the geographic samples of red snapper indicate present-day differences in demographic dynamics that may include the number of individuals that produce surviving offspring, and hence by inference, census size. The factors, ecological or otherwise, promoting these demographic differences are difficult to assess but likely relate in some way to variation in food availability, habitat quality, or mortality (or a combination of all three factors). Accordingly, one might expect one or more of these factors to differ among the sample localities, given the differences in variance effective size among localities. In addition, one might expect other demographic parameters to differ as well.

Our study was part of a larger, multidisciplinary project that involved studies of age-and-growth and reproduction of red snapper at the three localities. The age-and-growth studies of Fischer et al. (2004) documented that fork length, total weight, and age-frequency distributions differed significantly among localities. Red snapper sampled at the Texas locality were significantly smaller at age and reached smaller maximum size than did red snapper sampled at the Louisiana and Alabama localities; fish sampled at the latter two localities did not differ in size-at-age or maximum size. There also was a significantly higher proportion of smaller, younger fish at the Texas locality than at the other two. The studies of reproductive capacity (Woods et al., 2003) involved only fish sampled from the Louisiana and Alabama localities but revealed that females sampled from the Alabama locality reached sexual maturity at a smaller size and younger age than did females sampled from the Louisiana locality. The differences in growth rate are likely a function in part of the more productive, nutrient-rich waters found at the Louisiana and Alabama localities and caused by the plume produced from the Mississippi River (Fischer et al., 2004), a hypothesis reinforced by the observation (Grimes, 2001) that between 70–80% of fishery landings in the northern Gulf of Mexico come from waters surrounding the Mississippi River delta. The differences in female age and size at maturity, alternatively, are thought to indicate a stressed population and to reflect a compensatory response to growth overfishing or declining population size, or a response to both (Trippel, 1995; Woods et al., 2003). Collectively, the life-history differences and the differences in genetic-based estimates of effective size strongly suggest that red snapper at the three localities represent three different, demographic stocks.

A critical issue is whether the demographic differences in life history observed among red snapper in the northern Gulf are genetic or phenotypic (environmentally induced) in origin. Most discussions of stock structure in commercially exploited marine fishes involve an explicit genetics component (Gold et al., 2001a), and typically, the absence of genetic heterogeneity within a fishery leads to management planning for a single unit stock. However, life-history traits can change rapidly in response to environmental pressures (e.g., size-selective fishing), and it has been hypothesized that the pool of genotypes that code for life-history traits is a highly dynamic property of populations, and moreover, that local adaptation(s) differentiating populations can evolve even in the presence of extensive gene flow (Conover et al., 2005). Thus, demographically different stocks could differ genetically, but not necessarily in selectively neutral markers that respond primarily to the interaction between gene flow and genetic drift. The issue also is of importance to management planning because phenotypically plastic responses due to environmental differences generally can be reversed fairly quickly, whereas genetic responses are typically much slower (Hutchings, 2004; Conover et al., 2005).

The geographic differences in red snapper in growth rates and shifts in timing of female maturity in all likelihood are due to a mix of genetic and environmental factors, as are most life-history traits in a variety of animal species, including fishes (Mousseau and Roff, 1987; Conover and Munch, 2002). A significant genetic component to growth rate is well documented in a variety of fishes under aquaculture (Dunham et al., 2001)

[12] Nieland, D. 2005. Personal commun. Coastal Fisheries Institute, Louisiana State University, Baton Rouge, LA 70803-7503.

[13] Schirripa, M. J., and C. M. Legault. 1999. Status of the red snapper in U.S. waters of the Gulf of Mexico. Report SFD-99/00-75, 86 p. Southeast Fisheries Science Center, 75 Virginia Beach Drive, Miami, FL 33149-1099.

and genotypes for smaller size and younger age at maturity clearly exist (Gjerde, 1984; Tipping, 1991; Trippel, 1995). These considerations indicate that a genetic component to growth rate and age at maturity may exist in red snapper, and if so, stock-structure considerations solely on the basis of homogeneity in selectively neutral genetic markers may not be warranted.

Acknowledgments

We thank A. Fisher for providing individual age data, D. Nieland for providing life-history data, T. Turner for extensive assistance with statistical analysis, the Texas A&M supercomputing facility staff for help with parallel processing of MLNE, and S.C. Bradfield, C. Burridge, and L. Richardson for technical assistance. We also thank W. Patterson and T. Turner for helpful comments on early drafts of the manuscript, and J. Cowan and C. Porch for providing estimates of red snapper census size. Work was supported by the Gulf and South Atlantic Fisheries Development Foundation (Grant 70-04-20000/11824), by the Marfin Program of the U.S. Department of Commerce (Grant NA87-FF-0426), and by the Texas Agricultural Experiment Station (Project H-6703). This article is number 46 in the series "Genetics Studies in Marine Fishes."

Literature cited

Allendorf, F. W., and R. S. Waples.
1996. Conservation and genetics of salmonid fishes. *In* Conservation genetics: case histories from nature (J. C. Avise, and J. L. Hamrick, eds.) p. 238–280. Chapman and Hall, New York, NY.

Carvalho, G. R., and L. Hauser.
1995. Molecular genetics and the stock concept in fisheries. *In* Molecular genetics in fisheries (G. R. Carvalho, and T. J. Pitcher eds.) p. 55–80. Chapman and Hall, London.

Conover, D. O., S. A. Arnott, M. R. Walsh, and S. B. Munch.
2005. Darwinian fishery science: lessons from the Atlantic silverside. Can. J. Fish. Aquat. Sci. 62:730–737.

Conover, D. O., and S. B. Munch.
2002. Sustaining fisheries yields over evolutionary time scales. Science 297:94–96.

Cowen, R. K., K. M. M. Lwiza, S. Sponaugle, C. B. Paris, and D. B. Olson.
2000. Connectivity of marine populations: open or closed? Science 287:857–859.

Dunham, R. A., K. Majumdar, E. Hallerman, D. Bartley, G. Mair, G. Hulata, Z. Liu, N. Pongthana, J. Bakos, D. Penman, M. Gupta, P. Rothlisberg, and G. Hoerstgen-Schwark.
2001. Review of the status of aquaculture genetics. *In* Aquaculture in the third millennium (R. P. Subasinghe, P. Bueno, M. J. Phillips, C. Hough, S. E. McGladdery, and J. R. Arthur, eds.) p. 137–166. FAO, Rome.

Fable, W. A.
1980. Tagging studies of red snapper (*Lutjanus campechanus*) and vermilion snapper (*Rhomboplites aurorubens*) off the south Texas coast. Contrib. Mar. Sci. 23:115–121.

Ferber, D.
2001. Keeping the Stygian waters at bay. Science 291: 968–973.

Fischer, A. J., M. S. Baker Jr., and C. A. Wilson.
2004. Red snapper, *Lutjanus campechanus*, demographic structure in the northern Gulf of Mexico based on spatial patterns in growth rates and morphometrics. Fish. Bull. 102:593–603.

Frankham, R.
1995. Effective population-size adult-population size ratios in wildlife: a review. Genet. Res. 66:95–107.

Franklin, I. R.
1980. Evolutionary change in small populations. Chapter 8 *in* Conservation biology: an evolutionary-ecological perspective (M. Soulé, and B. Wilcox, eds.) p. 135–149. Sinauer, Sunderland, MA.

Gallaway, B. J., J. G. Cole, R. Meyer, and P. Roscigno.
1999. Delineation of essential habitat for juvenile red snapper in the northwestern Gulf of Mexico. Trans. Am. Fish. Soc. 128:713–726.

Gallaway, B. J., M. Longnecker, J. G. Cole, and R. M. Meyer.
1998. Estimates of shrimp trawl bycatch of red snapper, *Lutjanus campechanus*, in the Gulf of Mexico. *In* Fishery stock assessment models (F. Funk F, T. J. Quinn II, J. Heifetz, J. N. Ianelli, J. E. Powers, J. F. Schweigert, P. J. Sullivan, and C.-I. Zhang, eds.) p. 817–839. Alaska Sea Grant College Program, No. AK-SG-98-01. Fairbanks, AK.

Garber, A. F., M. D. Tringali, and K. C. Stuck.
2004. Population structure and variation in red snapper (*Lutjanus campechanus*) from the Gulf of Mexico and Atlantic Coast of Florida as determined from mitochondrial DNA control region sequence. Mar. Biotechnol. 6:175–185.

Gjerde, B.
1984. Response to individual selection for age at sexual maturity in Atlantic salmon. Aquaculture 38:229–240.

Gold, J. R., C. P. Burridge, and T. F. Turner.
2001a. A modified stepping-stone model of population structure in red drum, *Sciaenops ocellatus* (Sciaenidae) from the northern Gulf of Mexico. Genetica 111:305–317.

Gold, J. R., E. Pak, and L. R. Richardson.
2001b. Microsatellite variation among red snapper (*Lutjanus campechanus*) from the Gulf of Mexico. Mar. Biotechnol. 3:293–304.

Gold, J. R., F. Sun, and L. R. Richardson.
1997. Population structure of red snapper from the Gulf of Mexico as inferred from the analysis of mitochondrial DNA. Trans. Am. Fish. Soc. 126:386–396.

Goudet, J.
1995. F-STAT (Version 1.2): A computer program to calculate F-Statistics. J. Hered. 86:485–486.

Grimes, C. B.
2001. Fishery production and the Mississippi River discharge. Fisheries 26:17–26.

Guo, S., and E. Thompson.
1992. Performing the exact test of Hardy-Weinberg proportion from multiple alleles. Biometrics 48: 361–372

Hartl, D. L., and A. G. Clark.
1989. Principles of population genetics, 2nd edition, 669 p. Sinauer Assoc., Inc., Sunderland, MA.

Hauser, L., and R. D. Ward.
1998. Population identification in pelagic fish: the limits of molecular markers. *In* Advances in molecular ecol-

ogy (G. R. Carvalho, ed.), p. 2191–2242. IOS Press, Amsterdam.

Hauser, L., G. J. Adcock, P. J. Smith, J. H. B. Ramirez, G. R. Carvalho.
2002. Loss of microsatellite diversity and low effective population size in an overexploited population of New Zealand snapper (Pagrus auratus). Proc. Natl. Acad. Sci. USA. 99:11742–11747.

Hedgecock, D.
1994. Does variance in reproductive success limit effective population sizes of marine organisms? *In* Genetics and evolution of aquatic organisms (A. R. Beaumont, ed.) p. 122–134. Chapman and Hall, New York, NY.

Higgins, K., and M. Lynch.
2001. Metapopulation extinction caused by mutation accumulation. Proc. Natl. Acad. Sci. USA 98: 2928–2933.

Hoese, H. D., and R. H. Moore.
1977. Fishes of the Gulf of Mexico, 327 p. Texas A&M Univ. Press, College Station, TX.

Hutchings, J. A.
2004. Life history consequences of over-exploitation to population recovery in northwest Atlantic cod, *Gadus morhua*. Can. J. Fish. Aquat. Sci. 62:824–832.

Hutchinson, W. F., C. van Oosterhout, S. I. Rogers, and G. R. Carvalho.
2003. Temporal analysis of archived samples indicates marked genetic changes in declining North Sea cod (*Gadus morhua*). Proc. R. Soc. London, B 270: 2125–2132.

Jorde, P. E., and N. Ryman.
1995. Temporal allele frequency change and estimation of effective size in populations with overlapping generations. Genetics 139:1077–1090.
1996. Demographic genetics of brown trout (*Salmo trutta*) and estimates of effective population size from temporal change of allele frequencies. Genetics 143:1369–1381.

Morey, S. L., W. L. Schroeder, J. J. O'Brien, and J. Zavala-Hidalgo.
2003. The annual cycle of riverine influence in the eastern Gulf of Mexico. Geophys. Res. Letters 30:OCE 5.1–5.4.

Mousseau, T. A., and D. A. Roff.
1987. Natural selection and the heritability of fitness components. Heredity 59:181–198.

Nunney, L.
1993. The influence of mating system and overlapping generations on effective population size. Evolution 47:1329–1341.
1996. Influence of variation in female fecundity on effective population size. Biol. J. Linn. Soc. 59: 411–425.
1999. The effective size of a hierarchically structured population. Evolution 53:1–10.

Paetkau, D., R. Slade, M. Burden, and A. Estoup.
2004. Direct, real-time estimation of migration rate using assignment methods: a simulation-based exploration of accuracy and power. Mol. Ecol. 13:55–65.

Patterson, W. F., J. C. Watterson, R. L. Shipp, and J. H. Cowan Jr.
2001. Movement of tagged red snapper in the northern Gulf of Mexico. Trans. Am. Fish. Soc. 130:533–545.

Piry, S., A. Alapetite, J. M. Cornuet, D. Paetkau, L. Baudouin, and A. Estoup.
2005. GeneClass2: a software for genetic assignment and first generation migrants detection. J. Hered. 95:536–539.

Pruett, C. L., E. Saillant, and J. R. Gold.
2005. Historical population demography of red snapper (*Lutjanus campechanus*) from the northern Gulf of Mexico based on analysis of sequences of mitochondrial DNA Mar. Biol. 147:593–602.

Rannala, B., and J. L. Mountain.
1997. Detecting immigration by using multilocus genotypes. Proc. Nat. Acad. Sci. USA 94:9197–9201.

Raymond, M., and F. Rousset.
1995. Genepop (version 1.2): a population genetics software for exact test and Ecumenicism. J. Hered. 86: 248–249.

Rezak, R., T. J. Bright, and D. W. McGrail.
1985. Reefs and banks of the northwestern Gulf of Mexico, 259 p. John Wiley and Sons, New York, NY.

Rice, W. R.
1989. Analyzing tables of statistical tests. Evolution 43:223–225.

Schultz, S. T., and M. Lynch.
1997. Mutation and extinction: the role of variable mutational effects, synergistic epistasis, beneficial mutations, and degree of outcrossing. Evolution 51:1363–1371.

Shulman, M. J., and E. Bermingham.
1995. Early life histories, ocean currents, and the population genetics of Caribbean reef fishes. Evolution 49:897–910.

Szedlmayer, S. T.
1997. Ultrasonic telemetry of red snapper, *Lutjanus campechanus*, at artificial reef sites in the northeast Gulf of Mexico. Copeia 1997:846–850.

Szedlmayer, S. T., and R. L. Shipp.
1994. Movement and growth of red snapper, *Lutjanus campechanus*, from an artificial reef area in the northeastern Gulf of Mexico. Bull. Mar. Sci. 55:887–896.

Tipping, J. M.
1991. Heritability of age at maturity. North Am. J. Fish. Manag. 11:105–108.

Trippel, E. A.
1995. Age at maturity as a stress indicator of fisheries. BioScience 45:759–771.

Turner, T. F., J. P. Wares, and J. R. Gold.
2002. Genetic effective size is three orders of magnitude smaller than adult census size in an abundant, estuarine-dependent marine fish (*Sciaenops ocellatus*). Genetics 162:1329–1339.

Vucetich, J. A., T. A. Waite, and L. Nunney.
1997. Fluctuating population size and the ratio of effective to census population size. Evolution 51: 2017–2021.

Waite, T. A., and P. G. Parker.
1996. Dimensionless life histories and effective population size. Conserv. Biol. 10:1456–1462.

Wang, J.
2001. A pseudo-likelihood method for estimating effective population size from temporally spaced samples. Genet. Res. 78:243–257.

Wang, J., and M. C. Whitlock.
2003. Estimating effective population size and migration rates from genetic samples over space and time. Genetics 163:429–446.

Waples, R. S.
1989. A generalized approach for estimating effective population size from temporal changes in allele frequency. Genetics 121:379–391.

Weir, B. S., and C. C. Cockerham.
1984. Estimating F-statistics for the analysis of population structure. Evolution 38:1358–1370.

Whitlock, M. C., and N. H. Barton.
1997. The effective size of a subdivided population. Genetics 146:427–441.
Wilson, C. A., and D. L. Nieland.
2001. Age and growth of red snapper, *Lutjanus campechanus*, from the northern Gulf of Mexico off Louisiana. Fish. Bull. 99:653–664.
Woods, M. K., A. J. Fischer, J. H. Cowan, Jr., and D.L. Nieland.
2003. Size and age of female red snapper *Lutjanus campechanus* in the northern Gulf of Mexico. Proc. Gulf Caribb. Fish. Inst. 54:526–537.

Appendix Table 1

Summary statistics at 19 nuclear-encoded microsatellite loci for the 1995 cohort of red snapper (*Lutjanus campechanus*) sampled at three localities in the northern Gulf of Mexico. n is sample size, no. of A is the number of alleles, A_R is allelic richness, H_E *is* gene diversity (expected heterozygosity), P_{HW} is probability of conforming to expected Hardy-Weinberg genotypic proportions, and F_{IS} is an inbreeding coefficient measured as Weir and Cockerham's (1984) *f*. Boldface indicates significant departures from HW equilibrium following (sequential) Bonferroni correction.

Locus	Texas	Louisiana	Alabama	Locus	Texas	Louisiana	Alabama
Lca20				*Prs240*			
n	199	286	373	n	140	276	372
No. of A	5	5	6	No. of A	20	21	23
A_R	3.39	3.37	3.00	A_R	15.84	14.94	14.96
H_E	0.170	0.215	0.172	H_E	0.917	0.901	0.885
P_{HW}	0.088	0.816	0.007	P_{HW}	0.010	0.129	0.096
F_{IS}	0.053	−0.009	0.097	F_{IS}	0.065	0.079	−0.012
Lca22				*Prs248*			
n	198	281	376	n	195	285	372
No. of A	14	17	14	No. of A	21	21	23
A_R	8.45	9.62	8.92	A_R	13.40	12.61	12.88
H_E	0.686	0.741	0.712	H_E	0.889	0.851	0.874
P_{HW}	0.176	0.317	0.013	P_{HW}	0.468	0.393	0.291
F_{IS}	0.013	0.002	0.055	F_{IS}	−0.010	0.006	0.047
Lca43				*Prs257*			
n	202	275	340	n	165	273	269
No. of A	10	11	9	No. of A	16	16	16
A_R	6.41	5.98	6.19	A_R	12.95	12.57	12.50
H_E	0.535	0.553	0.530	H_E	0.903	0.909	0.904
P_{HW}	0.585	0.763	0.669	P_{HW}	0.350	0.140	0.392
F_{IS}	−0.028	−0.006	0.017	F_{IS}	0.021	0.013	0.005
Lca64				*Prs260*			
n	197	286	377	n	189	283	376
No. of A	12	14	13	No. of A	4	5	7
A_R	7.19	7.54	6.97	A_R	3.45	3.39	3.50
H_E	0.777	0.778	0.764	H_E	0.361	0.390	0.339
P_{HW}	0.239	0.684	0.028	P_{HW}	0.507	0.285	0.185
F_{IS}	0.027	−0.025	0.014	F_{IS}	−0.011	−0.005	−0.045

continued

Appendix Table 1 (continued)

Locus	Texas	Louisiana	Alabama
*Lca*91			
n	201	285	375
No. of A	6	7	7
A_R	4.49	4.16	4.43
H_E	0.608	0.559	0.580
P_{HW}	0.002	0.957	0.162
F_{IS}	0.002	−0.066	−0.021
*Prs*55			
n	184	277	377
No. of A	8	7	9
A_R	3.30	3.82	3.60
H_E	0.158	0.228	0.209
P_{HW}	0.353	0.326	0.102
F_{IS}	−0.030	0.001	0.073
*Lca*107			
n	189	286	375
No. of A	11	12	11
A_R	8.67	8.59	7.90
H_E	0.809	0.806	0.796
P_{HW}	0.871	0.451	0.776
F_{IS}	0.013	0.006	−0.031
*Prs*137			
n	201	286	376
No. of A	13	13	17
A_R	7.83	7.92	8.33
H_E	0.706	0.700	0.711
P_{HW}	0.103	0.331	**0.000**
F_{IS}	0.049	0.071	**0.125**
*Prs*221			
n	197	282	376
No. of A	16	20	19
A_R	9.78	10.26	9.73
H_E	0.791	0.802	0.792
P_{HW}	0.043	0.037	0.102
F_{IS}	0.018	0.050	0.053
*Prs*229			
n	201	285	376
No. of A	8	7	8
A_R	5.96	5.44	5.39
H_E	0.470	0.508	0.486
P_{HW}	0.689	0.392	0.782
F_{IS}	0.038	0.088	0.005
*Prs*275			
n	199	286	374
No. of A	9	10	9
A_R	5.46	4.91	5.25
H_E	0.635	0.595	0.590
P_{HW}	**0.000**	0.604	0.183
F_{IS}	**0.105**	−0.014	0.011
*Prs*303			
n	200	285	374
No. of A	7	13	11
A_R	5.02	5.77	5.29
H_E	0.365	0.416	0.375
P_{HW}	0.785	0.559	0.007
F_{IS}	−0.029	−0.012	−0.026
*Prs*282			
n	202	285	377
No. of A	14	14	14
A_R	8.57	8.62	8.06
H_E	0.664	0.669	0.623
P_{HW}	0.311	0.039	0.066
F_{IS}	−0.006	0.072	−0.035
*Prs*328			
n	200	286	377
No. of A	6	8	6
A_R	3.70	4.06	3.53
H_E	0.555	0.557	0.557
P_{HW}	0.008	0.002	0.034
F_{IS}	0.072	−0.086	0.020
*Prs*333			
n	202	283	371
No. of A	8	6	8
A_R	4.22	3.98	4.70
H_E	0.288	0.294	0.371
P_{HW}	0.008	0.638	0.002
F_{IS}	0.055	0.013	0.128

Appendix Table 2

Summary statistics at 19 nuclear-encoded microsatellite loci for the 1997 cohort of red snapper (*Lutjanus campechanus*) sampled at three localities in the northern Gulf of Mexico. n is sample size, No. of A is number of alleles, A_R is allelic richness, H_E *is* gene diversity (expected heterozygosity), P_{HW} is probability of conforming to expected Hardy-Weinberg genotypic proportions, and F_{IS} is an inbreeding coefficient measured as Weir and Cockerham's (1984) *f*. Boldface indicates significant departures from HW equilibrium following (sequential) Bonferroni correction.

Locus	Texas	Louisiana	Alabama	Locus	Texas	Louisiana	Alabama
*Lca*20				*Prs*240			
n	211	272	269	n	188	234	240
No. of A	6	6	6	No. of A	20	20	22
A_R	3.72	3.35	3.78	A_R	14.22	15.37	14.34
H_E	0.238	0.184	0.206	H_E	0.897	0.898	0.885
P_{HW}	0.121	0.561	0.009	P_{HW}	0.001	0.012	0.317
F_{IS}	0.042	0.043	0.082	F_{IS}	0.092	0.043	−0.021
*Lca*22				*Prs*248			
n	208	244	266	n	211	271	272
No. of A	16	14	15	No. of A	21	22	21
A_R	9.88	9.36	9.45	A_R	12.58	12.91	12.67
H_E	0.769	0.757	0.771	H_E	0.872	0.867	0.882
P_{HW}	**0.000**	0.892	0.086	P_{HW}	0.176	0.616	0.334
F_{IS}	**0.106**	0.004	−0.009	F_{IS}	0.001	0.030	0.017
*Lca*43				*Prs*257			
n	210	272	272	n	206	266	246
No. of A	8	12	11	No. of A	17	17	18
A_R	6.22	6.48	6.19	A_R	13.24	12.86	13.51
H_E	0.587	0.536	0.528	H_E	0.908	0.898	0.915
P_{HW}	0.325	0.669	0.981	P_{HW}	0.282	0.113	0.464
F_{IS}	0.010	−0.049	−0.003	F_{IS}	0.011	0.008	0.005
*Lca*64				*Prs*260			
n	211	271	271	n	211	272	272
No. of A	11	13	11	No. of A	6	6	6
A_R	7.33	6.93	6.90	A_R	3.70	3.41	3.88
H_E	0.784	0.765	0.769	H_E	0.367	0.344	0.429
P_{HW}	0.086	0.749	0.495	P_{HW}	0.275	0.780	0.311
F_{IS}	0.027	0.020	0.012	F_{IS}	−0.019	0.026	−0.002
*Lca*91				*Prs*275			
n	202	268	262	n	211	272	273
No. of A	7	8	8	No. of A	7	9	8
A_R	4.22	4.38	4.43	A_R	5.00	5.07	4.61
H_E	0.560	0.575	0.570	H_E	0.608	0.612	0.579
P_{HW}	0.895	0.927	0.005	P_{HW}	0.711	0.334	0.441
F_{IS}	−0.070	0.039	0.030	F_{IS}	0.034	0.015	0.031
*Lca*107				*Prs*282			
n	211	264	269	n	211	272	273
No. of A	10	11	11	No. of A	13	12	12
A_R	7.90	8.07	8.15	A_R	8.46	8.40	7.89
H_E	0.799	0.798	0.775	H_E	0.636	0.639	0.614
P_{HW}	0.249	0.669	0.346	P_{HW}	0.886	0.556	0.141
F_{IS}	−0.104	−0.015	−0.045	F_{IS}	−0.051	0.028	0.022

continued

Appendix Table 2 (continued)

Locus	Texas	Louisiana	Alabama	Locus	Texas	Louisiana	Alabama
*Prs*55				*Prs*303			
n				*n*	211	272	270
No. of A	7	6	6	No. of A	10	9	12
A_R	4.34	3.62	3.52	A_R	5.33	5.17	6.05
H_E	0.266	0.210	0.221	H_E	0.375	0.400	0.400
P_{HW}	0.100	0.525	0.199	P_{HW}	0.527	0.344	0.781
F_{IS}	−0.017	−0.052	0.051	F_{IS}	−0.010	−0.011	−0.055
*Prs*137				*Prs*328			
n	211	272	271	*n*	211	272	273
No. of A	13	13	12	No. of A	6	6	5
A_R	7.88	7.43	8.00	A_R	3.54	3.45	3.71
H_E	0.721	0.694	0.715	H_E	0.542	0.545	0.568
P_{HW}	0.127	0.001	0.051	P_{HW}	0.323	0.108	0.191
F_{IS}	0.008	0.105	0.019	F_{IS}	0.090	−0.018	0.007
*Prs*221				*Prs*333			
n	211	271	270	*n*	211	272	272
No. of A	19	18	17	No. of A	6	7	6
A_R	10.06	9.54	10.32	A_R	3.84	4.52	4.20
H_E	0.800	0.792	0.802	H_E	0.342	0.320	0.323
P_{HW}	0.108	0.006	0.797	P_{HW}	0.571	0.819	0.412
F_{IS}	0.016	0.100	−0.025	F_{IS}	0.029	−0.022	0.032
*Prs*229							
n	211	271	269				
No. of A	7	9	9				
A_R	5.05	5.08	5.51				
H_E	0.495	0.464	0.527				
P_{HW}	0.001	**0.000**	0.020				
F_{IS}	0.081	**0.181**	0.118				

The relationship between smolt and postsmolt growth for Atlantic salmon (*Salmo salar*) in the Gulf of St. Lawrence

Kevin D. Friedland

UMass/NOAA Cooperative Marine Education and Research Program
Blaisdell House
University of Massachusetts
Amherst, Massachusetts 01003
Present address: National Marine Fisheries Service
28 Tarzwell Dr.
Narragansett, Rhode Island 02882
E-mail address: kevin.friedland@noaa.gov

Lora M. Clarke

Department of Natural Resources Conservation
Holdsworth Hall
University of Massachusetts
Amherst, Massachusetts 01003

Jean-Denis Dutil

Ministère des Pêche et des Océans
Institut Maurice-Lamontagne
850 route de la Mer, Mont-Joli
Québec, G5H 3Z4, Canada

Matti Salminen

Finnish Game and Fisheries Research Institute
Viikinkaari 4
P.O. Box 2, FIN-00791
Helsinki, Finland

The interaction of ocean climate and growth conditions during the postsmolt phase is emerging as the primary hypothesis to explain patterns of adult recruitment for individual stocks and stock complexes of Atlantic salmon (*Salmo salar*). Friedland et al. (1993) first reported that contrast in sea surface temperature (SST) conditions during spring appeared to be related to recruitment of the European stock complex. This hypothesis was further supported by the relationship between cohort specific patterns of recruitment for two index stocks and regional scale SST (Friedland et al., 1998). One of the index stocks, the North Esk of Scotland, was shown to have a pattern of postsmolt growth that was positively correlated with survival, indicating that growth during the postsmolt year controls survival and recruitment (Friedland et al., 2000). A similar scenario is emerging for the North American stock complex where contrast in ocean conditions during spring in the postsmolt migration corridors was associated with the recruitment pattern of the stock complex (Friedland et al., 2003a, 2003b). The accumulation of additional data on the postsmolt growth response of both stock complexes will contribute to a better understanding of the recruitment process in Atlantic salmon.

Anadromous salmonids produce cohorts of juvenile smolts that migrate over a short period of time at a nearly uniform size; however, the variability that occurs in migration timing and the size spectra of smolts is of potential interest in the study of recruitment (Hoar, 1976; Wedemeyer et al., 1980). Enhancement and restoration programs provide data on the effect of smolt size on return rate where hatchery practices both intentionally and unintentionally produce fish of varying size and quality. There are many case studies that show positive correlations between smolt size and return rate in salmonids, but nonsignificant relationships have also been observed, which underscore the fact that the contrast in size that can be achieved in hatcheries is often outside ecologically relevant limits (Farmer, 1994; Salminen et al., 1994). The functional relationship between smolt size and return rate is probably more accurately described as nonlinear and as having some optimality within the range of hatchery releases (Bilton et al., 1982; Henderson and Cass, 1991).

Researchers have also considered the effect of smolt size at ocean entry and the effect of smolt size on the ensuing growth patterns of postsmolts. Ward and Slaney (1988) described a positive relationship between return rate and smolt size for rainbow trout (*Salmo gairdneri*), suggesting that the recruitment rate of a year class was mediated by the mortality that occurred when the fish migrated to sea. When new data were added to that relationship, the original conclusions were no longer supported, indicating that factors other than smolt size at ocean entry contribute to recruitment (Ward, 2000). Although size at ocean entry may contribute to mortality risk, postsmolt growth, and the biotic and abiotic factors affecting postsmolt growth, often play a dominant role (Salminen et al., 1995). However, what has remained obscure is whether size at ocean entry influences postsmolt growth. Skilbrei (1989) and Nicieza and Braña (1993) reported negative relationships between smolt size and

Manuscript submitted 4 February 2004 to the Scientific Editor's Office.
Manuscript approved for publication 10 April 2005 by the Scientific Editor.
Fish. Bull. 104:149–155 (2006).

marine growth in Atlantic salmon, whereas Lundquist et al. (1988) and Salminen (1997) reported positive relationships. Einum et al. (2002) reported an inverse relationship between pre- and postsmolt growth of Atlantic salmon and suggested that phenotypic characteristics favoring growth in one environment may not necessarily favor growth in another. The body of mixed results sheds little light on whether smolt size confers a growth advantage to postsmolts. It also leaves in doubt the importance of freshwater experience on postsmolt survival. Common to this body of work is the dependence on samples coming from river returns and fishery catches that may not be representative of the full range of growth signatures in postsmolt populations because they do not include data from mortalities and often do not include data from some return age groups.

In this study we report on an analysis of scale growth indices from a collection of postsmolts from the Gulf of St. Lawrence. We measured freshwater growth signatures representative of smolt size and freshwater growth prior to migration and postsmolt growth was partitioned by season. These are samples of a life stage in an intermediate phase of marine life that is infrequently sampled and may be free of some of the assumed biases associated with samples from spawning fish.

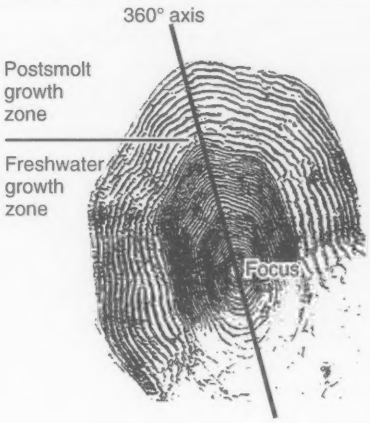

Figure 1

Postsmolt scale of Atlantic salmon (*Salmo salar*) in the Gulf of St. Lawrence showing focus, freshwater growth zone, and postsmolt growth zone.

Material and methods

We collected data on scale circuli spacing that was representative of the freshwater and postsmolt growth for juvenile salmon captured in the Gulf of St. Lawrence. These postsmolt salmon were collected in 1982–84 and were originally reported in Dutil and Coutu (1988). They were captured in experimental gill nets along the northwest shore of the Gulf during the months of August to October.

Freshwater and postsmolt growth descriptors were interpreted from circuli spacing patterns deposited on the scale. Scales were cleaned and mounted between glass slides and the spacings of scale circuli were measured with a Bioscan Optimas (Media Cybernatics, Inc., Silver Spring, MD) image processing system. Freshwater zone length (FZL) was taken as the total distance from the center of the scale focus to the transition between freshwater and postsmolt growth (Fig. 1). This transition zone is defined by the appearance of the first marine intercirculus spacing, i.e., as a wider spacing (according to the reader's judgment) than the progression of spacings in the freshwater zone. The FZL ends at the last freshwater circulus. FZL was interpreted as a proxy for smolt length at migration. The mean of the last five circuli spacings during the freshwater phase was computed for each sample (CSLF, circuli spacing during last freshwater period). This circuli spacing index was interpreted as an indication of freshwater finishing growth (the final phases of freshwater growth prior to migration). Two circuli spacing indices were extracted from the postsmolt zone, the mean spacing between intercirculi 2 through 6—an interval which was interpreted as the growth index for the early marine period (CSFM, circuli spacing during first marine period)—and the mean intercirculi spacing of the next five pairs occurring later in the postsmolt growth—an interval interpreted as an index of summer growth (CSSM, circuli spacing during summer marine period). The total length of the postsmolt growth zone was also extracted (MZL, marine zone length), which was the distance from the freshwater-marine transition, starting at the last freshwater circulus to the outer edge of the scale. All measurements were made on a single scale from each specimen along the 360° axis of the scale.

We tested the functional relationship between freshwater and marine growth, early and late marine growth, and seasonal progression of the growth zones using linear regression. We tested the significance of the slope parameters for each relationship as an indication of variable dependency.

We also considered whether these data might contribute to our understanding of size selective mortality by constructing a time series plot of FZL and MZL against date of capture. An anticipated positive trend in MZL would reflect growth during the marine phase, but any trend in FZL would reflect size-specific removals attributable to size at ocean entry.

Results

Measurements were taken from the scales of 587 postsmolts collected during 1982–84. FZL averaged 0.67 mm (SD=0.163) for all samples. CSLF averaged 0.022 mm (SD=0.0049), reflecting the slower growth and more narrowly spaced circuli of the freshwater zone. The two

circuli spacing indices from the postsmolt growth zone were larger in magnitude than the index from the freshwater zone. CSFM averaged 0.061 mm (SD=0.0109) and reflected a threefold increase in circuli spacing between the freshwater and marine zones. CSSM averaged 0.064 mm (SD=0.0100), reflecting the increased growth occurring within the duration of marine residency. MZL increased over time from approximately 0.6 mm in early August to 1.2 mm by mid-October.

The data we examined to test the relationship between smolt size and freshwater finishing growth and postsmolt growth indicate an absence of any linkage between the two growth environments. We found no significant relationships between smolt sizes as represented by FZL and either spring (CSFM) or summer (CSSM) postsmolt growth as represented by the circuli spacing indices. The scatter between CSFM and FZL suggests there were no linear trends for any of the study years (Fig. 2A). None of the three regressions had slopes significantly different from zero (Table 1). There was also an absence of any relationship between CSSM and FZL as evidenced by a similar pattern of scatter for the coordinates (Fig. 2B) and by an absence of significant slopes.

The relationship was further tested by considering the growth that occurs just prior to smolt migration as an indication of smolt condition at entry into the marine environment. As was the case with the bivariate relationships with FZL, CSLF was not a significant predictor of either CSFM or CSSM (Fig. 3). None of the slopes were significantly different from zero (Table 1).

Growth in the early and later part of the postsmolt season were correlated. There were significant positive linear relationships between CSSM and CSFM for all three years (Fig. 4), indicating that the postsmolts began their marine residence with rapid growth and continued to grow at a rapid rate through summer. The slopes of all three regressions were significantly different from zero (Table 1).

A time series plot of MZL, plotted by date of capture, shows an increasing trend reflecting the growth that postsmolts experience during early marine residence (Fig. 5). For the same fish, we also plotted FZL by date of capture and found a negative trend over time, indicating that FZL decreased during the period (Table 1), which would not be consistent with selective mortality of smolts of smaller initial size.

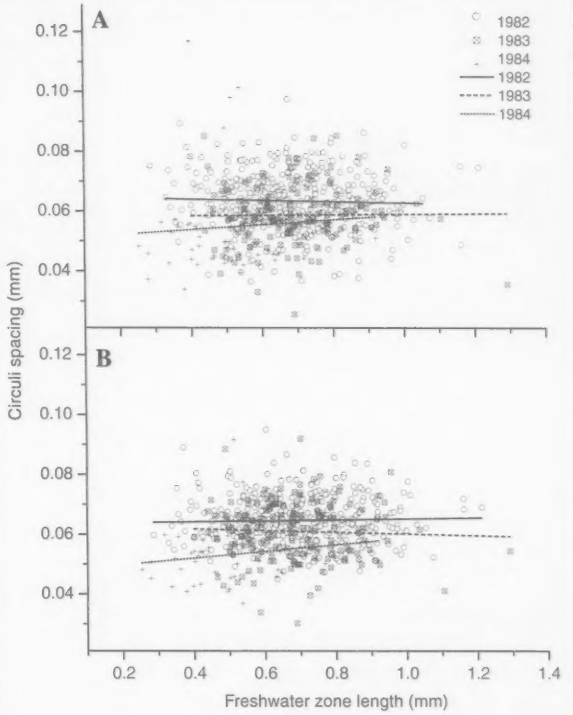

Figure 2

Relationships between circuli spacing during the early marine period (**A**) and circuli spacing during the summer marine period (**B**) and freshwater zone length for Atlantic salmon (*Salmo salar*) in the Gulf of St. Lawrence.

Table 1

Linear associations between scale growth indices and date of capture for Gulf of St. Lawrence Atlantic salmon (*Salmo salar*) postmolts. FZL=freshwater zone length; CSLF=mean of the last five freshwater intercirculi spacings; CSFM=mean spacing of intercirculi spacings 2 through 6; CSSM=mean spacing of intercirculi spacings 7 through 11; DOC=date of capture.

Linear associations		Probability H_0: slope = 0		
Predictor (X)	Dependent (Y)	1982	1983	1984
FZL	CSFM	0.53	0.87	0.57
FZL	CSSM	0.50	0.61	0.22
CSLF	CSFM	0.27	0.70	0.22
CSLF	CSSM	0.33	0.57	0.27
CSFM	CSSM	**<0.01**	**<0.01**	**<0.01**
DOC	FZL	**<0.01**		
DOC	MZL	**<0.01**		
Sample size		374	158	55

Discussion

Our main findings indicate that marine growth of postsmolt Atlantic salmon sampled from August to October in the Gulf of St. Lawrence was independent of freshwater growth history. Neither smolt size nor the last freshwater growth period of smolts prior to migration was related to postsmolt growth patterns. Furthermore,

there was no evidence that size at the smolt stage of postsmolts captured later in the season was larger than those captured earlier in the season, indicating that there was no size-selective attrition on smaller smolts during August to October. The strength of these data is that the samples were derived from collections of postsmolts, not river returns or fishery catches, and thus it is less biased and more representative of natural mortality factors. It will take considerably more data to fully test this hypothesis, but the highest priority should be given to similar sample collections, especially those collected earlier in the year (Holm et al., 2000). These data will be pivotal in interpreting the relative impact of size at ocean entry versus postsmolt growth for determing postsmolt survival.

Understanding survival during the postsmolt period is of great importance in the face of declining stock abundance and possible stock extirpations over portions of the range of Atlantic salmon (Anderson et al., 2000). With evidence showing the success of conservation efforts to increase freshwater populations (Swansburg et al., 2002), the range of potential life stages and habitats causing recruitment failure is reduced. Evidence at the population level showing coherence between early marine growth and survival at sea is still a long way from providing sufficient evidence to fully describe survival mechanisms or climate linkages. The hypothesized climate forcing appears to be related to a mismatch between ocean entry time for smolts and the thermal regime they find during their transition to marine life (Friedland et al., 2003b). The concept is supported by the growth response of postsmolts over a range of temperatures that they would likely encounter during that period of time. Atlantic salmon postsmolts follow a nonlinear growth response to temperature and optimum growth occurs at 13°C (Handeland et al., 2003). Variations in migration timing could result in fish encountering ocean conditions that are too warm or cool; these variations could explain the different associations of North American and European stocks to ocean temperatures. It would also be interesting to know if the thermal growth optimum is robust to varying feeding rations, which may be an issue for regional stock groups in the North Atlantic.

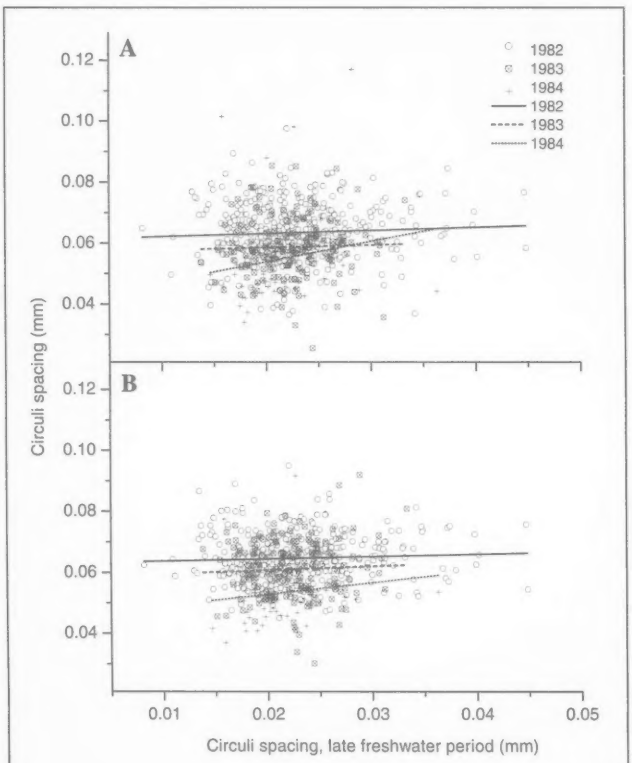

Figure 3

Relationships between circuli spacing during the early marine period (**A**) and circuli spacing during the summer marine period (**B**) and circuli spacing during the late freshwater period for Atlantic salmon (*Salmo salar*) in the Gulf of St. Lawrence.

The transition period from freshwater to marine life is characterized by a number of dynamic changes in growth and predation. The highest mortality rates for postsmolts occur during the first weeks at sea (Eriksson, 1994). As a consequence, even a minimal variation in these rates will have a large impact on adult recruitment. Size-selective mortality on juveniles has been demonstrated for other salmonids such as sockeye salmon (*Oncorhynchus nerka*) and has been shown to be seasonally concentrated (West and Larkin, 1987). Size-specific predation often occurs but predators, such as adult bird species, are not likely to grow at corresponding rates to those of the fish (Dieperink et al., 2002). Thus, size at ocean entry and the ability to grow out of the size range vulnerable to specific predators must affect the dynamics of predation rate. The period of predation vulnerability is mediated by growth rate; therefore the argument returns to what confers faster growth on postsmolts in some years?

One dynamic that challenges all stocks is the transition from predominantly invertebrate to piscivorous prey. Some authors suggest it is the success in making this transition, or the time it takes to make the transition, that dictates the amount of time the postsmolts take to grow out of the predation-vulnerable size range (Dutil and Coutu, 1988; Andreassen et al., 2001; Salminen et al., 2001). Depending on prevailing foraging conditions, this transition may be promoted by increased smolt size, as was the case in the northern Baltic Sea in 1990–93 (Salminen et al., 2001). One potential explanation for the contradictory views on the relationship between pre- and postsmolt growth in

Atlantic salmon may arise from geographical differences or year-to-year changes (or both) in prey regimes during the critical diet-transition period. In lake-run brown trout, Niva and Jokela (2000) found a positive correlation between hatchery growth rate and postsmolt growth in a lake with small fish as the main prey. In contrast, hatchery growth did not predict growth in a lake where the fish had to prey on bottom-dwelling invertebrates. This finding may indicate that assessment of individual performance may be highly specific to environments in migratory salmonids.

Size of postsmolts at ocean entry in salmonids also manifests itself in predictable patterns of life history variation. In sea trout (*Salmo trutta*) there is a close correspondence between size of juvenile stage and adult size, which is believed to have an impact on recruitment through size variation at critical life stages (Elliott, 1985). Hutchings and Jones (1998) found that smolt age and size had a small effect on the growth-rate threshold for maturity in Atlantic salmon. Smolt-size variation in sea trout has been associated with latitude, indicating that for this species recruitment strategies are likely adapted to local physical conditions, predators, and prey regimes (L' Abée-Lund et al., 1989). Wild smolts are often smaller than hatchery smolts for the same or allied strains, yet they consistently survive at higher rates (Poole et al., 2003). Obviously there are other cofactors that can explain why the wild fish overcome any advantage conferred on hatchery fish by their larger size at migration. The wild versus hatchery comparison is a relatively weak piece of evidence to use to dismiss the idea that smolt size is an important survival factor. However, a recent study of size at ocean entry in a Quebec stock of wild fish may provide more useful evidence (Dodson[1], Caron[2]). The investigators found that the size spectra of smolts were not different from the size spectra of back-calculated smolt sizes for returning adults, suggesting some factor other than size at ocean entry was controlling survival. It should be noted that postsmolts collected in the present study were of unknown origin, but the scale pattern for the freshwater zone clearly indicates that they were of wild origin.

The growth response of postsmolts may be governed by a simple response to temperature optima occurring in coastal marine waters, but it may also be more complex than that. The surface waters in the Gulf of St. Lawrence circulate in wide-scale

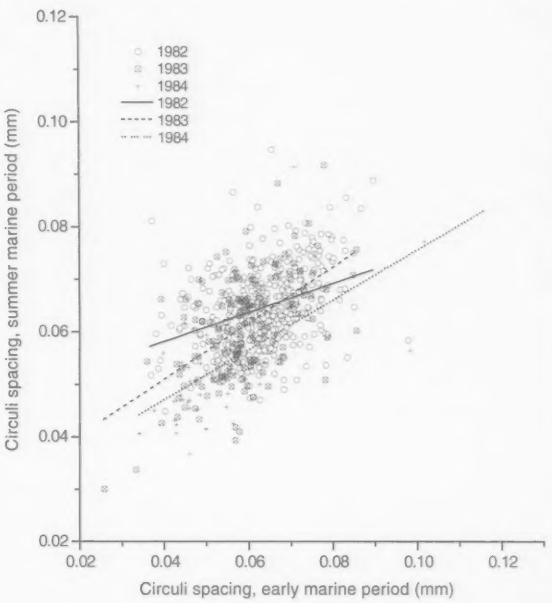

Figure 4

Relationships between circuli spacing during the summer marine period and circuli spacing during the early marine period for Atlantic salmon (*Salmo salar*) in the Gulf of St. Lawrence.

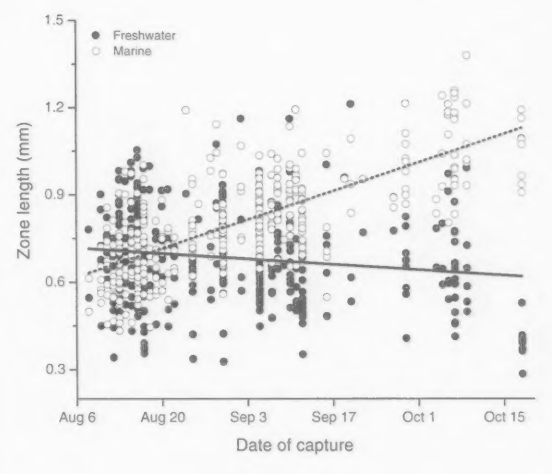

Figure 5

Freshwater zone length and marine zone length, by date of capture during the 1982 field season for Atlantic salmon (*Salmo salar*) in the Gulf of St. Lawrence.

[1] Dodson, J. 2004. Personal commun. Département de Biologie Pavillon Alexandre-Vachon, local 3058-B Université Laval, Québec, G1K 7P4, Canada.

[2] Caron, F. 2004. Personal commun. Direction de la Recherche Faune et Parcs Québec, 675 est, Boul. René-Lévesque Boîte 92, 11e étage, Québec, G1R 5V7, Canada.

gyres over the extremely cold waters of the cold intermediate layer (CIL), thus creating a thermally complex habitat. Strong winds periodically force cold waters from the CIL to the surface (Ouellet, 1997). Postsmolts appear to be opportunistic feeders in the ocean, and despite their predominant use of surface waters, they have been known to use benthic habitats and water column features as well (Levings, 1994; Sturlaugsson, 1994). These behaviors would distribute fish in a manner independent of surface temperatures because forage behaviors are not necessarily controlled by temperature preferences. Growth in postsmolts is also affected by other physical parameters, such as photoperiod (Forsberg, 1995), and possibly by variation in sea surface salinity as shown for chum salmon (*Oncorhynchus keta*) (Morita et al., 2001). We can predict migration timing and initial migration trajectories for postsmolts, but we are hard pressed to predict the physical nature of their habitats over time and the physiological effect of these habitats on postsmolt growth.

Acknowledgments

We thank T. Sadusky for help with the initial phases of this study and two anonymous reviewers for productive comments.

Literature cited

Anderson, J. M., F. G. Whoriskey, and A. Goode.
2000. Atlantic salmon on the brink. Endangered Species Update 17:15–21.

Andreassen, P. M. R., M. B. Martinussen, N. A. Hvidsten, and S. O. Stefansson.
2001. Feeding and pre-selection of wild Atlantic salmon post-smolts. J. Fish Biol. 58:1667–1679.

Bilton, H. T., D. F. Alderdice, and J. T. Schnute.
1982. Influence of time and size at release of juvenile coho salmon (*Oncorhynchus kisutch*) on returns at maturity. Can. J. Fish. Aquat. Sci 39:426–447.

Dieperink, C., B. D. Bak, L. F. Pedersen, M. I. Pedersen, and S. Pedersen.
2002. Predation on Atlantic salmon and sea trout during their first days at sea as postsmolts. J. Fish Biol. 61:848–852.

Dutil, J.-D., and J.-M. Coutu.
1988. Early marine life of Atlantic salmon, *Salmo salar*, postsmolts in the northern Gulf of St. Lawrence. Fish. Bull. 86:197–212.

Einum, S., E. B. Thorstad, and T. F. Næsje.
2002. Growth rate correlations across life stages in female Atlantic salmon. J. Fish Biol. 60:780–784.

Elliott, J. M.
1985. Growth, size, biomass, and production for different life stages of migratory trout *Salmo trutta* in a Lake District stream, 1966–83. J. Animal Ecol. 54:985–1001.

Eriksson, T.
1994. Mortality risks of Baltic salmon during downstream migration and early sea-phase: effects of body size and season. Nord. J. Freshw. Res. 69:100.

Farmer, G. J.
1994. Some factors which influence the survival of hatchery Atlantic salmon (*Salmo salar*) smolts utilized for enhancement purposes. Aquaculture 121:223–233.

Forsberg, O. I.
1995. Empirical investigation on growth of post-smolt Atlantic salmon (*Salmo salar* L.) in land-based farms. Evidence of photoperiodic influence. Aquaculture 133:235–248.

Friedland, K. D., L. P. Hansen, and D. A. Dunkley.
1998. Marine temperatures experienced by postsmolts and the survival of Atlantic salmon (*Salmo salar* L.) in the North Sea area. Fish. Oceanogr. 7:22–34.

Friedland, K. D., L. P. Hansen, D. A. Dunkley, and J. C. MacLean.
2000. Linkage between ocean climate, post-smolt growth, and survival of Atlantic salmon (*Salmo salar* L.) in the North Sea area. ICES J. Mar. Sci. 57:419–429.

Friedland, K. D., D. G. Reddin, D. G., and M. Castonguay.
2003a. Ocean thermal conditions in the post-smolt nursery of North American Atlantic salmon. ICES J. Mar. Sci. 60:343–355.

Friedland, K. D., D. G. Reddin, and J. F. Kocik.
1993. Marine survival of North American and European Atlantic salmon: effects of growth and environment. ICES J. Mar. Sci. 50:481–492.

Friedland, K. D., D. G. Reddin, J. R. McMenemy, and K. F. Drinkwater.
2003b. Multidecadal trends in North American Atlantic salmon (*Salmo salar*) stocks and climate trends relevant to juvenile survival. Can. J. Fish. Aquat. Sci. 60:563–583.

Handeland, S. O., B. T. Björnsson, A. M. Arnesen, and S. O. Stefansson.
2003. Seawater adaptation and growth of post-smolt Atlantic salmon (*Salmo salar*) of wild and farmed strains. Aquaculture 220:367–384.

Henderson, M. A., and A. J. Cass.
1991. Effect of smolt size on smolt-to-adult survival for Chilko Lake sockeye salmon (*Oncorhynchus nerka*). Can. J. Fish. Aquat. Sci. 48:988–994.

Hoar, W. S.
1976. Smolt transformation: evolution, behaviour, and physiology. J. Fish. Res. Board Can. 33:1233–1252.

Holm, M., J. C. Holst, and L. P. Hansen.
2000. Spatial and temporal distribution of post-smolts of Atlantic salmon (*Salmo salar* L.) in the Norwegian Sea and adjacent areas. ICES J. Mar. Sci. 57:955–964.

Hutchings, J. A., and M. E. B. Jones.
1998. Life history variation and growth rate thresholds for maturity in Atlantic salmon, *Salmo salar*. Can. J. Fish. Aquat. Sci. 55(suppl. 1):22–47.

Levings, C. D.
1994. Feeding behavior of juvenile salmon and significance of habitat during estuary and early sea phase. Nord. J. Freshwater Res. 69:7–16.

L' Abée-Lund, J. H., B. Jopnsson, A. J. Jensen, L. M. Sættem, T. G. Heggberget, B. . Johnson, T. F. Næsje.
1989. Latitudinal variation in life-history characteristics of sea-run migrant brown trout *Salmo trutta*. J. Animal Ecol. 58:525–542.

Lundquist, H., W. C. Clarke, and H. Johansson.
1988. The influence of sexual maturation on survival to adulthood of river stocked Baltic salmon, *Salmo salar*, smolts. Holarct. Ecol. 11:60–69.

Morita, S. H., K. Morita, and H. Sakano.
2001. Growth of chum salmon (*Oncorhynchus keta*) correlated with sea-surface salinity in the North Pacific. ICES J. Mar. Sci. 58:1335–1339.

Nicieza, A. G, and F. Branña.
1993. Relationships among smolt size, marine growth, and sea age at maturity of Atlantic salmon (*Salmo salar*) in northern Spain. Can. J. Fish. Aquat. Sci. 50:1632–1640.

Niva, T., and J. Jokela.
2000. Phenotypic correlation of juvenile growth rate between different consecutive foraging environments in a salmonid fish: a field experiment. Evol. Ecol. 14:111–126.

Ouellet, P.
1997. Characteristics and vertical distribution of Atlantic cod (*Gadus morhua*) eggs in the northern Gulf of St. Lawrence, and the possible effect of cold water temperature on recruitment. Can. J. Fish. Aquat. Sci. 54:198–210.

Poole, W. R., D. T. Nolan, T. Wevers, M. Dillane, D. Cotter, and O. Tully.
2003. An ecophysiological comparison of wild and hatchery-raised Atlantic salmon (*Salmo salar* L.) smolt from the Burrishoole system, western Ireland. Aquaculture 222:301–314.

Salminen, M.
1997. Relationships between smolt size, postmolt growth and sea age at maturity in Atlantic salmon ranched in the Baltic Sea. J. Appl. Ichthyol. 13:121–130.

Salminen, M., E. Erkamo, and J. Salmi.
2001. Diet of post-smolt and one-sea-winter Atlantic salmon in the Bothnian Sea, Northern Baltic. J. Fish Biol. 58:16–35.

Salminen, M., S. Kuikka, and E. Erkamo.
1994. Divergence in the feeding migration of Baltic salmon (*Salmo salar* L.); the significance of smolt size. Nord. J. Freshw. Res. 69:32–42.
1995. Annual variability in survival of sea-ranched Baltic salmon, *Salmo salar* L.: Significance of smolt size and marine conditions. Fish. Manag. Ecol. 2:171–184.

Skilbrei, O. T.
1989. Relationships between smolt lengths and growth and maturation in the sea of individually tagged Atlantic salmon (*Salmo salar*). Aquaculture 83:95–108.

Sturlaugsson, J.
1994. Food of ranched Atlantic salmon (*Salmo salar* L.) postsmolts in coastal waters, West Iceland. Nord. J. Freshw. Res. 69:43–57.

Swansburg, E, G. Chaput, D. Moore, D. Cassie, and N. El-Jabi.
2002. Size variability of juvenile Atlantic salmon: links to environmental conditions. J. Fish Biol. 61:661–683.

Ward, B. R.
2000. Declivity in steelhead (*Oncorhynchus mykiss*) recruitment at the Keogh River over the past decade. Can. J. Fish. Aquat. Sci. 45:298–306.

Ward, B. R., and P. A. Slaney.
1988. Life history and smolt-to-adult survival of Keogh River steelhead trout (*Salmo gairdneri*) and the relationship to smolt size. Can. J. Fish. Aquat. Sci. 45: 1110–1122.

Wedemeyer G.A., R. L. Saunders, and W. C. Clarke.
1980. Environmental factors affecting smoltification and early marine survival of anadromous salmon. Mar. Fish. Rev. 42:1–14.

West, C. J., and P. A. Larkin.
1987. Evidence for size-selective mortality of juvenile sockeye salmon (*Oncorhynchus nerka*) in Babine Lake, British Columbia. Can. J. Fish. Aquat. Sci. 44:712–721.

Erratum

Erratum: Fishery Bulletin 102(4): p. 568.
Calambokidis, John, Gretchen H. Steiger, David K. Ellifrit, Barry L. Troutman, and C. Edward Bowlby
Distribution and abundance of humpback whales (*Megaptera novaeangliae*) and other marine mammals off the northern Washington coast

Correction: Table 3 should read as follows

Table 3
Summary of marine mammal sightings by year during ship surveys off northern Washington. Opportunistic sightings (nontransect) are included.

	1995		1996		1997		1998		2000		2002		All years	
Species	No. of sightings	No. of animals	No. of sightings	No. of animals	No. of sightings	No. of animals	No. of sightings	No. of animals	No. of sightings	No. of animals	No. of sightings	No. of animals	No. of sightings	No. of animals
Baleen whales														
Humpback whale	25	40	54	86	23	44	27	36	24	57	79	139	232	402
Gray whale			1	1	2	3	2	3					5	7
Minke whale	3	3									1	1	4	4
Unidentified whale	4	8	3	3	11	12	1	1	3	3	4	6	26	33
Odeontocetes														
Dall's porpoise	27	72	20	64	16	43	13	46	14	48	25	133	115	406
Harbor porpoise	4	10	11	20	2	5	14	43	7	11			38	89
Pacific white-sided dolphin	4	596	16	149					4	369	4	19	28	1133
Northern right-whale dolphin									1	6			1	6
Risso's dolphin			5	57	1	5	2	11	1	6			9	79
Killer whale	3	16	2	38	2	21	2	5	3	36	2	8	14	124
Unidentified delphinid	6	9	8	56	2	4	3	5			4	18	23	92
Pinnipeds and otters														
Harbor seal	2	2	3	3	2	3	7	7	1	1			15	16
Elephant seal	6	6	10	10	2	2			2	2			20	20
California sea lion							1	1	3	3			4	4
Steller sea lion							3	5	1	1			4	6
Northern fur seal	6	6	5	5	1	2	9	9	1	1	6	6	28	29
Sea otter							3	3					3	3
Unidentified pinniped	4	4	3	3	1	2	4	4	1	1			13	14
Total sightings	94	772	141	495	65	146	91	179	66	545	125	330	582	2467

Fishery Bulletin

Guidelines for authors

Content of manuscripts

Contributions published in Fishery Bulletin describe original research in marine fishery science, fishery engineering and economics, as well as the areas of marine environmental and ecological sciences (including modeling). Although all contributions are subject to peer review, responsibility for the contents of papers rests upon the authors and not upon the editor or publisher. *Submission of an article implies that the article is original and is not being considered for publication elsewhere.* Manuscripts must be written in English. Authors whose native language is not English are strongly advised to have their manuscripts checked by English-speaking colleagues prior to submission. **Articles** may range from relatively short contributions (10–15 typed and double-spaced pages, tables and figures not included) to extensive contributions (20–30 typed pages). **Notes** are reports of 5 to 10 pages without an abstract and describe methods or results not supported by a large body of data.

Manuscript preparation

Title page should include *authors' full names and mailing addresses and the senior author's telephone, fax number, and e-mail address, and a list of key words to describe the contents of the manuscript.* **Abstract** should be limited to 150 words (one-half typed page), state the main scope of the research, and emphasize the author's conclusions and relevant findings. Do not review the methods of the study or list the contents of the paper. Because abstracts are circulated by abstracting agencies, it is important that they represent the research clearly and concisely. **Text** must be typed in 12 point Times New Roman font throughout. A brief introduction should convey the broad significance of the paper; the remainder of the paper should be divided into the following sections: **Materials and methods, Results, Discussion (or Conclusions),** and **Acknowledgments**. Headings within each section must be short, reflect a logical sequence, and follow the rules of multiple subdivision (i.e., there can be no subdivision without at least two items). The entire text should be intelligible to interdisciplinary readers; therefore, all acronyms, abbreviations, and technical terms should be written out in full the first time they are used. Include FAO common names for species in the list of keywords and in the introduction. Regional common names may be used throughout the rest of the text if they are different from FAO common names which can be found at http://www.fishbase.org/search.html. Follow the U.S. Government Printing Office Style Manual (1984 ed.) and the CBE Style Manual (6th ed.) for editorial style, and the most current issue of the American Fisheries Society's Common and Scientific Names of Fishes from the United States and Canada for fish nomenclature. Dates should be written as follows: 11 November 2000. Measurements should be expressed in metric units, e.g., 58 metric tons (t); if other units of measurement are used, please make this fact explicit to the reader. Write out the numbers zero through nine unless they form part of measurement units (e.g., nine fish but 9 mm).

Text footnotes should be inserted in 9-point font at the bottom of the page that displays the first citation of the footnote. Footnotes should be formatted in the same manner as citations. Footnote all personal communications, unpublished data, and unpublished manuscripts with full address of the communicator or author, or, as in the case of unpublished data, where the data are on file. Authors are advised to avoid references to nonstandard (gray) literature (such as internal, project, processed, or administrative reports, ICES Council Minutes, IWC Minutes or Working Papers, any "research" or "working" documents, laboratory or contract reports, Management Council reports, and manuscripts in review) wherever possible. If these references are used, present them as footnotes and list whether they are available from NTIS (National Technical Information Service) or from some other public depository. Cite all software and special equipment or chemical solutions used in the study, not in a footnote but within parentheses in the text (e.g., SAS, vers. 6.03, SAS Inst., Inc., Cary, NC).

Literature cited comprises published works and those accepted for publication in peer-reviewed literature (in press). Follow the name and year system for citation format. If there is a sequence of citations in the text, list chronologically: (Smith, 1932; Green, 1947; Smith and Jones, 1985). Abbreviations of serials should conform to abbreviations given in the Serial Sources for the BIOSIS Previews Database. Authors are responsible for the accuracy and completeness of all citations. Literature citation format: Author (last name, followed by first-name initials). Year. Title of report or manuscript. Abbreviated title of the series to which it belongs. Always include number of pages. If there is a sequence of citations by the same first author, list the works alphabetically according to the last name of following authors (e.g., Smith G. P., L. C. Brown, 1982; Smith, G. P., and T. P. Stuart, 1982). If the authorship is identical, list works chronologically.

Tables and figures—general format

- Zeros should precede all decimal points for values less than one.
- Sample size, n, should be italicized.
- Capitalize the first letter of the first word in all labels within figures.
- Do not use overly large font sizes in maps and for units of measurements along axes in figures.
- Do not use bold fonts or bold lines in figures.
- Do not place outline rules around graphs.
- Do not use horizontal lines in graphs to indicate measurement units on axes.

- Use a comma in numbers of five digits or more (e.g. 13,000 but 3000).
- Maps should have a North arrow (or compass sign) and degrees latitude-longitude (e.g., 170°E)

Tables are often overused in scientific papers; it is seldom necessary or even desirable to present all the data associated with a study. Tables should not be excessive in size and must be cited in numerical order in the text. Headings should be short but ample enough to allow the table to be intelligible on its own. All unusual symbols must be explained in the table legend. Other incidental comments may be footnoted with italic footnote markers. Use asterisks to indicate probability in statistical data. Do not type table legends on a separate page; place them on the same page as the table data. Do not submit tables in photo mode.

Figures include line illustrations, photographs (or slides), and computer-generated graphs and must be cited in numerical order in the text. Graphics will aid in the comprehension of the text, but they should be limited to presenting patterns rather than raw data. Figures are costly to print and should be limited to six. Figures must be labeled with author's name and number of figure. Avoid placing labels vertically (except on *y*-axis). Figure legends should explain all symbols and abbreviations and should be double-spaced on a separate page at the end of the manuscript. Please note that we do not print graphs in color.

FAILURE TO FOLLOW THESE GUIDELINES WILL DELAY PUBLICATION OF A MANUSCRIPT

Copyright law does not apply to *Fishery Bulletin*, which falls within the public domain. However, if an author reproduces any part of an article from *Fishery Bulletin* in his or her work, reference to source is considered correct form (e.g., Source: Fish. Bull 97:105).

Reprints are available free of charge to the senior author (50 copies) and to his or her laboratory (50 copies). Additional copies may be purchased in lots of 100 when the author receives page proofs.

Submission

The Scientific Editorial Office encourages authors to submit their manuscripts as a *single* PDF (preferred), Word (zipped), or WordPerfect (zipped) document by e-mail to Fishery.Bulletin@noaa.gov. Please use the subject heading "Fishery Bulletin manuscript submission." *Do not* send encrypted files. For further details on electronic submission, please contact the Scientific Editorial Office directly (see address below). Or you may send your manuscript on compact disc in one of the above formats along with four printed copies (one original plus three copies [stapled]) to the Scientific Editor, at the address shown below. Send photocopies only of figures with initial submission of manuscript; do not send original figures. Original figures and electronic copies of figures will be requested later when the manuscript has been accepted for publication.

Dr. Adam Moles
Scientific Editor, *Fishery Bulletin*
11305 Glacier Hwy
Juneau, AK 99801-8626

Once the manuscript has been accepted for publication, you will be asked to submit a final software copy of your manuscript. When requested, the text and tables should be submitted in Word or Word Rich Text Format. Figures should be sent as PDF files, Windows metafiles, tiff files, or as EPS files. Send a copy of figures in original software if conversion yields a degraded version.

Fishery Bulletin

Subscription form

Superintendent of Documents **Publications** Order Form

*5178

☐ YES, please send me the following publications:

____ Subscriptions to *Fishery Bulletin*
for $55.00 per year ($68.75 foreign)

The total cost of my order is $ _____ . Prices include regular domestic postage and handling and are subject to change.

_____
(Company or Personal Name) (Please type or print)

_____
(Additional address/attention line)

_____
(Street address)

_____
(City, State, ZIP Code)

_____
(Daytime phone including area code)

_____
(Purchase Order No.)

Charge your order. IT'S EASY!

VISA

MasterCard

Please Choose Method of Payment:

☐ Check Payable to the Superintendent of Documents

☐ GPO Deposit Account ☐☐☐☐☐☐–☐

☐ VISA or MasterCard Account

☐☐☐☐☐☐☐☐☐☐☐☐☐☐☐☐

☐☐☐☐ (Credit card expiration date)

To fax your orders (202) 512-2250

_____
(Authorizing Signature)

Mail To: Superintendent of Documents
P.O. Box 371954, Pittsburgh, PA 15250-7954
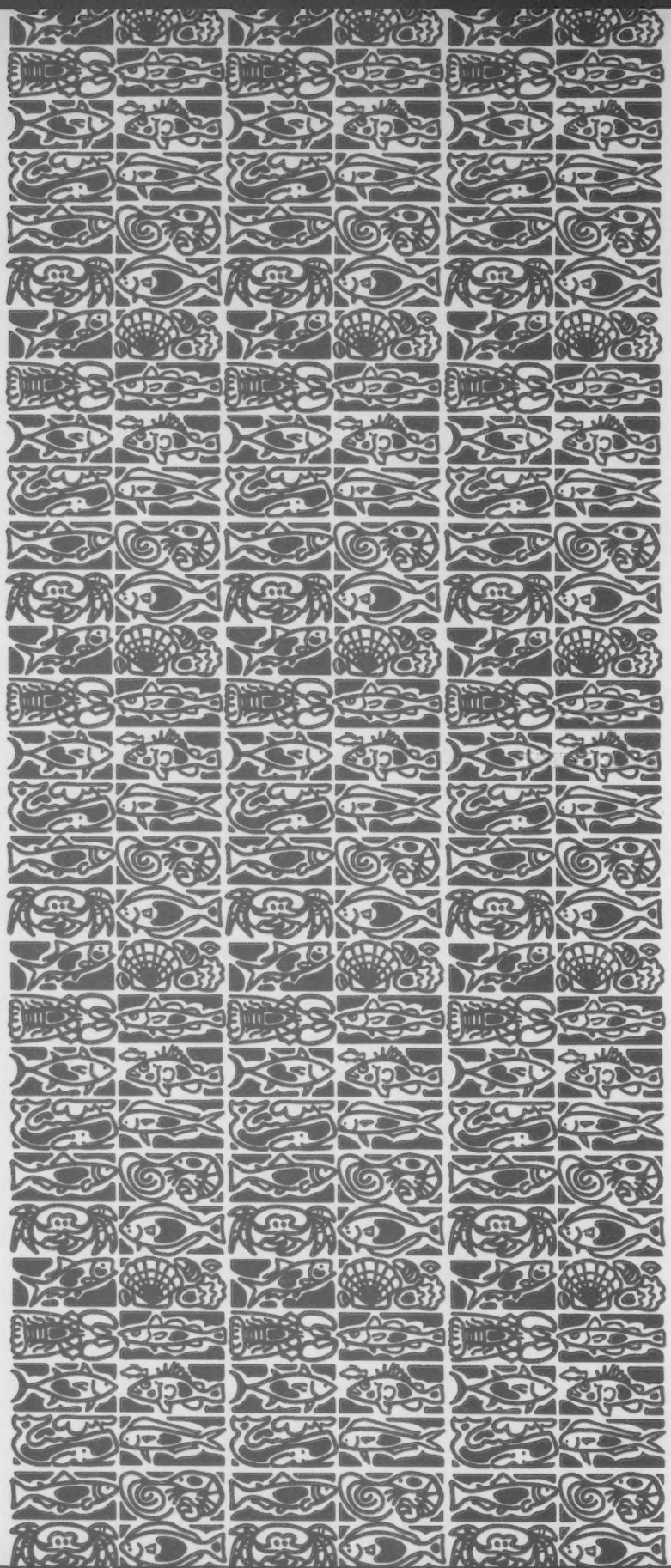
Thank you for your order!